4/10/2019

TU Delft
& Iv -Infra

Bicycle and pedestrian bridge for the circular economy: Technical and sustainability assessment

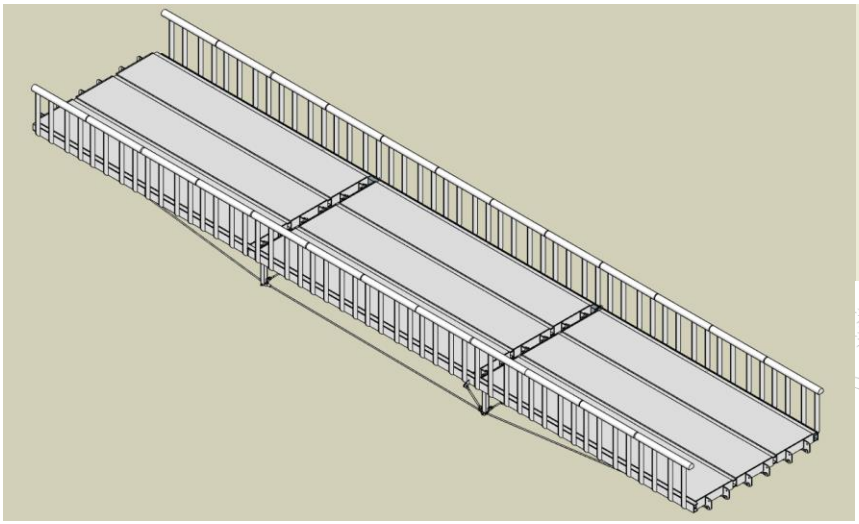

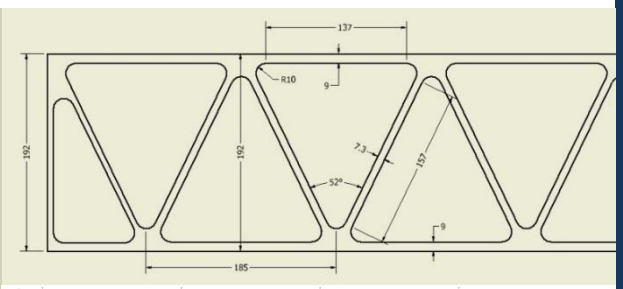

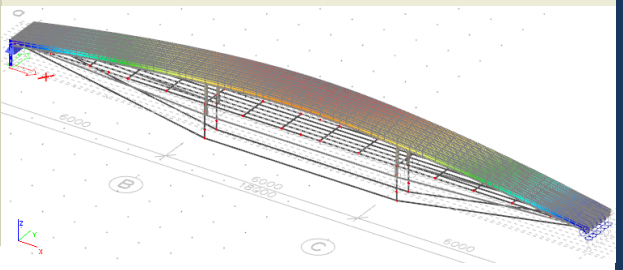

Master's Thesis | Luca Nicola Fausto Lopriore

Faculty of Civil Engineering and Geosciences
Delft University of Technology
April 2019, Delft

Bicycle and pedestrian bridge for a Circular Economy

Technical and sustainability assessment

by

Luca Nicola Fausto Lopriore

in partial fulfilment of the requirements for the degree of

Master of Science

in Structural Engineering

at Delft University of Technology,

to be defended publicly on Tuesday April 16th, 2019 at 9:00hrs.

Thesis committee:

Prof. Dr. M. Veljkovic	TU Delft
Ir. P. van Lierop	Iv-Infra
Prof. Dr. H. Jonkers	TU Delft
Ir. J. Smits	TU Delft

Preface

This thesis is submitted in completion of a Master's degree in Structural Engineering at Delft University of Technology. The subject of the thesis is the structural design and analysis of a bicycle and pedestrian bridge which meets the requirements of Circular Economy, the bridge is then compared to a structure designed using a traditional civil engineering approach to quantify its environmental impact.

I began work on this thesis in June of 2018 with research into Circular Economy in the context of civil engineering which forms the basis for the state of the art. In the following months I began to develop ideas regarding the different approaches to incorporating strategies of circularity in bridge design, a process which resulted in the design criteria for the structure. The months between October 2018 and March 2019 were spent performing the structural design and analysis of the structure; the girders, connections, and detailing of each element are all discussed in the body of the report. The month of March was spent preparing for the final submission and presentation in April 2019.

I would like to express my gratitude to the members of my Assessment Committee; prof. M. Veljkovic, ir. P. van Lierop of Iv-Infra, prof. H. Jonkers, and prof. J. Smits for their guidance. Furthermore, I would like to thank my colleagues at Iv-Infra in Haarlem for their continued advice and expertise.

L.N.F. (Luca) Lopriore
Delft, April 2019

Abstract

The aim of this thesis is to present a design for a bicycle and pedestrian bridge which meets the requirements of Circular Economy; by incorporating strategies such as design for disassembly and modularity a structure is created which improves upon the long-term value of existing bridges.

Circular Economy has in recent years begun to replace the sustainability paradigm as it provides more tangible strategies to achieve the same goals. Civil engineering is a large contributor to environmental impact and waste production therefore reducing this represented the main goal for this thesis; by designing a structure which uses alternative materials and connections to traditional methods the impact was reduced.
The design of the structure consisted of the following main aspects; girders, connections, and detailing, these were verified using European norms to demonstrate the feasibility of the proposed design. Analyses were performed for the key structural aspects of strength, stability, and dynamic response; together with detailing of the components it was demonstrated that implementation of such a bridge is possible in practice. Once the final design was determined it was compared to a set of bridges designed with a traditional civil engineering approach to demonstrate the benefits of circular design in terms of environmental impact.

It is concluded that a post-tensioned aluminium girder bridge represents a sufficiently strong and stiff solution for an 18m span and 3m width; the modular design allows for disassembly and modification on site meaning elements can be conveniently reused or replaced. In terms of environmental impact the result is dependent on the LCA method chosen; the Dutch method which allows bonus from reuse and recycling provides an even result while without this detraction the traditional structure is favoured significantly.

Table of contents

List of Figures

List of Tables

1. Introduction

1.1 Background and goals

The finiteness of Earth's resources and the role in industrial economies of resource inputs, waste outputs, and their inter-relation was first identified by Kenneth Boulding in his 1966 essay "Economics of the Coming Spaceship Earth" (Boulding, 1966). Many years before the advent of the Circular Economy paradigm which currently dominates discussions across disciplines, Boulding discusses the concept of the open economic systems which are still commonplace today, often described as the 'take-make-dispose' model, and how in reality they are closed systems as the resources and waste are shared across the global community. Due to increasing globalisation and environmental consciousness the validity and importance of these concepts has been demonstrated with policymakers and researchers beginning to take action in order to achieve sustainable development. This growing awareness is shown in the actions taken by governing bodies to promote Circular Economy through policy changes; notable examples include the European Circular Economy package introduced in 2015 and the Chinese Circular Economy Promotion Law of 2008. Common points of action include reducing consumption of resources, increasing life-span of products, and reducing and effectively managing waste (European Comission, 2015) (PRC, 2008).

A number of pilot projects for pedestrian bridges have been successfully realised which address the challenges posed by designing for a Circular Economy; these use the favourable properties of different materials, structural systems, and connections to maximise material efficiency and reduce environmental impact. The main structural material is often stipulated from the outset in the requirements of the engineering process; motivations for choosing a particular material traditionally surround strength, stiffness, and cost parameters. Often overlooked is the impact which a material may have in terms of recycling possibilities or freedom in design. Structures incorporating over-capacity or possibilities for upgrading are rarely seen in practice as the redundancy required to achieve this is seen as unnecessary cost, thereby rapidly being removed from the design considerations. As costs of ownership forecasts increase due to increasingly accurate and extensive life-cycle cost (LCC) analyses the value of structures which can remain in use for longer grows with it. Connections which allow disassembly can contribute to this in-built adaptability while simultaneously offering possibilities for reuse of components in different applications without compromising their quality. While individually these concepts are clearly displayed in a number of pedestrian bridges, a solution incorporating a combination hereof offers the opportunity to make valuable contribution to the promotion of a (local) Circular Economy system.

The goals of this thesis are to investigate the following topics:

- Identify and assess existing structures which implement Circular Economy strategies
- The structural design and analysis of a pedestrian bridge, specifically regarding the load-bearing structure, connections, and accounting for the fabrication process
- An LCC comparison of the proposed structure against a traditional solution

Through this investigation I aim to demonstrate the long-term value of a Circular Economy approach to small-scale infrastructure as well present a feasible but innovative solution to a practical case.

1.2 Objective and Research Questions

The main objective of this thesis is to design and perform a structural analysis of a bicycle and pedestrian bridge which meets the same functional requirements as a traditional structure but with optimised performance in terms of circularity. In order to reach this objective a research question and sub-questions have been formulated:

1. How should a structure and its components be designed such that they best meet the requirements of Circular Economy?
    a. Which type of structure best fits the 4R framework of Circular Economy?
    b. How should the connections in the structure be designed to enable modular assembly and disassembly?
    c. How can detailing of the structure take place such that feasibility is ensured?
2. To what extent were the design choices justified in terms of environmental impact and how does the structure perform when compared to traditional civil engineering solutions?

1. 3 Thesis structure

The opening of this thesis, Chapter 2, covers the state of the art for bicycle and pedestrian bridges, the design strategies, and components which should be implemented to achieve a circular economy design. The use of demountable connections plays a central role in this thesis as connections form a weak point in terms of strength and stiffness of the structure but are essential to modularity.

In Chapter 3 various methods are presented to determine which combination of load-bearing structure and upgradable or adaptable system could best be combined to maximise circularity, this was done first by means of a multi-criteria assessment and afterwards through an investigation of material use of structures in different configurations.

Taking the result from the previous chapter, Chapter 4 presents the complete structural design of the bridge; this consists of the deck, the support system, and the connections. Detailed finite element analysis of two variants of the longitudinal connections is performed to determine their suitability for the structure.

The life-cycle assessment for the structure is presented in Chapter 5, here a comparison is made between structures with and without implementation of circular design strategies to also demonstrate the benefits for sustainability.

Chapter 6 provides a brief discussion for the conclusions in each section and finally Chapters 7 and 8 contain the conclusions and recommendations regarding the investigation.

2. State of the Art

2.1 Concepts for Circular Economy bridges

2.1.1 Circular Economy Outline

Before discussing the different pilot projects and reviewing their strengths and shortcomings in the context of Circular Economy, I believe it is important to give a brief outline of Circular Economy as a concept to provide context to the analysis. Still in its infancy, the concept of Circular Economy has numerous definitions each differing slightly; the most commonly used definition is that of the Ellen MacArthur Foundation which reads:

"A circular economy is an industrial system that is restorative or regenerative by intention and design. It replaces the 'end-of-life' concept with restoration, shifts towards the use of renewable energy, eliminates the use of toxic chemicals, which impair reuse, and aims for the elimination of waste through the superior design of materials, products, systems, and, within this, business models." (Ellen MacArthur Foundation, 2013)

The Ellen MacArthur Foundation is a leader in the field of Circular Economy and collaborates with many prominent companies to bring about its establishment. In order to evaluate the aforementioned pilot projects however a concrete set of principles is required; the 9R-Framework (or waste hierarchy in more general terms), designing out waste, and building resilience through diversity are the most tangible Circular Economy principles which can be attributed to a product or system. The 9R-Framework (Figure 1) presents an extended version of the sustainability paradigm 'reduce, reuse, recycle'; first proposed by (Potting, Hanemaaijer, Delahaye, Ganzevles, Hokestra, & Lijzen, 2018)in a Dutch policy report entitled 'Circular Economy: Measuring Innovation in the Product Chain' it provides nine strategies in order of impact on circularity which can be used to achieve Circular Economy. This provides engineers with goals to strive for from the outset of a project which is when the greatest positive impact can be made. Designing out waste ties in closely with the 9R-Framework but with a greater focus on the end-of-life phase of products, this is of particular importance for civil and structural engineers as construction waste represents one third of total waste in the UK (WRAP, 2009) and 40% in The Netherlands (Vogels). This highlights a further point of motivation for the investigation in this thesis. The UK-based charity WRAP (Waste & Resources Action Programme) identifies the following strategies to design out waste:

- Design for reuse and recovery: this extends the effective life of materials and allows products, components or materials to be reused in new applications. If a structure is replacing an older one a site analysis should be performed in order to determine how much can be recovered and reused from the previous structure.
- Design for off-site construction (prefabrication): this involves producing as many and as large as possible elements of the construction in a factory.

- Design for materials optimisation: this involves simplifying the structure without compromising integrity, coordinating the design to minimise waste from cutting and joining, standardising the materials used to encourage reuse of offcuts, and creating repetitions in the design to promote reuse of components or manufacturing processes.
- Design for waste efficient procurement: considering work sequences, in collaboration with contractor(s) if possible, to identify and minimise sequences which produce waste.
- Design for deconstruction and flexibility: designing for multiple purposes within the lifespan, consider whether and how maintenance, upgrading, or replacement will produce waste, use of components which are reusable/recyclable, design for disassembly.

Adhering to these strategies will allow for the structure to improve its circularity performance in terms of waste reduction.

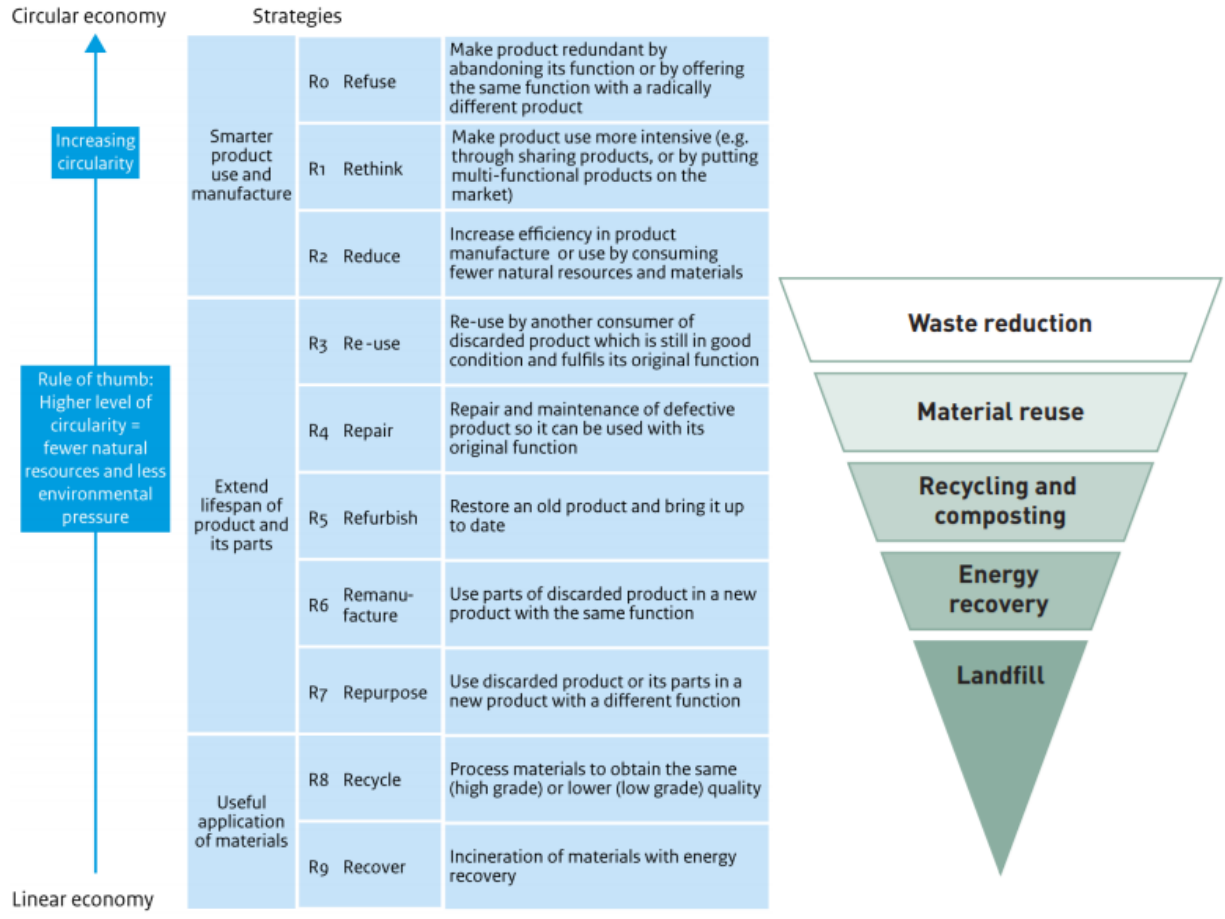

Figure 1: The 9R-Framework (Potting, Hanemaaijer, Delahaye, Ganzevles, Hokestra, & Lijzen, 2018) showing which actions should be prioritised (left) and the waste hierarchy presenting the same concept specifically for waste (WRAP, 2009) (right).

Finally, building resilience through diversity focuses on using strategies such as modularity, adaptability, and versatility of structures, and their components, in order to maximise their service life. Designing a structure in such a way that it can be reused requires insight into other potential functions and how these may change over time; the latter is particularly challenging as forecasts of transport are often erratic and require tailor made solutions to remain effective. The main strategies that can be used to achieve this are designing for disassembly and ensuring the structure incorporates upgradability in some regard; for example in the dimensions or the load-bearing capacity.

I believe this outlines the core aspects of Circular Economy and their relevance to structural engineering; by identifying both the tangible means of implementing circular engineering practices, and their merits, a better discussion of circular pilot projects is made possible.

2.1.2 Examples of circular bridges

Pedestrian bridge construction is a topic in which many structural engineers aim to innovate as the small scale and less stringent functional requirements allow for a greater freedom in design. In this section a number of pilot projects will be discussed which, through conscious circular/sustainable design practices or purely economic considerations, demonstrate successful implementation of the aforementioned Circular Economy strategies. Through this discussion of their strengths, but more importantly their shortcomings, opportunities for improvement can be identified and provide the knowledge gap which this thesis aims to address. Three examples will be presented to demonstrate the variety of possible approaches which exist, combining favourable aspects of each while mitigating the negative impacts will form the guidelines for an optimised circular structure.

Ultrabrug – Rotterdam, The Netherlands

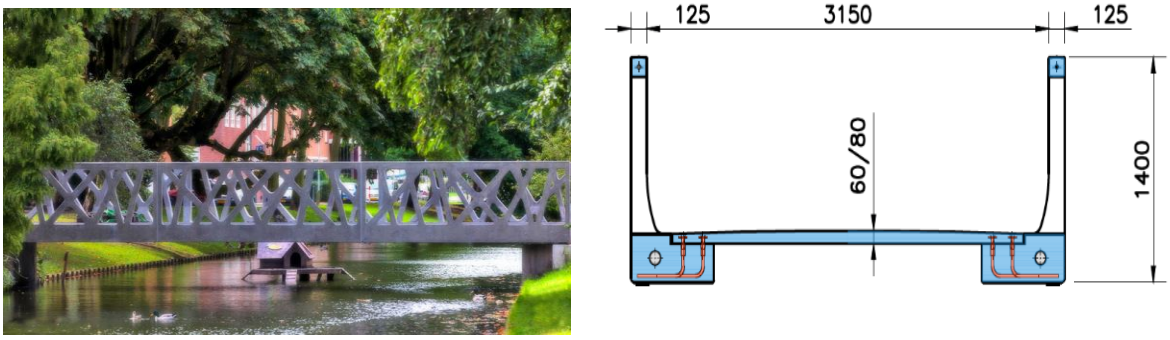

Figure 2: A picture of the Ultrabrige in use (left) and a cross-sectional view of the structure (right) (FDN Group)

The Ultrabrug, or Ultrabridge, produced by FDN Engineering is a pedestrian bridge produced from ultra-high performance concrete (UHPC) which allows for a very slender structure to be created with minimised material use. The bridge makes use of a prestressing system which consists of two sets of strands incorporated into the railing of the structure; a thin reinforced concrete deck is then place between the two railings which act as girders. The assembly is modular, consisting of deck and railing/girder elements, if a greater width is required the deck module can be replaced according to the new requirements while maintaining the same support system. The use of only two types of modules, railing and deck, facilitates reuse and offers possibilities for replacement in case of damage or

obsolescence. Disassembly of the deck takes place by means of a bolted connection shown in red on the right side of Figure 2. The structure makes use of segmental construction traditionally seen in prestressed concrete box girders used for traffic bridges, here the assembly is held together in transverse direction by the prestressing force and the bridge must be taken off-site in order to be modified, see Figure 3.

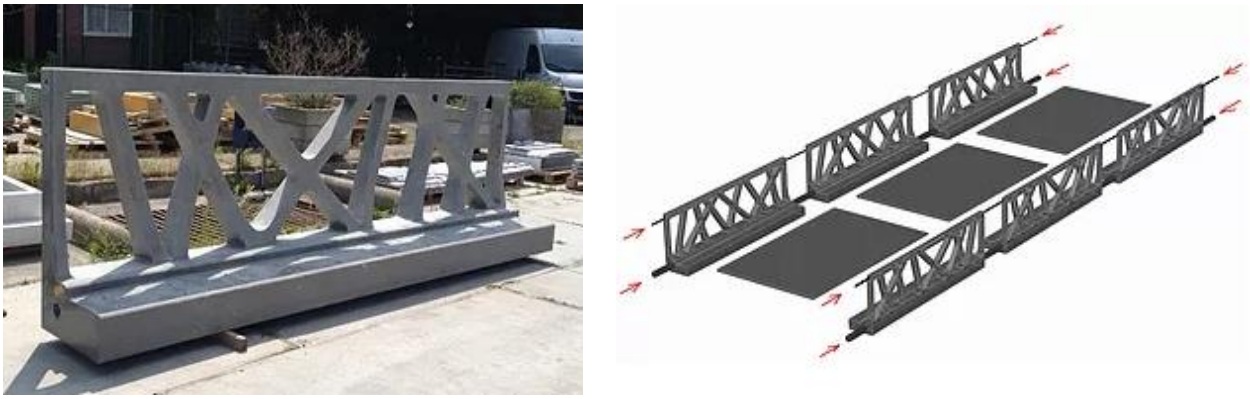

Figure 3: Railing module loose from the assembly (left) and an exploded view of the segmental assembly (right) (FDN Group)

The bridge can be produced in spans ranging between 6 and 25 metres (FDN Group), here the maximum span is determined by the maximum prestressing force to be taken by the girders/railings. UHPC has a chloride diffusion coefficient 100 times lower than traditional concrete (Tirimanna & Falbr, 2014) thus ensuring corrosion of reinforcement is significantly lowered; this improves both maintenance costs and maximum lifespan. Despite making efficient use of material and offering possibilities for adaptation, a number of issues and opportunities for improvement can be identified:

- Recycling of concrete is limited to down-cycling, the rubble can only be used for applications of lower value such as aggregate in new concrete or subgrade for road construction.
  → The use of a recyclable material would be preferable and create, at least in terms of raw materials, a closed loop of material recovery.
- Modifying the span and width requires destructive disassembly due to the grouting of the prestressing ducts (FDN Engineering), removing the prestressing tendon also nullifies structural integrity of the structure. Furthermore, (re-)jacking of the strands necessitates specialised equipment as well as access to the anchorage which is covered by the paving layer at the abutments.
  → The possibility to modify a structure on-site would reduce hindrance from construction work and transport to and from a factory, this could be achieved by means of an external support system and a load-carrying structure which maintains (a degree of) integrity during modification.
- The range of achievable spans is fairly limited and reduces the possibilities for reuse in different locations
  → A greater flexibility in the range of dimensions should be aimed for through the use of a more easily adaptable and robust load-bearing system.

Recycled plastic bridge – Peebleshire, Scotland

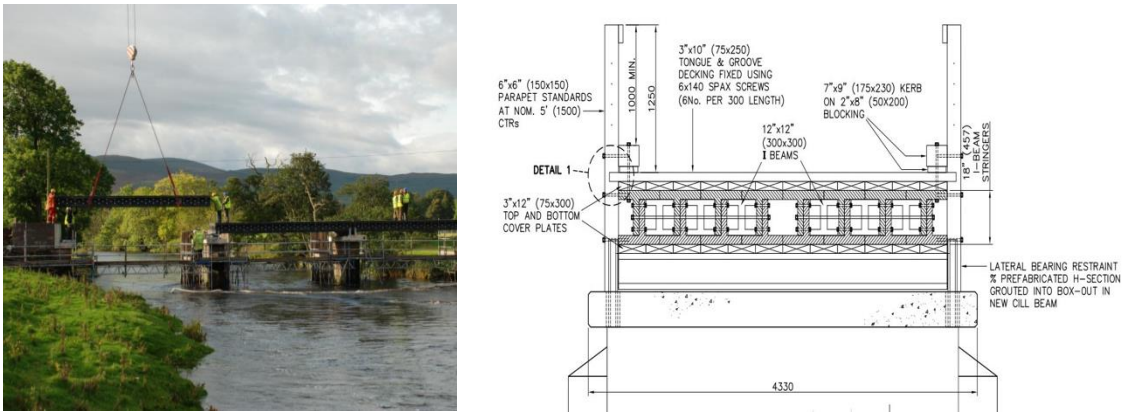

Figure 4: Assembly of the integrated deck girders of the bridge onto the supports (left) and a cross-section of the bridge (right) (Kim, 2011)

This structure, produced by Vertech, stands out for two main reasons; firstly, through the use of recycled waste material which is rarely up-cycled to a higher quality, and secondly due to the composite assembly of bolted I- and T-beams which make up the integrated deck girder. The structure makes use of two types of standard profiles which are repeated in both length and width directions, this greatly improves possibilities for reuse in a similar application or upgrading of the existing structure. The low density of the recycled thermoplastic also facilitates erection time and costs due to the lighter machinery which can be implemented. Finally, the structure makes extensive use of bolted connections to hold the structure together laterally meaning non-destructive disassembly is possible. Coupled with this there are negative aspects to be considered, such as:

- The stiffness of the plastic is approximately a factor 10 lower than that of timber products used in construction (Vertech) meaning that not only will extensive reinforcement be required to meet stiffness requirements but a greater number of intermediate supports must also be used; this will comprise large added costs and reduce the possibilities for passage below the bridge.
  → Stiffer but equally recyclable material alternatives such as steel and aluminium exist such that need for intermediate supports can be limited or altogether eliminated.
- The material is only available in a limited variety of standard cross-sections which limits freedom in design of both the structure and connections.
  → Choosing a material with a greater spectrum of available cross-sections increases the initial material and design costs but has greater potential to achieve a versatile structure which can adapt to different functions.

Modular steel bridges – Waagner-Biro and Janson Bridging

Figure 5: Waagner-Biro modular steel truss bridge (left) (Waagner-Biro, 2012) and temporary Janson bridging structure (De Waard, 2018)

Both Waagner-Biro and Janson Bridging make use of bolted steel assemblies to provide modular solutions for bridge construction. Trusses are used extensively in civil engineering due to their high strength-to-weight ratio; here material use has been limited greatly as the members are loaded in pure tension and compression. Furthermore, the truss structure uses square hollow sections (SHS) for the chords and H-girders for the braces which are both off-the-shelf cross-sections, extending the structure can therefore be achieved cost-effectively and without needing to wait for specially fabricated parts. The members are assembled by means of bolted gusset plates which make the structures demountable as well as allowing members to be changed as needed. Drawbacks to this assembly however are:

- While the span and width can be extended the maximum extent is limited by the resistance of the cross-sections used; increasing the height is not possible due to the fixed geometry of the gusset plates and fixed length of members. Alternatively the insufficiently strong members can be replaced by stronger ones while the existing ones are moved to where a lower capacity is admissible however this would require complex custom-made connections between members with different cross-sections thereby limiting the benefits of reuse.
  → While it is inevitable that increasing the required strength of structure creates a certain degree of obsolescence this should be mitigated as much as possible, particularly for elements optimised for a particular function.
- The chord members must be assembled from as great a length as possible to avoid splices else large forces must be taken by the gusset plates which have limited resistance, with these large continuous lengths the flexibility in span is reduced.
  → If a modular assembly is used a balance should be struck between flexibility, in terms of span, width, and/or load capacity, and the hindrance that the connections for this flexibility create for strength and stiffness of the structure.

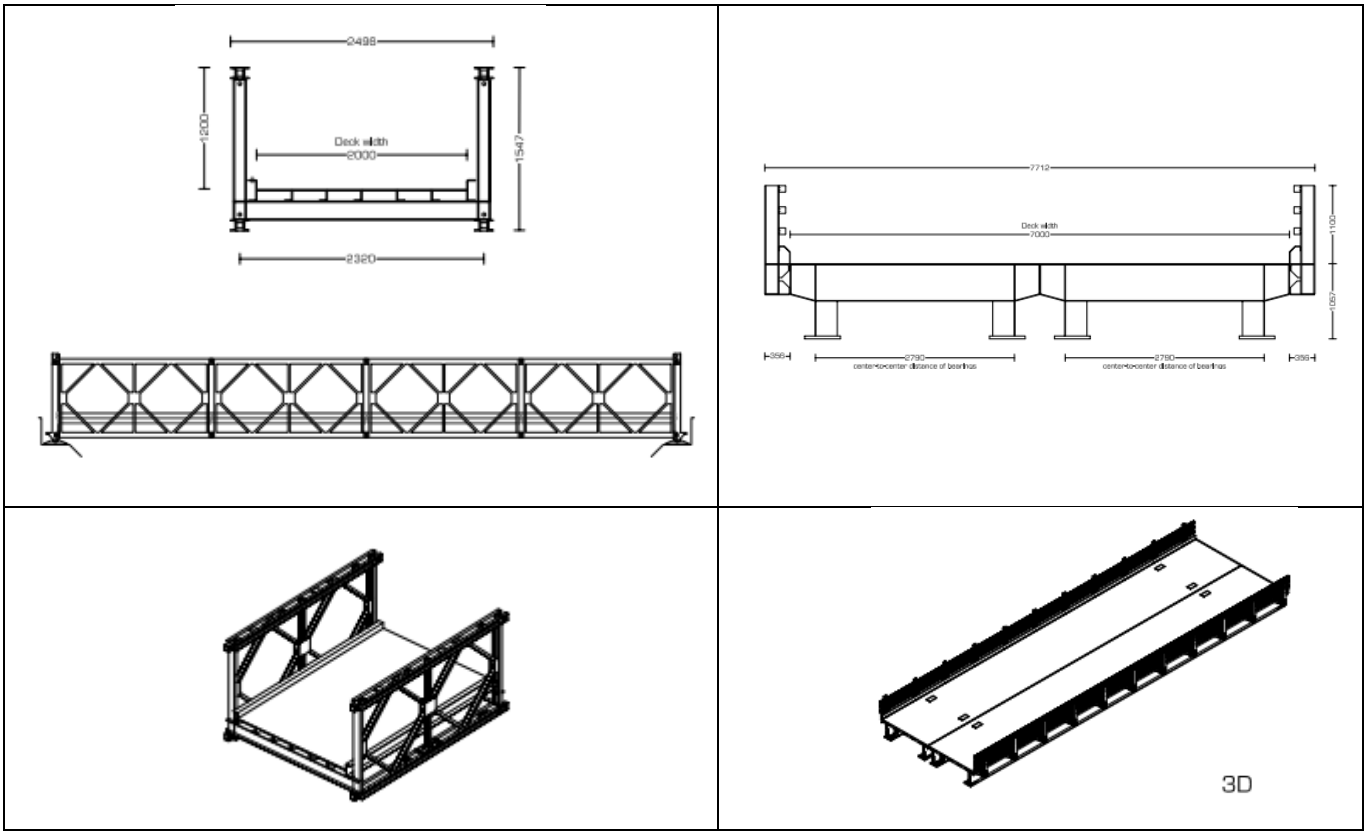

Figure 6: Figure 6: Janson Bridging modular girder bridges whose length (left pictures) and width (right pictures) can be extended by adding more identical modules (Janson Bridging, 2011)

The Janson bridging offer perhaps the most obvious representation of modular construction by creating an assembly made of building blocks; depending on the model these can be assembled in either transverse or longitudinal direction to meet the functional requirements. These structures are made from steel which provides high strength and stiffness and make use of bolts to form connections between modules which can fulfil a range of sizes in either span or width. Each structure is assembled from identical modules meaning costs can be minimised due to standardised production and assembly, furthermore these bridges are designed for temporary applications and can therefore be disassembled with relative ease. Aspects which offer opportunity for improvement for these structures are:

- The structure which extends in length is made up of identical modules regardless of the span, this means when using any other span than the allowable maximum, 33 metres, there is a significant portion of the material which is redundant.
  → Similarly to the truss bridge, a certain amount of redundancy is inevitable when designing for upgradability however the integration of all functions (deck, girders, railing) into a single module increases the degree of redundancy. Spreading functions across types of modules within an assembly may help reduce obsolescence.

- Steel requires coatings to be re-applied approximately every 25 years; this comes with increased costs and environmental impact (Hegger & de Graaf, 2013) as service life increases. When designing for reusability the need for coating and maintenance should be minimised.
  → The influence of the choice of material on the maintenance should be carefully considered from the outset and low maintenance or maintenance-free material should be favoured. Detailing of the connections should minimise entrapment of water and chlorides while facilitating inspection.
- While both structures are modular they can be extended in only one direction, span or width, which reduces the possible range of application if the structure is reused.
  → Designing a structure which can accommodate two degrees of flexibility by means of modular design and detailing would facilitate reuse and better contribute to circularity.

2.1.3 Identifying opportunities for circular design of bicycle and pedestrian bridges

Bicycle traffic in Amsterdam, specifically the number of bicycle journeys, has increased steadily over the last 20 years however projected growth numbers are uncertain; Amsterdam city council predicts two equally possible scenarios of 0% or 20% growth as shown in Figure 7.

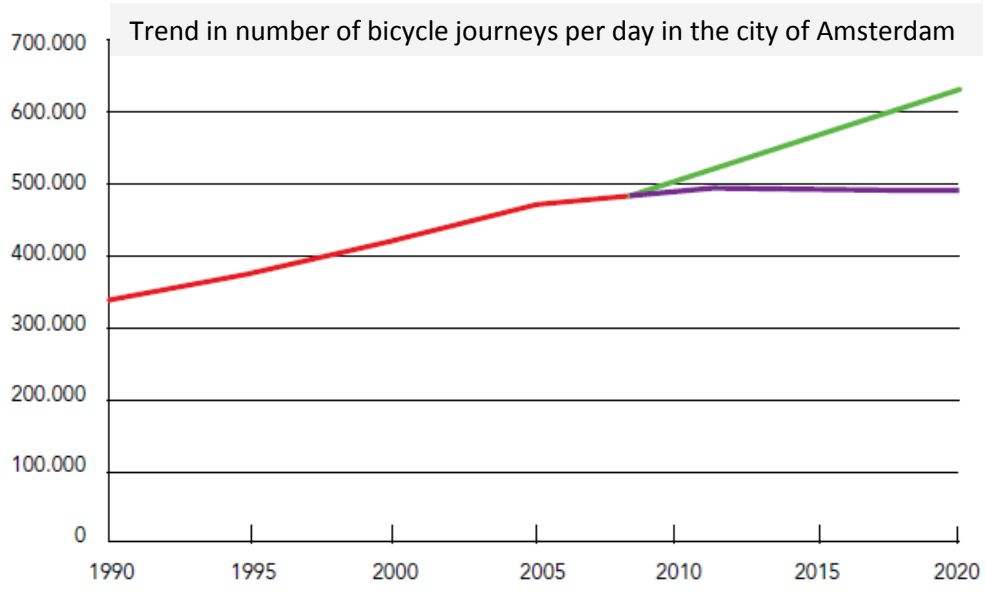

Figure 7: Number of bicycle journeys in Amsterdam (red) together with the predicted scenarios for continued growth (green) and plateauing (purple)

Next to the increase in bicycle traffic there have been a steady number of four wheel electric vehicles in The Netherlands over the past 10 years (CBS, 2018); these can reach speeds of over 45 km/h and pose a significant potential threat to normal bicycles. Together with the influx of new delivery vehicles in the city, shown in Figure 8, the nature of bicycle and pedestrian traffic may be on the verge of a drastic change. Allowing for additional space to accommodate mixed vehicle traffic, together with the uncertainty in future bicycle displacements offers opportunities for implementation of the upgradability and flexibility strategies present in Circular Economy.

Figure 8: New generation electric vehicles present in Amsterdam (De Telegraaf, 2017) (inStore, 2017)

2.2 Demountable Connections

In order to realise a structure suited for disassembly the elements must be connected by demountable connections; these are of great importance to the structure as they are often the weakest points within the assembly while contemporarily having a significant impact on the deformation due to the required tolerances. In this chapter two main groups of demountable connections will be described together with the opportunities they present for creating a demountable structure.

2.2.1 Bolted connections

2.2.1.1 Bearing bolted connections

Bolts create a connection between two or more plates by means of a fastener and a clamping package tightened with a nut along the screw thread. Bolted connections are applied in a variety of structures and have a great degree of flexibility; different bolted configurations can be used depending on the required characteristics. In practice however welded connections are often preferred for their greater strength and disassembly not being seen as a primary concern.

One application of bolted connections is to connect splices within a structure and extend it in the direction of the elements. The bolted connection can be used to form a connection between modules similar to the column splices in steel framed buildings, as shown in Figure 9, or as for the gusset plates in the truss girders mentioned previously. Spliced connections between girders use plates to increase the number of bolts which can fit in an assembly and can provide spacing to create a lever arm necessary to transfer bending moments. In Figure 9 two challenges of using beam splices for girders are shown; in the above portion of the figure the poor accessibility of the bolts can be seen, this makes such types of splices suited only to open cross-sections with sufficiently large spaces. The splice in the lower part of the figure shows an outstanding flange which is used to fix the bolts, while this does allow full access to the bolts the resistance will be significantly lowered due to the load being transferred in tension rather than shear.

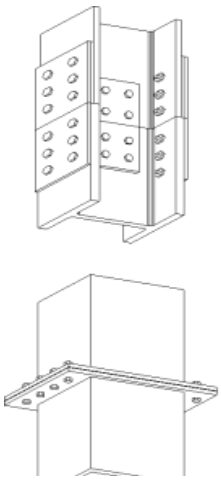

Figure 9: Bolted connection forming a column splice (SteelConstruction.info)

The capacity of bolted connections in steel is given EN 1993-1-8 depends first on the category of which there are five; here category A and B will discussed which are bolted connections loaded in shear with load transfer through bearing at ultimate limit state. Parameters influencing the resistance include the ultimate strength of the plate material, the bolt classes used (e.g. 5.6, 8.8), thicknesses of plates, diameters of bolts, edge and inner distances of bolts, types of holes, and the loads to be transferred (tensile, shear, or a combination of both). The governing resistance of a bolt is the lowest of the shear and bearing resistance and the total resistance of the joint is given by the sum of the governing resistances of each bolt in the group, this applies to bolted assemblies both steel and aluminium.

In order to demonstrate the feasibility of using bolted connections for beam splices in girder bridges an example has been taken from the Janson Bridging portfolio, a bolted beam splice connection from an assembly video has been matched to the corresponding bridge type. From this the girder dimensions have been determined and together with the loads on traffic bridges from EN 1991-2 an example calculation has been made.

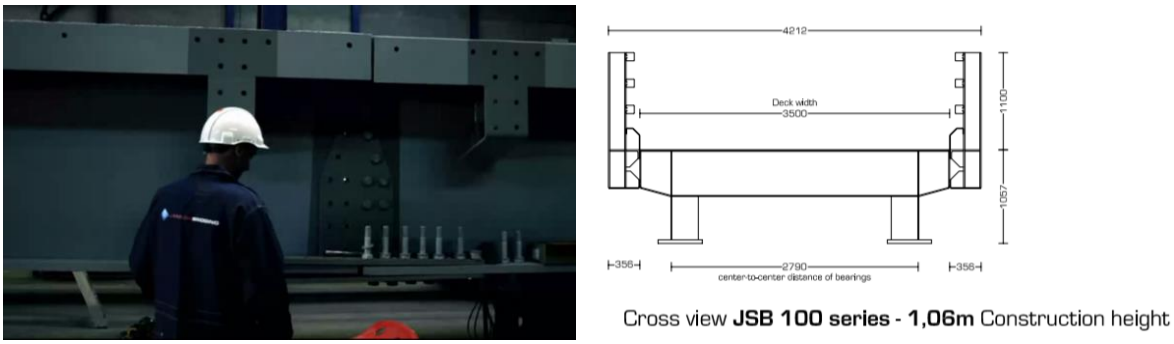

Figure 10: Beam splice used in Janson modular bridge (left) (Janson Bridging) and cross-section from the brochure of the corresponding type (right) which has been used to determine cross-section properties (Janson Bridging , 2011)

Each module is the same and must therefore be designed for the greatest possible traffic load, in accordance with EN 1991-2 the most heavily loaded traffic lanes must take:

- A distributed load of: $\alpha_{q1}q_{1k} = 1{,}0*9{,}0 = 9kN/m^2$
- A tandem system of two point loads each of: $\alpha_{Q1}Q_{1k} = 1{,}0*300 = 300\ kN$

The value of α is taken assuming 1st class/international heavy vehicle traffic which is the most unfavourable situation. The dimensions of the girder are derived from the drawings in the brochure together with the allowable deflection at serviceability limit state (SLS) of 3/1000*L.
This results in a design bending moment at mid-span of $M_{Ed} = 6766$ kNm, the full calculation is shown in Appendix A.

2.2.1.2 Slip-resistant bolted connections

The final category of bolts loaded in shear, category C, relies on a preloaded torque to be applied to the bolt such that at ULS the load transfer will occur only by means of friction between the faces of the clamping package. The application of such bolted connections originated in splices of wind turbines where considerable cost savings could be achieved by replacing the manufacturing and welding of the

bolts flange as well as offering greatly improved fatigue performance. Using a similar connection for column splice in buildings offers another advantage which is the possibility to pre-assemble the connection by using long, open slotted holes. The bolts can be placed in their holes at one end of the slice after which the open slotted connections can be slid into place and the bolts tightened from one side.

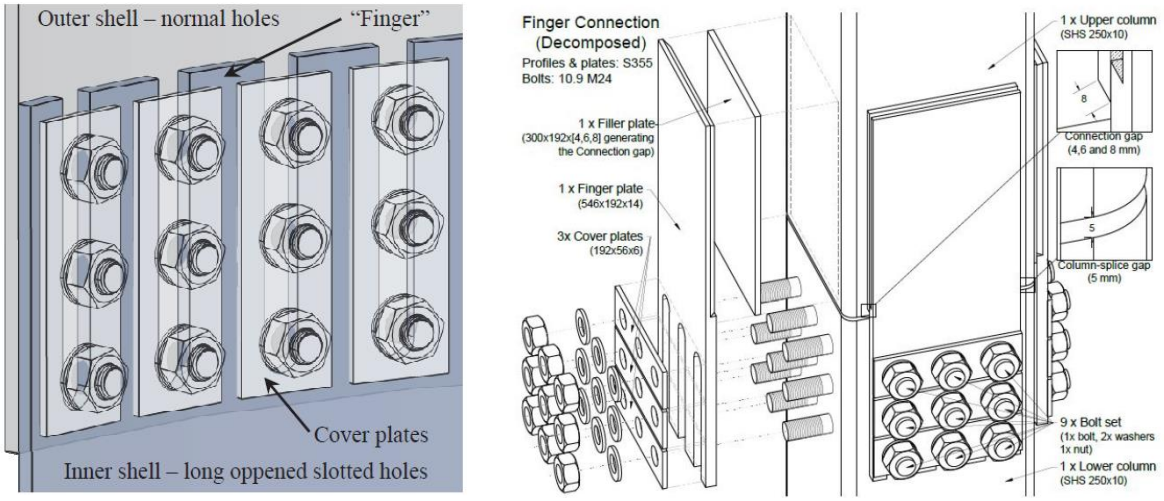

Figure 11: Friction connection for use in wind turbines (left) (Heistermann, 2014) and a column splice suitable for one-sided assemblies (right) (Piniarski, 2014)

The possibility to use connections accessible from only one side reduces the limitations set by accessibility requirements of normal bolted connections, this increases design flexibility through the use of closed sections such as box girders or hollow core sandwich panels. The feasibility of using such a connection in a structure depends mainly on the achievable resistance which will be lower than a normal bolted connection. Furthermore, it is important to note that this connection cannot be used by itself due to the poor shear resistance of the open slotted plates; therefore a different, shear-resistant, connection must be used in conjunction to ensure safety.

2.2.1.3 Bolted connections in aluminium

Although aluminium bolts exist their use is limited to small-scale, mechanical engineering applications, for this reason (stainless) steel bolts are most commonly used in in combination with aluminium for structural applications. However this creates the risk for galvanic corrosion in the connection, this occurs when metals with different electrode potentials are brought in contact. Introducing (salt) water creates a galvanic couple which will corrode the less noble of the two metals. The "Aluminium Structures" lecture handbook of the Eindhoven University of Technology recommends using steel bolts in combination with the following guidelines (Soetens, Maljaars, van Hove, & Pawiroredjo):

- Excessively high pressure on the surface of the aluminium when the fastener is tightened can be avoided by fitting hard aluminium washers under de head of the bolt and the nut.

- When bolts are frequently loosened and subsequently re-tightened, the thread in the aluminium component or on the bolt itself can quickly become worn. In such cases it is recommended to use inserts.
- For joints exposed to moisture the aluminium bolts should be sealed

2.2.1.4 Resin injected bolted connections

Resin injected bolts fill the tolerance gap left by the bolt between the bolt shank and the plates; this ensures that slip is minimised, or altogether eliminated, without the need to preload the bolt. The use of injected bolts is of particular value when the high resistance developed by bearing forces is needed but tolerances for fabrication or assembly require large gaps.

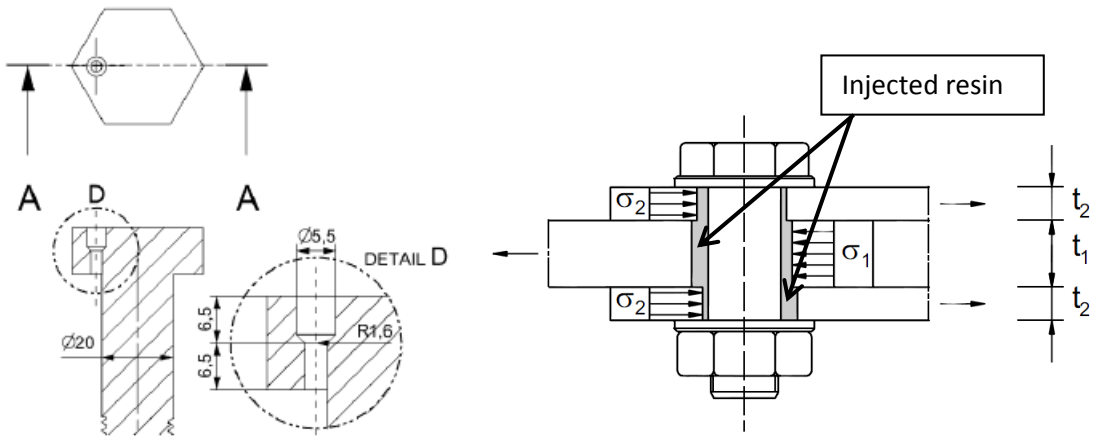

Figure 12: Diagram of an M20 bolt with channel for resin injection (left) (Nijgh, 2017) an bearing stresses being developed in a double lap joint due to the resin injection (right)

The resistance of such a joint is given by the smallest of the shear resistance of the bolt and the bearing resistance of the resin; the latter depends on the strength of the resin, the duration of the load, and the clearance of the holes. The strength of the resin varies on the type, composition, and execution of the injection; for example Araldite/RenGel SW 404 + HY 2404 which is commonly used in practice has a strength of 110 – 125 MPa (Inter-Composite) making it weaker than standard bearing.
Recent research performed at The Delft University of Technology (Nijgh, 2017) has also demonstrated the feasibility of disassembling injected bolted connections; several non-destructive (for the bolt and plates) methods are available to disassemble the connection and reuse its components. Wax-based release agents, silicon spray, and polyvinyl alcohol all allowed the bolt to be separated from the resin with little or no residue.

2.2.2 Plug-and-play connections

Within the scope of this thesis a plug-and-play (PAP) connection is defined as a set of interlocking parts which transfer load by means of friction between them, assembly of such a connection should take place only via a particular type of displacement and rely on no other on-site processes such as gluing, bolting, or welding. The aim of implementing such connections is increasing the speed of assembly, thereby reducing costs and hindrance, as well as facilitating disassembly such that reuse is incentivised through cost-effectiveness and mitigation of damage from the disassembly processes. The use of such connections in structures is starting to become more commonplace as the benefits are recognised, however research is on-going and both new types and resistance of existing types of PAP connections are being investigated. In this chapter, two main types of PAP connections will be discussed: slotted and wedged connections.

2.2.2.1 Slotted connections

Slotted joints describe a system in which a hole in a plate fits around a stud to form a fixed connection; this can be achieved by means of a displacement or a rotation. An example of a rotating connection is shown in Figure 13 where an S-shaped plated is rotated and then slides onto two studs. This type of slotted joint is less likely to be disconnected due to small displacements however it requires complete rotation of the module for assembly which may be difficult in practice. The displacement connection is shown in Figure 14 below.

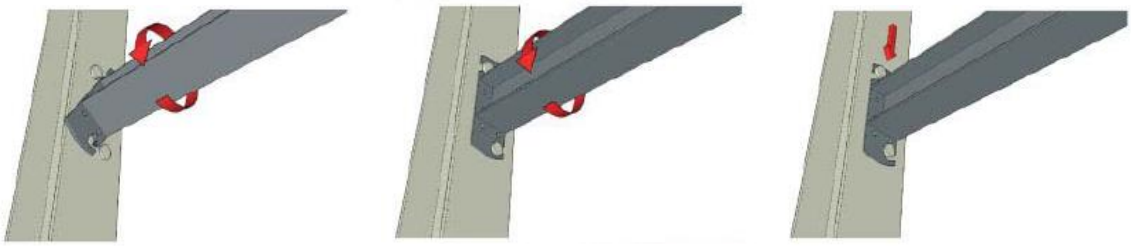

Figure 13: Slotted connection using an S-shaped end plate (Bijlaard, Girao Coelho, & Magalhaes, 2009)

Figure 14: Slotted connection assembled by displacement (Bijlaard, Girao Coelho, & Magalhaes, 2009)

Designing the mechanism to slide horizontally rather than vertically ensures that the connection will not be disassembled through deformation of the structure due to vertical loading which is most common in bridges. In both cases creating lighter modules is of particular interest as it facilitates the moving of modules to fit into the connection. The capacity of these connections depends on the type of loading, geometry, and dimensions of the studs and plates which determine the behaviour of the joint. As an

initial estimate the resistance of the connection can be assumed to be directly derived from the shear resistance and tensile resistance of headed steel studs.

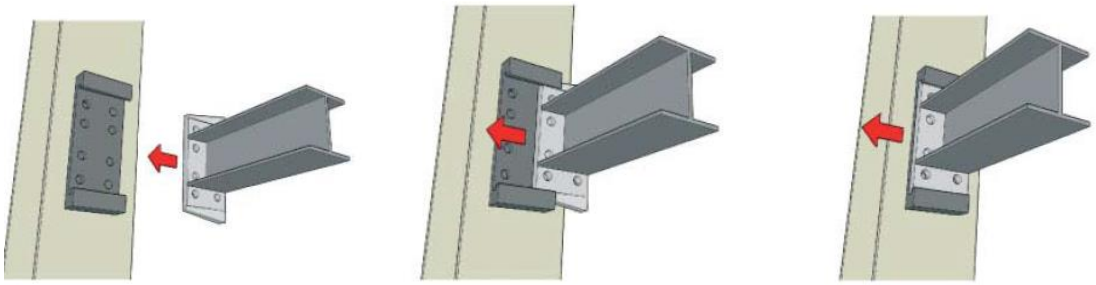

Figure 15: 'Concept 2' from (Bijlaard, Girao Coelho, & Magalhaes, 2009)

2.2.2.2 Wedged connections

A wedged connection in the scope of this thesis describes a male-female configuration in which a solid element slots into a gap made to fit it, this can be a plate or a more complex shape and is similar to dovetail joints used in wood joinery. One such concept has been put into practice by the American company

ConXtech in which rails slot into guided tracks thereby demonstrating the effectiveness of such a system even on a large scale. Research at Eindhoven University of Technology (TUE) has also been performed to determine the resistance of a wedged steel wedged joint together with the parameters influencing it. While both applications focus on buildings, specifically beam to column joints, applying this system to bridges could bring with it the same benefits of fast and labour-efficient assembly.

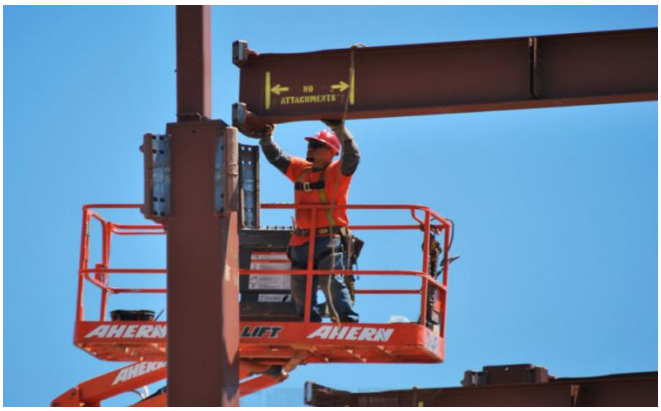

Figure 16: Large scale wedged connection assembly by ConXTech (ConXTech)

Behaviour of plug-and-play connections

As mentioned previously, a student of the Eindhoven University of Technology, Sergio Moriche-Quesada, investigated a PAP connection in steel; this produced information regarding strength, stiffness, and the effect of different configurations of the joint (shown in Figure 17) such as angle, depth, and length of the steel-to-steel dovetail connection.

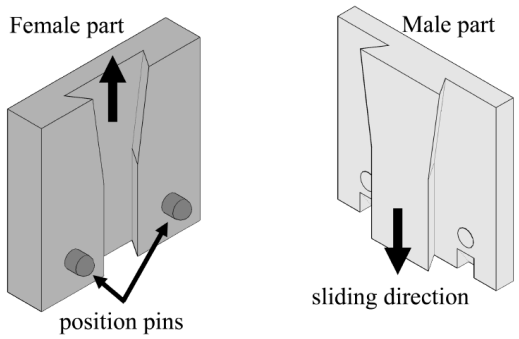

Figure 17: Plug-and-play (referred to as snap-fit) connection investigated by (Moriche Quesada, 2016)

Through his thesis Moriche-Quesada aims to establish and validate numerical (fine element) models for the behaviour of a particular design for a PAP joint. Three physical tests were set up in which a cantilevering HEA-profile applied a displacement-controlled force to create a moment – rotation graph for each case. Physical model Test A used the standard joint with no position pins which created moment-displacement diagram with zones that can be approximated as linear, plateauing, and plastic.

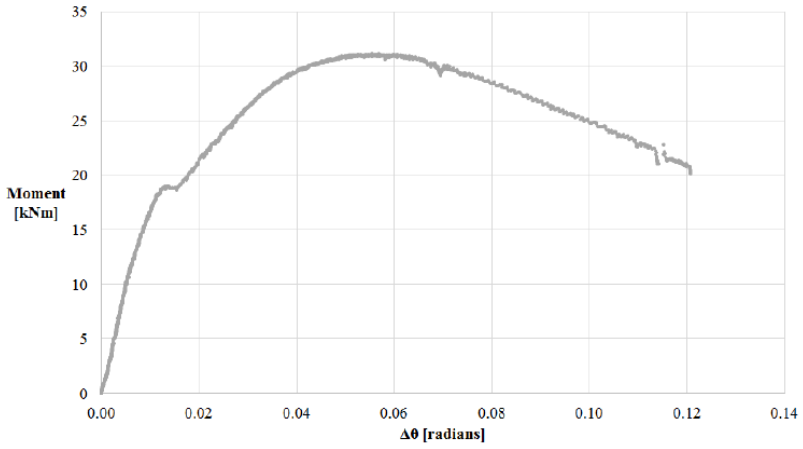

Figure 18: Physical model Test A moment-rotation diagram (Moriche Quesada, 2016)

The maximum capacity was of 30 kNm while the maximum rotation was of 0.12 rad. The presence of a yielding zone at 18kNm, similar to that present in steel coupon tests, is favourable for use in a structure as it demonstrates additional resistance and deformation capacity. Numerical verification of this setup was mostly unsuccessful due to the idealised situation of the numerical model which was unable to include the significant influence that small geometric imperfections had on the physical model.

In order to address the issue of uplift of the joint present in Test A the second physical test uses position pins on either side of the dovetail. This resulted in an increased capacity of the connection but caused brittle failure at 40 kNm. This is less favourable for direct implementation in practice as a brittle failure mechanism does not provide a warning of failure; the absence of a yielding zone could be resolved in the same way as for yielding of aluminium in which a proof value is used to ensure safety. Numerical

modelling until the point of fracture showed good agreement with the physical model and makes this configuration a viable candidate for practical implementation.

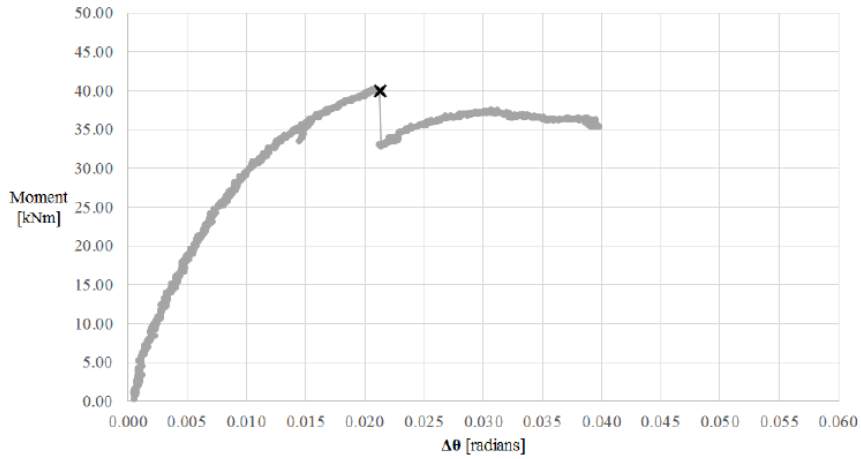

Figure 19: Physical model Test B moment-rotation diagram (Moriche Quesada, 2016)

Test C used a more squared geometry for the connection in order to reduce the stress concentrations at the corners of the dovetail and relying primarily on frictional contact to ensure resistance (see Figure 20 right). The resultant behaviour of the connection was much more ductile but with a lower capacity as the overlapping area of the male and female parts was significantly smaller than previous tests. The behaviour is again different to the previous two tests in that there no yield zone and no brittle failure point.

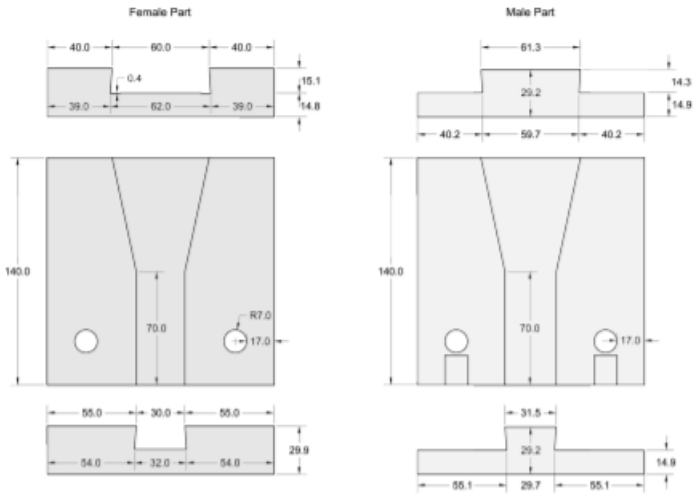

Figure 20: Geometry of the connection used in Test C (Moriche Quesada, 2016)

The final rotation of the joint was increased to 0.14 rad in this way while the capacity fell to 12 kNm. While the overall behaviour of the connection was supported through the numerical modelling the sensitivity to the frictional behaviour resulted in unstable results. The lower capacity and difficult to verify behaviour of this connection configuration make it less suited than the other two investigated.

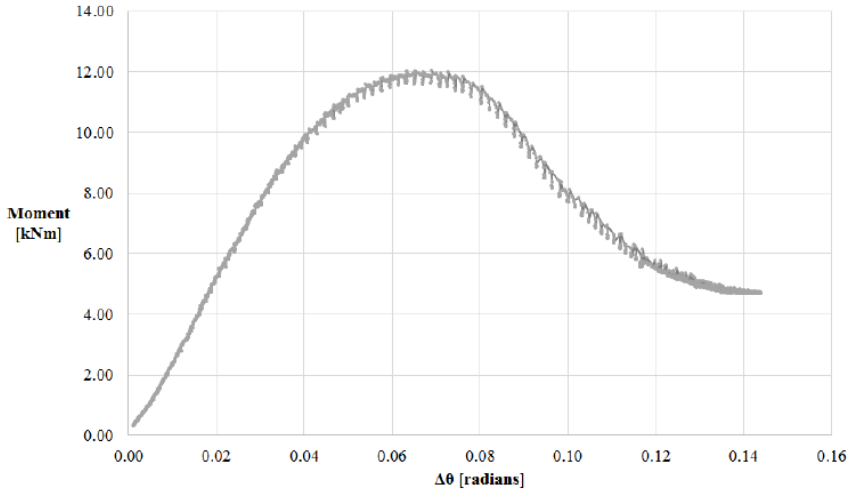

Figure 21: Physical model Test C moment-rotation diagram (Moriche Quesada, 2016)

Parametric studies performed showed that the most important aspects were the inclination of the dovetail, its thickness, and above all the gap between male and female parts; the larger this was the greater the capacity. Finally, an alternative configuration of the connection was proposed in which two, thinner connections were applied instead of one, wider one. This activates a larger amount of material in the connection during rotation which increased the moment capacity. A comparison with a traditional extended beam to column end-plate connection demonstrates that the same strength can be achieved with a higher rotation capacity.

Comparing this to the beam splice examples used for the other connections it can be seen that the resistance, taking 18kNm as a reference value, is significantly lower. However this resistance is for a connector of only 140mm x 140mm which due to the complexity of the connection cannot easily be scaled based on height or width. Using this system for a smaller, lower-capacity connection rather than a primary splice would allow for successful implementation despite the lower strength.

3. Choice of structural system

3.1 Development of Circular Economy bridge concepts

In order to determine the most suitable load-bearing structure for the bridge a brainstorm was created; here different types of bridge structures were combined with different strategies of upgradable design. The structure types include standard girders, integrated deck girders, and trusses while the upgradability strategies are using a building block approach, using telescopic elements, and using (un)folding components.

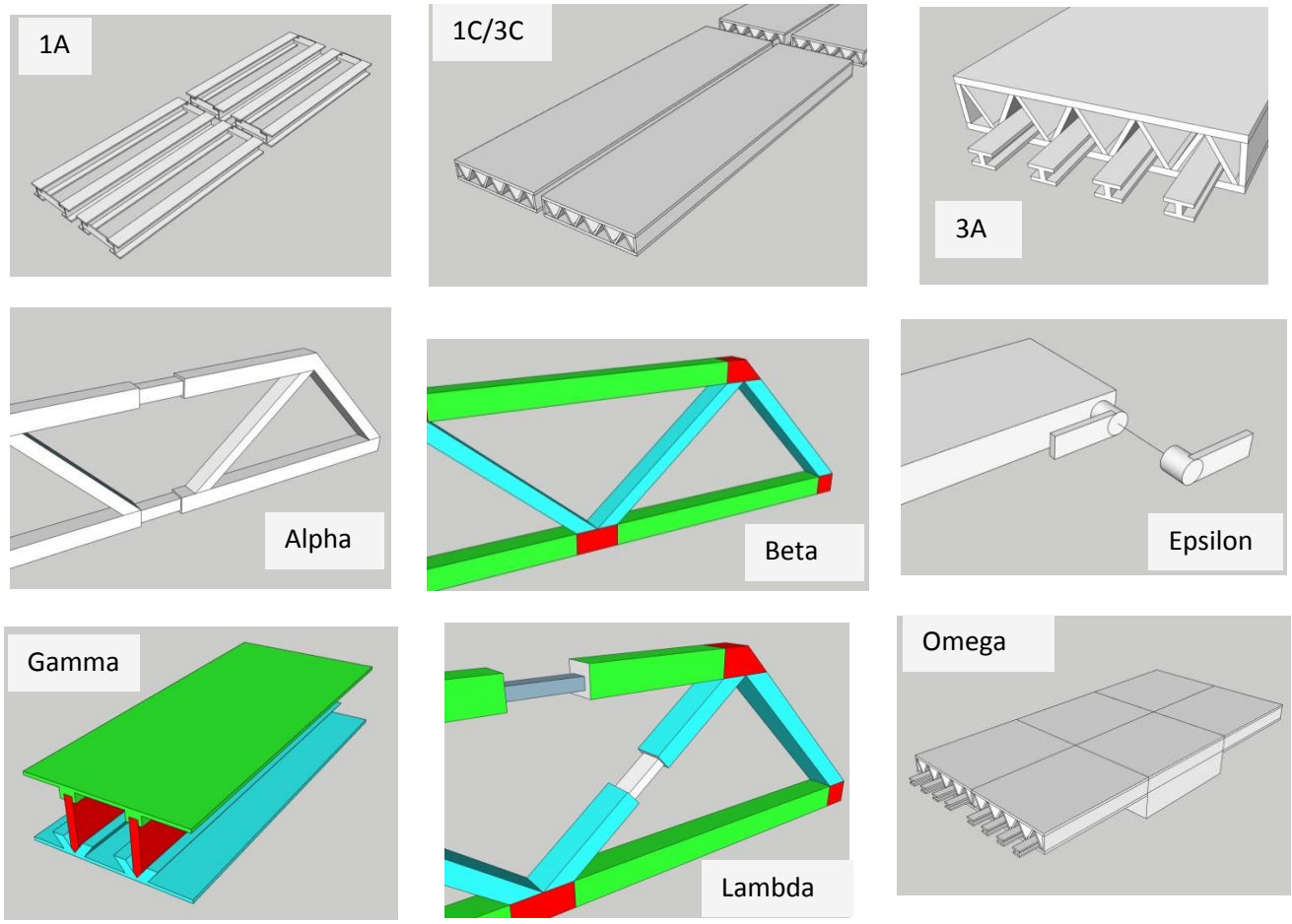

Figure 22: Circular economy bridge concepts

3.2 Design Criteria and Multi-Criteria Analysis

3.2.1 Design Criteria

The design criteria were set up in order to compare the various brainstorm alternatives; these are divided into the categories of: optimised material use, adaptability and upgradability, ease of maintenance and repair, disassembly and reusability, and miscellaneous sustainability aspects. The criteria were developed from the literature research into Circular Economy as well as collected research from variety of researchers as Mayyas et al. (2012), Fernandez (2001), and Smith and Babb (1973)). By evaluating each alternative against the established criteria an optimal solution can be found together with a clearer picture of which criteria are most significant to achieve a circular structure. While the evaluation of each alternative was performed as thoroughly as possible it was based on a preliminary structural design which led to inconclusive results in certain cases. Criteria which resulted in being inconsequential or difficult to grade were the use of higher strength materials and the ecological footprint of materials, this is due to the fact that all structures were conceived with steel in mind.

3.2.2 Qualitative Multi-Criteria Analysis

In this chapter a brief summary will be given of the qualitative multi-criteria analysis (MCA), the complete version can be found in Appendix C1. A traditional girder bridge is used as a '0 alternative' to provide an indication of the relative improvement each alternative offers.

Starting from the most basic options, Alternative 1A and 3A implement a building block approach to girder and integrated girder bridges respectively. Alternative 1A is the same structure proposed by Janson bridging which offers the greatest benefits in terms of simplicity and robustness, which can also be said of the fabrication and the assembly method; both aspects favour reuse and re-assembly by lowering costs of such operations. Less favourable are the degrees optimisation and flexibility which are hindered by the use of standard I- or H-sections which only come in stock dimensions, custom profiles are possible but would increase costs. Overall Alternative 1A is considered good as the constituent components can be re-used as a whole without significant modification. Alternative 3A offers the same basic concept but using integrated hollow core deck girders rather than standard profiles. These will be made specifically to meet the requirements and give a high degree of optimisation as well as offering a reduction in material use, furthermore there is no need to apply a deck meaning further material and weight savings can be achieved. The drawbacks are the high costs associated with producing custom cross-sections as well the difficulty of creating connections between hollow core panels without welding.

Alternatives 1C and 3C have been grouped together due to their similarity, for this structure girders extend telescopically from inside the central module to allow for the span to be adjusted. The main advantage of this system is the accuracy of increments which can be made as well as the speed and ease by which this can be done. By using only two modules however, the outer housing and inner extending profiles, there will be a higher degree of over-specification with redundant material use. Due to the limited possibilities for upgrading this alternative scores above average however the detailing will play a significant role in determining feasibility.

Alternative 2A (or BETA) represents the Waagner-Biro modular trusses with the difference that every node and module can be separated. The advantages of such a structure are the high degree of optimisation possible in each member as well the degree of upgradability through the possibility to replace any component according to changing needs. The main issue is the same as for the Waagner-Biro truss which is the limited resistance of connections. Furthermore issues during assembly due to tolerances and deformations associated with the required gaps are likely to occur. The feasibility of such a structure is again strongly dependent on the detailing should it be chosen to be investigated further.

Alternative 2C (or ALPHA) consists of a truss system in which the end chord members can extend telescopically, here fewer connections are used and similarly to 1C and 3C the adjustments can be made quickly and accurately. On the other hand increases in span are limited by the resistance of the central chord members which would rapidly become obsolete due to the increased load. Overall the structure is given an average rating as it does not offer significant advantages with respect to the added complexity.

Alternative Gamma combines Alternative 3A with an added degree of modularity which is the interchangeability of the webs in order to create a taller, and therefore stronger, cross-section. The main advantage is the very high degree of upgradability however creating demountable connections between flanges and webs would prove challenging in practice. Inspection, maintenance, and connections being inaccessible within the structure all contribute to making this alternative a poorer than average choice.

Alternative Epsilon is similar to 1C and 3C but uses (un)folding modules together with telescopic girders to adjust the span, in this way the extension can be retrofitted when the functional requirements change. The retrofitted modules allow for fast modification as they only affect the external structure but are limited in the added span and width they can provide, this system would also require many specially made components which increase cost and hinder reuse. Overall this option is poor in comparison to the other alternatives.

Alternative Omega combines the building block approach of 1A and 3A with the flexibility of 1C and 3C, placing the telescopic modules at the ends where the resistance is less critical provides a viable alternative. The challenge lies in finding several different demountable connections with sufficient strength and stiffness to meet the requirements as well as sensitivity to tolerances. If the feasibility can be demonstrated this alternative offers distinct advantages.

Finally, Alternative Lambda extends the concept of 2C to all members such that the span of the bridge and length of the truss members can be extended. This structure offers a high degree of freedom but is limited by the great number of connections required; these can create problems for the strength and robustness as well as having a complex assembly process. This alternative is mostly interesting from a theoretical standpoint as the costs and complexity of manufacturing would not be achievable in practice.

3.2.3 Second round Multi-Criteria Analysis

In order to support the points discussed in the qualitative analysis the same analysis is performed with weighting factors for the criteria, the criteria are given a score of 1 to 10 based on how important they

are for circularity, 10 being the best. This gives a more accurate representation of the suitability of structures with respect to one another as well as forcing a comparison of the different criteria which can help future design considerations. The most important criteria which were given weightings of 8 to 10 are: designing without over-specification, use of optimised cross-sections, range of span, width, and strength expandability, and ease of disassembly. These have the most influence on reduced material use and reusability.

The grades from the first MCA were converted to scores of 1 to 5 and multiplied by the weighting factors to give the final score, from this analysis the two best solutions were found to be Alternative Beta and Omega with scores of over 580 however these are closely followed by Alternatives 1A and 3A both at over 570 points. The other structures scored around 550 or below however the spread is not very large with none scoring far under 500, demonstrating the options studied all show favourable characteristics in some regard. The second MCA reinforced the conclusion that the chosen solutions are the most suited however it demonstrated the importance of creating a simple and strong structure. The complete results are shown in Appendix C2.

3.3 Material Use Analysis

The MCA proved unable to provide a single optimal solution due to the variety of criteria included and only preliminary development of design concepts. For this reason a different analysis was set up with a more limited set of parameters; in this analysis the key functionality criteria to be considered are span, width, and lifespan. Changing the span and width represents a significant change in function of the structure, here conventional civil engineering practices would dictate that the structure be replaced in its entirety. In order to favour a circular approach however the service life of the structure will be made indefinite, this makes changes in span and width adjustments rather than changes in function which represents an important strategy in designing for Circular Economy.

Quantifying circularity is one of its most challenging aspects and currently there is no recognised way of estimating how effective a product is (Ellen MacArthur Foundation, Granta Design, 2015); while the use of circularity indicators is cited as the best available approach this has proven insufficiently specific for this thesis. Referring back to the 9R-Framework it can be seen that the three most circular strategies are refuse, rethink, and reduce. In performing this research the strategies refuse, choosing to not apply standard civil engineering practices, and rethink, trying to develop new approaches to existing problems, are seen as an integral and implicit part of this thesis. For this reason the most circular strategy which can be implemented is to reduce the amount of material used, the weight of each structure over its service life will be used to determine how suitable it is for a Circular Economy and will be used as the governing criterion in this analysis. As the service life is increase the additional material required for modification becomes increasingly important as cumulatively more material is used over time. Choosing an indefinite service life means that rather than looking only at the net amount of material used, the percentage of reused material should be considered to better capture the impact over time. The importance of this cumulative material use and the service life to be considered is illustrated in Figure 23 below.

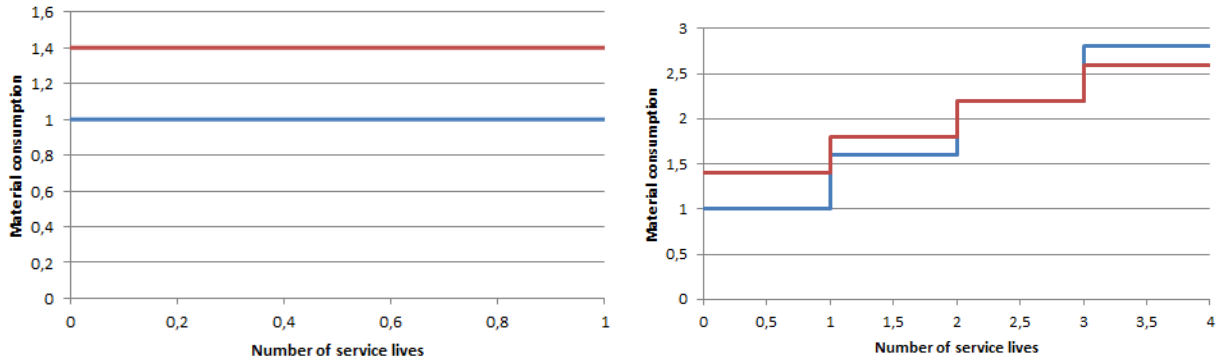

Figure 23: Influence of chosen service life and cumulative material use illustrated

As can be seen in Figure 23, when only one service life is considered the structure represented by the blue line is clearly favourable; this is representative of the standard engineering approach of single use structure with no in-built adaptability or redundancy. However taking into account more service lives the initially more material intensive alternative, shown in red, begins to close the gap as the amount of new material required per service life is lower. The final graph on the right shows that as the service life increases the lower the slope, i.e. the higher the rate of reuse, the more favourable the structure is in terms of total material use. Where the line of the heavier but more adaptable structure meets the line of the other can be considered a type of break-even-point (expressed in time) indicating the time scale which should be considered for small-scale infrastructural project. This gives an insight into how realistic implementation of these principles would be in practice as a very distant break-even-point would not be of interest to current policymakers.

In order to determine the changes in weight over the service life a number of scenarios are defined, these represent different potential functions which the structure is fulfilling. The scenarios chosen represent increases in either span or width, these are:

- 15m span and 5m width: increase span by 10m
- 25m span and 5m width: increase width by 2m
- 25m span and 5m width: increase span by 8m
- 33m span and 5m width: increase width by 2m

The spans were chosen based on 10m increments however 33m is given as the maximum span for steel girder bridges according to the Short Span Steel Bridge Alliance (Short Span Steel Bridge Alliance) which is why the final increment is reduced to 8m. The starting width of 5m is chosen based on the requirement for the highest bicycle traffic intensity (CROW, DTV Consultants, 2018) to provide as much buffer as possible for future increase. It is also possible that a structure will be reused where a shorter span or smaller width is necessary. It is chosen to exclude these scenarios from the analysis as the preceding structure can be reduced to the required size without needing further modification and maintaining the over-specification and capacity from its previous function. It is assumed each structure is assembled from sufficiently small elements such that all changes in dimensions can be made completely accurately. For example, if a longer member is needed only the difference in length is added

rather than complete replacement with a member of the newly required length as would likely occur in practice for convenience and strength reasons. Despite not being quantifiable and playing no further role in the analysis this assumption highlights the importance of designing for disassembly and the fact that certain structures are more suited to Circular Economy when practical considerations are taken into account. The structures are designed according to the functional requirements from the aforementioned scenarios with the ultimate limit state (ULS) for strength taken as governing. In the following paragraph the structural parameters for each alternative will be discussed in further detail.

3.3.1 Truss girders

The first structure analysed consisted of a deck supported by two steel warren trusses composed of steel square hollow sections (SHS). These were arranged in equilateral triangles such that the height of the truss was 2m based on a span of 25m, a favourable arrangement for a relatively short span truss bridge which allowed for lighter cross-sections to be used. The geometry of the trusses was maintained for every scenario such that reuse of members would not be constrained by lengths of available members. The trusses were connected by I-beams and SHS sections were used to support the deck, both of these were included in the analysis while the deck was not under the assumption a timber deck with little environmental impact could be applied. An overview of the structure is shown below. The loads applied were of 5kN/m^2, this was applied along the longitudinal members, and 3kN/m vertically on the top chord of the railings in accordance with the Dutch national annex of the Eurocode.

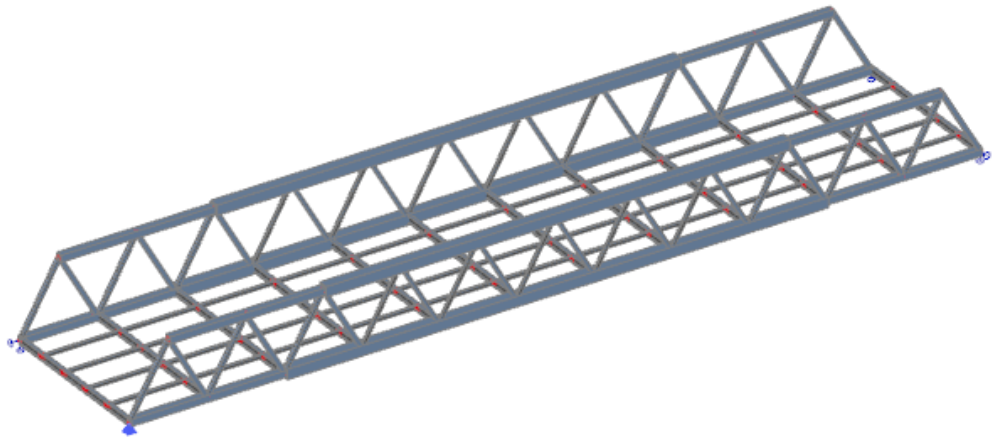

Figure 24: SHS truss used for the analysis

The governing check was the buckling of the top chord of the truss while for the integrated deck girder the bending stress was used for calculation. In order to allow for more balanced comparison the truss was considered to be assembled from easily demountable members (e.g. using gusset plates), in practice this would rarely be the case however this compares the structures from the same departure that all structures use demountable connections.

3.3.2 Adaptable integrated deck girder

The integrated deck girder consists of modules built up of two flanges connected by a web which can be substituted to increase construction height, between the webs are four open stiffeners spaced at

regular intervals as shown in the figure below. These modules are placed side-by-side and end-to-end as many times as is necessary to achieve the required dimensions of the structure. It is assumed the girder functions fully compositely even with the demountable connection between flanges and webs.

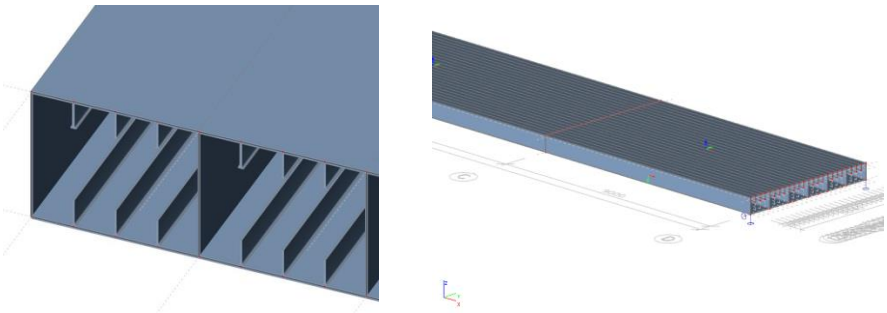

Figure 25: Integrated steel deck girder used for the analysis

The geometry of the deck was chosen such that local buckling did not need to be considered, i.e. all parts of the cross-section were Class 1 according to Eurocode 3 (EN1993-1-1), and the structure was designed based on bending stress. The deck is loaded with a distributed load of 5 kN/m^2 and 3 kN/m along the two longitudinal edges.

3.3.3 Tied arch bridge

The tied arch bridge structure is built up from an arch composed of straight sections where each configuration uses the same geometry where possible, this is the same way in which reuse for the truss was maximised in order to homogenise the analysis as much as possible. The arches are simply supported such that the outward horizontal forces are taken by the deck, again to ensure the support conditions are the same as for the other two structures investigated. The arches are connected by bracings at a height of approximately 3 metres to improve the out of plane buckling resistance which was governing in all cases. The deck was suspended from cables placed at the transitions in the arch segments to avoid bending moments within beams, the deck is further supported by cross-girders at regular intervals. The weight of the cables is not taken into account for the analysis.

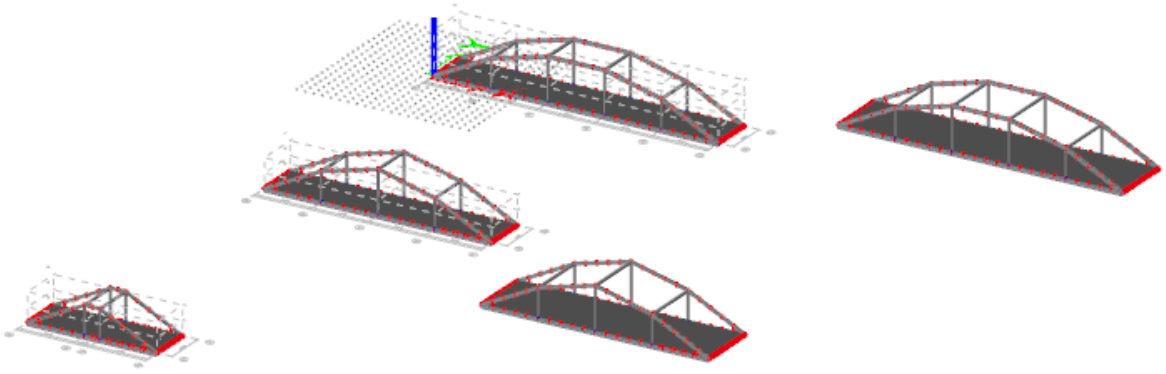

Figure 26: Tied arch bridges used in the weight analysis

The buckling resistance of the arches was determined according to Annex D of NEN-EN 1993-2 using the same distributed line and area loads as for the other two structures.

3.3.4 Results of material use analysis

The ratio of the weight of the structures was calculated as roughly 1:2:3 for the truss, girder, and arch structures respectively throughout the scenarios. This makes the tied arch structure the heaviest in every scenario, as the dimensions increased its weight relative to the other structures decreased. This confirms the expectation that the tied arch structure is most suited to long spans where greater material, and although not considered here also the cost of fabrication, is required. The main contribution to the weight for this structure came from the deck and cross-girders, this was however favourable for the reuse and these could be applied in other configurations effectively. This resulted in an average reuse per modification of 46% which is almost precisely halfway between the other two structures. Despite this, the initial material use of the structure is such that the break-even-point is extremely distant whereby the tied arch no longer becomes feasible. Reuse of the main structural components, the arches, was not possible as the structure was modified as each new configuration increased the buckling load significantly; this meant the previous cross-sections became obsolete.

The truss was lightest by several thousand kilograms in every scenario; this is not surprising as trusses see widespread use in civil engineering structures for their excellent strength-to-weight ratios and efficient use of material. The chosen spans also fit comfortably within the effective range for bridges made with truss girders, which is up to around 75 metres (Short Span Steel Bridge Alliance, 2012), such that light industry standard cross-sections could be implemented. The governing check was the buckling of the top chord; the required cross-sections gave the largest contribution to the weight and could not be reused in different configurations as the buckling load was exceeded. The trusses therefore had the lowest reuse percentage of the three alternatives with an average of 20% for the scenarios analysed. The possibility to accurately optimise the truss members for a particular configuration meant that the most commonly reused elements were the girders supporting the deck which were very light and only slightly contributed to reuse.

Finally, the adaptable girder was intermediate in terms of total weight but allowed for 64% to be reused on average for each configuration. Similarly to the truss structure the integrated girder was dimensioned based on the middle span of 25m while reducing the weight as much as possible. Comparing the truss and integrated girder bridges over time it can be seen that if the structure is modified around 4 times, depending on the type of modification made, the integrated girder reaches its break-even-point with the truss despite it being twice as heavy initially. Given the rapidly changing nature and demand for bicycle and pedestrian bridges, a structure which adapts easily but also effectively in terms of material use is valuable in the context of Circular Economy. The complete overview of the material use per structure is given in Appendix D.

3.4 Conclusions for choice of structural system and material use analysis

Performing a multi-criteria analysis on the various alternatives developed demonstrated the difficulty in assigning priority to the various strategies which can be implemented in Circular Economy design. When the analysis was refined to include only values assigned to each criterion the alternatives did not prove sufficiently distinguishable in large part due to the lack of detail which could be included in such an early stage of the design process. The difference in score between the best and worst alternatives came to less than 20% and between the best four of the nine alternatives investigated the scores varied only 3% which provides markedly inconclusive results.

The material use analysis served to set a clear distinction based on the amount of material used in each structure, this criterion is set as the top priority in the 9R-Framework for circularity. Reuse follows reduction in material use in priority therefore the material use spread across several reuse phases was set as the governing criterion for three types of traditional structures: girders, trusses, arches. The results were consistent with the expectations; as a single use structure trusses represent a light and material-efficient solution saving over 60% with respect to the next best structure which was the girder bridge. When the structures were modified to different dimensions however the truss was only able to reuse 20% of the material while the girder bridge achieved 65%. If the structure is designed for reuse and this takes place in practice an estimated three reuse phases are needed for the girder bridge to surpass the truss in terms of material use efficiency, therefore the girder is chosen as the main structural system for the bridge.

4. Structural Design

4.1 Development of the integrated deck girder

The adaptable integrated girder was therefore chosen for further investigation, the following step involved choosing the cross-section required for achieving a deformation below the allowable limit. For the allowable deformation the criterion according to NEN-EN 1990 was chosen which states that the maximum deflection at serviceability limit state (SLS) should not exceed L*3/1000, where L is the span of the bridge. Using cross-section similar to that of the girder in the material use analysis a construction height of 800mm was necessary to meet this requirement and the weight of the structure rose to almost 70.000kg which represents an unacceptable increase in material use.

In order to address the issues of deflection and a lack of adaptability, a structure combining the integrated deck girder with external prestressing tendons was investigated. This structure uses an integrated girder deck in which post-tensioned elements provide the added resistance against deformation. This approach is commonly used in concrete girders where imposed loads are large and tensile stresses must be mitigated, however the benefits for applications in other materials are being increasingly investigated, as is shown in the figure below.

Figure 27: Timber beam with external prestressing tendons (Miljanović & Zlatar, 2015)

Two alternative configurations of this concept were investigated; a tendon with a single kink in the centre, and a tendon with two kinks at even distances from the supports. The former provides support where the deflection is greatest while the latter creates a wider angle of the kink thus increasing the upward vertical component of the prestressing force. For the remainder of this chapter these alternatives will be referred to as I (single kink) and II (two evenly spaced kinks), schematic drawings of both are given below.

Alternative I:

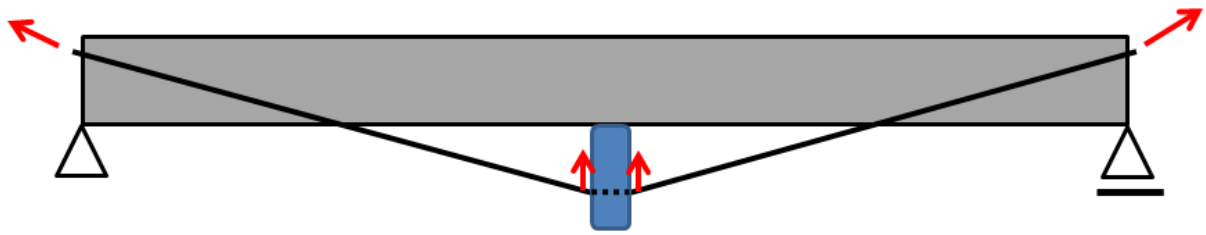

Alternative II:

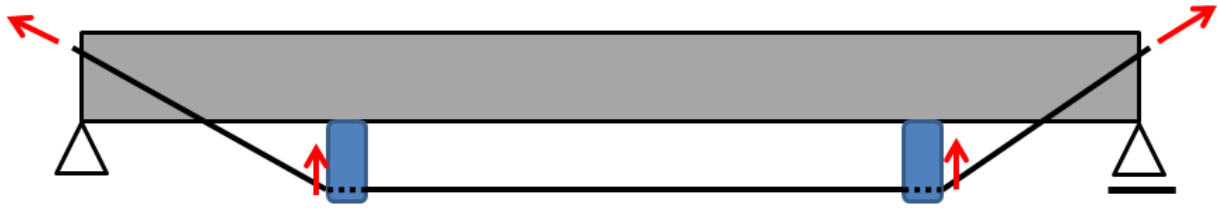

Figure 28: Schematic drawings of Alternatives I and II

4.1.1 Deflection calculation

As the governing criterion it is necessary to calculate the deflection for both alternatives, this was done through the following steps:

1. The vertical force (upward) from the tendon onto the beam
   For alternative I:

   $$\tan(\alpha) = \frac{dz}{dx} = \frac{f + w_{mid}}{l/2}$$

   $$V = H \cdot \tan(\alpha)$$

   From the equilibrium of the strut and the tendon system it follows:

   $$F_{tendon,I} = 2V + 2F$$

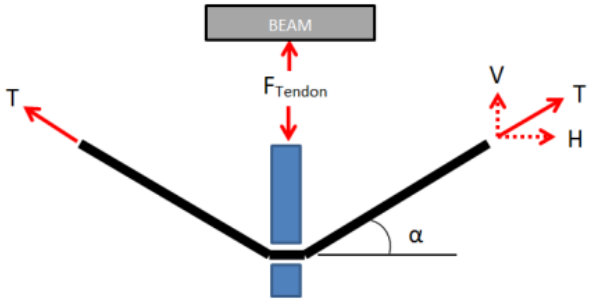

Figure 29: Free body diagram of the prestressing system for Alternative I

   For alternative II:

   $$\tan(\alpha) = \frac{dz}{dx} = \frac{f + w(a)}{a}$$

   $$V = H \cdot \tan(\alpha)$$

   $$F_{tendon,II} = V + F$$

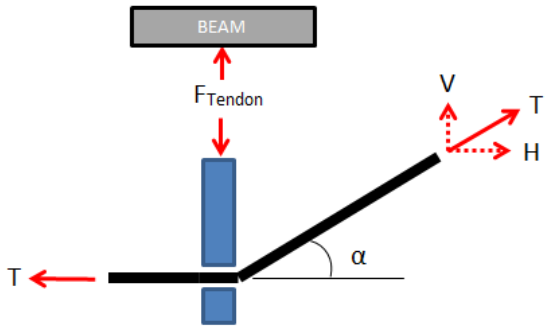

Figure 30: Free body diagram of the prestressing system for Alternative II

   The vertical force due to elongation of the tendon is:

   $$\Delta l = \sqrt{a^2 + (f + w(a))^2} - \sqrt{a^2 + f^2}$$

   $$\varepsilon = \Delta l \Big/ \sqrt{a^2 + f^2}$$

   $$F = E_{tendon} \cdot A_{tendon} \cdot \varepsilon \cdot \sin(\alpha)$$

   In which:
   f is the vertical distance the tendon spans
   w_{mid} is the downward displacement of the system (beam and strut) at mid span
   l is the length of the beam
   T is the tensile force in one tendon

V and H are the vertical and horizontal components respectively
α is the angle the tendon forms with the horizontal axis
a is the distance of the kink from the support
w(a) is deflection of the system at the kink (x = a)

2. The anchoring force at the ends also creates a bending moment due to its eccentricity from the geometric neutral axis (NA) of the beam(s). For one tendon this the moment due to eccentricity is given by:

$$M_{ecc} = H \cdot e_0$$

In which:
e_0 is the eccentricity of the tendon from the NA, downward is positive and creates a constant negative bending moment resulting in an upward deflection

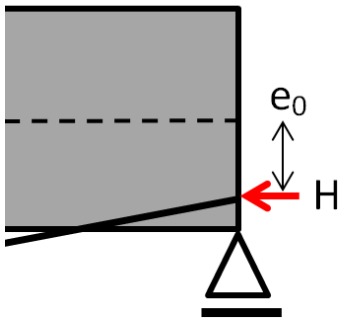

Figure 31: Moment at the support due to eccentricity (e_0) of the anchorage

3. The deflection of structure is derived from the basic cases for a simply supported beam:
For alternative I:

$$w_{mid} = \frac{5}{384}\frac{q \cdot l^4}{EI} - \frac{1}{48}\frac{F_{tendon,I} \cdot l^3}{EI} - \frac{1}{8}\frac{M_{ecc} \cdot l^2}{EI}$$

For alternative II, at point x = a:

$$w(a) = \frac{1}{24}\frac{q \cdot a^4}{EI}(l^3 - 2l \cdot a^2 + a^3) - \frac{1}{6}\frac{F_{tendon,II} \cdot a}{EI}(3la - 3a^2 + a^2) - \frac{1}{8}\frac{M_{ecc} \cdot l^2}{EI}$$

The calculated deflections were then used to calculate the new angle α which subsequently influenced the deflection; this iterative process was repeated until the deflections converged to within 5% of one another. The calculations were set up in Maple, this allowed for the contribution of the bending moment from the deformation of the structure with respect to the axial load to be accounted for; the fourth order differential equation for Euler-Bernoulli beams was used to calculate deflection, rotation, moment, and shear force. The main calculation steps are shown below.

Definition of the fourth order DE's

The beam was split into three fields each with its own fourth order ordinary differential equation and solutions with four unknowns, given by the constants C1 through C12. The beam was split at the position of the kinks (distance 'a' from each end) and the same uniform distributed load was applied on each segment.

$$ODE1 := EI\left(\frac{d^4}{dx^4} w1(x)\right) = q \qquad w1 := \frac{q\,x^4}{24\,EI} + \frac{\_C9\,x^3}{6} + \frac{\_C10\,x^2}{2} + \_C11\,x + \_C12$$

$$ODE2 := EI\left(\frac{d^4}{dx^4} w2(x)\right) = q \qquad w2 := \frac{q\,x^4}{24\,EI} + \frac{\_C5\,x^3}{6} + \frac{\_C6\,x^2}{2} + \_C7\,x + \_C8$$

$$ODE3 := EI\left(\frac{d^4}{dx^4} w3(x)\right) = q \qquad w3 := \frac{q\,x^4}{24\,EI} + \frac{\_C1\,x^3}{6} + \frac{\_C2\,x^2}{2} + \_C3\,x + \_C4$$

To solve these unknowns 12 conditions were set; 4 boundary conditions (BC's) and 8 matching conditions (MC's) at the ends and between beams respectively.

$$x := 0 : eq1 := w1 = 0 : eq2 := M1 = 0 :$$
$$x := a : eq3 := w1 = w2 : eq4 := phi1 = phi2 : eq5 := M1 = M2 : eq6 := V1 - V2 + F = 0 :$$
$$x := a + b : eq7 := w2 = w3 : eq8 := phi2 = phi3 : eq9 := M2 = M3 : eq10 := V2 - V3 + F = 0 :$$
$$x := a + b + a : eq11 := w3 = 0 : eq12 := M3 = 0 :$$

From this the deflection of the beam along the length could be plotted, the same can be done for rotation, bending moment, or shear force.

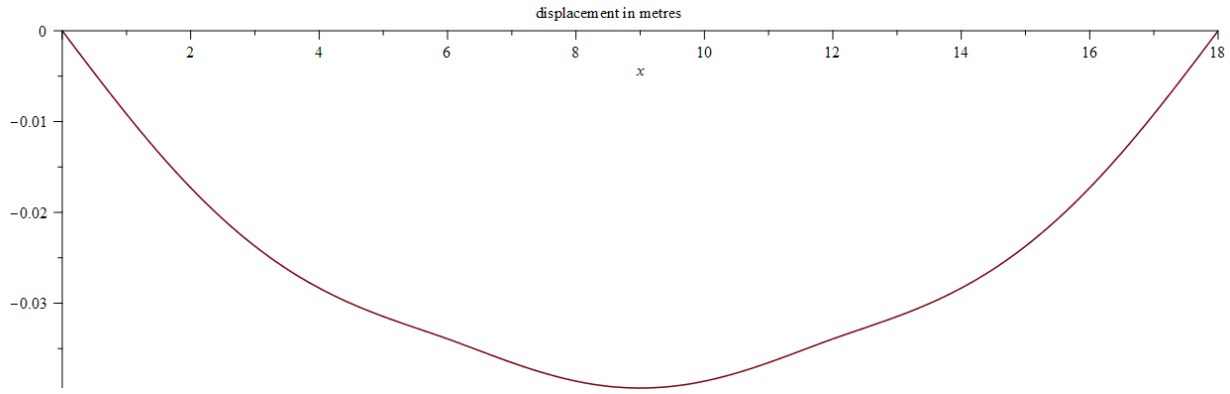

Figure 32: Deflection of the girder in metres along the length

These calculations were performed parametrically in order to set up a functioning sheet to be used in the testing of the two configurations. It should be noted that the moment due to eccentricity was set to zero for each calculation to facilitate detailing later in the design process, eccentricity of the normal force with respect to the neutral axis of the cross-section would lead to complex stress distributions in the girder which it is easiest to avoid from the offset.

4.1.1 Choice of material

A number of standard construction materials were considered for the girder, their respective benefits and disadvantages are collected in Table 1 below. The aspects are considered within the framework of a demountable, reusable, and recyclable girder bridge.

Table 1: Advantages and disadvantages of different construction materials

Construction material	Advantages	Disadvantages
Concrete	- Low initial costs - Low maintenance - High strength and stiffness	- High self-weight hinders reuse - Grouted connections prevent (easy) disassembly - Poor recycling possibilities
Carbon steel	- Low initial costs - Large variety of available grades and manufactured products - High strength and stiffness	- Requires regular maintenance which increases costs and environmental impact
Stainless steel	- Large variety of available grades and manufactured products - High strength and stiffness - Maintenance free	- High initial costs - High environmental impact
Weathering steel	- Moderate/low initial costs - Large variety of available grades and manufactured products - High strength and stiffness - Maintenance free	- High sensitivity to corrosion from chloride intrusion (de-icing salt) - Sensitive to corrosion near welds - Long-term resistance to moisture is uncertain
Aluminium alloy	- Freedom in design of cross-sections / elements - Low self-weight - Maintenance free - Extrusion allows serial production of elements	- High initial costs - Low stiffness - High environmental impact
Timber	- Minimal environmental impact	- Short service life / degrades quickly, cannot be reused - Low strength and stiffness - Limited options for connections
Fibre Reinforced Polymer (FRP)	- High strength and stiffness - Maintenance free -Large freedom in (initial) design	- Moderate/high initial costs - High environmental impact - Sensitive to damage / difficult to repair - Poor recycling possibilities

Based on the considerations in the above table the most favourable options are: carbon steel, stainless steel, and aluminium alloy. These materials offer freedom in manufacturing possibilities as well favouring reuse and long-lasting design practices. Concrete was eliminated due to the self-weight and demountability of connections and weathering steel due to the limitations for welding. Timber limits the range of possible applications due to its low strength and FRP lacks options for repair or modification, therefore these materials are also not analysed further.

Given the significant and continuous environmental impact of coating carbon steel (Hegger & de Graaf, 2013) this option is seen as the least favourable of the first three choices as reuse will lead to a larger cumulative impact. When comparing stainless steel and aluminium alloy the main differences are the respective stiffness and freedom in design; given the need to create custom shapes in order for the

wedged connection to be manufactured, and the fact that the majority of the stiffness is provided by the support structure, aluminium alloy is chosen for the girder(s). Furthermore, it is expected that the lower self-weight of aluminium favours ease of assembly and environmental impact of transport.

4.1.2 Dimensioning of the cross-section of modules

The structure must be adaptable and therefore be built up from modules in both length and width direction. In accordance with my company supervisor it was chosen to set 12 metres as the minimum span, this is a common length for bicycle and pedestrian bridges and will serve as the point of departure for the module sizes. This 12m span must also be constructed such that if the width or load are increased the capacity can be upgraded to match, for this reason the 12m span must be further sub-divided to allow the prestressing system to be applied. For both alternatives the spans are of 6m which will be governing module used for the design, a simply supported span of 6m designed to meet the deflection requirement of L*3/1000 was used to determine the minimum cross-section. This process has the added benefit of starting out with a light, optimised module for which strength becomes governing as the span increases. This imposes a natural limit on the maximum span rather than choosing an arbitrary value as the requirement, this approach is taken due to the lack of fixed requirements.

For the girder it is chosen to use a cross-section consisting of a top and bottom flange connected by a truss-shaped core. This cross-section offers high torsional stability and resistance to local loads due to the core's geometry as well as high strength in longitudinal direction provided by the continuous flanges. This cross-section is also well suited to the extrusion manufacturing process which offers a high degree of standardisation and repetition within the structure. An example of a similar cross-section is shown in Figure 33, the cross-section used will be built up from modules 1m wide.

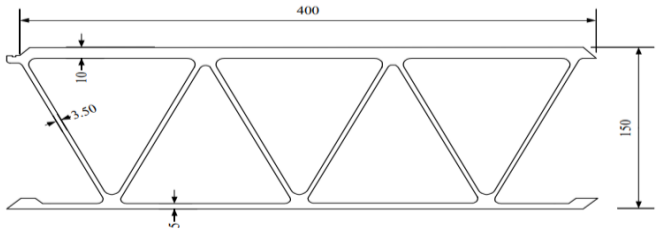

Figure 33: Example of a truss core aluminium cross-section used for a traffic bridge (Soetens, Maljaars, van Hove, & Pawiroredjo)

Minimum dimensions of the cross-section were be determined based on simplified local verifications using a service vehicle from NEN-EN 1991-2. The configuration of service vehicle load model is shown below.

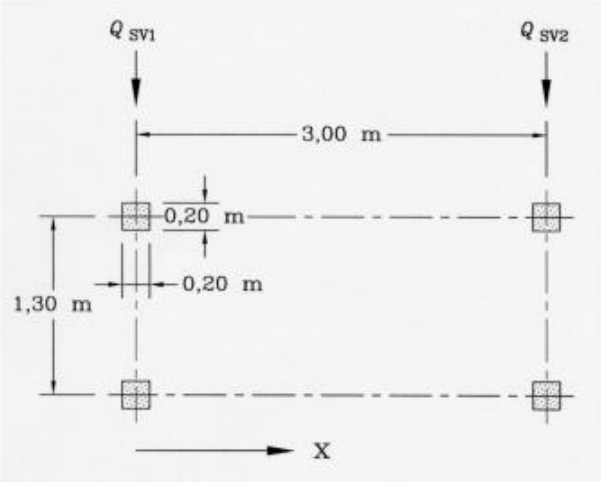

Key
x : Bridge axis direction
Q_{sv1} = 80 kN
Q_{sv2} = 40 kN

Figure 34: Service vehicle load model from NEN-EN 1991-2 (NEN, 2003)

A wheel load of 40kN (80kN axle load on two wheels) over an area of 0,2m*0,2m was used to determine the thickness of both the flanges and the webs. The distance between two contact points between web and flange was set to maximum 200mm such that the load will always rest on at least two webs. The corresponding internal height of the cross-section is set to 180mm such that the geometry of the triangles in the truss core is approximately equilateral. To perform a conservative initial hand calculation the load from one wheel from the axle is placed on the inclined webs which are modelled as pinned columns and the flange was modelled as a beam clamped at both ends. The calculations and schematisations of the girder are shown below.

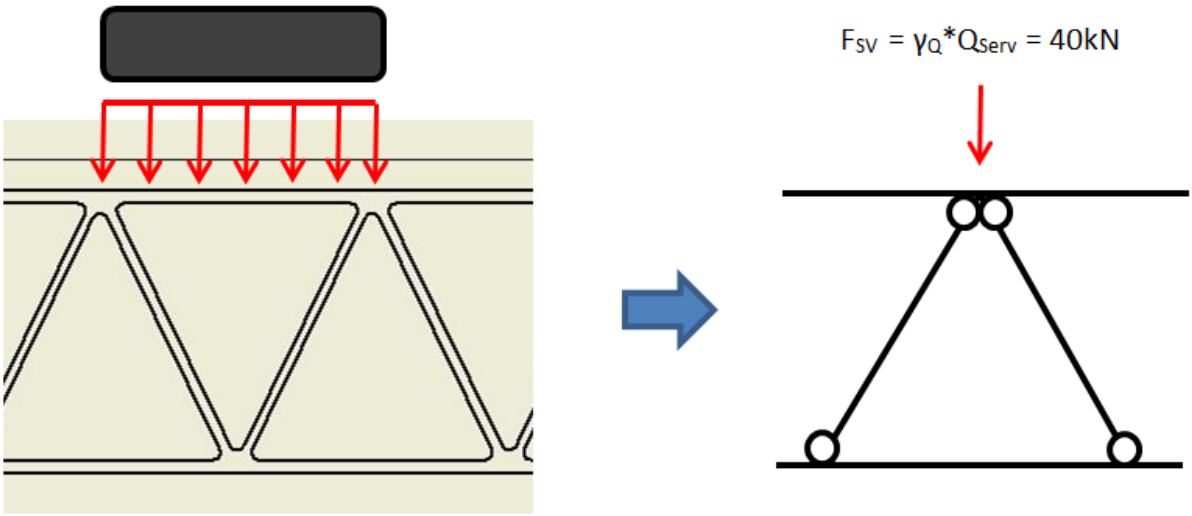

Figure 35: Schematic loading from the service vehicle on the girder

Buckling resistance of the webs

Euler buckling load: $N_{Euler} = \frac{\pi^2 EI}{l^2}$

With:
E = 70 GPa = 70 *10^6 kN/m^2
I = (1/12) * 200 * 6^3 = 3600 mm^4 = 3,6 * 10^{-9} m^4
L = h' / cos(29) = 206 mm = 0,206 m

N_{Euler} = 59 kN

N_{Ek} = (1/2)*F_{SV}*(1/cos(29)) = 23 kN
N_{Ed} = γ_Q * N_{Ek}

In accordance with 5.3.2.3 (1) of EN 1991-2 for a service vehicle on a pedestrian bridge (accidental loading) γ_Q = 1,0. Therefore N_{Ed} = N_{Ek} = 23 kN.

N_{Ed} < N_{Euler} therefore buckling will not occur.

Bending resistance of the flange
Section modulus of the flange: W_{fl} = (1/6) * 200 * 9^2 = 2700 mm^3 = 2,7*10^{-6} m^3

Distributed load from the wheel: q_d = 40 / 0,2 = 200 kN/m
Bending moment in clamped beam: M_{Ed} = (1/12) * 200 * $0,17^2$ = 0,48 kNm

Stress from bending moment: σ = M/W = 0,66 / 2,7*10^{-6} = 178395 kN/m^2 = 178 N/mm^2 < f_o = 260 N/mm^2 therefore the flange will no fail due to bending.

The following parameters therefore satisfy the requirements for local loading:

- Web thickness of 6mm
- Flange thickness of 9mm
- Internal height of 180mm
- Angle of inclined web to vertical of 29°

Limiting the stresses of stresses in the cross-section provides the two final constraints for the design of the structure; the first which has already been mentioned is the maximum span, the second is the choice between Alternatives I and II. Increasingly large spans were investigated for the two alternatives, as the prestressing force was increased to meet the deflection requirement the unity check for bending and compression increased also. The final span is chosen as 18 metres with a width of 3 metres, these were determined based on; limiting the prestressing force to only counter balance the self-weight and allowing only two prestressing elements per module for ease of assembly.

The resistance of the girder is calculated using EN 1999-1-1 which gives the rules for the structural design of aluminium structures. The use of a prestressing system results in significant compressive stresses in the girder, therefore the critical check for the cross-section will be buckling of the elements in compression. In order to ensure the cross-section is fully effective, i.e. the reduction factor $\rho_c = 1$, the thickness of the flanges and webs are set to 9mm and 7,3mm respectively such that the slenderness limit for Class 3 is met. The calculation is given in Section 4.1.3.1 to follow.

The resulting cross-section of one module in the girder is shown schematically below; each one has a width of 1018mm and for a width of 5m five modules will be connected next to one another.

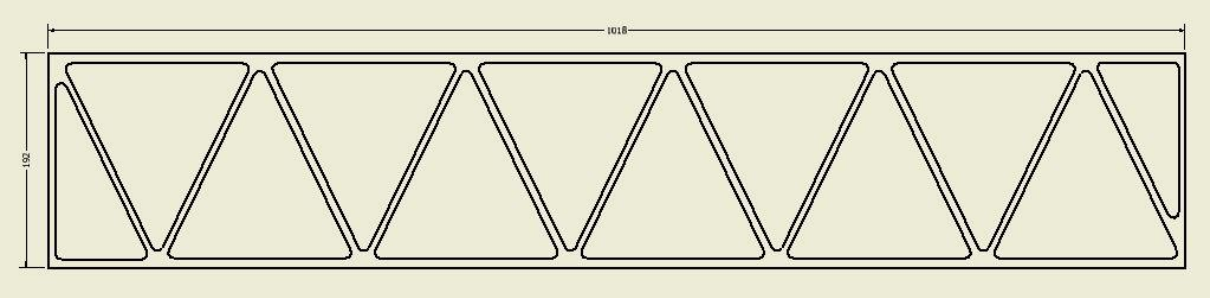

Figure 36: Overview diagram of the cross-section of one module

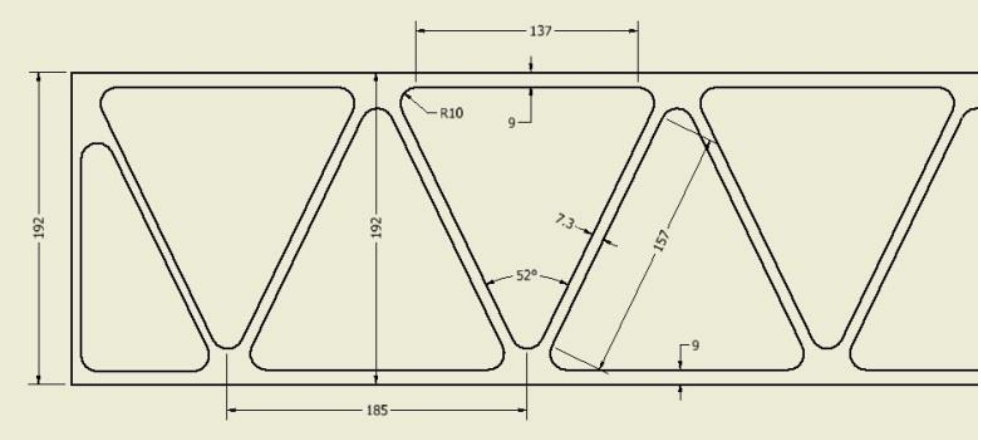

Figure 37: Dimensions of the extruded module

Having determined the cross-section to be used in each configuration the analysis to calculate the maximum span can take place. The longitudinal stress is calculated as the summation of the bending stress, from the global bending moment and the eccentricity of the axial load, and the axial compressive stress; $\sigma = \frac{M}{W} \pm \frac{N}{A}$ in which M is the bending moment, W is the section modulus, N is the axial compressive force from the horizontal component of the prestressing system, and A is the area of the cross-section.

4.1.3 Overview of the structure

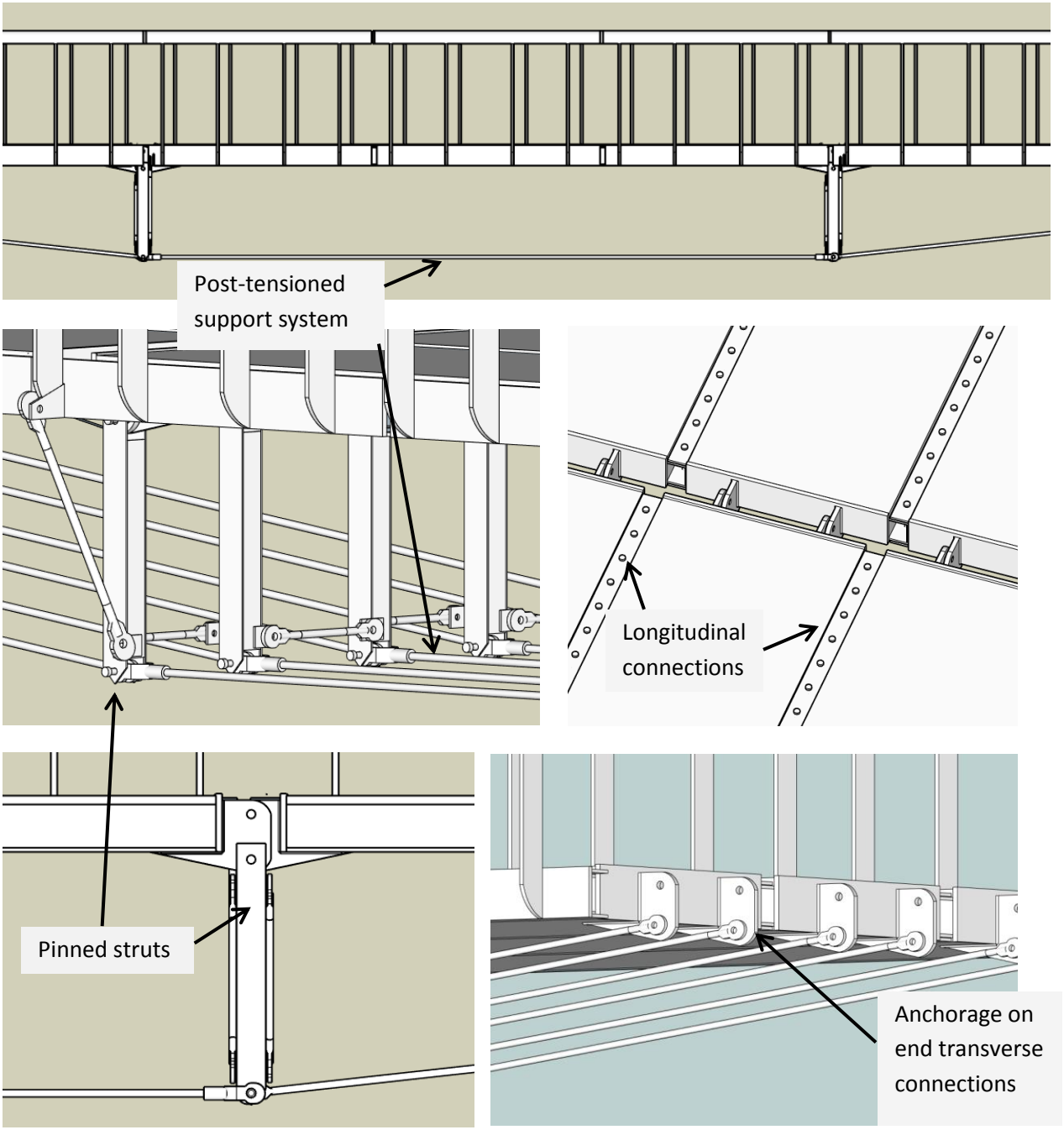

Figure 38: Overview of main components of the structure

4.1.3 Strength verifications of the structure (ULS)

4.1.3.1 Load factors for post-tensioned structures

The complete calculation of the structure can be found in Appendices E1 and E2, however the most important design aspects are summarised in this chapter. In accordance with NEN-EN 1993-1-11 for a prestressed system the load cases of self-weight (G) and prestressing force (P) must be joined into one load combination (G+P) which must be multiplied by one of two factors:

- Superior load factor, $\gamma_{G,sup}$ = 1,35, if the load is unfavourable
- Inferior load factor, $\gamma_{G,inf}$ = 1,0, if the load is favourable

The greater the load the greater the deflection which results in a greater upward force, it is unknown whether this will be favourable or not in terms of bending moment and axial force from the outset. For this reason both load cases were used for the complete calculation in order to determine which scenario would result in the most critical outcome.

4.1.3.2 Classification of the cross-section

The cross-section consists of two elements to be classified; the flanges and the inclined webs, both are internal elements with a constant stress over the length, this is for the critical situation in which the bending moment along the span is zero and the cross-section is under pure compression.

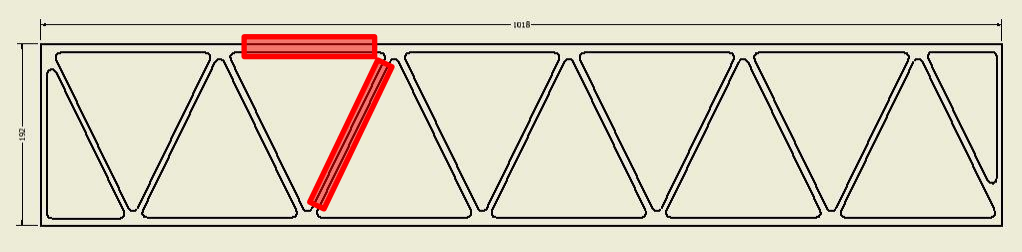

Figure 39: Elements governing the cross-section classification of the cross-section

In accordance with Chapter 6.1.4 of NEN 1999-1-1 slender parameter β for an internal element with a constant stress gradient is β = b/t, for the elements this yields:

- Flanges: β = b/t = 137 / 9 = 15,2
- Webs: β = b/t = 157 / 7,3 = 21,5

The parameter ε for accounting for the 0,2% proof-stress is: $\varepsilon = \sqrt{(250/f_0)} = 0,98$.
According to Table 6.2 of NEN 1999-1-1 for an internal element with welds, as is the case for the flanges, the limit value of the slenderness for Class 3 is $\beta_3/\varepsilon = 18$. The webs do contain any welds therefore the slenderness limit for Class 3 is $\beta_3/\varepsilon = 22$, this results in the following classification:

- Flanges: β = 15,2 < 0,98*18 = 17,6 → Class 3
- Webs: β = 21,5 < 0,98*22 = 21,6 → Class 3

Therefore the cross-section is Class 3. In accordance with Equation 6.11 of NEN 1999-1-1 the reduction factor for local buckling may be taken as $\rho_c = 1,0$ for $\beta < \beta_3$ meaning no reduction is required.

4.1.3.3 Load cases

The following load cases (LCs) were investigated for the structure:

- LC1: Crowd loading (5 kN/m^2) over the full span
- LC2: Service vehicle (120kN point load) at mid span
- LC3: Crowd load on the field left of the left strut

- LC4: Crowd load on the fields left and between struts
- LC5: Upward wind load

LC1: Crowd loading over full span

The strength checks which are most critical in LC1 are:

- Strength: Combined bending and compression
- Stability: Buckling and buckling with a transverse load

Governing loads

Bending moment: M_{Ed} = 85 kNm
Axial force: N_{Ed} = 970 kN
Shear force: V_{Ed} = 166 kNm

Axial compression

In accordance with Chapter 6.2.4 of NEN 1999-1-1 the axial compressive force N_{Ed} must satisfy the equation:

$$\frac{N_{Ed}}{N_{Rd}} \leq 1{,}0$$

In which N_{Rd} is the resistance of the cross-section, given by:

$$N_{c,Rd} = A_{eff} \cdot f_o/\gamma_{M1}$$

In which:
A_{eff} is the effective surface area of the cross-section based on the reduced thickness due to local buckling and the reduction due to the heat-affected zone.
The 0,2% proof stress of EN-AW 6082, f_o = 260 N/mm^2.
The material factor for aluminium, γ_{M1} = 1,1.

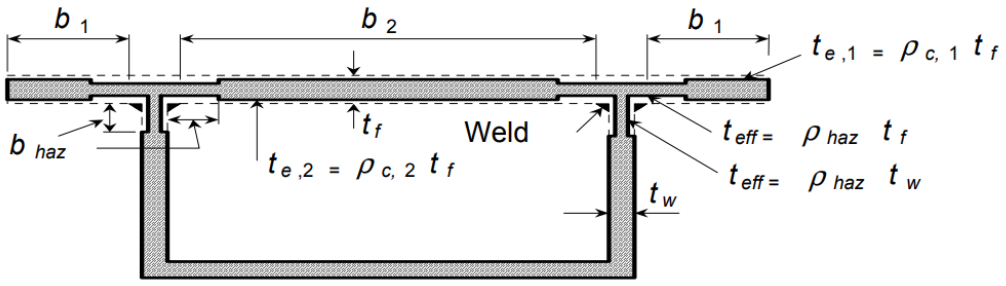

Figure 40: Visual representation on an example cross-section of the reduction in thickness due the HAZ introduced by welds

The total area of the cross-section is A = 98787 mm^2, the area of the heat-affected zone (HAZ) will be subtracted from this. Each of the five modules consists of five extrusions welded together along the length; in accordance with Section 6.1.6.3 (3) of NEN 1999-1-1 the HAZ for elements of 6mm to 12mm

thick is of 30mm. The resistance of the material is reduced by multiplying with the HAZ-factor $\rho_{0,HAZ}$ = 0,48; this will be applied as a reduction in thickness to the HAZ area. The area to be subtracted is therefore: A_{red} = 3 * 2 * 4 * 30 * 9 * (1 – 0,48) = 3370 mm^2.

This results in an effective area of:
A_{eff} = 98787 – 3370 = 95417 mm^2.

This yields:

$$N_{c,Rd} = 95417 \cdot \frac{260}{1,1} \cdot 10^{-3} = 22553\ kN \rightarrow \frac{N_{Ed}}{N_{Rd}} = \frac{959}{22553} = 0,04 \rightarrow \text{OK}$$

Bending moment
In accordance with Chapter 6.2.5 of NEN 1999-1-1 the bending moment M_{Ed} must satisfy the equation:

$$\frac{M_{Ed}}{M_{Rd}} \leq 1,0$$

In which M_{Rd} is the resistance of the cross-section, given by:

$$M_{Rd} = \alpha \cdot W_{el} \cdot f_o / \gamma_{M1}$$

In which:
The shape factor α is given in Table 6.4, for a cross-section in Class 3 with longitudinal welds:
$\alpha = \alpha_{3,w} = W_{el,haz} / W_{el}$
The elastic section modulus, W_{el} = 3*((1/6)*1018*192^2 – 5,5*(1/6)*165*174^2) = 5026041 mm^3.
$W_{el,haz}$ is the reduced elastic section modulus when taking the HAZ into account, using the same method as for the effective area it can be calculated as:
$W_{el,haz} = W_{el}$ – 5*(4*(1/16)*30^2*(192-174)*(1-0,48)) = 5009193 mm^3.

This yields:
$$M_{Rd} = 5009193 \cdot \frac{260}{1,1} \cdot 10^{-6} = 1184\ kNm \rightarrow \frac{M_{Ed}}{M_{Rd}} = \frac{85}{1184} = 0,07 \rightarrow \text{OK}$$

Combined bending and axial compression
For double-symmetric cross-sections the following condition must be met:

$$\left(\frac{N_{Ed}}{\omega_0 N_{Rd}}\right)^{\xi_0} + \frac{M_{y,Ed}}{\omega_0 M_{y,Rd}} \leq 1,0$$

In which:
ζ_0 = 0,8 can be taken as a conservative value in accordance with NEN1999-1-1 and for longitudinally welded sections $\omega_0 = \omega_x = (\rho_{u,haz} * f_u / \gamma_{M2}) / (f_o / \gamma_{M1})$ = (0,6 * 310 / 1,25) / (260 / 1,1) = 0,63.

This yields:

$$\left(\frac{970}{0,63 \cdot 22553}\right)^{0,8} + \frac{85}{0,63 \cdot 1184} = 0,18 \leq 1,0 \rightarrow \text{OK}$$

Buckling with bending moment

The buckling resistance of beams under combined axial compression and bending must satisfy the equation:

$$\left(\frac{N_{\mathrm{Ed}}}{\chi_{\mathrm{y}}\,\omega_{\mathrm{x}}\,N_{\mathrm{Rd}}}\right)^{\xi_{\mathrm{yc}}}+\frac{M_{\mathrm{y,Ed}}}{\omega_0\,M_{\mathrm{y,Rd}}}\leq 1{,}00$$

With $M_{y,Rd} = M_{Rd}$ from the previous calculation and the resistance to axial load given by:

$$N_{Rd} = A_{eff}\, f_o/\gamma_{M1}$$

The buckling reduction factor is determined using NEN1999-1-1 Chapter 6.3.1.2:

$$\chi = \frac{1}{\phi+\sqrt{\phi^2+\bar{\lambda}^2}} \leq 1{,}0$$

$$\phi = 0{,}5(1+\alpha(\bar{\lambda}+\bar{\lambda}_0)+\bar{\lambda}^2)$$

The imperfection factor α and limiting value of the slenderness λ_0 are given in Table 6.6 as 0,20 and 0,10 respectively for alloys in Class A.
A_{eff} is the effective area after reduction due to the influence of the HAZ.
The 0,2% proof-stress: $f_0 = 260$ N/mm^2.
The partial safety factor for the stability check: $\gamma_{M1} = 1{,}1$.

To determine the reduction factor for welds, κ, the relative slenderness, $\bar{\lambda}$, was first determined. This is determined using: $\bar{\lambda} = \sqrt{\frac{A_{eff} f_0}{N_{cr}}}$ in which N_{cr} is the elastic critical buckling load. The girders of the bridge are schematised as a sway column with rotational supports.

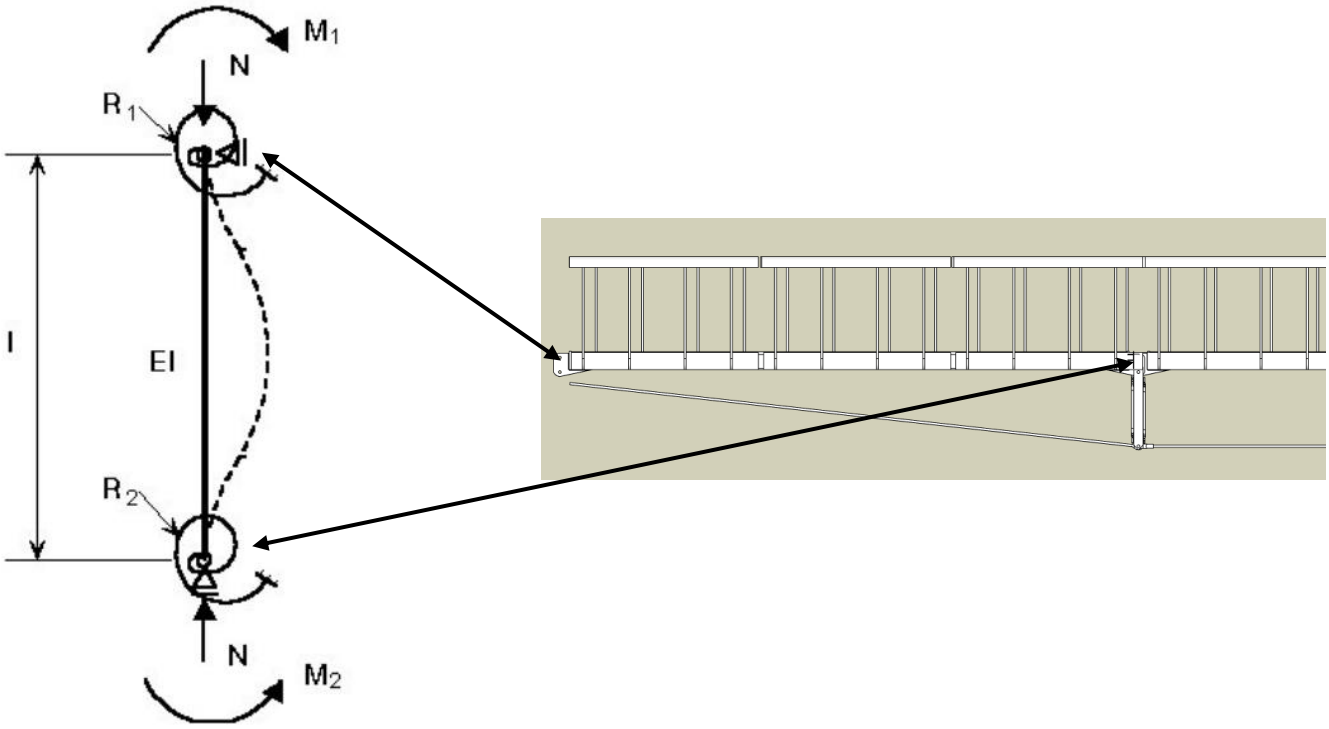

Figure 41: Schematisation of the girders for Donnell's equation (ESDEP, sd)

The schematisation allows for the use of Donnell's equation for buckling, the buckling length of a column with rotational springs at the supports must be multiplied by a factor K calculated using:

$$K = \frac{1}{\sqrt{n}}$$

$$n = \frac{1{,}2(f_1+f_2)+7{,}2f_1f_2}{1+1{,}4(f_1+f_2)+1{,}8f_1f_2}$$

$$f_i = \frac{1}{6{,}5\ EI}\frac{M_i}{\theta_i}$$

For the spring stiffness, M/θ, the value of the bending moment and rotation at the location of the struts will be taken for the maximum load at ULS; this is the critical scenario for the axial load which causes buckling. The complete calculation is given in Appendix E3. The first iteration of the calculation was performed using the conservative assumption that the support is pinned and has no rotational stiffness; for $f_1 = 0$ the buckling resistance was found to be insufficient. For this reason the influence of the eccentricity of the anchorage was included resulting in rotational stiffnesses of $f_1 = 0{,}03$ and $f_2 = 0{,}14$.

This yielded a multiplication factor for the buckling length of k = 2,1; in the schematisation of the girders the length considered is the distance to the struts meaning L = 6m. The buckling length of the girders therefore comes to L_{cr} = 12,6m with a corresponding elastic critical buckling load of N_{cr} = 2297 kN.

The reduction factor for welds κ is determined according to Table 6.5:

Table 6.6 - Values of α and $\bar{\lambda}_0$ for flexural buckling

Material buckling class according to Table 3.2	α	$\bar{\lambda}_0$
Class A	0,20	0,10
Class B	0,32	0,00

This allowed the parameters λ and κ to be determined resulting in:

$$\left(\frac{970}{0{,}084 \cdot 0{,}63 \cdot 23286}\right)^{0{,}8} + \left(\frac{85}{0{,}63 \cdot 1184}\right) = 0{,}94 \leq 1{,}0$$

Therefore buckling of the girders does not occur due to combined bending and axial compression.

LC2: Service vehicle at mid-span

- Strength: Shear force under the point load

Shear resistance of the cross-section
The shear resistance of the cross-section is given by:
$V_{Rd} = A_v * (f_o / \sqrt{3})$

The area of the shear webs: $A_v = 3 * 11 * 7{,}3 * 174 = 41917$ mm^2. This yields:
$V_{Rd} = 41917 * (260 / \sqrt{3}) * 10^{-3} = 6292$ kN.

U.C. = 120 / 6292 = 0,19 → OK.

LC3 and LC4: Partially distributed pedestrian load

The partial loading of pedestrians on the bridge does not lead to a critical scenario for the strength verifications.

LC5: Upward wind load

- Strength: Bending moment resistance due to upward wind load

Governing loads
Bending moment: $M_{Ed} = -147$ kNm
Axial force: $N_{Ed} = 0$ kN (rod assumed to take zero compressive force)
Shear force at the supports, $V_{Ed,supp} = -33$ kN (uplift force)

Calculation procedure for upward wind load
Given the low self-weight of the structure the effect of upward wind loading was investigated using the simplified method given in NEN 1991-1-4. Assuming a conservative scenario in which the bridge is at an elevation of z = 10m and is found in Zone 1, the exposure factor is determined as $c_e = 2{,}8$.
The girders are assumed to remain level giving an incidence angle of Θ = 10°, this results in a factor $c_f = 0{,}9$. The total correction factor comes to C = 2,8 * 0,9 = 2,52.

In accordance with the Dutch National Annex the reference wind speed is v_b = 29,5 m/s and the density of air is ρ = 1,25 kg/m^3. The total upward wind load is of:
$F_{w,z}$ = 0,5 * ρ * v_b^2 * C * $A_{ref,z}$ = 0,5 * 1,25 * 29,5^2 * 2,52 * 3 * 18 = 74014 N = 74 kN.
This is a distributed load of: $q_{wind,z}$ = 1,37 kN/m^2.

Bending moment (negative)
In accordance with Chapter 6.2.5 of NEN 1999-1-1 the bending moment M_{Ed} must satisfy the equation:

$$\frac{M_{Ed}}{M_{Rd}} \leq 1{,}0$$

From the previous bending moment resistance calculation M_{Rd} = 1184 kNm.

This yields:
$$\frac{M_{Ed}}{M_{Rd}} = \frac{147}{1184} = 0{,}12 \rightarrow \text{OK}$$

4.1.4 Dynamic analysis of the structure

In order to determine the natural frequency the bridge was modelled in SCIA Engineer, one module is modelled separately as a continuous beam, simply supported at both ends with the steel rods and struts connected by pins below. In the model no prestressing force is applied to the tie rods, this creates a conservative approach as the structure made taught by this force would have a higher natural frequency. A second simplification of the model is the absence of connections between the three sections of the span, these would however provide a positive influence from damping due to the friction between components. Given however that the bolts used in the connections will be pre-tensioned to prevent slip at SLS, and that the deformation of 36mm occurring at the first harmonic corresponds to a load smaller than that to be taken by the bolt preload (see Chapter 4.3.4), the assumption that the girder is continuous is both conservative and realistic. Only the self-weight is considered in the analysis as this results in the lowest, and therefore most critical, natural frequency.

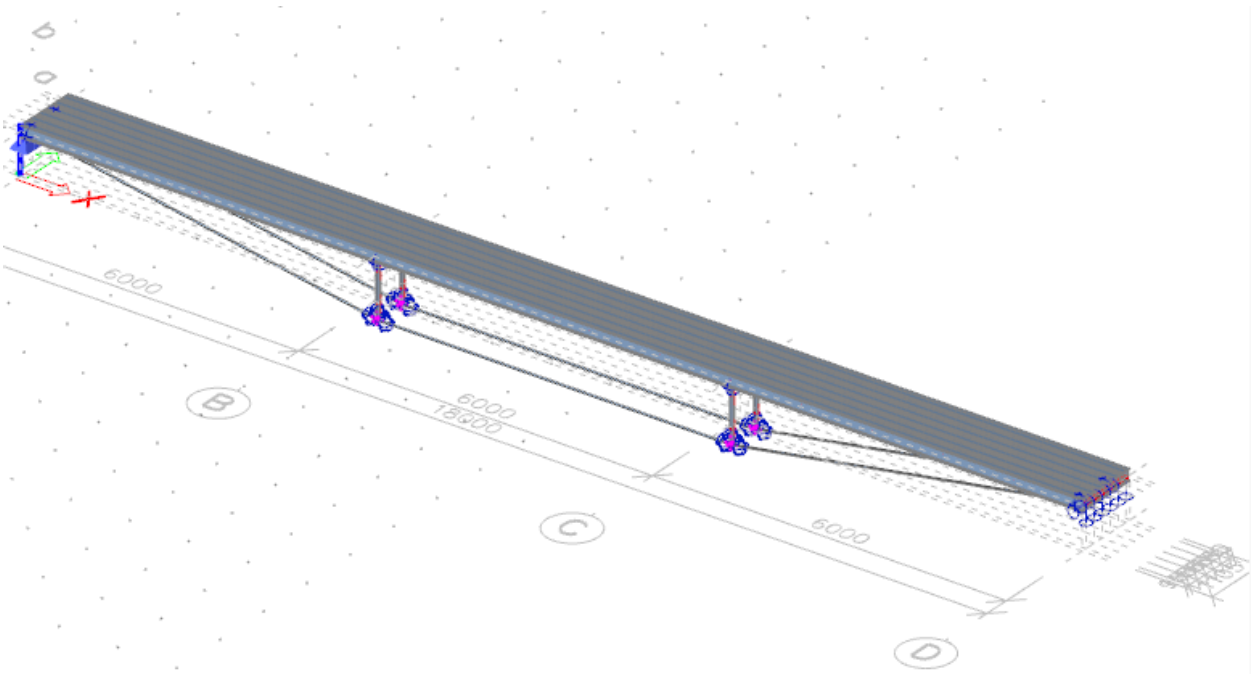

Figure 42: SCIA Engineer model used to determine dynamic behaviour of the structure

From the analysis it was found that the first vertical harmonic frequency of the structure occurs at $f_{n,1}$ = 5,03 Hz, the corresponding modal shape is shown in Figure 43. Achieving a frequency above the required 5Hz required increasing the height/length of the struts from 0,7m to 1,03m as the favourable influence of the post-tensioning is not present in the model.

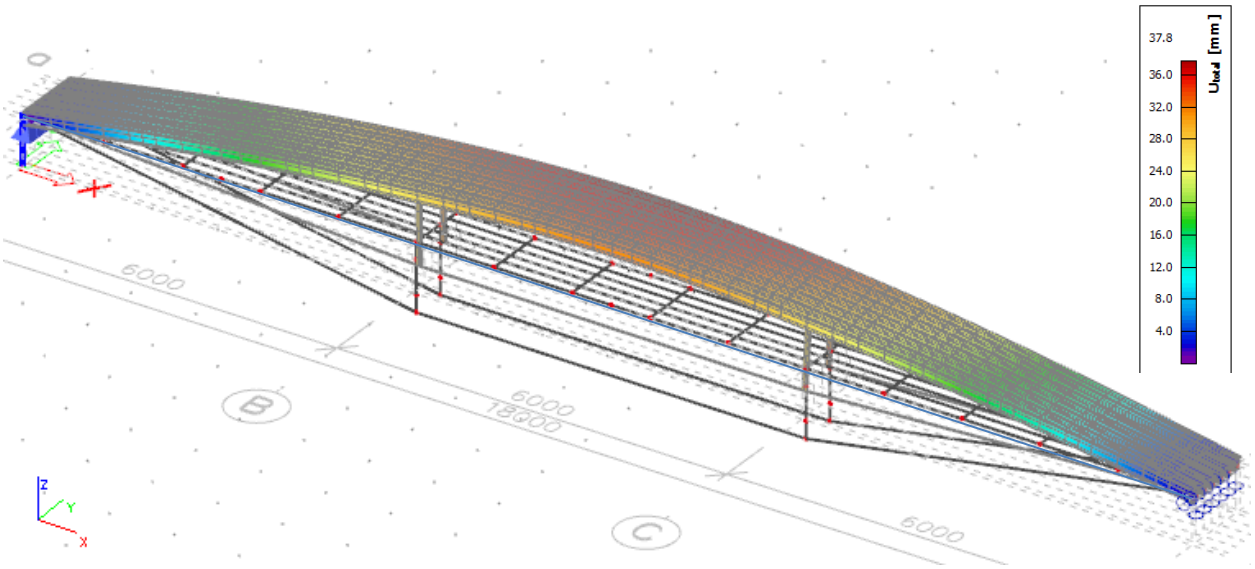

Figure 43: Deflection shape corresponding with the first vertical harmonic frequency

The lateral excitation is also verified, comfort requirements state that resonance frequencies above 2,5Hz are safe (Hoorpah), with the first harmonic occurring at $f_{n,1,lat}$ = 3,53Hz according to the shape shown in Figure 44 below.

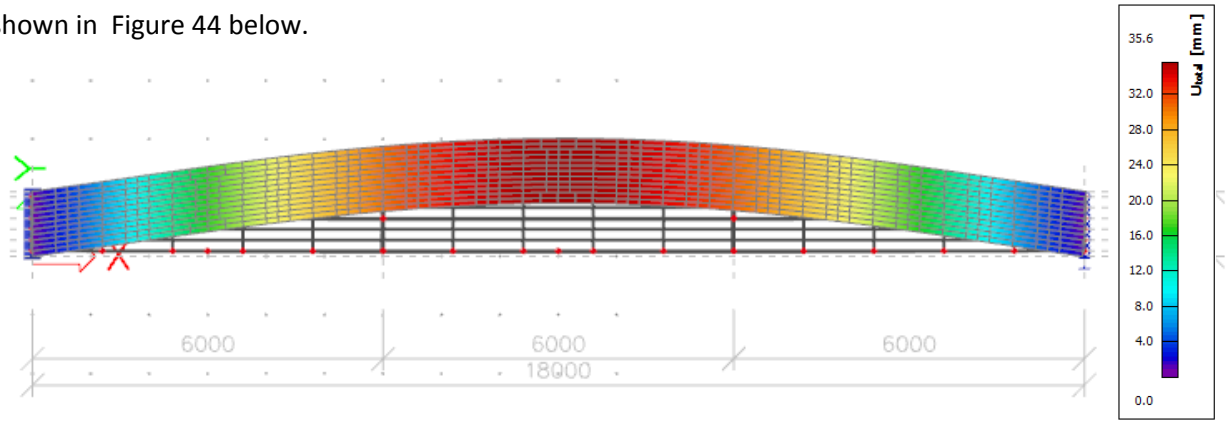

Figure 44: Deflection shape corresponding with the first lateral harmonic frequency

Both first harmonic frequencies are shown to be above the required limits meaning the structure is not susceptible to dynamic effects from pedestrians.

4.1.5 Conclusions for the girder dimensioning and strength verification

A configuration with two tendon kinks was chosen, this offered a greater reduction of the bending moment along the span for the governing load case. Aluminium alloy was chosen for the girders; the high natural corrosion resistance, low self-weight, and possibility to extrude custom profiles were selected as characteristics to be prioritised in the structure. The girders are built up from symmetric truss-core panels, 200mm tall and 1018mm wide, which provide high torsional stiffness (across the structure) and optimised material use. Extrusion of the section allows for large fillet radii to be created between the webs and flanges such that the slenderness, and therefore sensitivity to local buckling, is reduced.

The resistance of the cross-section has a significant margin of safety with peak stresses below 100 N/mm^2 compared to a resistance of 260 N/mm^2, stability was verified using both a traditional approach, approximating the girders as a pinned - rolling clamped column, and a method accounting for transverse loading in combination with compression. Both methods yielded unity checks of around 0,4 indicating that the verification is fairly accurate and with sufficient margin of safety.
Dynamic effects proved to be critical for the structure due in large part to the low self-weight of aluminium; in order to fall outside of the critical range of 5 Hz the height of the struts needed to be increased to 1 metre, with a strut height of 0,7 metres the bridge is safe but not comfortable for users. Lateral excitation was also checked and found not to be critical therefore needing to further measures. The dynamic model used in the structure omitted both the pre-tensioning in the tie rods and damping from flexibility in the bolted connection, both provide more favourable behaviour thereby providing a conservative result.

4.2 Post-tensioned support system and anchorage

The post-tensioned system represents a crucial detail in the structure as it provides the required strength and stiffness which allows for the reduced material use of the integrated deck girder modules. Two options were investigated; firstly a cable system as would be used in a traditional prestressed concrete girder, and secondly a system using steel rods tensioned by turnbuckles as is used in wind bracing. A solution is presented for both options in order to accurately compare the feasibility and make a choice as to which is most suited, once this has been determined the components requiring further development will be analysed and discussed.

4.2.1 Turnbuckle and tie rod assembly

Turnbuckles are metal frames with threaded inserts at each end which allow metal rods to be screwed in, rotating the frame pulls the rods together thereby creating tension in the assembly. The advantages of using turnbuckles include: their availability and widespread use in the construction sector, meaning maintenance and modification of the structure are easily achieved, as well as their fast assembly which requires only basic tools. Finally, the turnbuckles can be used anywhere on the bars so that they can be placed in accessible areas to further facilitate inspection and maintenance; key aspects in extending the lifespan of the structure.

Figure 45: Various examples of uses of tied rod constructions with turnbuckles: timber roof structure (top left) (Architectural Timber & Millwork, Inc.), close-up of turnbuckles and threaded rods (bottom left) (Portland Bolt), stability bracing for a walkway (right) (HALFEN)

The engineering design is based on the initial assumption that the rods are evenly divided among the modules each with a turnbuckle to apply a pre-tension; this allows for an even distribution along the width of both support from the struts and compressive stresses. To ensure feasibility when assembling the structure the number of rods per module was limited to two, meaning six in total for the 3m wide structure, with each rod taking a combination of load from pre-tensioning of the turnbuckles and stress due to elongation:

- Pre-tensioning force, T = 27 kN.
  Determined to give zero deflection due to self-weight at SLS.
- Axial force due to elongation, N = 164 kN.
  Calculated using vertical deflection of the structure at the end of the rod.

This yields a total load in the rod and turnbuckle of: $F_{turn,Ed}$ = 27 + 137 = 164 kN
As shown in Table 2 below the M24 turnbuckle and tie rod assembly provides sufficient resistance and can be used safely. The complete calculation can be found in Appendix E2.

Table 2: Engineering data of Willems Anker turnbuckles indicating rod diameter and design resistance (at ULS) (Willems Anker). The first column shows the metric diameter of the rod while the second is the resistance at ULS.

Trekstang	Rekenwaarde van de bezwijkkracht (zie opmerking)	Benodigde bouten tbv. aansluitplaat	diameter rondstaal	B (zaag-maat)	Alle maten zijn vermeld in mm.														
					C	D	E	F	G	H	J	K	L	M	P	R	S	Z	SW
M16	58 kN	M 20*70	14,55	A-/- 230	25	12	Ø20.5	115	30	50	77	Ø23	194	24	Ø34	55	30	42.5	13
M20	138 kN	M 20*70	18,22	A-/- 230	25	12	Ø20.5	115	30	50	77	Ø23	194	24	Ø34	55	30	42.5	16
M24	203 kN	M 24*90	21,86	A-/- 238	25	20	Ø24.5	119	40	71	63	Ø27	210	26	Ø44	50	25	58.3	20
M30	323 kN	M 27*110	27,51	A-/- 322	25	25	Ø28.0	161	49	80	100	Ø30	271	36	Ø56	70	40	67	24
M36	436 kN	M 30*130	33,18	A-/- 322	25	25	Ø31.0	161	55	97.5	97	Ø33	279	38	Ø66	80	45	79	30
M42	561 kN	M 42*150	38,84	A-/- 444	25	30	Ø44.0	222	72	112	152	Ø45	373	54	Ø79	100	55	90	36
M48	742 kN	M 42*150	44,49	A-/- 444	25	30	Ø44.0	222	72	112	150	Ø45	371	52	Ø79	115	65	90	41
M60	1180 kN	M 52*200	56,16	A-/- 722	25	40	Ø54.0	361	95	142	220	Ø55	551	70	Ø110	130	75	130	50
M80	2115 kN	M 64*280	75,82	A-/- 820	25	50	Ø66.0	410	111	176	264	Ø66	626	80	Ø125	200	115	157	70

Next, the design and verification must take place for the anchorage which carries the axial load from the tie rods into the span; initially a scenario was investigated in which the rod ends are connected to the transverse connections present at each end of the module. By assigning a second function to these connections a separate support module does not need to be designed and manufactured; this simplifies the structure thereby facilitating reuse as well as reducing the amount of material and manufacturing processes needed. The dimensions of the transverse connections used as anchorage are taken from Chapter 4.3, there the detailing procedure will be given in full; the only parameter to be determined is the thickness of the plates which are governing for the anchorage.

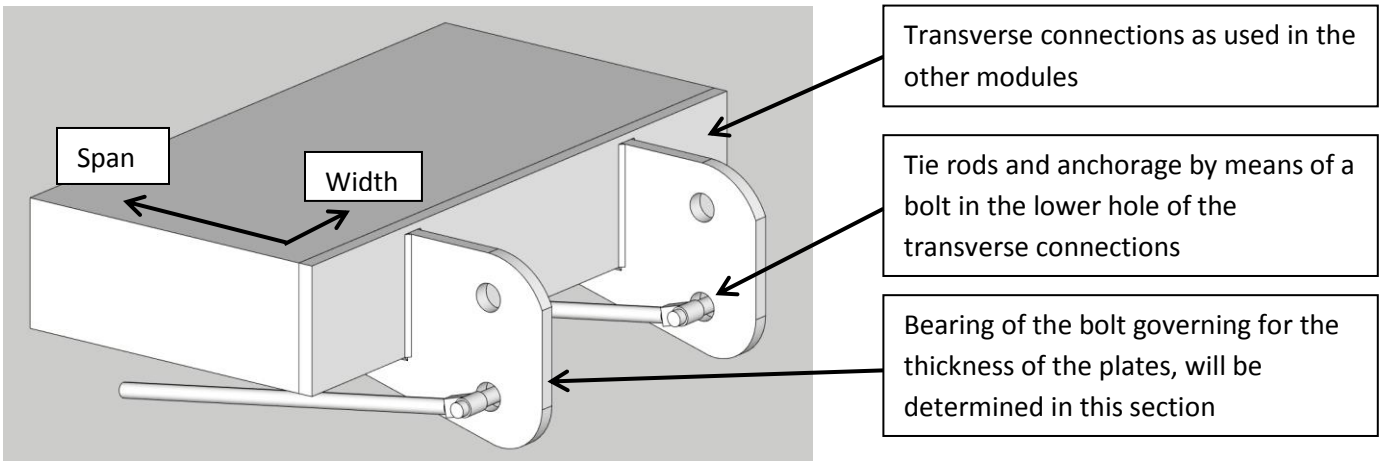

Figure 46: End view of the anchorage of the tie rods by means of a bolted connection in the transverse connection

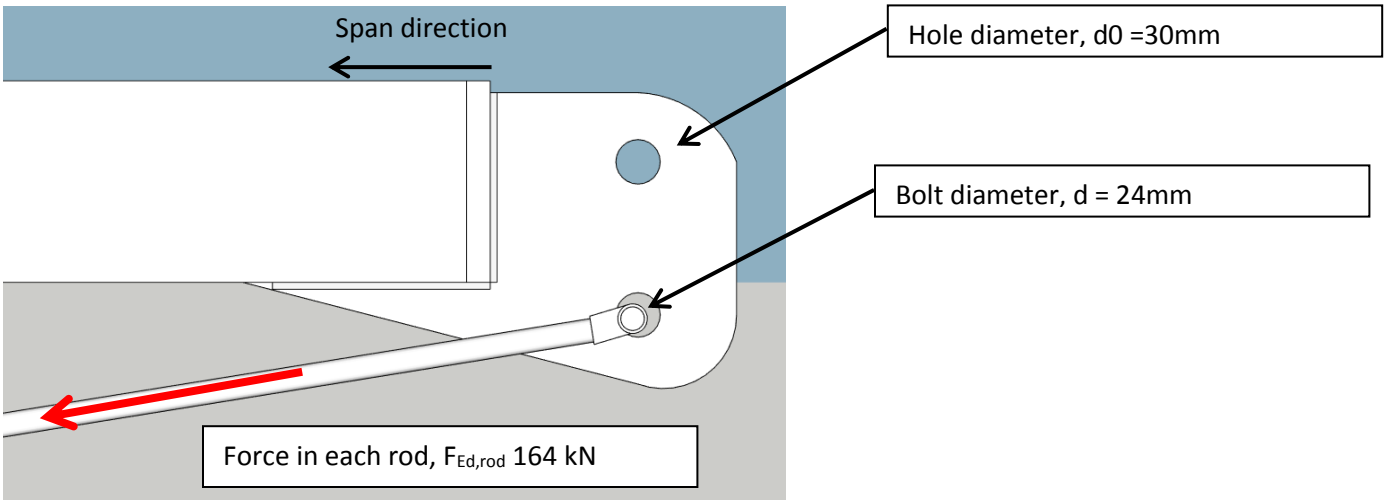

Figure 47: Key parameters for the anchorage system calculation

To determine the thickness of each plate the following input parameters will be used:
Diameter of the bolt: d = 24mm
Hole diameter: d_0 = 30 mm
End distance in the direction of load transfer: e_1 = 68mm
k_1 = 2,5
$\alpha_d = e_1 / (3*d_0) = 0,74$

Equating the force in each rod, $F_{Ed,rod}$, to the bearing resistance of one of the plates in each module, $F_{b,Rd}$, results in an equation in terms of the required thickness of the plate, t_{req}:

$$F_{Ed,rod} = F_{b,Rd} = 0,8 \cdot \frac{k_1 \cdot \alpha_d \cdot f_{u,p} \cdot d \cdot t_{req}}{\gamma_{M2}}$$

$$164 \cdot 10^3 = 0,8 \cdot \frac{2,5 \cdot 0,74 \cdot 295 \cdot 24 \cdot t_{req}}{1,25} \rightarrow t_{req} = 20\ mm$$

The calculation of parameters k_1 and α_d is given in Chapter 4.3 as these parameters depend on the dimensioning depending on the diameter of the bolt hole.
The bolt diameter was chosen based on the hole diameter of the clevis as given by the supplier, dimension E shown in Figure 48, which in accordance with Table 2 can be a maximum of 24mm.

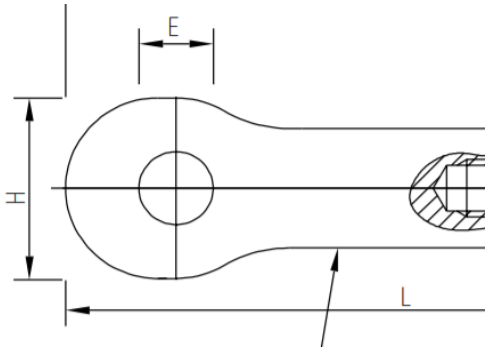

Figure 48: Dimension E of the clevis supplied by Willems Anker

The factor of 0,8 is derived from EN1999-1-1 which states that for oversized holes, as are applied in the M24 bolt inside a 45mm hole, the bearing resistance must be reduced by the given factor. The resistance of the bolt and the connection between the plates and the extruded sections will be discussed in Chapter 4.3.

4.2.2 Post-tensioned cable system

A second option was investigated; a cable system similar to those used in concrete girder with external tendons. The procedure was very similar to the tie rod system however due to the high resistance of the tendons a single tendon could be implemented per module, the technical data is taken from an engineering data sheet provided by VSL; a foremost supplier of both strands and anchorages for post-tensioning systems. The advantages of using a cable system are the high resistance and possibility to increase capacity or reduce deflection by adding more cables, as well as requiring fewer assembly stages and using hydraulic jacks which ensure a greater level of precision.

Figure 49: External prestressing tendons in concrete box girder (left) (Karlsruhe Institute of Technology) and tensioning of tendons using a jack (right) (Công Ty Cổ Phần Kỹ Thuật Namcong, 2015)

The force to be taken by each tendon (five in total) is given by:
$F_{tendon,Ed}$ = 984 / 3 = 328 kN
To satisfy this requirement VSL 5-3 tendons can be used which consist of three strands of 13mm diameter; these have a breaking load of 519kN (VSL, 2013). For the anchorage the same component as for anchoring in concrete is used, this ensures a strong and reliable connection despite the non-standard application. The VSL Type-E Anchorage can be used in combination with a variety of materials and transfers its load by means of a bearing plate, furthermore its can hold up to 55 strands per tendon allowing for high degree of upgradability should it be necessary.

Figure 50: VSL Type-E anchorage (VSL)

For the anchorage a separate module must be implemented as a combination with the existing structure would be overly complex, a design consisting of a plate with open stiffeners is proposed. The force will be concentrated around the bearing plate two thicker stiffeners are placed near the edges. Taking the

anchorage plate to be used with the highest strength material (C43/53) dimensions of 210mm x 210mm should be used however this exceeds the maximum height of the cross-section which is 190mm.

Reducing the height of the plate to 190mm and supporting it along the top edge and sides with the top flange and stiffeners as shown in Figure 51 below results in a stress of 204 N/mm^2. Although high this compressive stress is taken by very stocky plate elements which are not sensitive to buckling.

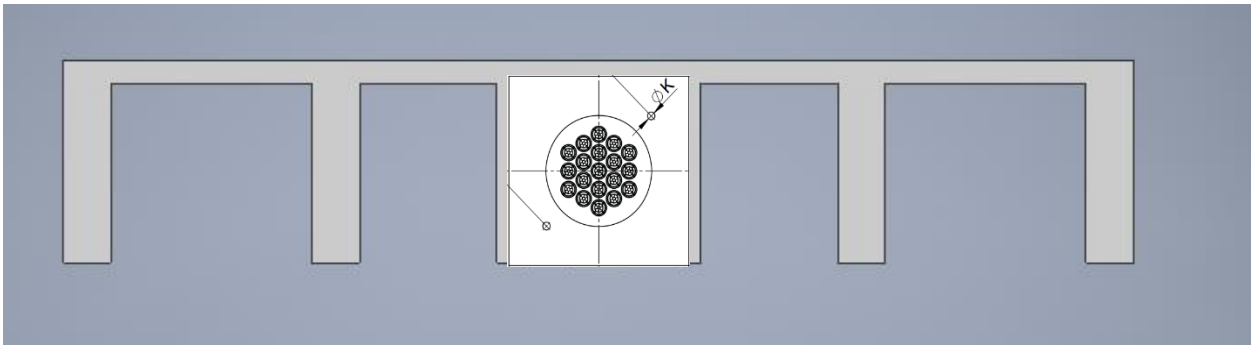

Figure 51: Anchorage bearing plate laid over support module sketch

4.2.3 Choice of post-tensioning system

In order to choose between the tie rod and cable system a comparison was made based on the characteristics considered most important for modularity and durability of the structure. Firstly, the inspection, maintenance, and ease of repair represents a foremost aspect in extending the service life of the structure both while in use and then afterwards if it is to be refurbished and reused. In the tie rod assembly all components are accessible and can be replaced on site without complete disassembly of the structure; conversely the anchorage in the cable system can only be accessed from the end sections which will be covered by a layer of paving at the abutments.

Upgrading and adjusting the structure is also easier in the tie rod system as turnbuckles can be tuned at any point during the service life, this allows for greater flexibility when it comes to possible reuse of the structure as strength and stiffness can be tailored to fit the changing needs.

According to a comparative life-cycle analysis (LCA) of bicycle and pedestrian bridges of different materials the coating required for a steel structure “represents the most important possibility for reducing environmental impact”, this came from the need to coat this structure every 25 years in order to avoid deterioration (Hegger & de Graaf, 2013). While this detracts from the advantages of the tie rod system this impact has been mitigated by limiting the use of steel, particularly small in terms of surface area, as well as the ease of applying this coating.

The option to use existing connections for the anchorage of the steel rods also represents a saving in materials and cost with regard to the special anchorage module needed for the cable system. Finally, the stiffness of the system is significantly improved as the tie rods do not have any slack and the structure has greater in-built redundancy due to the greater number of elements; thereby contributing to both safety and longevity.

For these reasons the tie rod system is chosen over the cable system and will be analysed further.

4.2.4 Conclusions for prestressed support system and anchorage

Steel tie rods post-tensioned with turnbuckles are used to support the structure, these provide greater stiffness than cables and the turnbuckles can be adjusted without disassembly of the structure. For the 18m long and 3m wide configuration of the bridge 6 tie rods with a 24mm diameter will be used, each module will be supported by 2 rods along the span. The total tensile load to be taken by the rods is of 984 kN at ULS which was the governing force for the thickness of the plates used in the transverse connection, these serve as anchorage for the tie rods. The initial preload in the tie rods is set to 20kN which results in a level resting position of the deck when only the self-weight is present.

4.3 Transverse connections

4.3.1 Choice of transverse connection

The transverse connections form an integral part of the design of the structure requiring both high strength and stiffness to ensure the structure meets the requirements of safety and function. From the state of the art four possible types of connections could be implemented: bolted, bolted frictional, wedged, and slotted. In order to determine the suitability of each type of connection the governing loads were determined for the maximum span of 18m and a corresponding width of 3m; the calculation was performed using Maple. Two load cases are critical for the transverse connections:

- LC1: Fully loaded span → Most unfavourable combination of axial force and bending moment
- LC5: Upward wind load → Most unfavourable effect from the negative moment

The appropriate connection was chosen by process of elimination, starting with the experimental steel dovetail connection of Moriche-Quesada of TUE. This connection was not used due to the connection being made from steel which cannot be welded to aluminium; while a bolted connection is theoretically possible the extensive contact area to be isolated as well the added challenge of creating sufficiently strong blind connections between connection and webs of the modules made this an impractical solution. Next, the slotted connection was considered; the capacity was shown to be most dependent on the resistance of the backing plates. According to the example calculation from Appendix B, the resistance can be found to be significantly below the requirement such that major modifications to the structure would be required. Furthermore the slotted connection relies on being under (partial) tension to ensure the stud does not leave the slot/channel which is not the case due to the constant compressive axial load from the prestressing system. Finally, only the bolted connections remain as possible solutions; due to the poor shear resistance of the frictional bolted connection these are also unsuited for the purpose of longitudinal connections. This leaves standard bolted connections as the only suitable solution; these have a high shear resistance and offer the opportunity for preloading to prevent slip at SLS.

4.3.2 Schematic view of loading on components

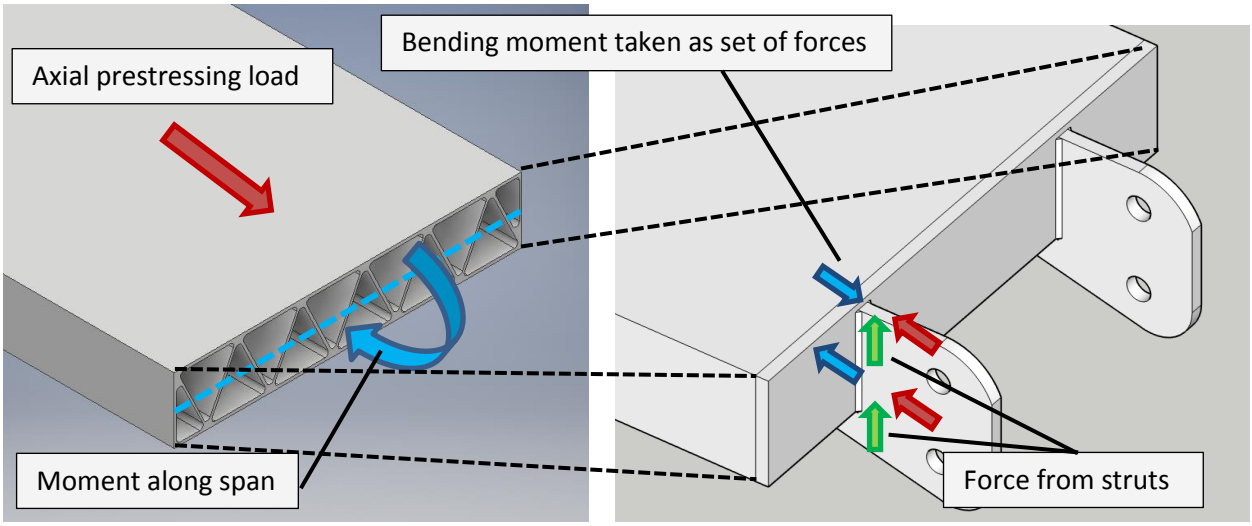

Figure 52: Overview of loads on the structure and how they are applied on the connection

4.3.3 Geometry and dimensions

The connectors shown in Figure 53 each consist of two vertical plates welded to a backing plate, which is then welded to the module. Two fillet welds of 177mm connect the vertical plates, with holes for the bolts, to the backing plate while another two horizontal fillet welds of 210mm connect these plates to the underside of the module. The backing plate is connected to the face of the module by means of two sets of welds along the top (fillet) and bottom (butt) edges (1018mm). The backing plate extends slightly above the top fibre of the top flange, the purpose of this is two-fold; firstly a fillet weld can be used which does not require any type of bevel, secondly the outstanding part of the plate forms a lip for when the epoxy granulate is applied on the deck layer to prevent excessive spreading or leaks. For bicycle and pedestrian bridges this layer is usually between 6 and 7mm thereby creating a flush surface with the protruding part of the plate. At the bottom a butt weld is used to allowing for a continuous weld along the tails below the modules.

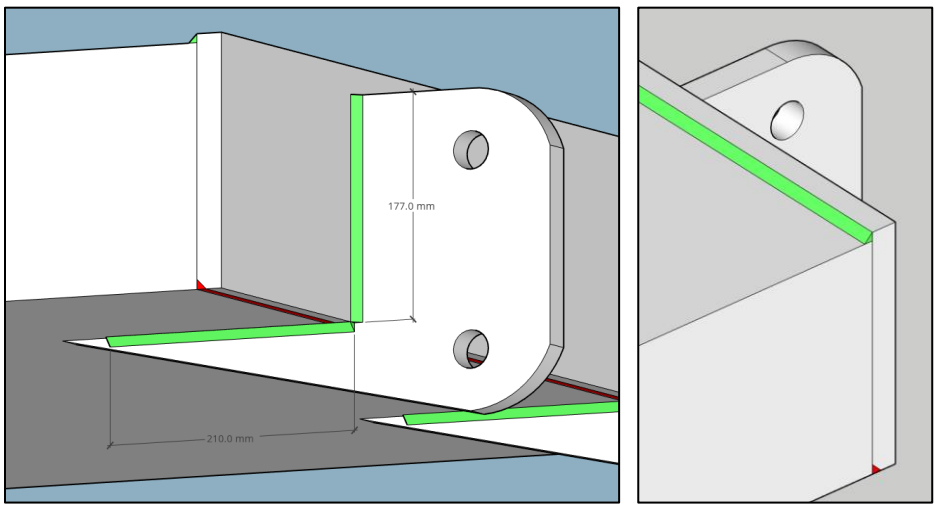

Figure 53: Welds in the transverse connection, green indicates fillet welds while red is for butt welds

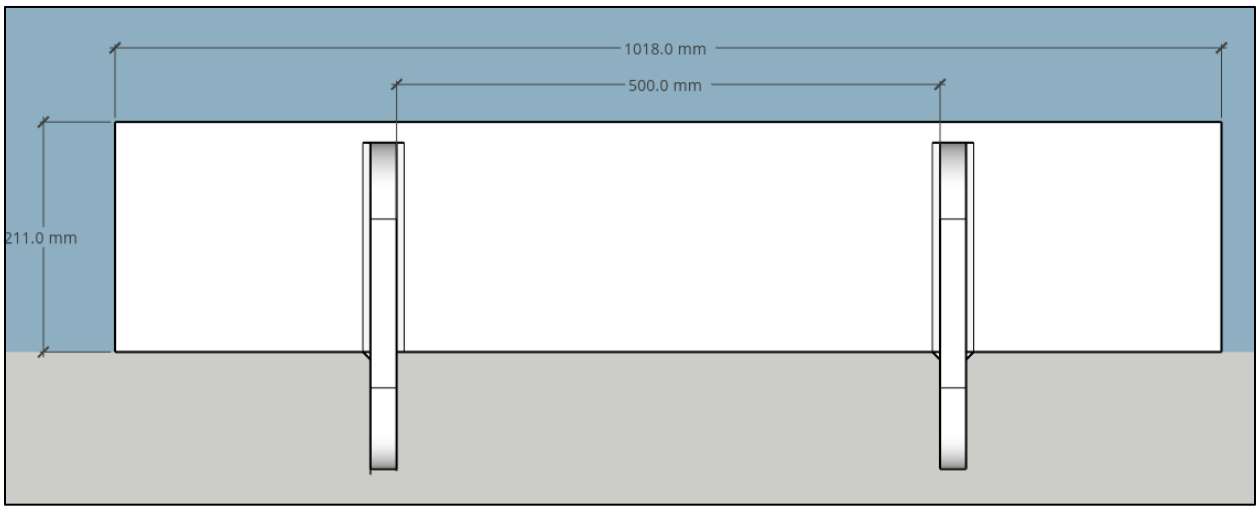

Figure 54: Front view of the connector joining modules end to end along the span

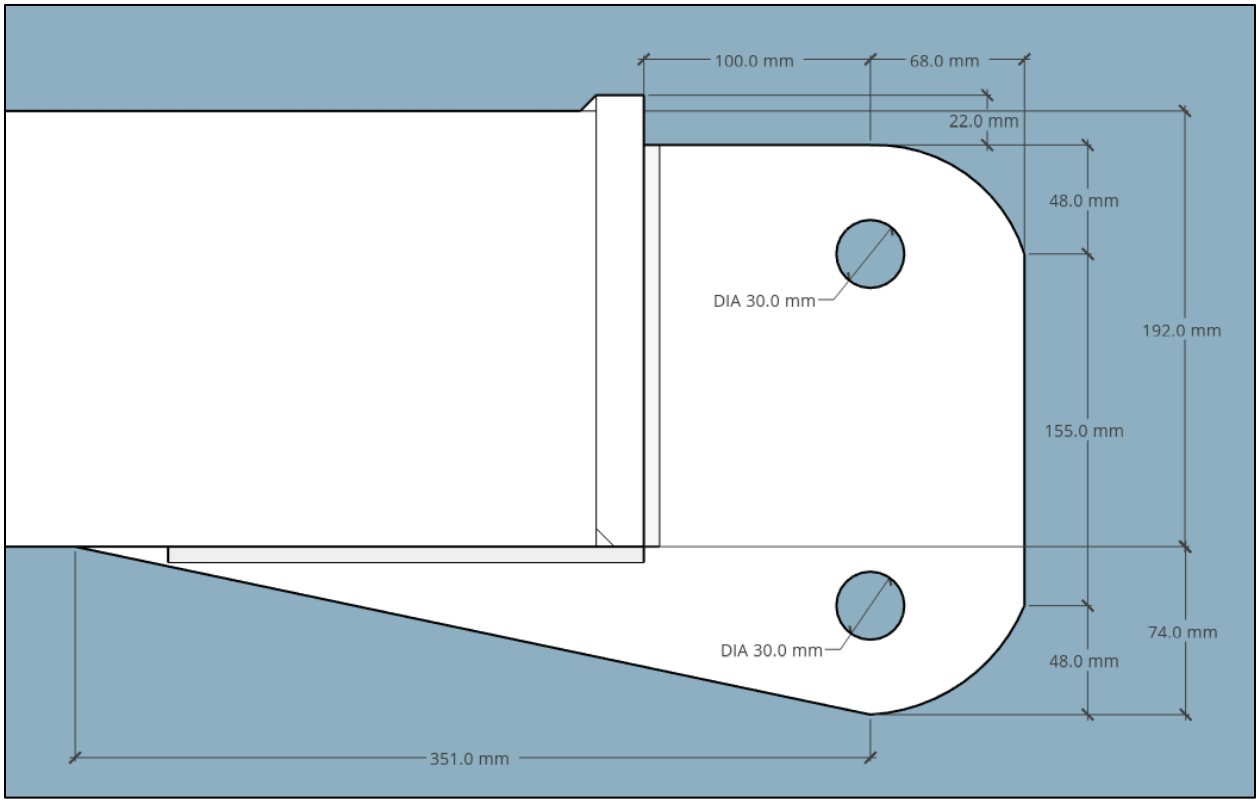

Figure 55: Side view of the connector joining modules end to end along the span

4.3.4 Stiffness of the connection at SLS

One of the key reasons a bolted connection was opted for rather than a dowel is the possibility to pretension the bolt. While pretensioning is not necessary for the structural integrity, i.e. slip-resistant at ULS, the deflection at SLS due to the gaps left by the bolt holes leads to excessive rigid body rotations of the modules. For the transverse connection the slip resistance is governing for the bolt diameter, the hole required, and dimensions of the plate therefore it is verified first.

Assuming bolts M27 Grade 10.9 the allowable preloading force is given by:

$$F_{p,c} = 0{,}7 \cdot f_{ub} \cdot A_s = 0{,}7 \cdot 1000 \cdot 459 = 321.300N$$

The slip resistance is given by:

$$F_{s,Rd} = \frac{n \cdot \mu}{\gamma_{M3,ser}} \cdot F_{p,c}$$

In which:
The number of friction surfaces: n = 1, for two plates in contact
The friction coefficient, μ = 0,40. This is derived from Table 8.6 of EN 1999-1-1 as the total joint thickness Σt = (24mm+24mm) > 30mm such that a roughness value of R_a 12,5 can be achieved for grit blasting.
The partial factor for bolted connections at serviceability limit state: $\gamma_{M3,ser}$ = 1,1

Therefore the slip resistance of one bolt comes to:

$$F_{s,Rd} = \frac{1 \cdot 0{,}4}{1{,}1} \cdot 321300 = 116836\ N = 117\ kN$$

The governing load case for the slip resistance of the bolted components of the connection is LC1 in which the structure is fully loaded by pedestrians, the governing loads for the structure at SLS are:
Bending moment: M_{Ed} = 44 kNm
Axial force: N_{Ed} = 643 kN
Shear force: V_{Ed} = 109 kN

The critical bolt must withstand a load of:

$$F_{Ed,bolt} = \frac{\frac{44\ [moment]}{0{,}155\ [lever\ arm]} + \frac{643\ [axial]}{2\ [bolts\ per\ plate]} + \frac{109\ [shear]}{2\ [bolts\ per\ plate]}}{2\ [plates\ per\ module] \cdot 3\ [modules]} =$$

$$F_{Ed,bolt,SLS} = 110\ kN$$

The unity check is: U.C. = $F_{Ed,bolt,SLS}$ / $F_{s,Rd}$ = 0,94 < 1, therefore no slip occurs at SLS.

4.3.5 Resistance of the connection

4.3.5.1 Resistance of the bolted components

The governing load case for the resistance of the bolted components of the connection is LC1 in which the structure is fully loaded by pedestrians, the governing loads for the structure at ULS are:
Bending moment: M_{Ed} = 84 kNm
Axial force: N_{Ed} = 956 kN
Shear force: V_{Ed} = 164 kN

The critical bolt must withstand a load of:

$$F_{Ed,bolt,ULS} = \frac{\frac{84\ [moment]}{0{,}155\ [lever\ arm]} + \frac{956\ [axial]}{2\ [bolts\ per\ plate]} + \frac{164\ [shear]}{2\ [bolts\ per\ plate]}}{2\ [plates\ per\ module] \cdot 3\ [modules]} =$$

$$F_{Ed,bolt,ULS} = 183kN$$

This load must be taken by both the plate in bearing and the bolts in shear.

Bearing resistance of the plate

The bearing resistance of the plate is given in Table 8.5 of EN 1999-1-1 as:

$$\boldsymbol{F_{b,Rd} = \frac{k_1 \cdot \alpha_b \cdot f_u \cdot d \cdot t}{\gamma_{M2}}}$$

In which:
Ultimate tensile strength of the bolts: f_{ub} = 1000 N/mm^2
Ultimate tensile strength of the plate material (AW6082): $f_{u,plate}$ = 295 N/mm^2
Diameter of the bolt: d = 27mm
Diameter of the bolt hole: d_0 = 30mm
Thickness of the plate: t = 24mm
Edge distance in the direction of load transfer: e_1 = 68 mm
Edge distance perpendicular to the direction of load transfer: e_2 = 48 mm
Partial safety factor for connections: γ_{M2} = 1,25

$$\alpha_b = \min\left\{\frac{e_1}{3d_0}; \frac{f_{ub}}{f_u}; 1{,}0\right\} = \min\left\{\frac{68}{3 \cdot 30}; \frac{800}{295}; 1{,}0\right\} = 0{,}74$$

$$k_1 = \min\left\{2{,}8\frac{e_2}{d_0} - 1{,}7; 2{,}5\right\} = \min\left\{2{,}8\frac{48}{30} - 1{,}7; 2{,}5\right\} = 2{,}5$$

This yields:

$$F_{b,Rd} = \frac{2{,}5 \cdot 0{,}74 \cdot 295 \cdot 27 \cdot 20}{1{,}25} = 235763\ \text{N} = 236\ \text{kN}$$

The unity check is: U.C. = $F_{Ed,bolt,ULS}$ / $F_{b,Rd}$ = 0,78 < 1, therefore bearing failure does not occur.

Shear resistance of the bolt

The shear resistance of the bolt per shear plane is:

$$F_{v,Rd} = \frac{\alpha_v \cdot f_{ub} \cdot A}{\gamma_{M2}}$$

In which:

α_v = 0,5 for Grade 10.9 bolts

f_{ub} = 1000 N/mm^2

A = 459 mm^2

This yields :

$$F_{v,Rd} = \frac{0{,}5 \cdot 1000 \cdot 459}{1{,}25} = 183600\ N = 183{,}6\ kN$$

The unity check is: U.C. = $F_{Ed,bolt,ULS}$ / $F_{v,Rd}$ = 0,99 < 1, therefore shear failure of the bolt does not occur.

4.3.4.2 Resistance of the welded components

Strength of weld material

In accordance with Table 8.8 of NEN1999-1-1 filler metal 5356 is chosen to be used in combination with alloy AW6082, the characteristic strength is of f_w = 210 N/mm^2.

Effective weld length

For the weld along the top and bottom edges of the backing plate a reduction of the length must be applied in accordance with 8.6.3.3 of NEN1999-1-1, here the length of the weld of 1018mm exceeds 100 times the throat thickness of 7mm. The effective length of the weld is therefore:

$L_{w,eff}$ = (1,2 – (0,2*L_w)/(100*a))*L_w = (1,2 – (0,2*1018)/(100*7))*1018 = 923 mm.

Schematisation of loading

The loads on the connection (axial force (N), bending moment (M), and shear force (V)) are transmitted by means of the two bolts connected to the vertical plates; these loads are then transferred by the welds to the backing plate and girder. Two load cases are governing for these welds, LC1 and LC2, these were used to verify the strength of the three fillet welds shown in Figure 56 depending on which is critical. The loads from the top bolt are applied to Fillet weld 1 (vertical) and those on the bottom bolt are applied to Fillet weld 2 (horizontal), the governing scenario for Fillet weld 3 is the same as that for Fillet weld 1.

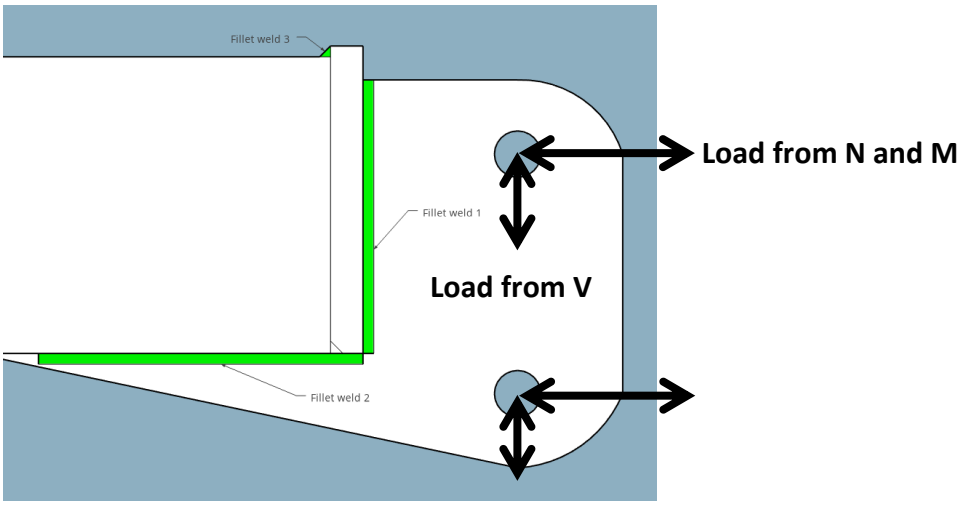

Figure 56: Schematisation of loading on the transverse connection with welds highlighted in green

<u>Fillet weld 1 under LC5 loading:</u>

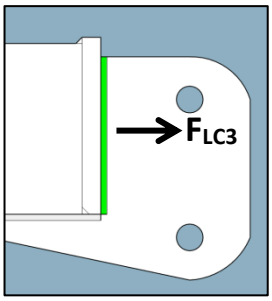

F_{LC3} = (125 / 0,155) / (3 [modules] * 2 [plates/module]) = 135 kN

$\tau_{\perp} = \sigma_{\perp}$ = 135*10^3 / (√2 * 2 * 177 * 7) = 38 N/mm^2

$\sigma_{Ed,a}$ = √(σ^2 + 3 τ^2) = √(38^2 + 3*38^2) = 76 N/mm^2

$f_{w,d} = f_w / \gamma_{Mw}$ = 210 / 1,25 = 168 N/mm^2

U.C. = 76 / 168 = 0,45 < 1 → OK

<u>Fillet weld 2 under LC1 loading:</u>

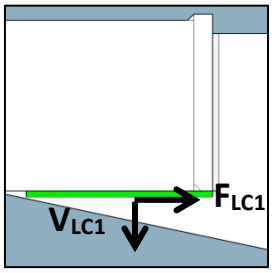

F_{LC1} = ((20 / 0,155) + (1206/2)) / (3 [modules] * 2 [plates/module]) = 135 kN

V_{LC1} = 160 / (3 [modules] * 2 [plates/module] * 2 [bolts/plate]) = 13 kN

$\tau_{//}$ = 135*10^3 / (2 * 210 * 7) = 46 N/mm^2

$\tau_{\perp} = \sigma_{\perp}$ = 13*10^3 / (√2 * 2 * 177 * 7) = 4 N/mm^2

$\sigma_{Ed,a}$ = √(σ^2 + 3 τ^2) = √(4^2 + 3*(4^2 + 46^2)) = 80 N/mm^2

U.C. = 80 / 168 = 0,48 < 1 → OK

<u>Fillet weld 3 under LC3 loading:</u>

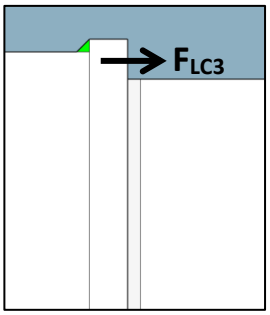

F_{LC3} = (125 / 0,155) / 3 [modules] = 270 kN

$\tau_{\perp,} = \sigma_{\perp,}$ = 270*10^3 / (√2 * 923 * 7) = 30 N/mm^2

$\sigma_{Ed,a}$ = √(σ^2 + 3 τ^2) = √(30^2 + 3*30^2) = 60 N/mm^2

U.C. = 76 / 168 = 0,45 < 1 → OK

Verification under maximum shear

The connection of the backing plate to the ends of the extruded girders must also be verified as the connection is only present at the edges of both elements. A finite element model was created to determine the load distribution in the welded connections; the maximum shear force from the self-weight and crowd loading was applied to the plates with the welded connections modelled as fixed supports. The governing shear force at the support is given by:

V_{supp} = ½ * q * L = ½ * (1,5 * 15 + 1,35 * 0,27) * 18 = 213,3 kN.

The applied load per plate is F_{supp} = 213 / (3 * 2) = 34 kN.

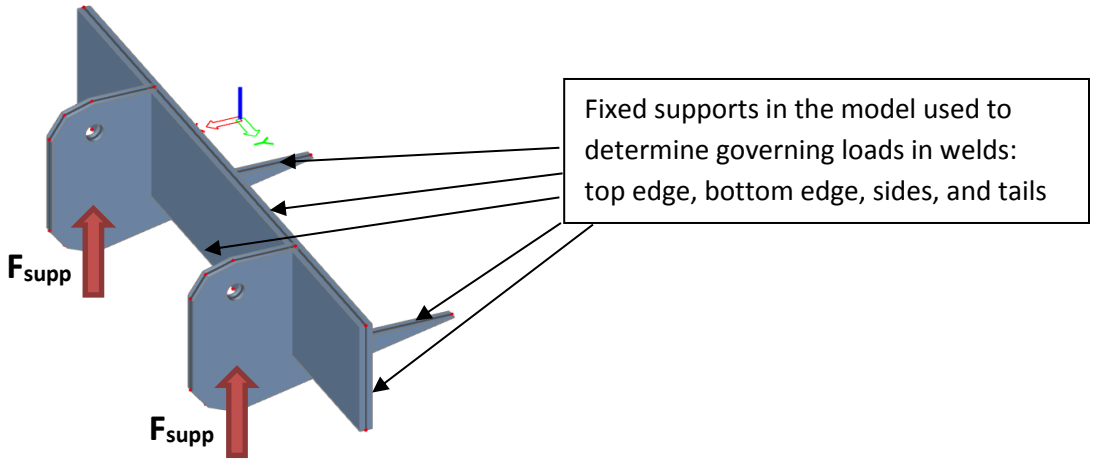

Figure 57: Finite element model of the transverse connection at the supports

The resulting loads along the length of the welds are:

- Top edge: 31 kN/m over 1018mm
- Bottom edge: 44 kN/m over 1018mm
- Sides (individual): 0,6 kN/m over 200mm
- Tail plates (x-direction is critical for welds) (individual): 32,5 kN/m over 251mm

The verification for the welds is given below:

- Top edge: $\tau_{\perp} = \sigma_{\perp} = 31*10^3 * 1,018 / (\sqrt{2} * 1018 * 7) = 3,1$ N/mm² << f_w = 168 N/mm²
- Bottom edge: $\tau_{//} = 44*10^3 * 1,018 / (1018 * 7) = 6,3$ N/mm² << f_w = 168 N/mm²
- Sides: $\tau_{//} = 0,6*10^3 * 0,2 / (200*7) = 0,1$ N/mm² << f_w = 168 N/mm²
- Tail plates: $\tau_{//} = 32,5*10^3 * 0,251 / (2 * 251 * 7) = 2,3$ N/mm² << f_w = 168 N/mm²

With these verifications it has been shown that the welds in the structure have sufficient resistance.

4.3.5 Conclusions for transverse connections

By process of elimination a bolted assembly was chosen for the transverse connections; these offer high versatility, resistance, and the possibility for pre-tensioning to create non-slip conditions. The connection is comprised of two M27 Grade 10.9 bolts separated by a vertical lever arm of 155mm to reduce the contribution of the axial force to the bending moment in the connection. These bolts slot into a connector consisting of two vertical plates each with a thickness of 20mm, each plate has a tail which is welded to the underside of the girder to provide additional resistance.

The connection transfers the axial load from prestressing (984kN), the bending moment along the span as a set of horizontal forces (84kN), and vertical forces from the tie rods through the struts (109kN). The critical check for the connection at ULS is shear resistance of the bolts, at SLS the bolts can be sufficiently pretensioned to prevent slip thereby ensuring no kinks will be present along the deck.

4.4 Longitudinal connections

In order to connect the modules longitudinally (along the span) three options were investigated; a slotted connection, a plug-and-play connection, and a traditional bolted connection. Next to having sufficient resistance the connection must also provide a level deck for users, meaning openings and excessive rotation of the connection must be prevented. While the bolted connection offers good strength and stiffness properties the frictional plug-and-play connection would allow for a faster and less labour-intensive erection process. This may offer competitiveness with respect to traditional methods in terms of cost and safety; furthermore as hindrance from construction work becomes increasingly undesirable the value of efficient erection increases. Aluminium to aluminium contact as used in the plug-and-play connection also eliminates the risk of galvanic corrosion present when (stainless) steel fasteners are implemented.

4.4.1 Determining governing loads

In order to determine the governing loads on the connections the bridge was modelled in SCIA-Engineer, the modules were built up from 2D plate elements connected rigidly to one another in both longitudinal and transverse direction. The bridge is simply supported at both ends using a line support with the tie rods and struts modelled as pinned rods without any prestressing load applied. Figure 58 gives an overview of the model and the cross-section used, the longitudinal connection is modelled as a set of vertically spaced plates used as dummy elements (highlighted in pink) to determine the bending moment and shear force along the span. The bending moment in the connection is derived from the axial force across the span (N_y) multiplied by the vertical lever arm of 192mm, the shear force can be calculated from the sum of the shear forces (V_y) in the two plates.

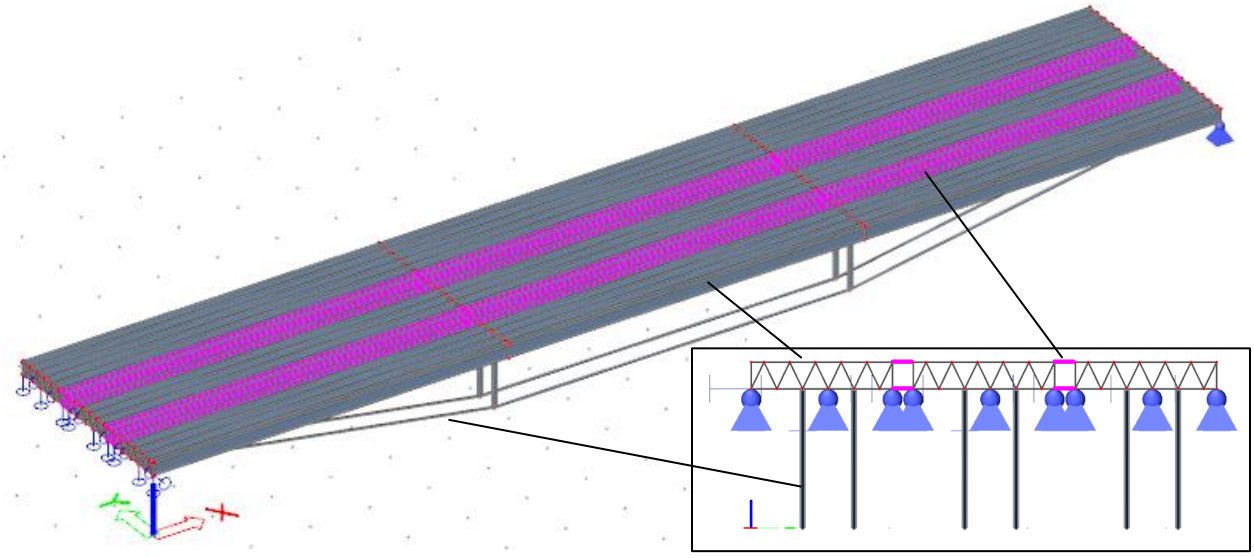

Figure 58: Plate and beam model from SCIA Engineer, the dummy elements are shown in pink

The imposed loads creating the governing scenario had to be determined; four load cases were investigated using a combination of self-weight, full pedestrian loading, partial pedestrian loading, upward wind load, and one axle of a service vehicle:

- LC1: Fully loaded structure (crowd load of 5kN/m^2)
- LC2: Line of pedestrians directly beside the connection (strip of 5kN/m^2 over 2 modules)
- LC3: Upward wind load and reduced self-weight (1,37 kN/m^2)
- LC4: Service vehicle directly beside connection (Two 40kN point loads 1,2m apart)

An overview of these load cases is shown below with the position of the connection highlighted in pink.

LC1

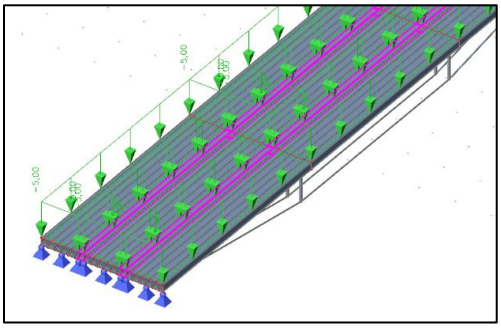

LC2

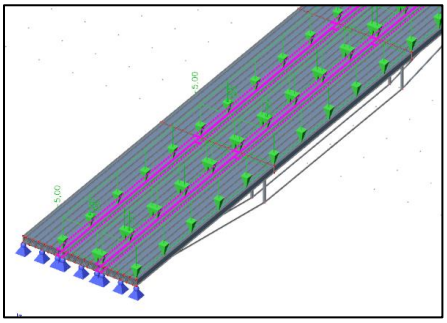

LC3

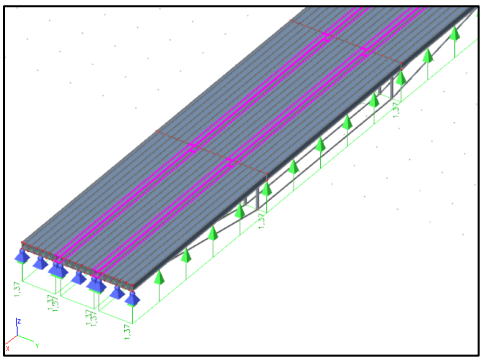

LC4

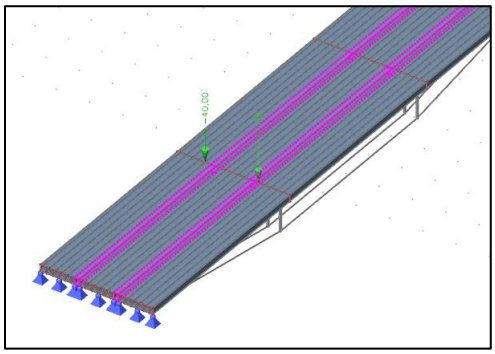

Figure 59: Load cases investigated for transverse connections and locations of dummy elements in pink

From this analysis the governing loads were calculated as:

- N_y = 62 kN/m' → M_{xy} = 62*0,192 = 12 kNm/m'
- V_y = 12 kN/m'

The governing scenario was given by LC4 due to the point loading from the service vehicle, while this loading is concentrated over a small length the service vehicle may be placed anywhere meaning the entire connection must be calculated according to this load.

The results are given per meter length along the x-axis which is indicated with the m' index, these loads can be used directly in a 2D analysis and represent the governing scenario for all possible configurations of the structure 18m long, 3m wide and smaller.

4.4.2 Slotted connections

In order to determine the suitability of a slotted connection a calculation was made based on a set of studs made to fit slots which transfer the bending moment and shear forces, the general design is shown in Figure 60. Assembly of the connection takes place in two steps: firstly the studs are aligned with the larger diameter holes and afterwards the modules are pushed or pulled in opposite directions so that the shaft of the stud is resting in the smaller diameter hole.

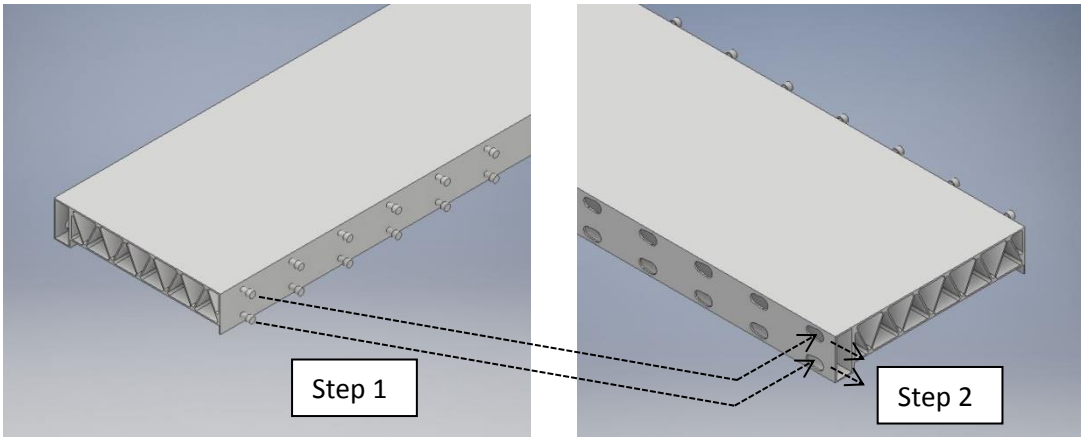

Figure 60: Isometric view of the two parts forming the connection: studs left and slots right

4.4.2.1 Dimensions of the connecting parts

Slotted connector

The slotted connector consists of a set hole which tapers along the length; the vertical plate must resist punching shear from the head of the stud when the connection is subjected to bending and resist bearing when the connection is loaded in shear

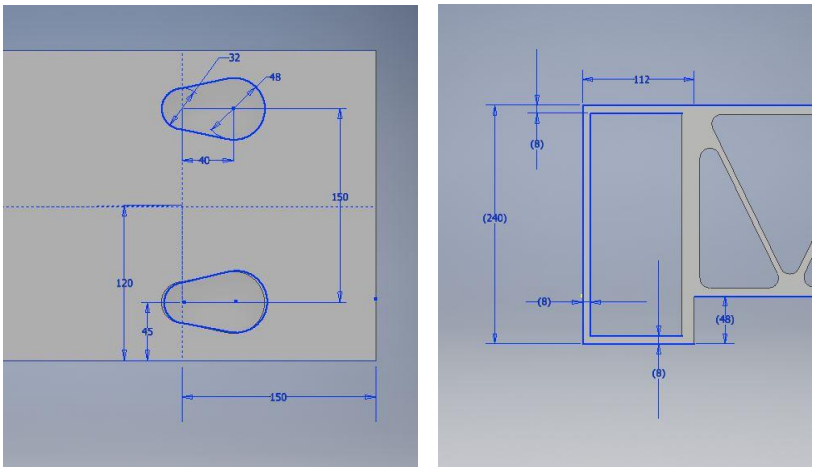

Figure 61: Dimensions of the slotted part of the connection

Studded connector

The studded connector consists of aluminium studs welded to the side faces of the modules; these transfer moments through a set of opposing tensile and compressive forces and transfer shear across the shank area. The overall behaviour can be equated to a set of bolts in tension and shear. Originally, in order to increase the lever arm of the connection the outermost web was made to extend downward, as shown in Figure 62 (left) however given the limitations on extrusion shape (size of the die) this was not feasible. Welding a vertical end plate with stiffeners was also considered but would require extensive and careful welding which is likely to result in insufficient strength along the top edge, this configuration is shown on the right side of Figure 62.

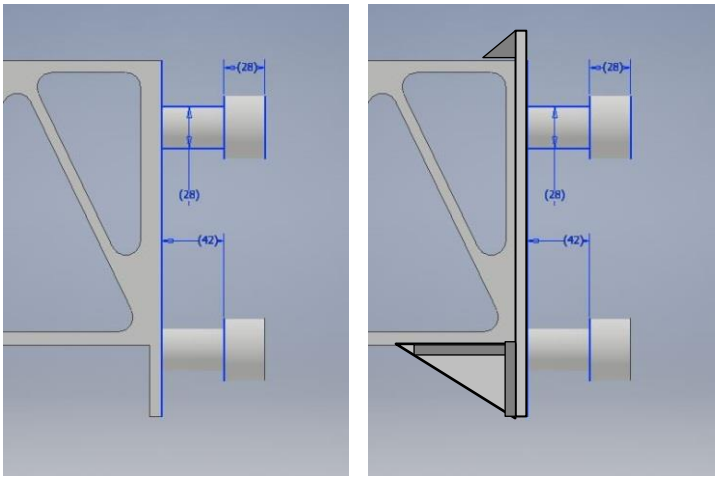

Figure 62: Concepts for extended end plate to be used in the studded connection, extruded (left) and welded (right)

The connection tested consisted of two studs with diameters of 20mm and a spacing of 130mm such that the studs could be welded to the end webs of the modules.

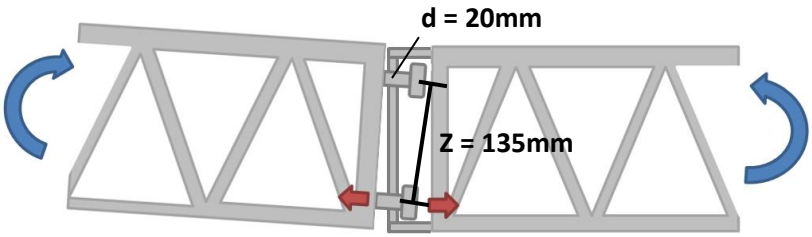

Figure 63: Key dimensions for the slotted connection shown here being loaded in bending

4.4.2.2 Resistance of the slotted connection

Loads on the connection

M_{Ed} = 12 kNm/m → Set of opposing forces: $F_{T,Ed} = M_{Ed} / z = 12 / 0{,}13 = 92{,}3$ kN/m'

V_{Ed} = 12 kN/m'

Bending moment – Studs under tension and punching of the plate

Tensile strength of the studs:

$$F_{T,Rd} = \frac{k_2 \cdot f_{ub} \cdot A}{\gamma_{M2}}$$

From NEN 1999-1-1: $k_2 = 0{,}9$ and $\gamma_{M2} = 1.25$

For ultimate tensile strength of the bolt the HAZ-affected 0,2% proof-stress is taken: $f_{o,haz} = 185$ N/mm^2

The area of the shank of the stud: $A = 0{,}25 * \pi * 20^2 = 314$ mm^2

This yields: $F_{T,Rd} = \frac{0{,}9 \cdot 185 \cdot 314}{1{,}25} \cdot 10^{-3} = 41{,}8\ kN$ → $n_{req} = 80 / 41{,}2 = 1{,}92$ → 2 sets of studs per meter required

Punching resistance of the plate:

$$B_{p,Rd} = 0{,}6 \cdot \pi \cdot d_m \cdot t_p \cdot \frac{f_u}{\gamma_{M2}}$$

In which:

The diameter of the head of the stud: $d_m = 30$ mm

Thickness of the plate: $t_p = 8$mm

Ultimate strength of the plate material: $f_u = 295$ N/mm^2

This yields: $B_{p,Rd} = 0{,}6 \cdot \pi \cdot 30 \cdot 8 \cdot \frac{295}{1{,}25} \cdot \frac{2}{3} \cdot 10^{-3} = 98{,}7\ kN$ → $n_{req} = 80 / 71{,}1 = 1{,}1$ → 2 sets of studs per meter required. The resistance has been reduced by a third to account for the partial opening due to the larger hole used for assembling the connection.

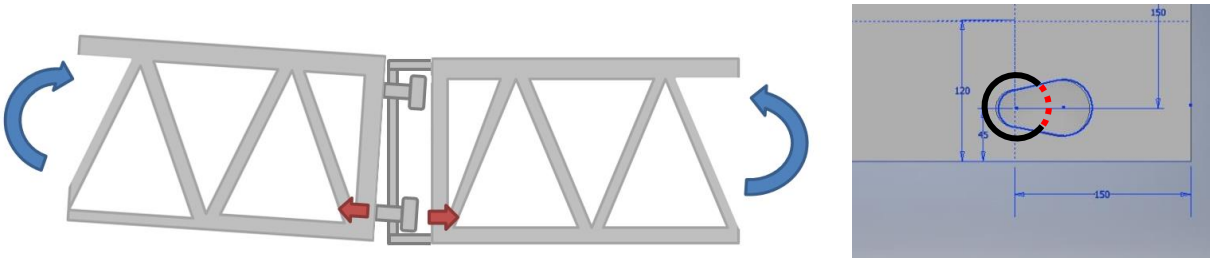

Figure 64: Loading of the connection under bending moment (left) and reduced contact area for the punching resistance (right)

Shear - shear resistance of the studs

Shear resistance of the studs:

$F_{V,Rd} = \frac{\alpha_v \cdot f_{ub} \cdot A}{\gamma_{M2}} = \frac{0{,}6 \cdot 185 \cdot 314}{1{,}25} \cdot 2 \cdot 10^{-3} = 83{,}6\ kN$ → n_{req} = 12 / 83,6 = 0,14 → 1 set of studs per meter required.

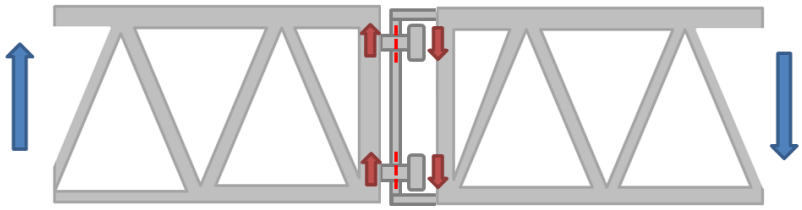

Figure 65: Loading of the connection under shear

From the calculation it was determined that 2 rows of studs two studs each are needed per meter length to ensure sufficient resistance of the connection, this means for a module of 6 metres 24 individual connectors must be fitted. Given manufacturing and assembly tolerances, ensuring all studs fit into their respective slots would be challenging, this would further be hindered further by the lack of flexibility in the connection. Should one stud not fit the entire series cannot fall into their designated slots; on site modification of these connections would be either impossible or too expensive to be feasible given the accurate welding and cutting processes required. For this reason the slotted connection will not be used due to the significant challenges it poses for practical application.

4.4.3 Plug-and-play connection

4.4.3.1 Geometry

The plug-and-play, or friction fit, connection was designed based on the dovetail connection found in wood joinery, the principle relies on a male and female part fitting into one another and resisting the load through frictional forces between the two. While a traditional dovetail consists of angular parts the design chosen for the analysis was modified to reduce sensitivity to fabrication errors and increase the contact area of the faces.

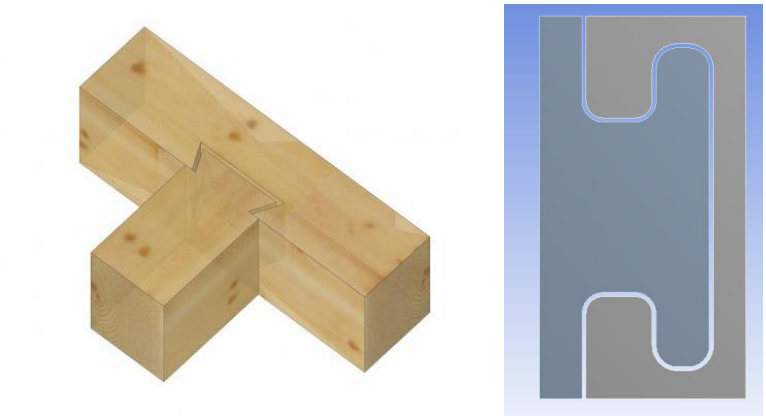

Figure 66: Dovetail used in joinery (left) and first version of the plug-and-play joint analysed in ANSYS (right)

5.4.3.2 ANSYS analysis settings

The modelling of the connection in ANSYS required thorough adaptation of the settings such that despite the non-linear behaviour an accurate and converging result could be achieved. Where possible the settings were left to the default setting, what follows is a brief discussion of the settings that were modified. The connection was modelled in ANSYS in 2D to reduce the solution time; the out-of-plane effects, axial compression and bending moment along the length which act normal to the 2D faces, do not influence the behaviour of the connection.

In ANSYS Mechanical this was indicated through the setting Geometry > 2D Behaviour > Plane Strain, this setting "assumes zero strain... [while] the stress in the z direction is non-zero" (SHARCNET). According to the Shared Hierarchical Academic Research Computing Network (SHARCNET), a group of academic institutions dedicated to high performance computing, a plane strain analysis should be used "for structures where the z dimension is much larger than the x and y dimensions". In this case the working plane of the 2D face is the XY-plane while the Z-axis represents the depth or out-of-plane axis which is indeed much larger than the dimensions of the connection (6m and 0,2m respectively).
Next, the contact region between the male and female parts was defined under the 'Connections' tab. The resistance of the connection is realised by bending of the components of the connection however before this can occur stable contact between these parts must be achieved. Accurate definition of the frictional behaviour of the contact interface is therefore essential as this largely determines if a converged solution can be reached. In ANSYS the behaviour is set to "Frictional" and the friction coefficient is set to 0,2, according to Table 18 of NEN 1090-2 this corresponds to Class D surface treatment and is the most conservative assumption. The behaviour is set to "Asymmetric" which defines ones face of the connection as the contact and the other as the target, in accordance with (Johnson) the convex faces were set as the contact and the concave as the target. For the contact formulation theory ANSYS offers several options, three of which are suited to any type of contact behaviour (SHARCNET), namely:

- Pure penalty: A normal force is generated equal to the contact stiffness multiplied by the penetration, the distance which one face overlaps with another in the contact region. The normal force is therefore given by: $F_{Normal} = k_{normal} * x_{penetration}$.

- Augmented Lagrange: This also a penalty-based method which uses the same calculation method as the Pure penalty method but adds an extra term thereby increasing solution time but reducing sensitivity of the solution to the contact stiffness. For the Augmented Lagrange method the normal force is given by: $F_{Normal} = k_{normal} * x_{penetration} + \lambda$.
- Normal Lagrange: This method isolates the contact pressure as a degree of freedom to be solved and removes penetration from the calculation, this negates the influence of a normal contact stiffness but increases required computation requirements.

For this analysis Augmented Lagrange was chosen to provide an accurate result while mitigating the required calculation time and influence of the normal contact stiffness. Finally, under Geometric Modification the Interface Treatment setting is set to "Add Offset, Ramped" with an offset of 0,08mm to bring the bodies into initial contact.

4.4.3.3 Fabrication and assembly tolerances

The allowable tolerances on aluminium extrusions are given in EN 775-9; depending on the type of cross-section, thickness, and location of an element the desired dimension van vary by several millimetres. Figure 67 shows the different categories of these dimensions; the right side of the sample extrusion bears a clear resemblance to the female connector for which A, E, and H are relevant.

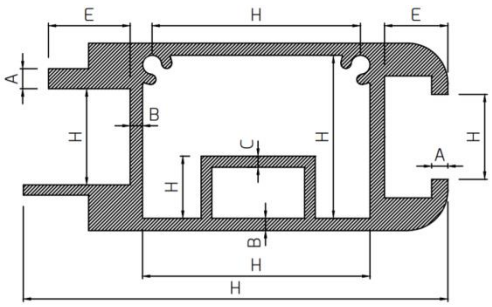

Figure 67: Definition of dimensions A, B, C, E, and H (Alunoor)

Given the dimensions of the main girder cross-section the dimension H will fall between 100 and 150mm, E will be less than 100mm, and A around 30mm. The circumscribing circle (CD) is the diameter of the extrusion press through the profile is formed, for the height of the chosen cross-section a diameter of 200mm was taken. This resulted in the following tolerances:

- For H between 100 and 150mm and CD < 200mm: H ±1,1mm
- For E between 80 and 100mm and CD < 200mm: H ±0,6mm
- For A between 20 and 30mm and CD < 200mm: A ±0,5mm

To allow for smooth assembly of the connection a gap must be left equal to the sum total of the tolerances namely 2,2mm. Next to the variation in dimensions, the straightness of the cross-section along the extrusion direction must also be considered. Speaking with Reint van de Wakker of HYDRO Extrusions it was agreed that a deflection of 1mm per meter is a realistically achievable production tolerance meaning an additional tolerance of 6mm is needed.
Summing the tolerances would result in a total gap of over 8mm which is very large relative to the dimensions of the connection; a more forgiving gap of 5mm is taken to allow better chances for successful implementation.

4.4.3.4 Plug-and-play connection 1

The first analysis was performed with a connection with the same basic geometry as the one shown in Figure 66 however the two horizontal prongs of the female connecter were widened/thickened for a more even distribution of strength in the connection. The dimensions of the male and female parts are shown in Figure 68 below. In ANSYS the left connector is supported along the left edge with a fixed support while a bending moment is applied along the right edge of the right connector. While the calculated magnitude of the moment is 12 kNm/m' a previous design iteration with a greater width gave a governing moment of 31,35 kNm/m'. For a 2D analysis ANSYS applies units in accordance with those specified by the user therefore for results and input in Newton and millimetre, and a model depth of 1mm, a moment of $31{,}4*10^3$ Nmm was applied.

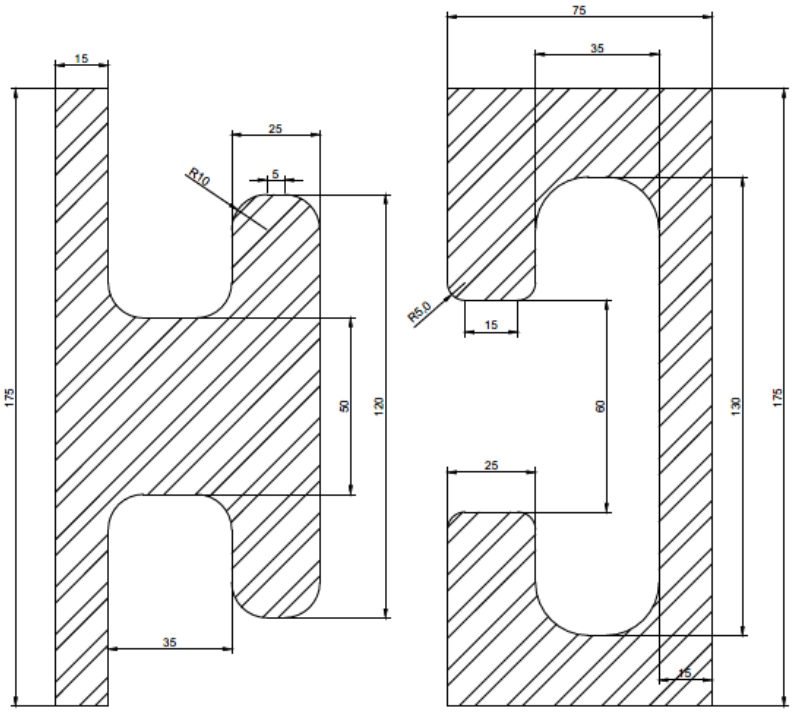

Figure 68: Dimensions of the male (left) and female (right) components of the connection in mm

By analysing the results for the deformation of the connection and the contact information generated by ANSYS, shown in Figure 69, it can be concluded that the behaviour is being accurately modelled; the positive bending moment applied which produces tension in the bottom and compression at the top match the deformation of the connection. The contact status also indicates that the bottom prong of the female connector is being 'hooked' by the male part and that the resistance is generated through frictional contact.

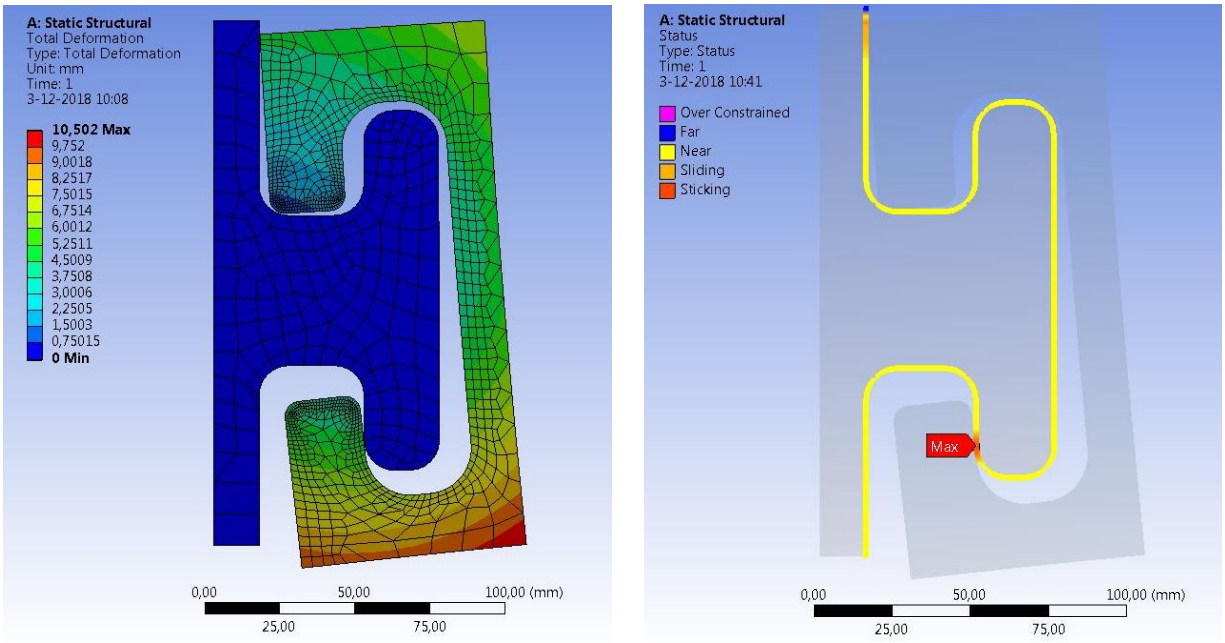

Figure 69: Deformation of the connection and information on interface contact

The results for the global stresses were skewed by a singularity in the top left corner of the female part, this sharp edge produced the highest results in a single node while nearby nodes displayed stress well below yield stress. For this reason this result will be regarded as anomalous and disregarded further in the analysis.

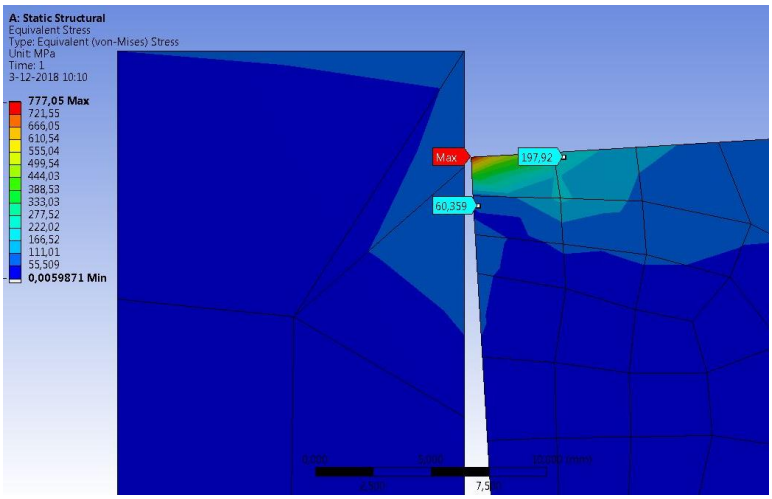

Figure 70: Stress singularity due to sharp geometry at a corner

In the lower part of the connection two critical points can be identified; the contact area between the connectors and the lower prong of the female connector. In the former the pressure is of 356 MPa which exceeds the yield strength of the material, however given the minute area over which it acts this will be redistributed to a safe equilibrium position. The foremost issue with this connection, and the reason for which an improved configuration will be proposed, are the tensile stresses in the lower prong

of the female connector; here the stresses are well in excess of the allowable stress and thereby compromise the structural integrity as well causing permanent deformations which may hinder disassembly and future reuse. An overview of these stresses is given in Figure 71.

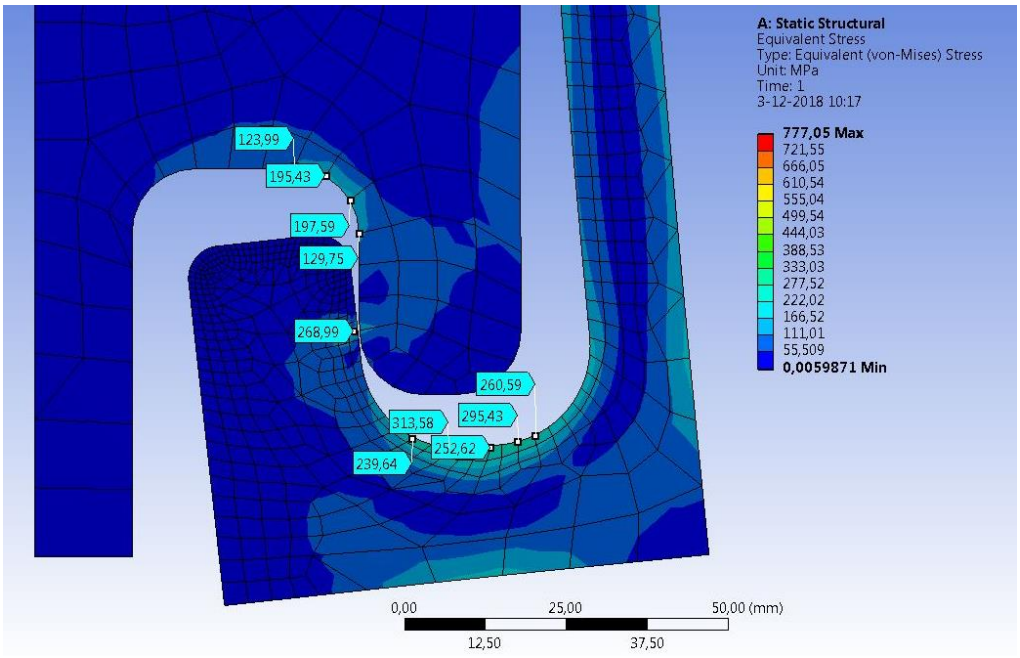

Figure 71: Equivalent von Mises stresses in the lower half of the connection

4.4.3.5 Plug-and-play connection 2

Based on these results a modified plug-and-play connection is proposed in which the lower prong extends further to increase the stiffness in this region while the top prong is reduced in thickness. The top left corner of the female connector has also been rounded off to remove the singularity from the stress calculation and improve the quality of the displayed results. In the previously critical area along the lower prong the stresses have been significantly reduced to around 50MPa while an increase occurs in the top prong due to the now reduced thickness. The stress is highest in this part of the connection however it remains below 100MPa over the majority of the thickness with peaks of 140MPa, this is still well below the 0,2% proof stress of 260MPa at which plastic deformation occurs.

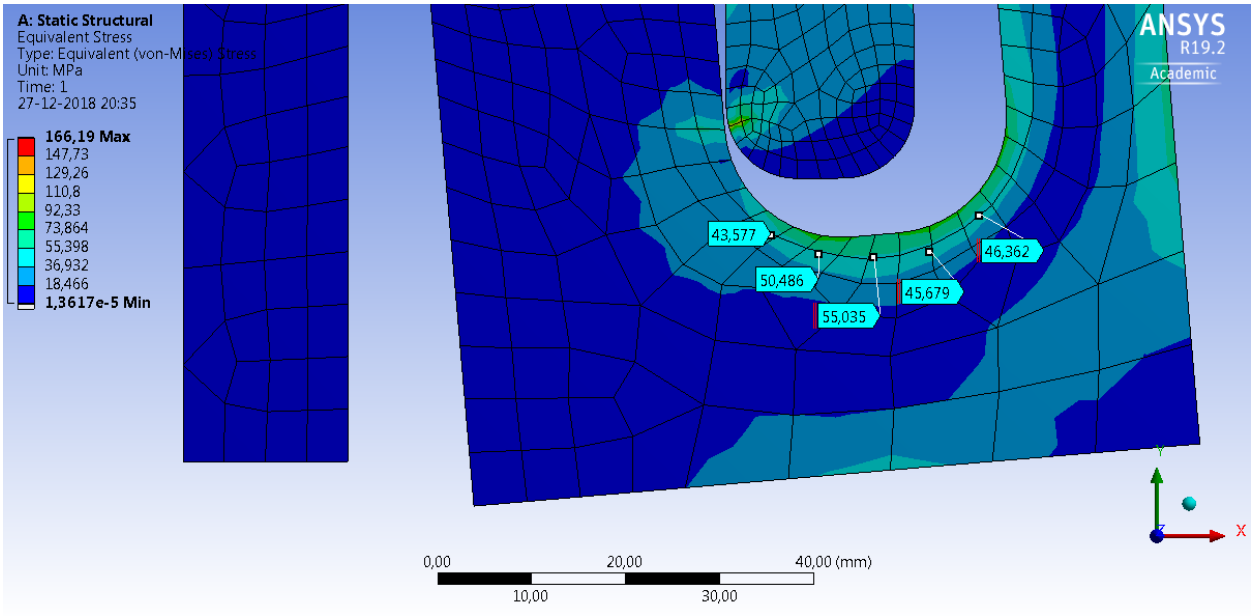

Figure 72: Von Mises stresses in the bottom prong of Plug-and-play connection 2

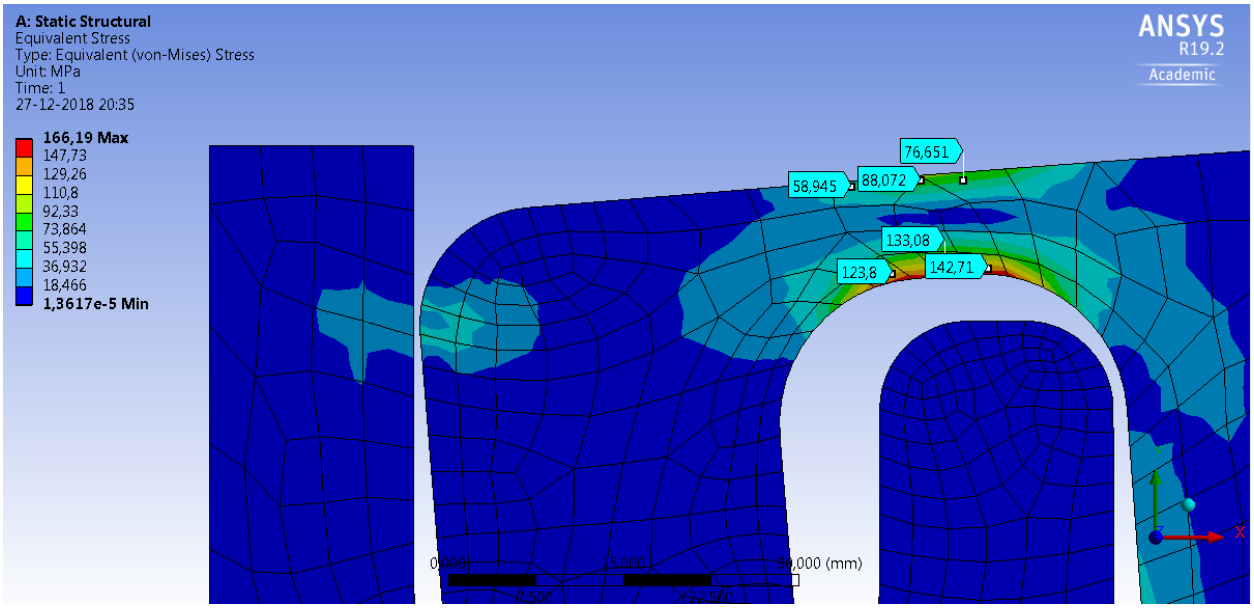

Figure 73: Von Mises stresses in the top prong of Plug-and-play connection 2

From these analyses it can be concluded that the plug-and-play connections have ample resistance given appropriate design however the main issue is the rigid body rotation caused by the gaps left between the male and female connectors. An idealised version of Plug-and-play connection 2 was analysed in which the gap was set to 2mm to minimise its influence on this rotation, the deformation results are shown in Figure 74.

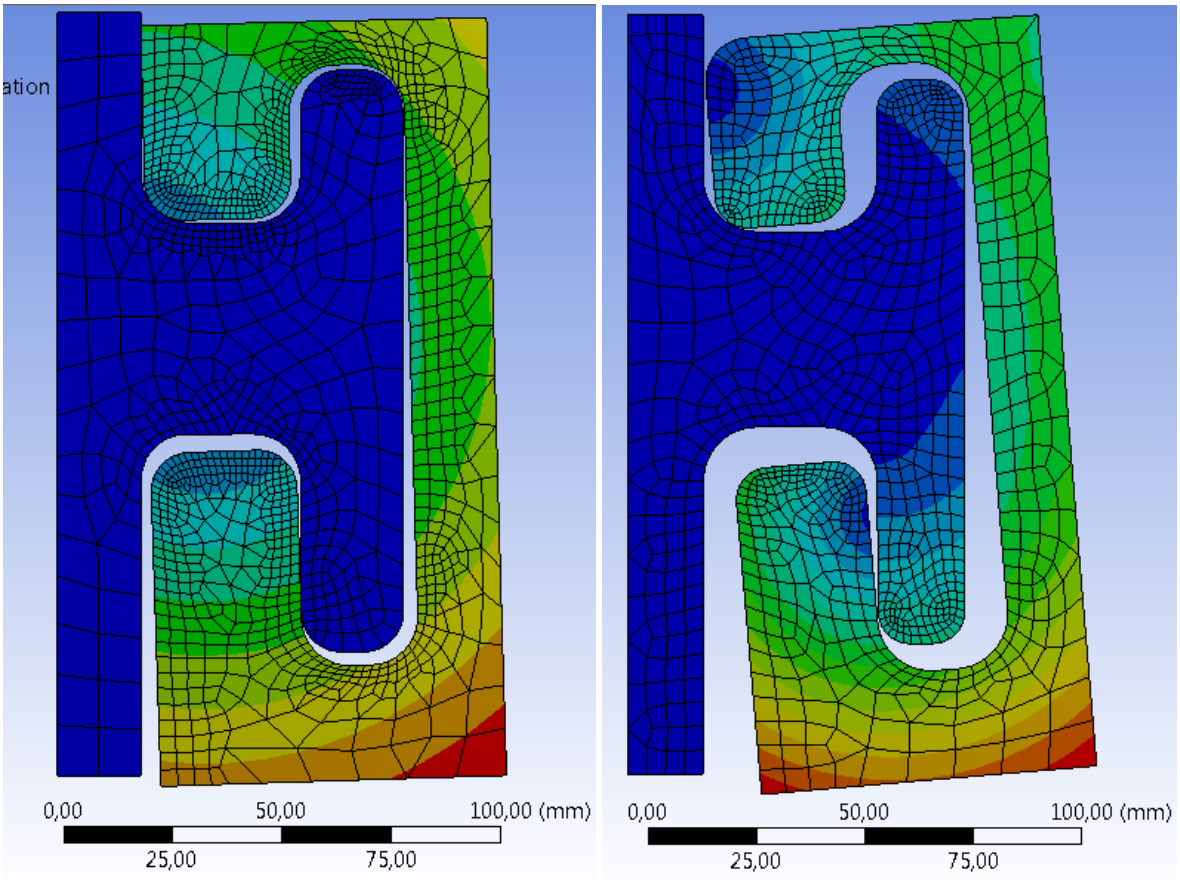

Figure 74: Comparison of total deformation of the idealised (left) and 'real' (right) versions of Plug-and-play connection 2

Comparing the idealised and non-idealised versions of Plug-and-play connection 2 it can be seen that the majority of the rotation indeed occurs due to the gap required for assembly. Current fabrication tolerances determined by the extrusion process due not allow for a gap as small as shown in the idealised situation to be used therefore the plug-and-play connection must be rejected on this basis.

4.4.4 Bolted connection

4.4.4.1 Geometry of the connection

In order to ensure that the structure can be fabricated and assembled a bolted connection will be used; the assembly is composed of an overlapping end segment of the extrusion as shown in Figure 75. It was chosen to provide a connection in which one side can fit into the other to provide added stability during erection and symmetry for moment transfer. Furthermore, a gap has been left above the connection to allow for a filler piece to be installed creating an even deck.

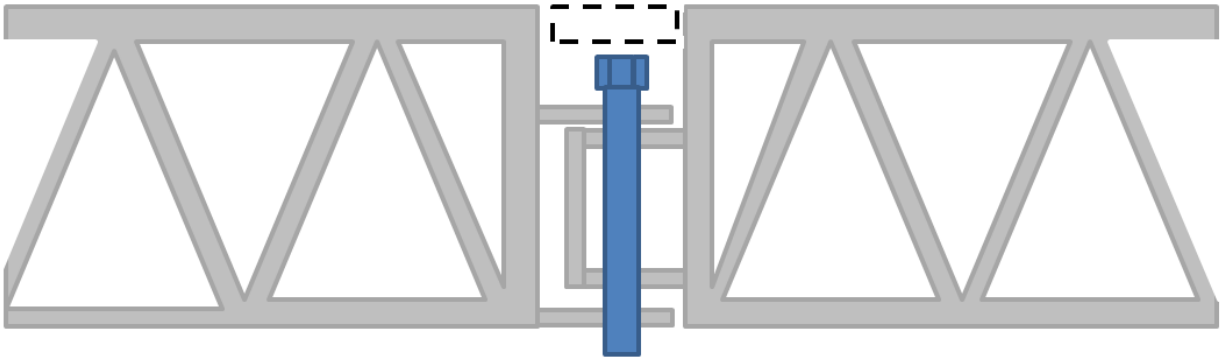

Figure 75: Sketch of the bolted geometry for the transverse connections

5.4.4.2 Effect from the moment: Shear resistance of the bolt

From Table 8.5 of EN1999-1-1 the shear resistance of the bolt per shear plane is given by:

$$F_{v,Rd} = \frac{\alpha_v \, f_{ub} \, A}{\gamma_{M2}}$$

In which:

α_v = 0,6 for steel bolts of class 8.8

f_{ub} = 800 N/mm^2 for steel bolts of class 8.8

A = A_s = 245 mm^2 for bolts M20

γ_{M2} = 1,25

This yields:

$F_{V,Rd}$ = (0,6 * 800 * 245) / 1,25 =-94.080 N = 94,1 kN per shear plane, per bolt.

Assuming the moment is distributed evenly across the horizontal shear planes the governing load on the connection is:

$F_{V,Ed} = M_{xy} / z' = 12 / 160*10^{-3}$ = 75 kN/m'

The required number of bolts per meter is $n_{req} = F_{V,Ed} / F_{V,Rd}$ = 75 / 94,1 = 0,80 → 1 bolt per meter

4.4.4.3 Effect from the moment: Bearing resistance of the plate

From Table 8.5 of EN1999-1-1 the bearing resistance of the plate is given by:

$$F_{b,Rd} = \frac{k_1 \alpha_b f_u d t}{\gamma_{M2}}$$

In which:
Single bolt row therefore all bolts are end bolts for which: $\alpha_d = e_1 / (3*d_0)$
Assuming $d_0 = 20+2 = 22$ mm and $e_1 = 28$ mm ($>1{,}2d_0 = 26{,}4$ mm): $\alpha_d = 28 / (3*22) = 0{,}42$
$f_{ub} = 800$ N/mm^2
d = 20 mm
t = 12 mm per plate, two plates per side (top and bottom)
$\alpha_b = \min\{\alpha_d ; f_{ub}/f_u ; 1{,}0\} = \alpha_d = 0{,}42$
$f_u = 295$ N/mm^2 for the chosen alloy AW6082

Assuming $e_2 = 100$ mm
Governing moment due to point load can occur anywhere, edge bolt has the lowest resistance and is therefore critical:
$k_1 = \min\{2{,}8*(e_2/d_0) -1{,}7 ; 2{,}5\} = 2{,}5$

This yields:
$F_{b,Rd} = (2{,}5 * 0{,}42 * 295 * 20 * 12) / 1{,}25 = 59.472$ N = 59,5 kN
$F_{V,Ed} = M_{xy} / z' = 12 / 148*10^{-3} = 81{,}1$ kN/m'.
$n_{req} = F_{V,Ed} / F_{b,Rd} = 81{,}1 / 59{,}5 = 1{,}36 \rightarrow$ 2 bolts per meter

Bearing is therefore governing with 1 bolt per meter length required.
This results in a pitch of $p_2 = 6000 / (12n+1) = 462$ mm.

In compliance with Table 8.2 of EN1999-1-1 for members in compression, as is the case with the modules, a maximum distance is specified to prevent corrosion in exposed members. The maximum allowable pitch is:
$p_{2,max} = \min\{14*t ; 200\text{mm}\} = 200$ mm $< p_2 = 462$mm.
The number of bolts must therefore be increased to reduce the pitch, applying n = 5 bolts per meter length results in:
$p_2 = (6000 – 2*100) / ((5 * 6) + 1) = 187$ mm < 200 mm.
Therefore 5 bolts per meter length is the minimum number that meets the requirement.

The maximum allowable edge distance is given by:
$e_{2,max} = \max\{12*t ; 150\text{mm}\} = 150$ mm > 100mm.
Therefore the assumed edge distance of 100mm does not need to be changed.

4.4.5 Finite Element Analysis of the bolted longitudinal connection

Given the slenderness of the components of the connection a verification using Finite Element Analysis (FEA) was set up to ensure that failure due to local loading does not occur. Here influence of the stiffness of the deck girder and interaction between the connecting plates will be taken into account to verify whether the behaviour of the connection is consistent with the theory for bolted assemblies.

4.4.5.1 Geometry and boundary conditions

The model required a sufficiently fine mesh to provide detailed results of stress and strain near the bolts, non-linearity due to plastic deformation of the aluminium, and frictional contact between plates. For these reasons it was chosen to model a segment of the span with only three bolts in accordance with the strength requirement of two bolts per meter; the girder is then further simplified by isolating two adjacent modules and the longitudinal connection between them. The bolts in the model have a diameter of 36mm, instead of the 20mm determined in the previous calculation, as they were dimensioned based on an outdated configuration of the structure. This represents the only difference between the model and the structure dimensioned with the preceding hand calculation as the geometry and model setup remain unchanged. The behaviour of the connection can be expected to remain the same with a lower resistance as the outcome.

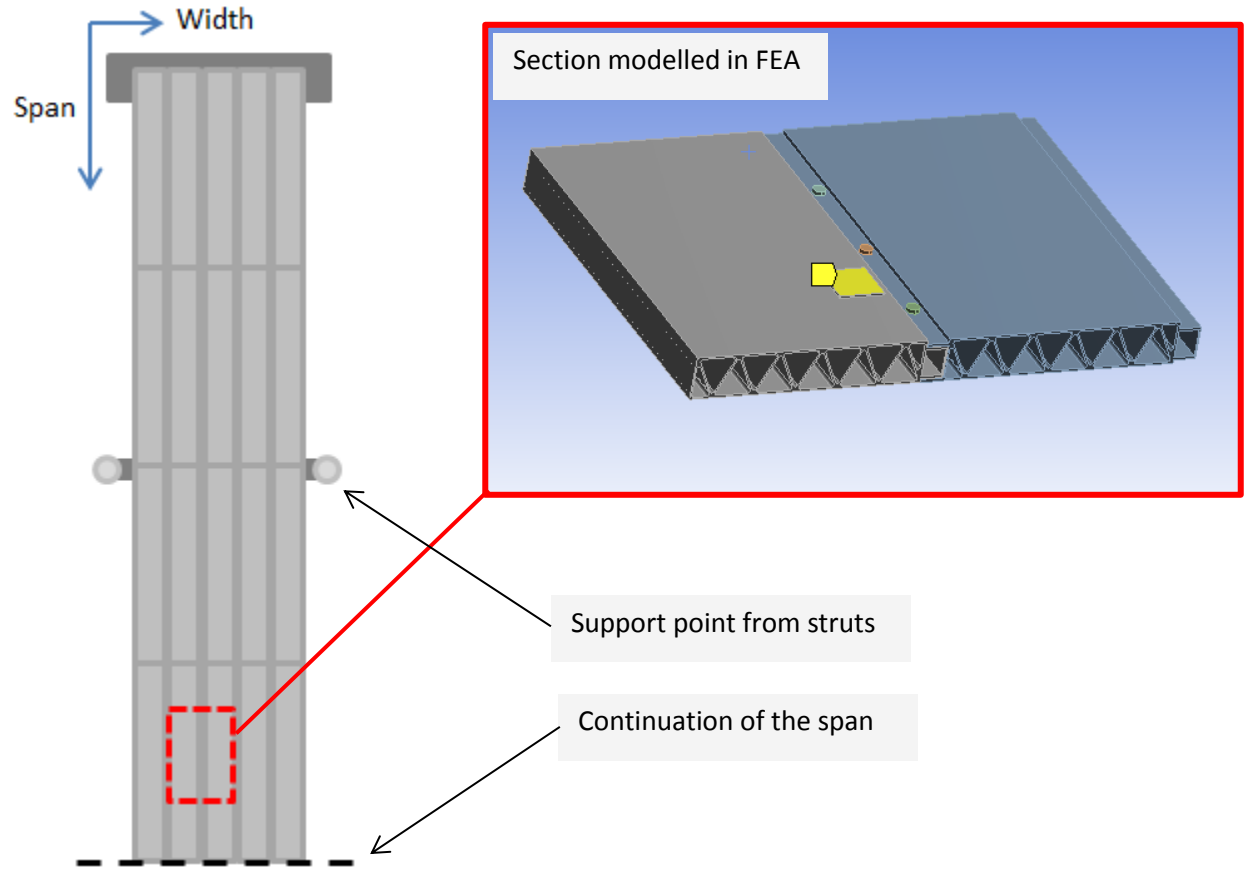

Figure 76: Location of the modelled section within the overall structure

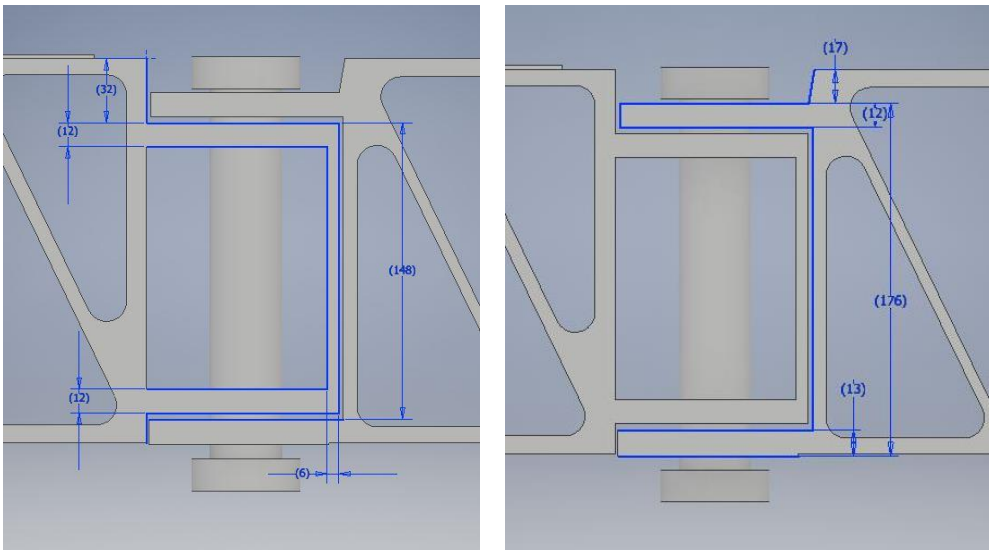

Figure 77: Dimensions of the inner (left) and outer (right) plates of the bolted connection used in the FEA

The critical section is in the span between the support lines of the struts; here the behaviour of the deck girders tends towards plate-like behaviour which results in the bending moment verified in section 5.4.4. The geometry of the structure for the rest is unaltered with respect to that discussed in the preceding chapters.

The two sections of the modules are modelled as a simply supported girder; this is consistent with the assumed situation for the hand calculation of the connection in which a moment is developed in the connection due to vertical loading.

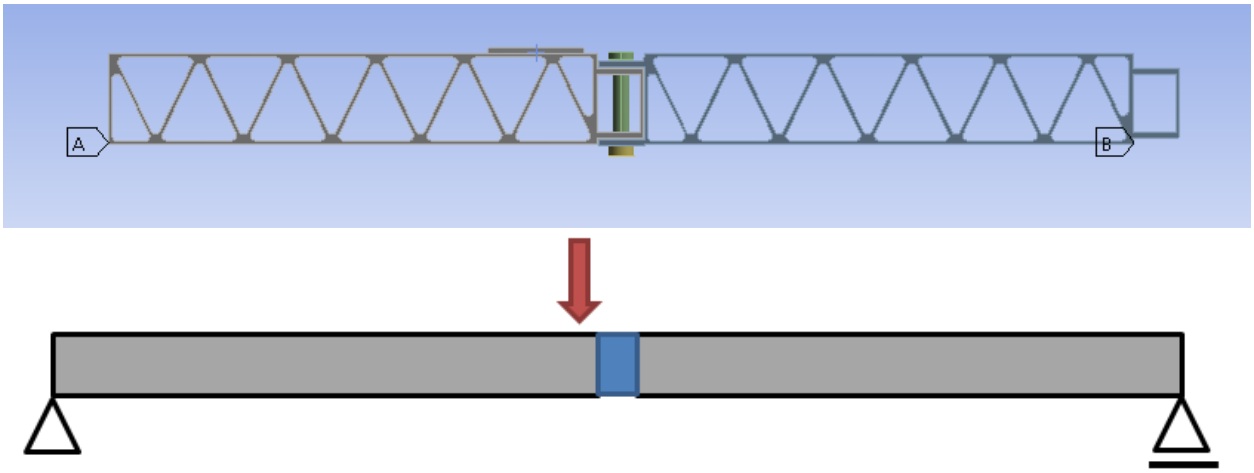

Figure 78: Cross-sectional view of the module/deck girders (above) and sketch of the schematic system used to represent it (below), in blue the connector joining the two girders at mid-span while the red arrow shows the position of the load

The square area, highlighted in yellow in the three-dimensional view of Figure 76, is not a physical part of the model but serves as a point on which to apply the load. It is consistent with the wheel of a service vehicle 200mm x 200mm which is used to investigate the effects of local loading on the connection.

Two main boundary conditions present in the real structure but omitted from the model are; the stiffness of adjacent connections, these would be present at the supports of the girder shown in Figure 78, and secondly the self-weight and bending moment along the span, which acts out of the plane of the above diagrams. The goal of this analysis is the verification of the hand calculation according to NEN1999-1-1 as well as investigating the effect of local loading from a service vehicle. Omitting these additional loads therefore creates a model more consistent with the hand calculation to be verified and creates the mid span bending moment which will be taken by the two horizontal shear planes of the connection. Furthermore, the simplified analysis provides a conservative result as the influence of both the adjacent connections and the global bending moment work in opposite direction, and therefore favourably, with respect to the imposed load.
The axial load from prestressing at ULS is included in the analysis as it provides a significant contribution to the stress and therefore lowers the threshold for plastic deformation begins.

4.4.5.2 Contact and interaction

Unlike the plug-and-play connection investigated previously the bolted connection does not rely on frictional forces to transfer load but rather contact pressure between components; all surfaces have therefore been set to frictionless contact. This reduced the run time of the model without neglecting any significant aspect of the behaviour of the connection; contact forces developed between plates provide a negligible contribution to the resistance and would provide a less conservative analysis.

4.4.5.3 Element type and mesh

Three main types of mesh were used in the analysis depending on the location within the connection; firstly, multizone meshing was used for the bolts creating elements which match the cylindrical shape with quadrilateral elements, this created a uniform mesh for all the bolts. The connected plates used a fine mesh consisting of triangular elements however around the bolt holes the mesh becomes irregular with a greater number of slender triangular elements. The accuracy of the results in these points will be somewhat reduced by these uneven elements however results from single elements or nodes will be not be used meaning the influence of anomalous results concentrated in one location will be minimised. Treatment of the mesh around the bolt holes was unsuccessful and may be caused the need for the mesh to vary in type across the same body (from connecting plates to extruded girder).

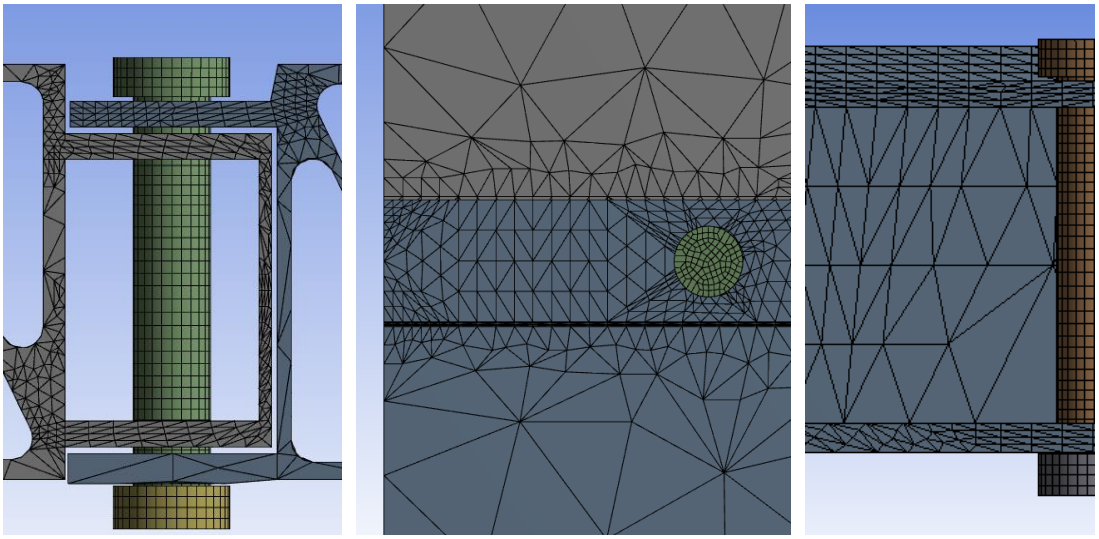

Figure 79: Detailed view of the mesh for the bolts and plates in the connection

A coarse mesh was used for the extruded girders as the detailed results for these are not needed and their significant size makes them the greatest contributor to size and run time of the analysis.

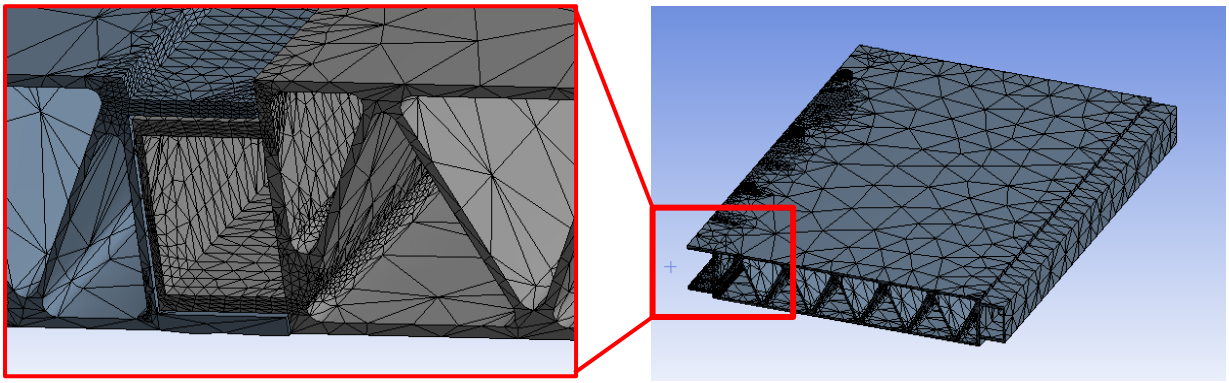

Figure 80: Difference in mesh size for the connecting plates and the extruded girder

4.4.5.4 Test parameters and material properties

The analysis was performed using a displacement controlled setup; this ensures that if failure occurs the model does not deform abruptly thereby causing issues with convergence and compromising previous analysis results. The displacement was applied at the at the wheel load area which is placed between two bolts to maximise the negative influence on the deformation, the sum of the reaction forces from the pinned supports can be used to calculate the vertical force required to achieve the imposed deformation. The displacement was applied at a constant rate of 40 mm/s, the rate of displacement has no influence on the results and this rate is used for convenience so as limit the analysis to one step.

Table 3: Applied displacement for the finite element testing of the connection

Tabular Data

	Steps	Time [s]	Z [mm]
1	1	0,	0,
2	1	0,1	-4,
3	1	0,2	-8,
4	1	0,3	-12,
5	1	0,4	-16,
6	1	0,5	-20,
7	1	0,6	-24,
8	1	0,7	-28,
9	1	0,8	-32,
10	1	0,9	-36,
11	1	1,	-40,
*			

The model consists of two materials; aluminium alloy for the girders and plates and stainless steel for the bolts, the linear elastic properties for both were left as the ANSYS default values. For the aluminium alloy data for the plastic behaviour needed to be input manually, this was achieved through using experimental stress-strain data in combination with the multi-linear isotropic hardening input for ANSYS. Options for both kinematic and isotropic hardening are available in ANSYS; these affect the behaviour under cyclic loading but display the same behaviour under fixed loading as the yield criterion is exceeded only once. The plastic strain rate was set to 0 for a stress of 250 MPa, the 0,2% proof-stress of the material, and subsequent points were derived from data shown in Figure 81. It is important to note that plastic strain graph from ANSYS begins at a stress of 250 MPa however the Young's modulus is linear from 250 MPa to 310 MPa and is consistent between the two graphs.

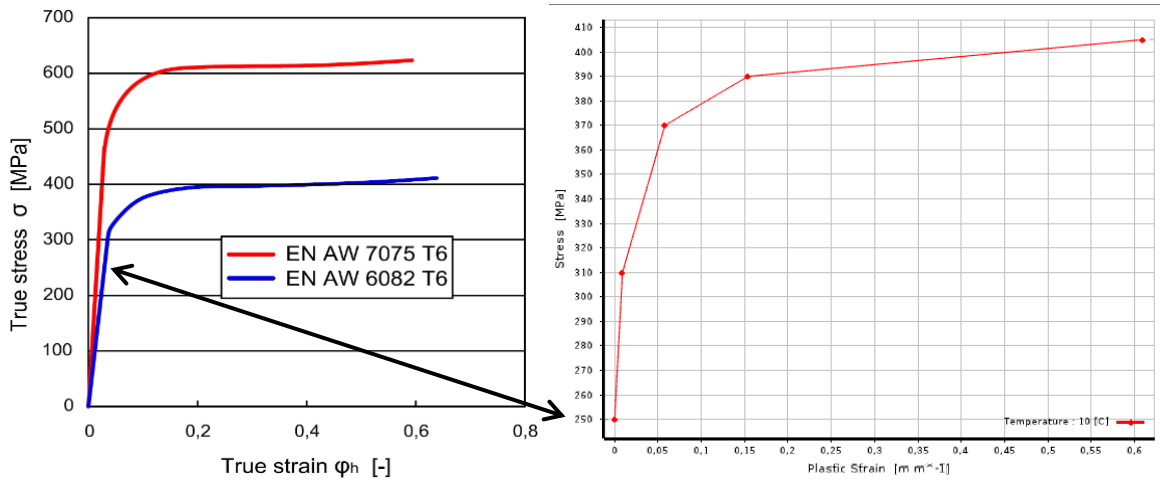

Figure 81: Experimental data for stress-strain behaviour of AW6082 (Kovacova, Kvackaj, Kocisko, & Tiza, 2014) and input data for ANSYS

The stress-strain diagram shows elastic behaviour of aluminium alloy between the stresses of 250 MPa 310 MPa, the aluminium will only begin to exhibit plastic behaviour once the latter stress is reached. These stresses coincide with the 0,2% proof-stress and ultimate strength of the alloy as given

NEN1999-1-1 thereby providing results consistent with the norms. The true ultimate strength of the alloy at which failure occurs is at 410 MPa, in the area between 310 MPa and 390 MPa the alloy undergoes some hardening providing a small added margin of safety which does however come paired with significant deformations which should be avoided.

4.4.4.5 Behaviour of the connection

As mentioned previously, the finite element analysis was performed to ensure the connection was able to withstand concentrated loading from a service vehicle, specifically considering the influence of the slenderness of the plates and spacing of the bolts. Furthermore, a comparison with the theory for bolted connections in shear is needed to ensure the hand calculations do not provide an over-simplification of the true behaviour and show more favourable results than the true situation.

General behaviour

Looking first at the deflection it can be seen that the modelled section behaves consistently with the imposed loading and boundary conditions; the rotation of the two girders is approximately symmetrical with the maximum offset occurring beneath the point at which the imposed deflection is applied. Both supports have zero or negligible reaction forces in x- and y-direction with the rolling support on the right side having total horizontal displacement of 13mm at the final load step. The black outline in Figure 82 shows the position of the model at time t = 0s when no loading has been applied.

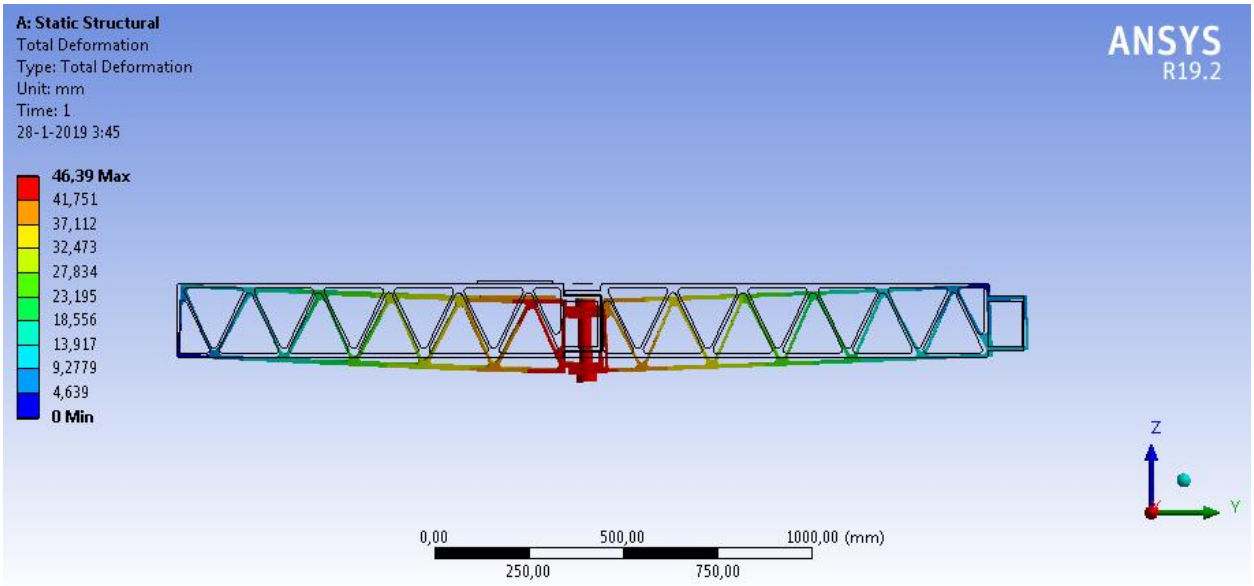

Figure 82: Deflection of the model at the final load step

Starting from the time immediately after t = 0s, as the first displacement is applied the expected set of forces is developed in the connection, two horizontal shear planes separated by a vertical lever arm resist the bending moment created by the displacement at mid-span. In Figure 83 this principle is illustrated through the yellow arrows on the left picture, on the right side the areas circled in red show the rigid body rotation of the connection taking place due to the small gap left between bolt shank and hole.

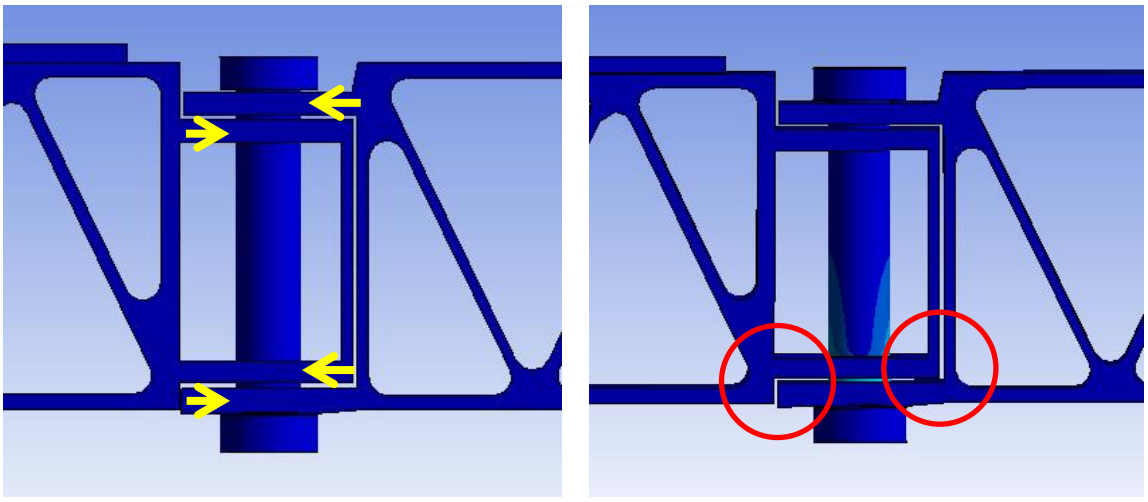

Figure 83: Moment resistance developed through two horizontal shear planes (left) and red circles indicating rotation occurring (right)

In the early steps of the loading process the connection continues to exhibit the behaviour assumed in the hand calculation and rotation takes place around the geometric centre, it is clear from the stress in the bolts however that the distribution of forces is not even across shear planes.
This is illustrated in Figure 84 below; initially the axis of the bolt remains straight but the increased stress and deformation at the bottom side can be seen.

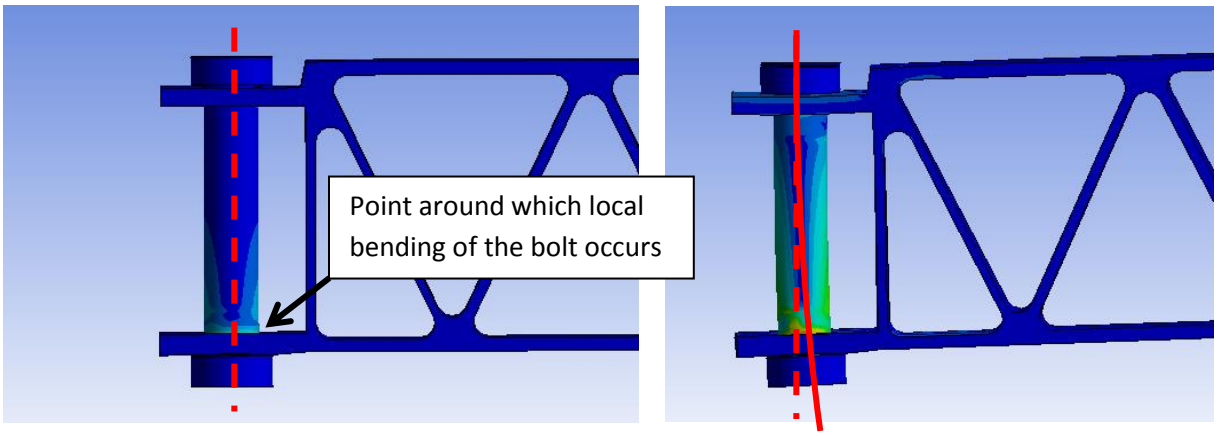

Figure 84: Deformation of the bolt along its axis as the imposed deflection increases over time

This indicates a clear discrepancy between the model and the reality as an M36 Grade 8.8 bolt, as was used in the retired structure, must have a significantly higher stiffness. The stress distribution near the holes also indicate an error in the model as stresses which develop in bolt should closely resemble those in the plate surrounding it which, as shown in Figure 85, is not the case; the bolt experiences stresses a factor 3 or more higher.
Looking at the contact settings for the interface between the bolt shank and the two holes it passes through it was found that the contact regions are ‘bonded’; in ANSYS this means that the faces in contact (bolt shank to inner plate and bolt shank to outer plate) cannot deform and furthermore cannot change separation.

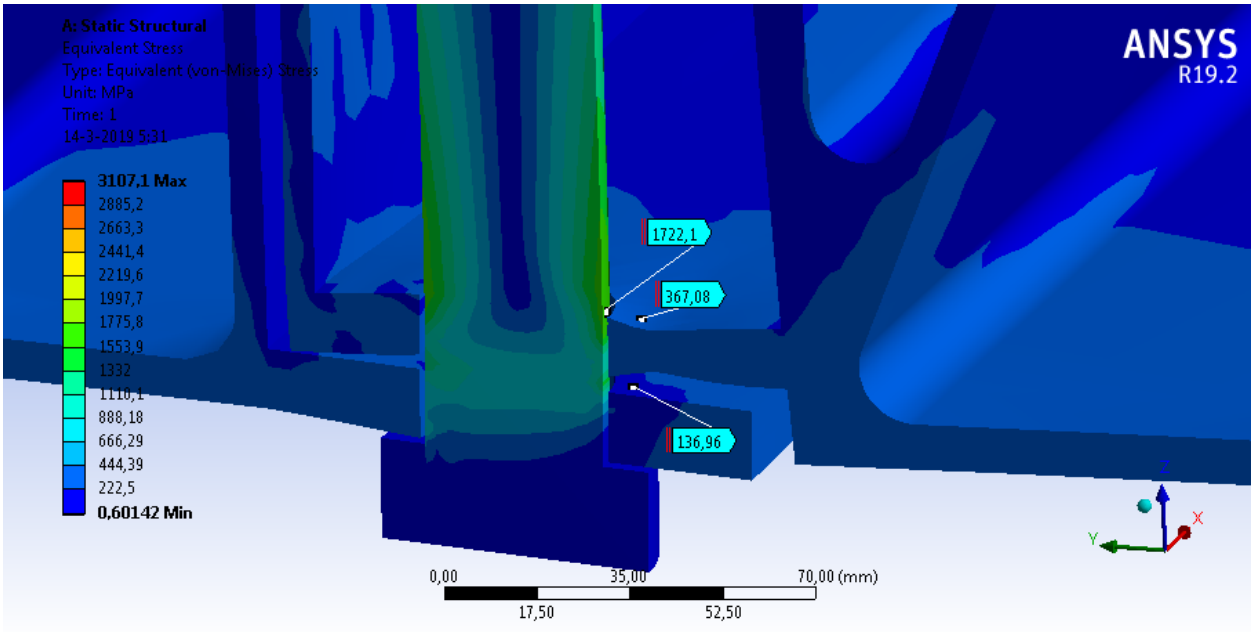

Figure 85: Discrepancy in stresses between the bolt and the connected plates

This has as a consequence that the faces of the bolt holes (red in Figure 86) and their projection on the bolt shank (blue in Figure 86) work as a 'master – slave' system in which one dictates the deformation which the other must follow, which ANSYS calls 'contact' (red) and 'target' (blue).

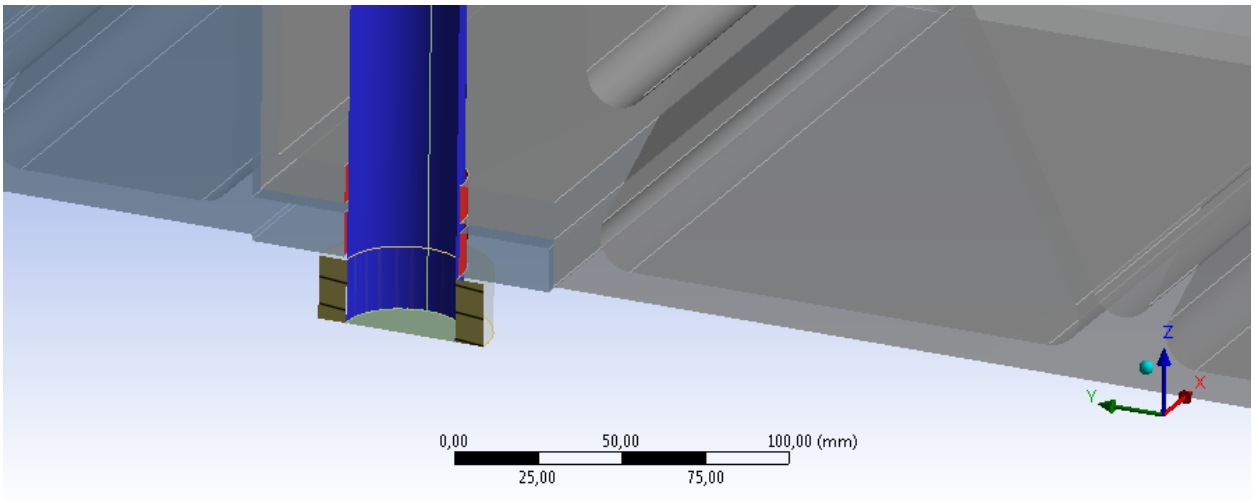

Figure 86: 'Contact' faces (master) shown in red and 'target' face (slave) shown in blue in the same cross-section as Figure 85

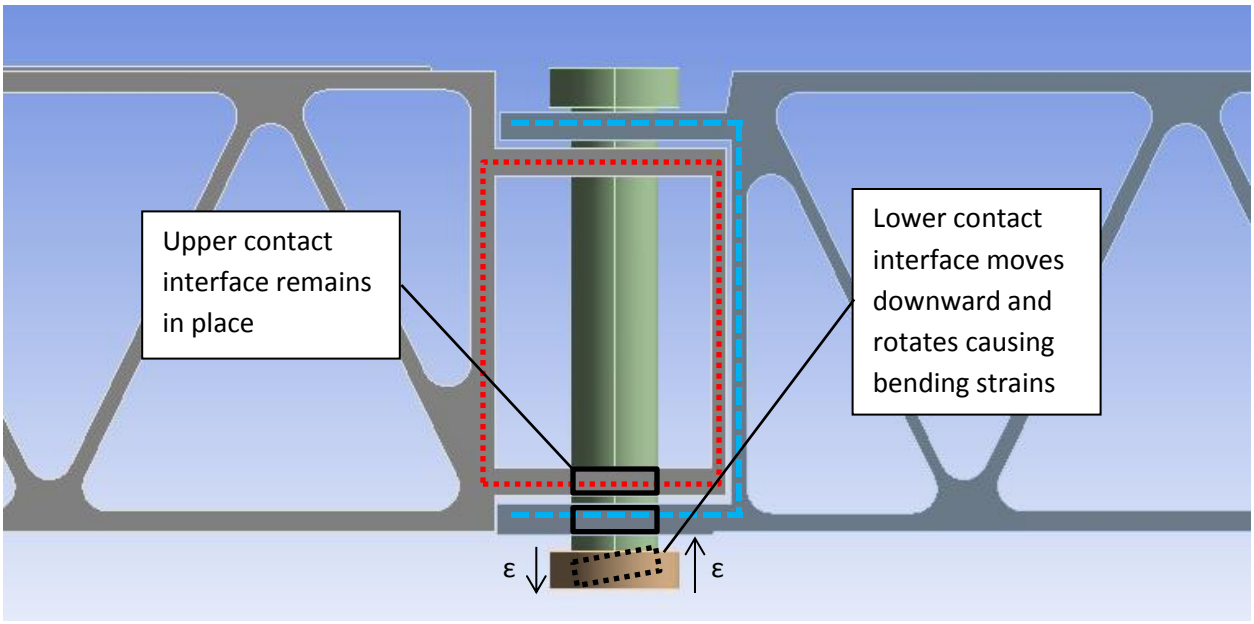

Figure 87: Inner (red) and outer (blue) plates with high and low torsional stiffness respectively

The inner plates form a closed section with high torsional stiffness and maintain their position when the structure is loaded. The lowest plate rotates due to lack of constraints from other elements and position of the load, this forces the area of the bolt shank on which it is projected to rotate with it; this does not occur due to contact between elements but instead due to the manner in which the interface is defined. The difference in rotation between the two bottom shear planes, the top remaining horizontal and the bottom rotating counter clockwise, creates strains in the bolt shank which due to the high E-modulus of steel result in the bending stresses seen.

This demonstrates that the first iteration of the finite element analysis contains an error in the modelling of the interface between bolt shank and plates, a second analysis will be performed ensuring all contact is set to frictionless and accurate modelling of the connection takes place.

4.4.6 Finite Element Analysis of the modified bolted longitudinal connection (increased number of bolts / reduced pitch)

In the hand calculation the number of bolts was required to be set to 5 in order to negate the possibility of corrosion in the presence of a compressive axial load, in the second run the number of bolts per meter is increased to five so that a conservative analysis is performed which better coincides with the hand calculation from the norm.

4.4.6.2 Changes in model setup

In terms of model setup no significant changes were made; the geometry, constant downward displacement, and support conditions were kept the same. The mesh of the lower plate of the outer connection was slightly refined to better match the rest of the mesh in the connection. Finally, the bolts were assigned bilinear plastic behaviour by which after the stress of f_{ub} = 800 MPa is reached the tangent modules becomes almost horizontal, this was done in order to achieve a clearer failure result in the Force-displacement diagram should the bolts reach their allowable stress.

Bilinear stress-strain behaviour of the bolt material for input in ANSYS

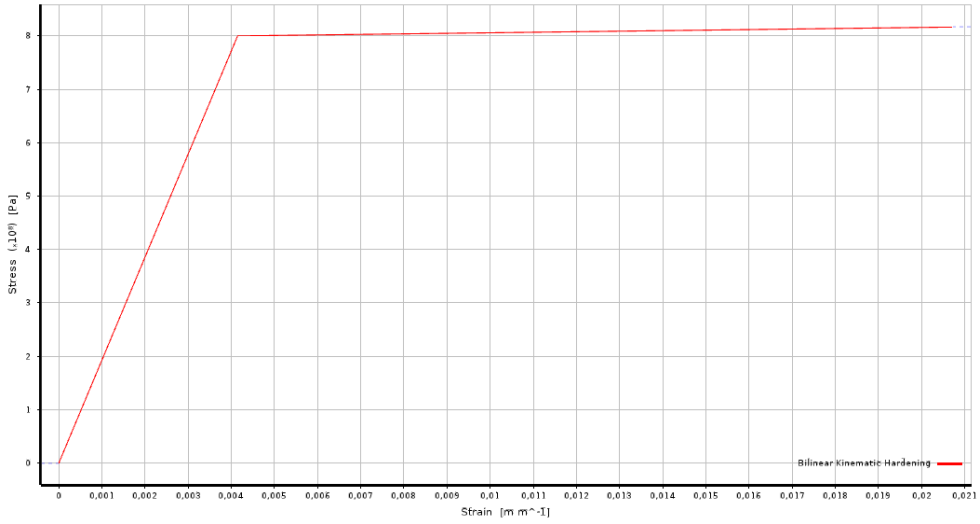

Figure 88: Bilinear stress-strain behaviour of the bolts after f_{ub} is reached

4.4.6.2 Behaviour of the connection

Using the global deformation to once again determine the overall functioning of the model, it can be seen that the behaviour is similar and consistent with the previous FEA run.

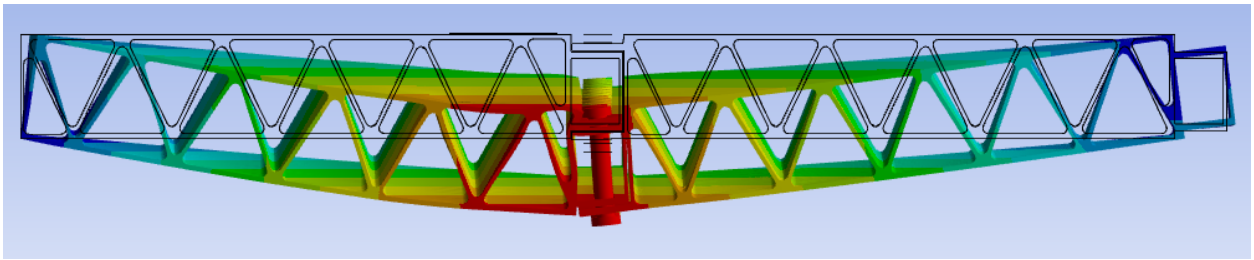

Figure 89: Total deformation of the model at the end of the run, time t = 1s

Focusing on the behaviour of the connection near the point of applied displacement, the behaviour of the elements differs significantly from that of the first FEA run. Due to a combination of deformation of the corner of the left girder, which begins to curl inwards, and rotation of the right girder due to the rolling support, the plates make contact at t = 0,21s.

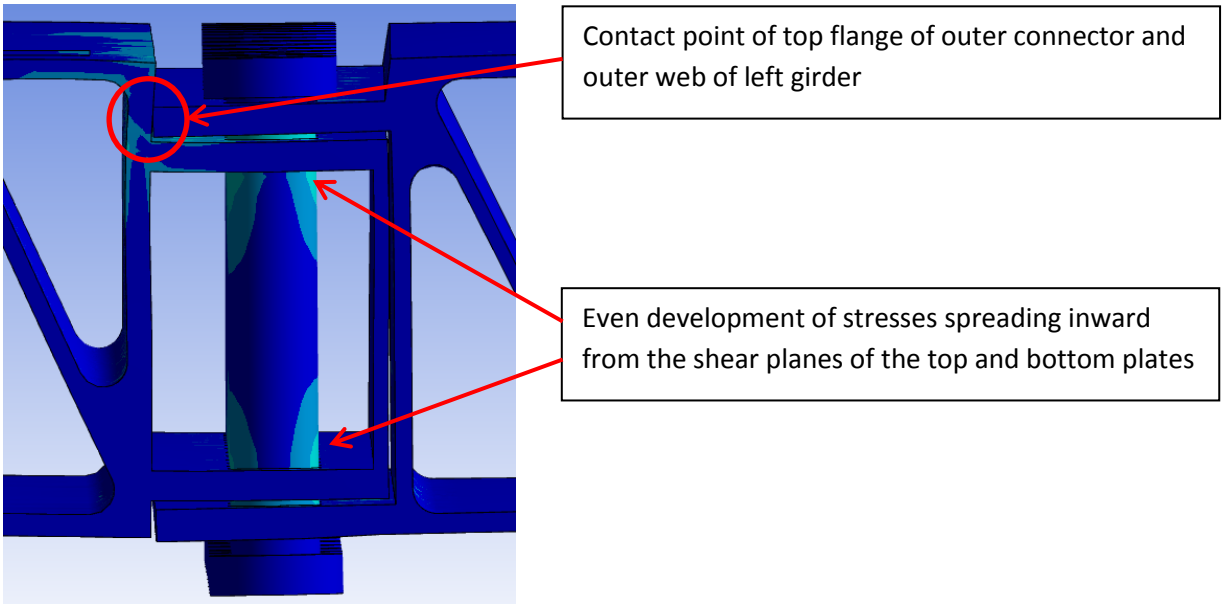

Figure 90: Stress and deformation of the connection at t = 0,21s

The first stresses to develop are in the outer plate and are consistent in shape with the theory for bolted connections (see Figure 91 right); together these indicate that despite the occurrence of undesired contact in the connection the bearing stresses develop evenly in the top and bottom outer flanges.

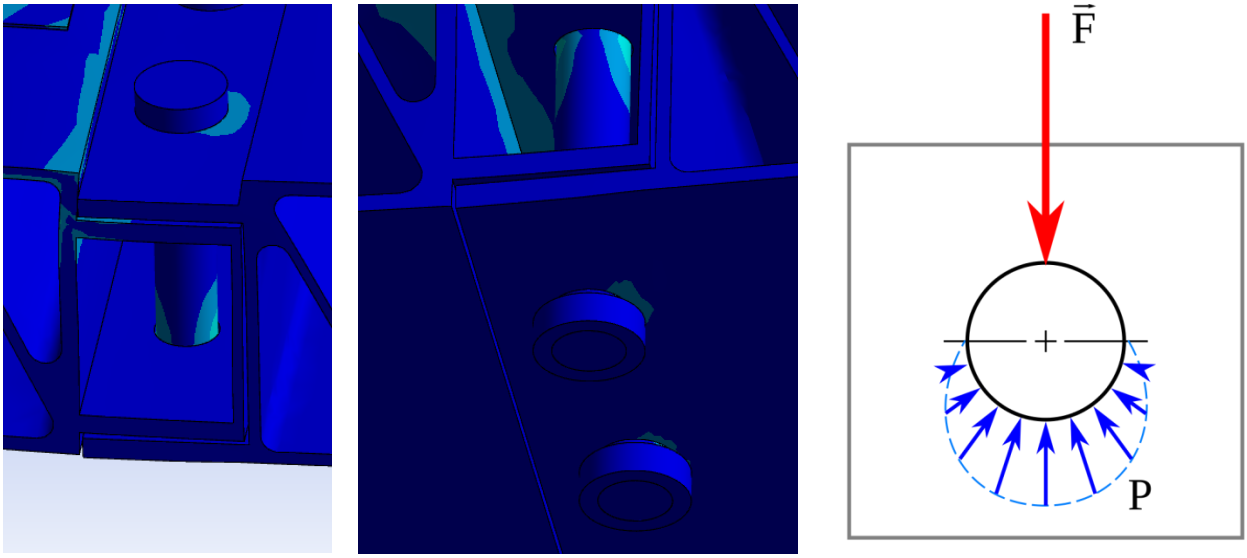

Figure 91: Stress distributions consistent with theory for bearing stress at the top (left) and bottom (middle) of the connection. Distribution of stresses is shown on the right (Cdang, 2015).

As the imposed deformation continues to increase the two sides of the connection maintain their shape, the outer top flange continues to be forced into the web however both deform evenly in such a way that general shape of the two connectors is maintained almost regular without the contact point at the top left creating a change in stiffness. This ensures that the mechanical schematisation of the bending moment due a point load can be taken by a set of horizontal shear planes in the connection.

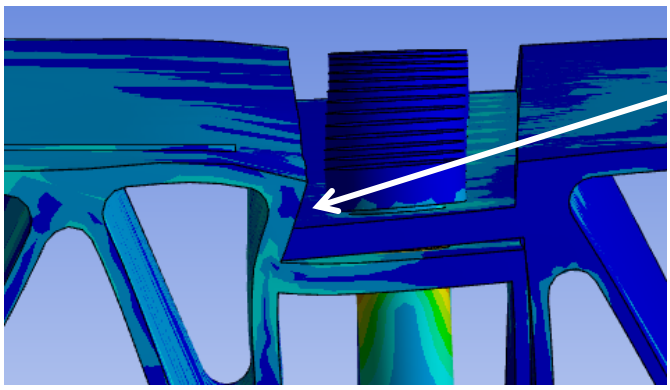

Compression of the plate and deformation of the web, additional resistance due to bearing area

Figure 92: Contact being developed at the top of the connection

The main results from the second run of the FEA are shown in the graph below; the blue line shows the experimental data, the black line is a forecasting trend line, and finally the red dotted line shows the predicted maximum load which can be taken by the connection corresponding to F_{max} = 1350 kN.

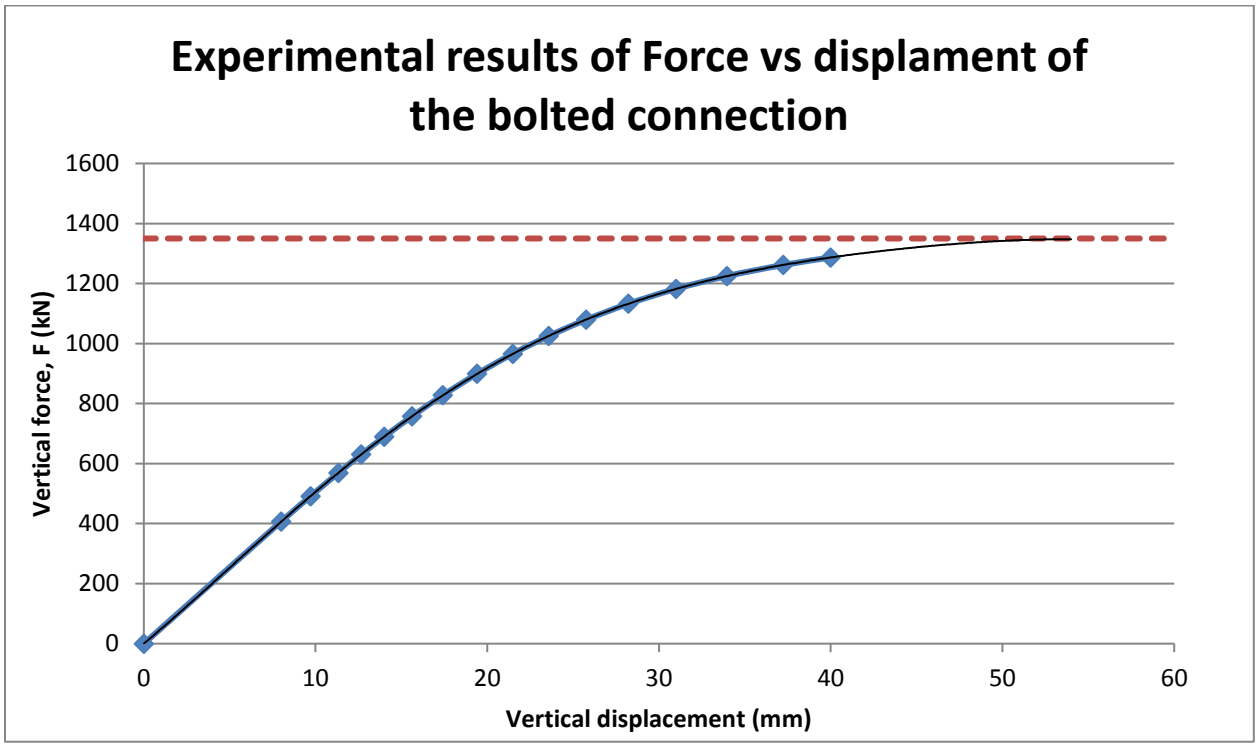

Figure 93: Force-displacement diagram of Run 2

The maximum load as determined by NEN 1999-1-1 is calculated by setting global bending moment in the girder, M = 0,25*F*L, equal to the moment transferred in the connection, M = $F_{B,Rd}$*z, which gives:

$$F_{max,NEN} = \frac{F_{b,Rk,M32} \cdot n_{bolts} \cdot z}{L} \frac{1}{0{,}25} = \frac{282 \cdot 13 \cdot 0{,}176}{2{,}136} \frac{1}{0{,}25} = 1208\ kN$$

This is in the same order of magnitude as the value of 1350kN predicted by the results of the FEA and represents a significant improvement on the first run. It is important to note that the characteristic

value of the bearing resistance was used for the above calculation to provide an accurate comparison between the theory and the FEA, the latter of which does not take any reduction due to safety factors into account. The additional resistance of the FEA result compared to the calculation according to the norms can be attributed to the conservative nature of Eurocode calculations which must account for imperfections or residual stresses that are present in practice. The contact which occurs between the top plate of the outer connecter and the web of the left module also provides an additional 'bearing' force which contributes to the resistance.

In the FEA the peak stresses occurred in the bolt with a magnitude of 870 MPa which is in excess of the allowable stress of f_{ub} = 800 MPa, looking at a cross-sectional view of the critical bolt showed however that this stress was concentrated at a single node. Stresses at surrounding nodes showed significantly lower values indicating that this peak represents an anomaly due to contact pressure with the sharp edge of the bolt hole. Furthermore, shear stresses in the bolt made a significant contribution to the total stress showing that bending of the bolt did not play a critical role in this analysis and further affirming the expected behaviour from the norms.

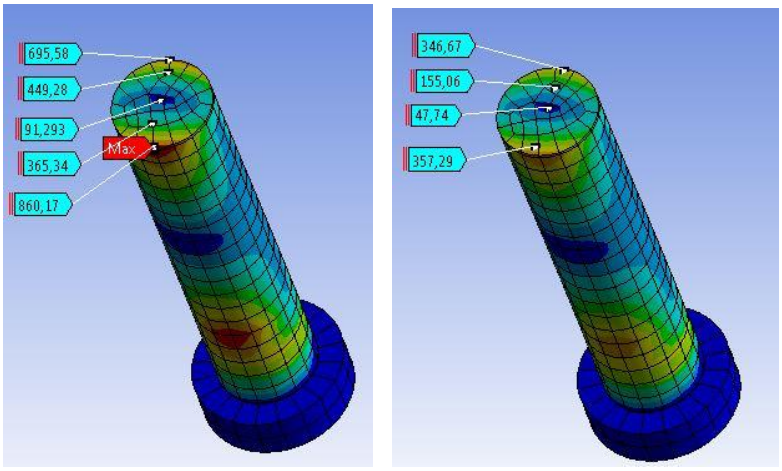

Figure 94: Total stress across the critical cross-section of the bolt (left) and shear stress across the same cross-section

Overall the second FEA run provided results which better matched the behaviour and resistance according to the hand calculations from NEN 1999-1-1; this demonstrated that the configuration using 5 bolts per meter can be implemented with a higher degree of reliability for practical applications. The results of the second FEA run are collected in Figure 95 below; here the loads and resistances of the connection are shown.

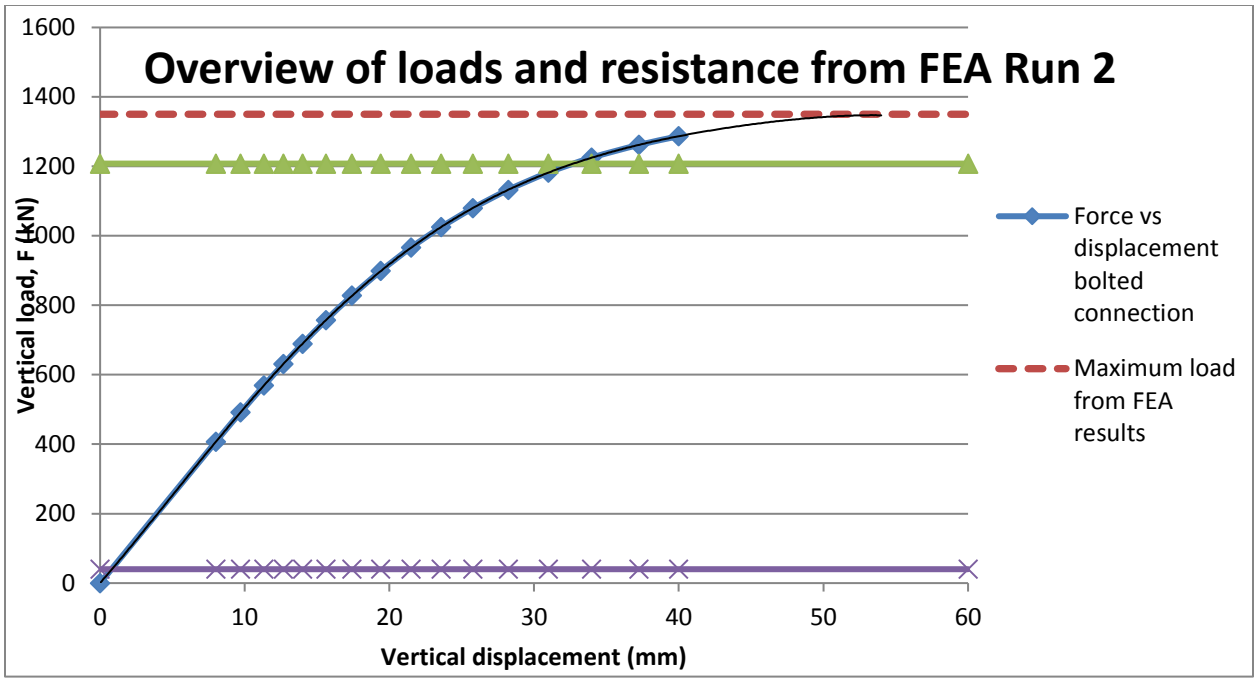

Figure 95: Overview of the loads and resistances for the connection with 5 bolts per meter

4.4.7 Conclusions for the longitudinal connections

The governing load at ULS was calculated to be 12kNm per meter length however which was used to dimension and check the resistance of the longitudinal connections, three types were investigated: slotted, wedged (or plug-and-play), and standard bolted connections. Calculations from a previous iteration of the structure took place with a moment of 31,4 kNm/m' which was kept for the plug-and-play connection test as it provided a conservative analysis.

The slotted connection was dimensioned based on a schematisation in which the bending moment is transferred through a set of horizontal forces divided across the two studs; this resulted in three sets of studs being required per meter length. Given a maximum length of the module of 6 metres 24 individual studs would be need to fit correctly in order to form the connection, in practice ensuring a correct for each would challenging with the added issue of on-site adjustments requiring significant amounts of added time and costs.

The goal of the wedged connection was to create a connection which similarly to the slotted connection could be slid/pushed into place, thereby reducing hindrance, time, and costs associated with assembly, with the advantage of having no welded components with reduced resistance due to the presence of a heat-affected zone. The connection proved to be able to resist the required bending moment however the gaps required for assembly to compensate for the extrusion tolerances contributed to 85% of the 4° total rotation of the connection, this represented unacceptable deflection along the width of the structure as this would be repeated several times within the structure. Resin injection of this connection was investigated and yielded promising results; the resistance remained high and rigid body deformation was eliminated. The connection cannot be implemented due to lack of data regarding physical tests however it is recommended that these tests take place in future research.

The bolted connection was initially evaluated using a hand calculation according to NEN 1999-1-1, this

resulted in two bolts being required to meet the bending moment resistance. Given the slenderness of the plates and the low stiffness of aluminium a finite element analysis was set up to verify the resistance and stiffness of the connection when subjected to local loading, in this case the wheel of a service vehicle in accordance with EN 1991-2. The first FEA run was performed such that the minimum number of bolts was met however errors in the model required a second iteration to be made; here the number of bolts was increased to 5 per meter to match the corrosion requirement. With this correction the total resistance came to 1350kN, which provides ample margin of safety for the 40kN wheel load of the service vehicle, this is around 15% higher than the resistance than that predicted by the Eurocode and demonstrates the connection can safely be implemented in practice.

4.4 Detailing of the structure

In order to ensure the feasibility of the structure a number of modifications must be made or additional details must be added, the most important of these are; the railing of the bridge and its connection to the girders, bracing of the struts and verifying the resistance of connected elements, covers for the transverse and longitudinal connections, and the supports.

4.4.1 Detailing of the railing

The railing will be connected to the girders using the existing longitudinal connections; this is shown in the figure below. In accordance with NEN1990 the load to be taken by the railing is 3 kN/m', taking a standard railing height of 1,1 metres this results in a governing moment of 3,3 kNm/m'. The load can be applied either vertically or horizontally depending on the most critical scenario; given the contact area of the plates the vertical (shear) loading is negligible.

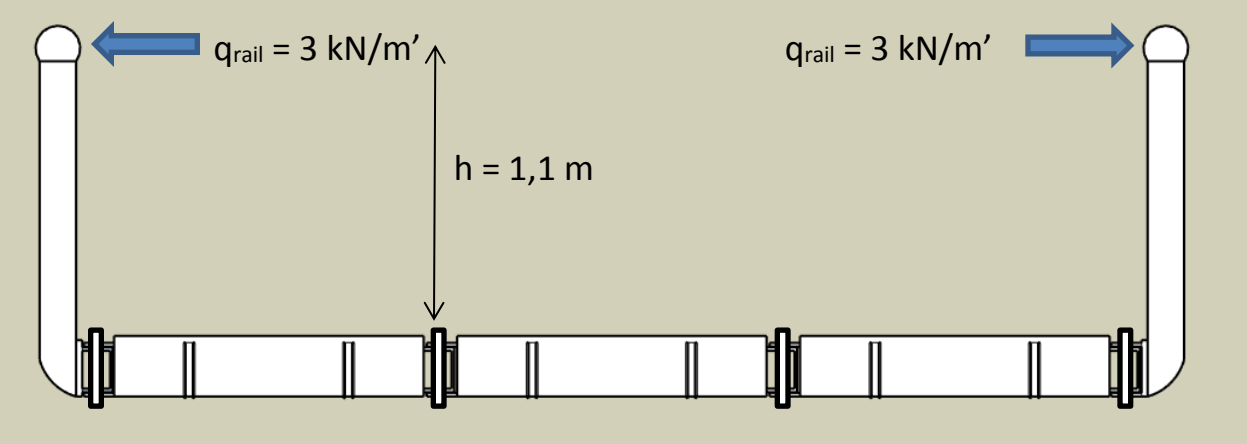

Figure 96: Use of the existing longitudinal connection for the railing and governing load conditions

The critical moment therefore comes to M_{Ed} = 1,5 * 3 * 1,1 = 4,95 kNm/m'.
The governing load for the longitudinal connection was found to be 12 kNm/m', the resistance for this connection is met amply by the configuration with 5 bolts per meter and only 1 bolt per meter would be sufficient to resist this load.

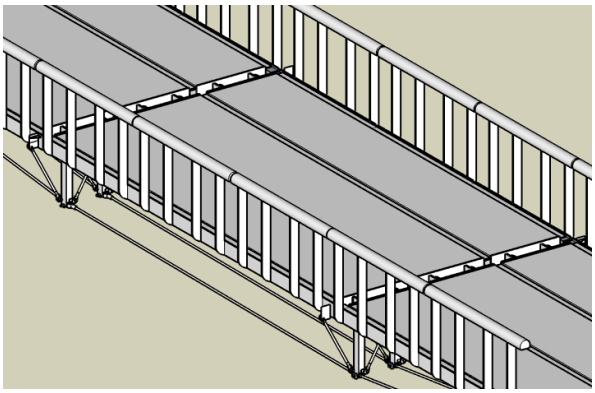

Figure 97: View of the railing as it appears on the structure

4.4.2 Detailing of the struts

The struts transfer the vertical load from the kink in the tie rods to the bottom bolt in the transverse connection, given that these elements are loaded in compression they are susceptible to instability; in particular sway of struts as a group must be prevented.

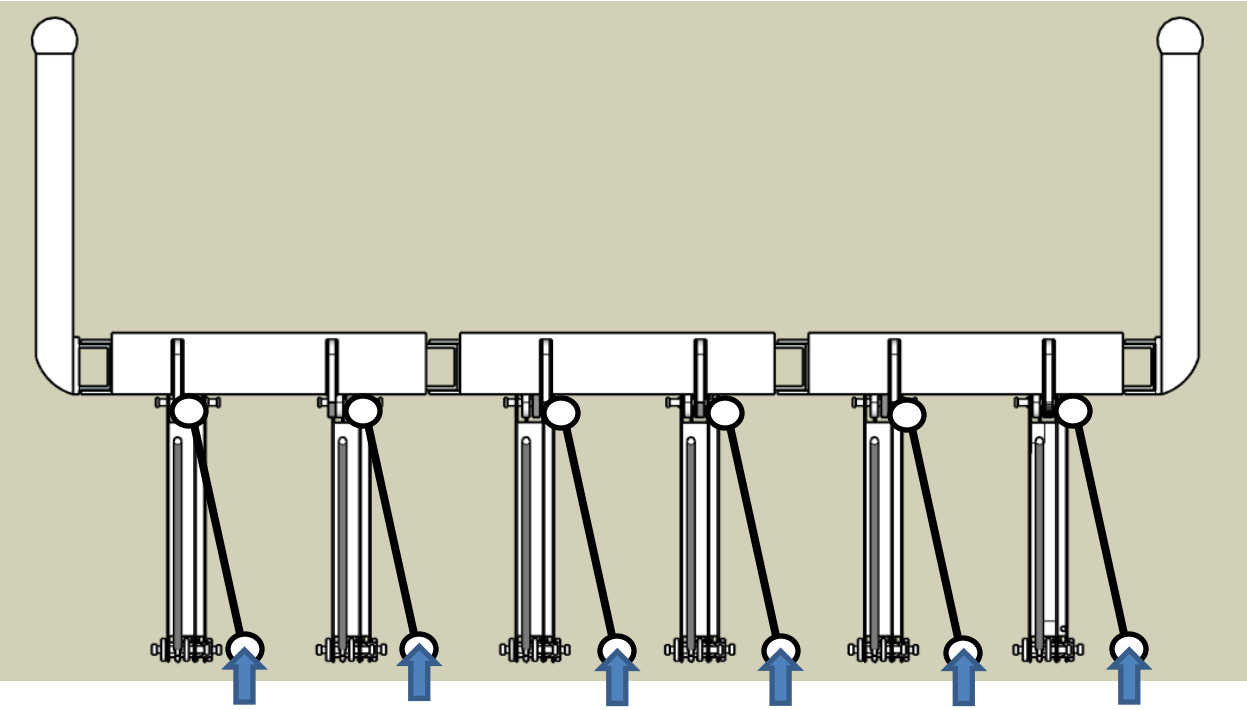

Figure 98: Sway of the struts under compressive loading

A series of pinned rods connected to the struts by means of gusset plates are used to prevent sway, given the limited load on these struts the resistance is assumed to be sufficient and only an overview of the bracing system and its connections is shown.

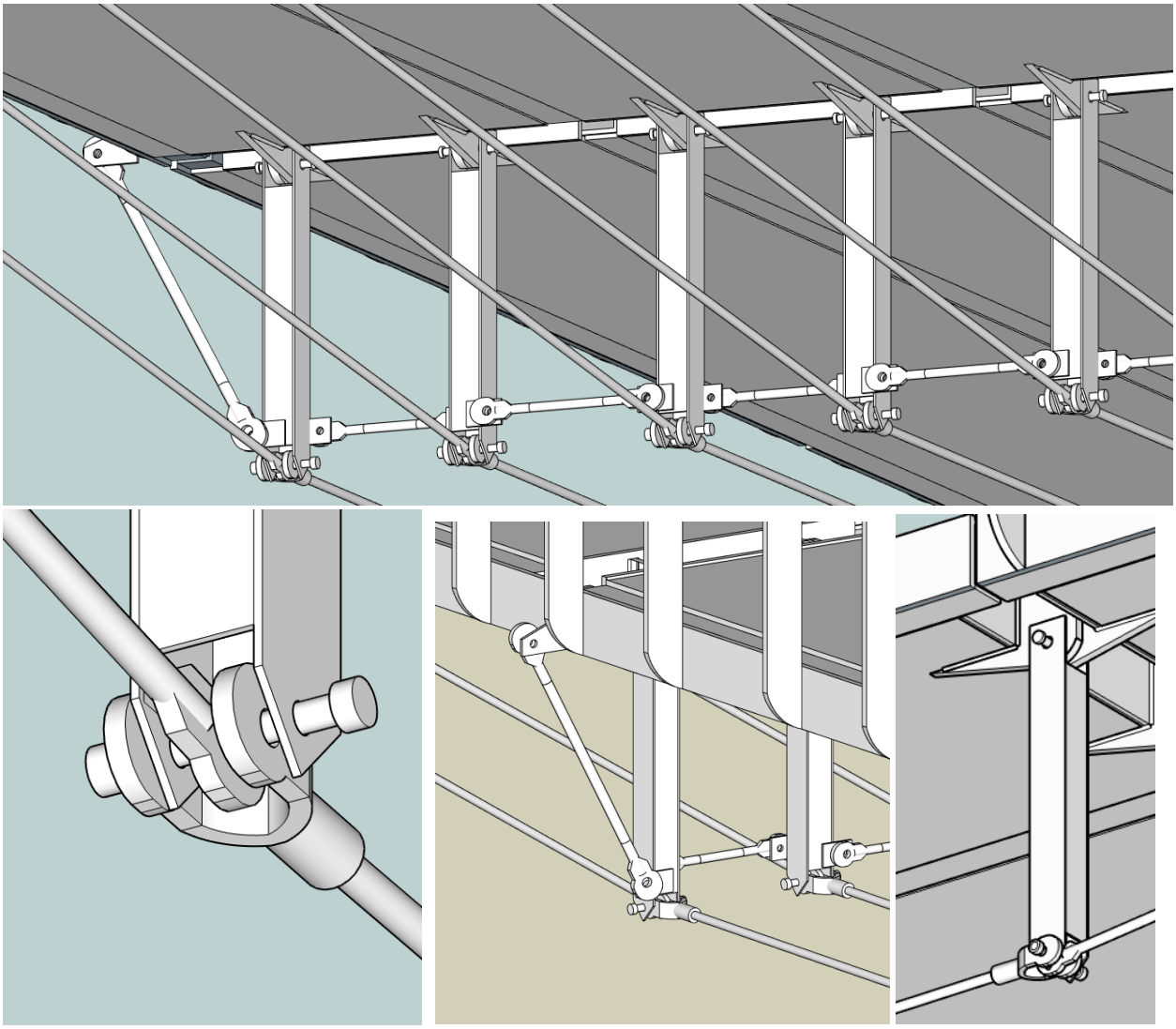

Figure 99: Overview of the bracing system (top), connection tested for shear and bearing resistance (left), end bracing element connected to the railing (middle), and connection between struts and transverse connection without bracing (right)

The struts are dimensioned based on the width of the vertical plates plus additional gaps left for tolerances, each strut consists of a steel S355 rectangular hollow section in which two flanges extend and both ends to allow for a bolted connection be created. The dimensions of the struts are shown in Figure 100.

The following strength verifications are necessary for the struts:

- Buckling resistance of the struts under axial compression
- Bearing resistance of the bolt due to vertical load
- Shear resistance of the bolt due to tension in the tie rods

Buckling of the struts

$N_{euler} = \pi^2 * E * I / L^2$

$E = 210*10^6$ kN/m^2

$I = 2{,}7344*10^{-6}$ m^4

L = 1 m

N_{euler} = 5658 kN

The maximum vertical load in the struts is of N_{Ed} = 24,9 kN, this is significantly smaller than the governing load therefore axial compression is not critical for the struts.

Bearing resistance of the plates on the struts

The bearing resistance of the plates of the struts is given in NEN1993-1-8 as:

$$F_{b,Rd} = \frac{k_1 \cdot \alpha_d \cdot f_u \cdot d \cdot t}{\gamma_{M2}}$$

In which:

e_1 = 40 mm

e_2 = 28 mm

d_0 = 24 mm

$p_2 = \infty$

$k_1 = \min\{ 2{,}8(e_2/d_0) - 1{,}7 ; 1{,}4(p_2/d_0) - 1{,}7 ; 2{,}5\} = 1{,}57$

$\alpha_d = e_1/3d_0 = 0{,}56$

f_u = 470 N/mm^2

d = 22 mm

t = 12 mm (two plates 6mm thick)

This yields: $F_{b,Rd}$ = 86 kN > F_{Ed} = 25 kN therefore yielding of the plates does not occur.

Shear resistance of the bolt

The shear resistance of the bolt, per shear plane, is given by NEN1993-1-8 as:

$$F_{v,Rd} = \frac{\alpha_v \cdot f_{ub} \cdot A}{\gamma_{M2}}$$

In which:

α_v = 0,6 for Grade 8.8 bolts

f_{ub} = 800 N/mm^2

A = 303 mm^2 for bolts M22

This yields: $F_{v,rd}$ = 234 kN > $F_{Ed,rod}$ = 202 kN therefore failure of the bolt does not occur.

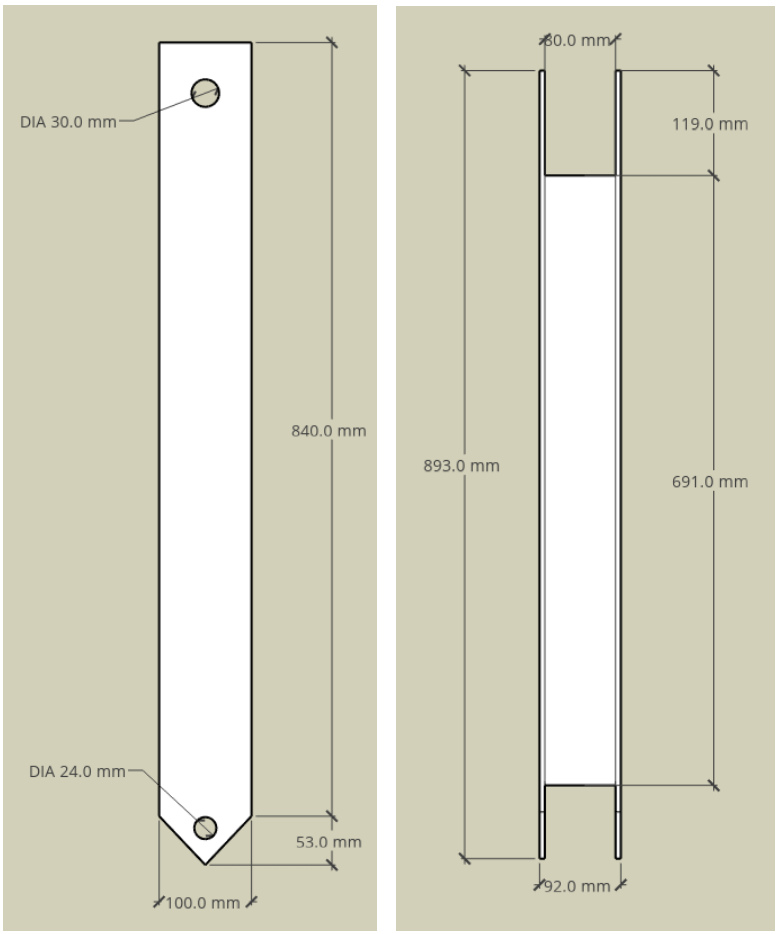

Figure 100: Dimensions of the struts

4.4.3 Detailing of the covers

4.4.3.1 Covers for the transverse connection

The area to be covered is of 1128mm by 200mm and will consist of a girder connecting to the top set of bolts in the transverse connection.

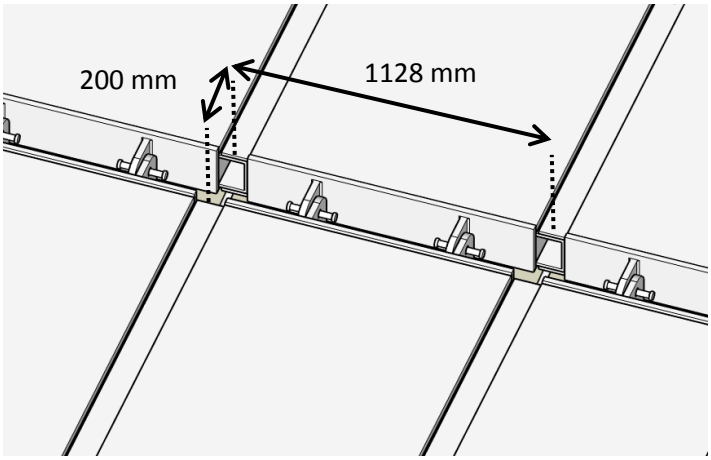

Figure 101: Dimensions of the cover plate required

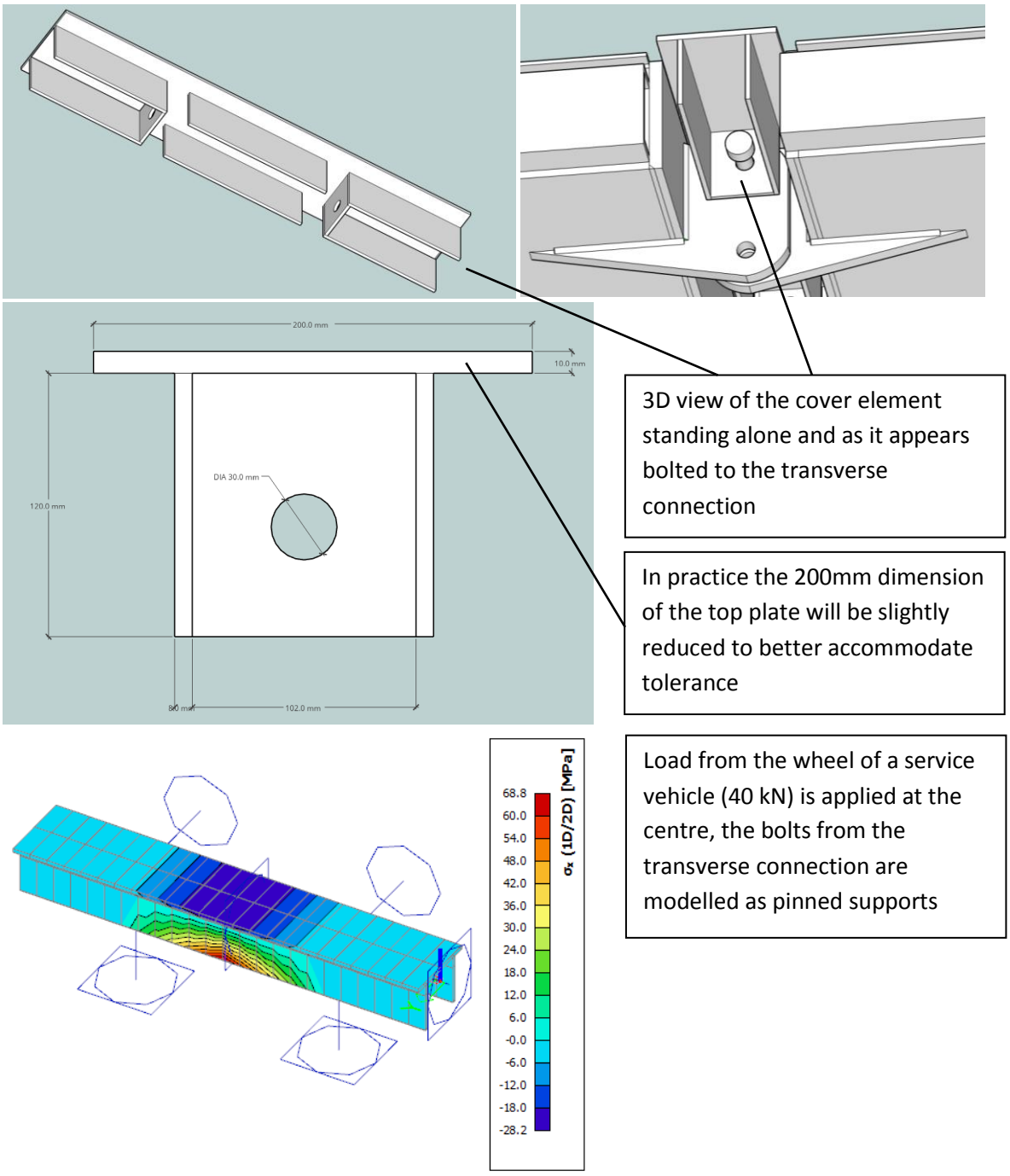

Figure 102, Figure 103, Figure 104, Figure 105: View of the transverse connection cover (top), dimensions of the component (middle), stresses in the component due to wheel load (bottom)

4.4.3.2 Covers for the longitudinal connection

In order to ensure demountability of the longitudinal bolted connection intrusion of the epoxy for the deck must be prevented, this is done by creating an extended flange which covers the connection. This element can be extruded together with the connection or welded on afterwards.

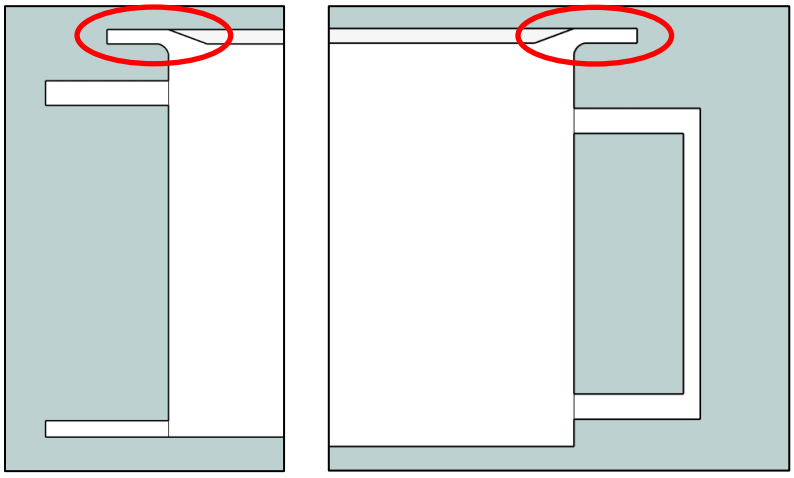

Extended flange at each end of the module to cover the bolted connection

Figure 106: Extended flange plates at the left and right sides of the modules

Covering the top side of the connection however prevents the use of standard bolts, for this reason hammerhead bolts in combination with long slotted holes must be applied. The configuration and assembly method is shown below.

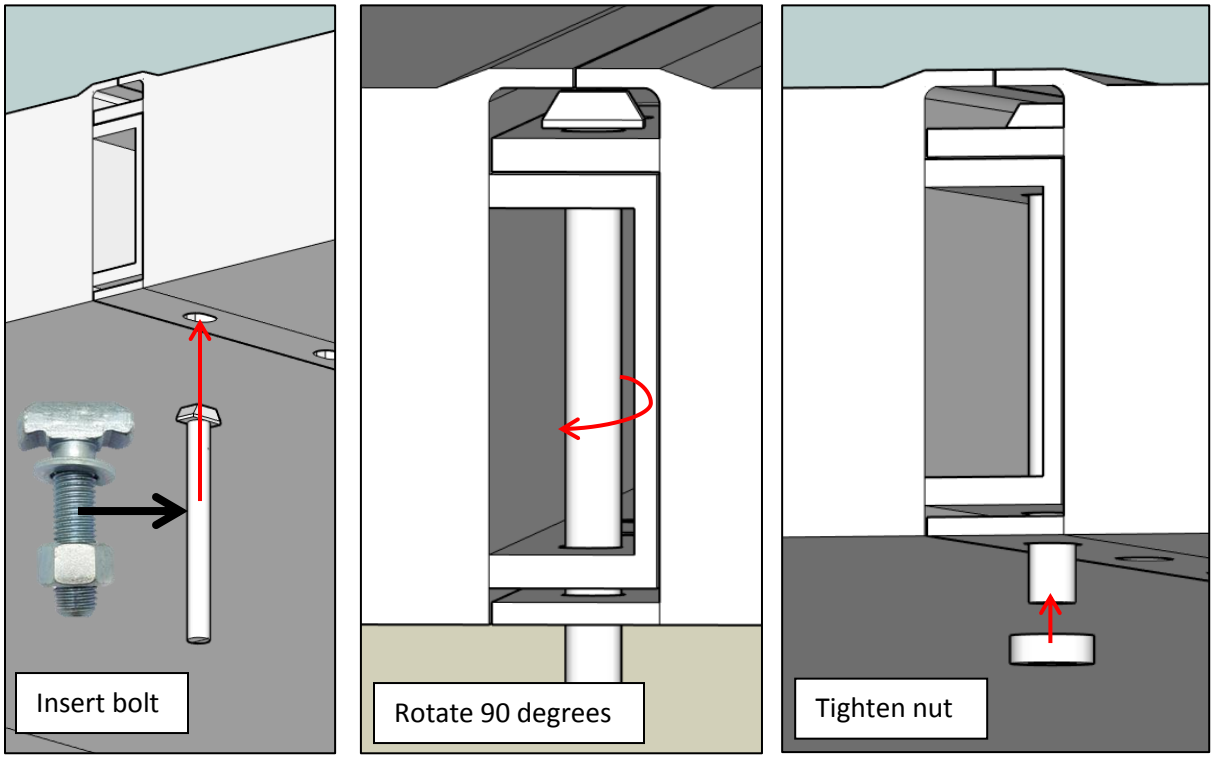

Figure 107: Assembly procedure for the hammerhead bolt

In accordance with Table 8.5 of NEN1999-1-1 the following conditions must be met for bolts in slotted connections:

- The factor α_b must be limited to 0,66 instead of 1,0: in the connection implemented the factor α_b = 0,42 therefore no reduction is necessary.
- The bearing resistance of the bolts in holes longer than 1.5 to 2.5 the diameter must be multiplied by a factor 0,65: the resistance of the connection must be reduced by this factor however given that 5 bolts are used rather than the required 2 a significant margin of safety remains for the connection.

The connection therefore has sufficient resistance and can be assembled in practice.

4.4.4 Detailing of the supports

The structure consists of a simply supported beam; one end must prevent displacement and allow rotation (pinned) while the other must also allow displacement in the longitudinal direction of the span (rolling) to prevent stresses due to thermal expansion. The low self-weight of the structure is such that uplift of the structure due to wind loads is possible, the supports must therefore also be anchored to prevent upward displacement.

Pinned support

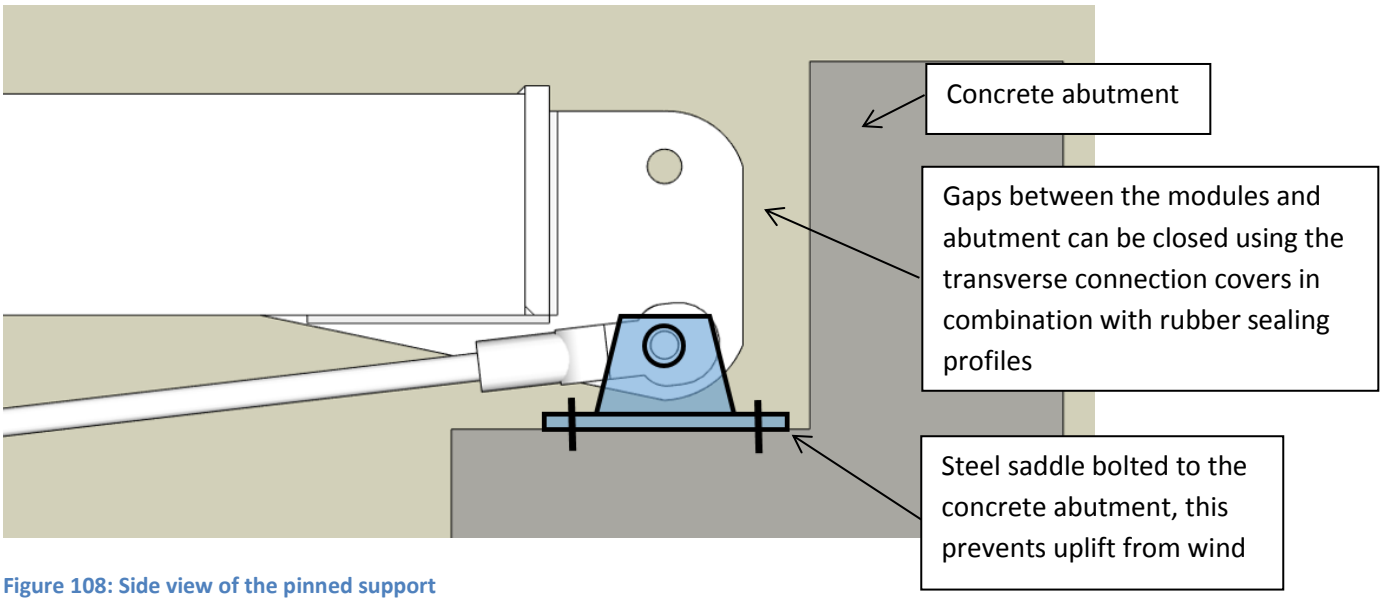

Figure 108: Side view of the pinned support

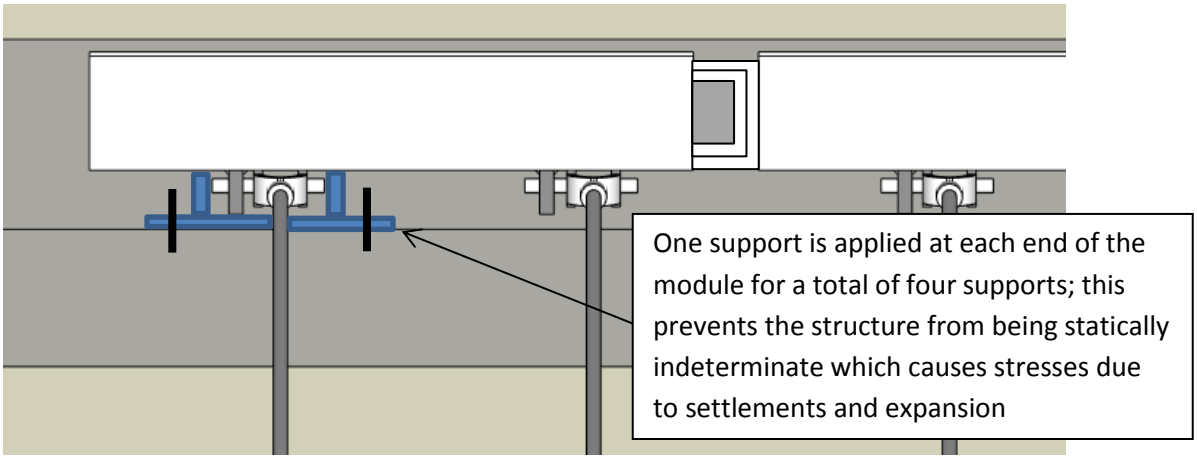

Figure 109: Front view of the pinned support

Rolling support

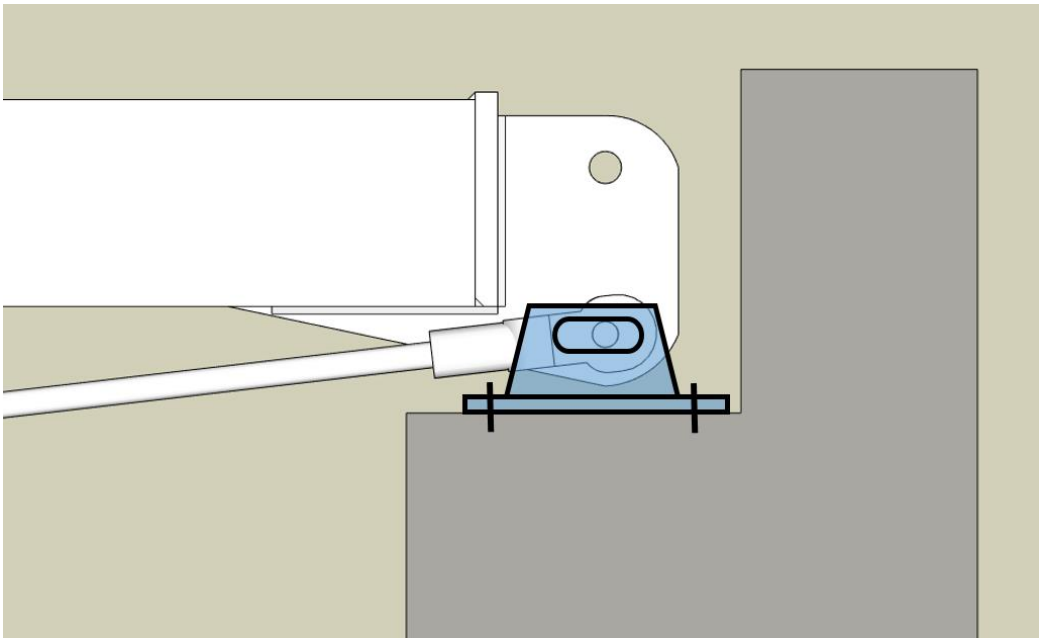

Figure 110: Side view of the rolling support

The length of the slot was determined based on the unrestrained thermal expansion:

$\Delta L^T = L * \alpha * \Delta T$

The linear coefficient of thermal expansion: $\alpha = 24*10^{-6}$ m / (m K)
As a conservative value for the temperature variation a value is taken of: $\Delta T = 80$ K
The length is the span of the bridge: L = 80 m

Therefore the minimum length of the hole is: $L_{hole} = 35$ mm.

For the resistance of the steel saddle the bearing resistance of the slotted holes is governing, the required thickness of the steel plates was calculated based on the maximum shear force at the supports.

Maximum shear force at the supports:
$V_{Ed,supp}$ = ½ * (1,35*q_G + 1,5*q_Q) * L = ½ * (1,35*0,27 + 1,5*15) * 18 = 206 kN

Bearing resistance of the slotted hole:

$$F_{b,Rd} = 0{,}6\frac{k_1\alpha_b f_u dt}{\gamma_{M2}} \rightarrow 206 \cdot 10^3 = 0{,}6 \cdot \frac{\left(2{,}8 \cdot \frac{30}{26} - 1{,}7\right) \cdot \left(\frac{60}{3 \cdot 26}\right) \cdot 470 \cdot 24 \cdot 2t}{1{,}25} \rightarrow t = 9\,mm$$

With this it has been shown that the structure can be supported by four saddle elements in the corners consisting of two 9mm plates each.

4.4.5 Conclusions for the detailing of the structure

The railing uses the same connection as the modules thereby allowing it to be disassembled; this reduces the probability of obsolescence due to the aesthetics of the railing, reduces the number of specialised elements which need to be created, and facilitates widening of the structure. The governing load of 4,9 kNm/m' is lower than the governing load on the longitudinal connection meaning strength is not a critical aspect.
The struts were braced with a standardised approach similar to what is found in wind bracing for framed structures; the tie rods are connected to the struts by means of gusset plate with a single bolt which allows rotation as well as demountability. The end struts are connected to the railing using the same system of tie rods; the addition of a turnbuckle ensures stability of the struts and eliminates slack in the structure. The connection between the struts and transverse connection and between the struts and the tie rods all use bolts; these have been dimensioned in accordance with the required resistance and dimensions provided by Willems Anker.
The covers of the transverse connection consist of a small girder connected to the top bolts of the transverse connection; these undergo minimal deformation (0,5mm) and can withstand the stresses (100 N/mm^2) from the imposed wheel load. Covering of the longitudinal connections required extending the top flanges, in order to assemble the connection from one side hammerhead bolts were used in combination with slotted holes. The capacity must be reduced by around 30% however this is covered by the ample margin of safety in the connection.
The supports of the structure consist of a steel saddle bolted to the concrete abutment to prevent uplift; at the pinned support the bottom hole of the transverse connection is joined using a normal bolt hole while at the rolling support a slotted hole is used to allow movement in longitudinal direction.

5. Life Cycle Analysis

5.1 Goals and scope

5.1.1 Goals

The Life Cycle Analysis (LCA) in the context of this thesis has several goals. First and foremost, the advantage of implementing circular design strategies for a bridge structure should be demonstrated by a quantification of the impact. As mentioned in the introduction of this thesis, circularity represents a means of achieving sustainability and this should be visible in the LCA results. By comparing this result to that of a bridge designed using a traditional structural engineering approach, i.e. take-make-dispose, the benefits can be more accurately discussed as well as weighed against costs.
Secondly, areas of the structure which make significant contributions to the environmental impact can be identified. This allows targeted improvements to be made to the structure focusing on particular components or materials.

5.1.2 Scope

5.1.2.1 Functional Unit

The functional unit (FU) defines and describes that which is assessed in the LCA such that the boundaries are clearly defined from the outset of the analysis as well as allowing for fair comparison between alternatives. In the case of this analysis two separate FUs are defined, both regarding bicycle and pedestrian bridges, such that a scenario in which the structure undergoes modification is presented; this provides favourable conditions for the demountable structure which are however valid as such a structure would only be implemented where modification is expected.

The first functional unit for the LCA, FU1, is defined as follows:
A simply supported bicycle and pedestrian bridge with a span of 18 metres and a width of 3 metres with a maximum allowable deflection of L*3/1000. The loads considered are the self-weight of the structure and a distributed load of 5 kN/m^2 over the entire span and width.
The second functional unit, FU2, is the same as FU1 with the exception that the bridge must have its width increased by 2 metres while maintaining the same structural system.

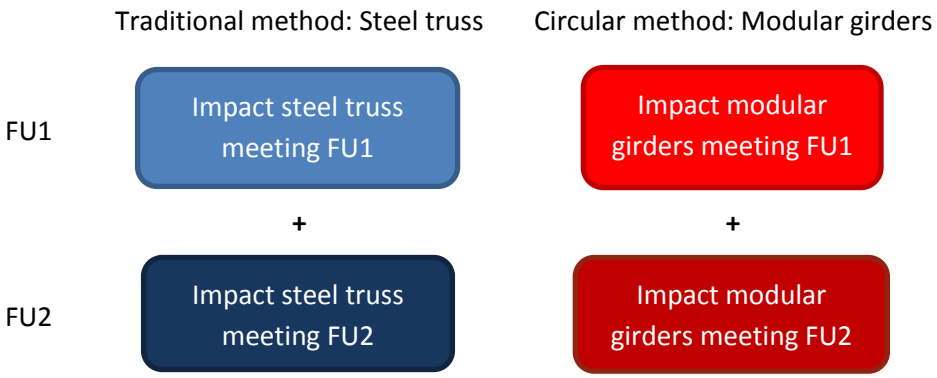

Comparison of total impact for traditional vs. circular method

5.1.2.2 System boundaries and assumptions

The LCA is performed using the following system boundaries and assumptions:

- In terms of material analysed only the load-bearing structure and deck are included; abutments, railings, and deck surface are assumed to be identical between the two methods and therefore irrelevant when compared.
- The service life, or duration of one functional unit, is taken as 50 years.
- For the steel truss girder bridge:
    - The trusses will be comprised of two types of circular hollow sections, one for the chords and one for the braces, for short span bridges this is commonly done to reduce costs of supply and manufacturing. I-profiles are used for the cross-girders supporting the deck as they are light and robust.
    - The deck plate of the steel bridge a 10mm plate stiffened by 6mm ribs is used, this consistent with other examples of steel pedestrian bridges (Felix & Helzel, 2005).

Figure 111: Ribbed steel deck for pedestrian bridge (ipv Delft)

- Recycled content of steel is taken as 50% and 80% for aluminium (see LCA inventory in the appendices) in accordance with Dutch National Environmental Database (NMD)
- Welding is expressed as a length and is determined based on the dimensions of elements being joined.
- Coating of steel is the only maintenance process considered in the analysis, this is assumed to take place every 25 years with 0,48 kg/m^2 density.
- End of life:
    - Steel truss: In accordance with NEN8006 51% and 49% of steel elements used in construction are recycled and reused respectively, transport to a sorting site has a reference transport distance of 50km.
    - Modular girders: it is assumed that after the first service life full reuse of the structure takes place however after the second the aluminium will be 95% recycled, the steel will be 51% recycled and 49% reused
- Transport is divided into three stages:
    - From the supplier to the manufacturing site: Structural elements are assumed to be bought outside of The Netherlands; a reference transport distance of 240km is taken representing the distance by road between Amsterdam and Dusseldorf, Germany.

- From the manufacturing site to the use site: this is assumed to be 100km.
- End-of-life: disassembly of the structure takes place at reuse and recycling centre which is assumed to be 150km from the use site.
- Transport takes place by lorry as all components and processes are assumed to take place within continental Europe.

An overview of these assumptions within the framework of the life of the structure is shown in the Life Cycle Inventory (LCI).

5.2 Life Cycle Inventory (LCI)

5.2.1 Steel truss first and second service lives (FU1 and FU2)

The diagram below shows the four main stages of the service life considered in the functional units; production of structural elements, assembly of the structure through welding, coating, and reuse and recycling. Each stage is connected by a transport flow corresponding to the weight of the stage preceding it.

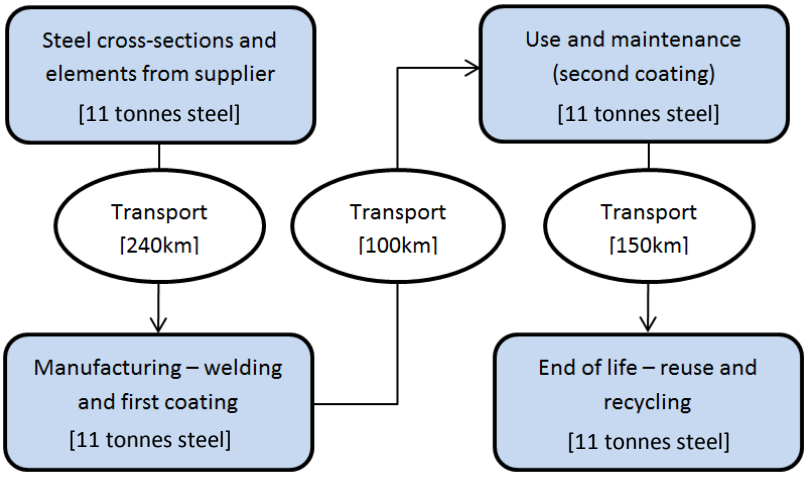

Figure 113: LCI diagram for the steel truss in FU1

The LCI diagram for the steel truss in FU2 is identical with the exception that the amount of steel at each stage is 16 tonnes instead of 11.

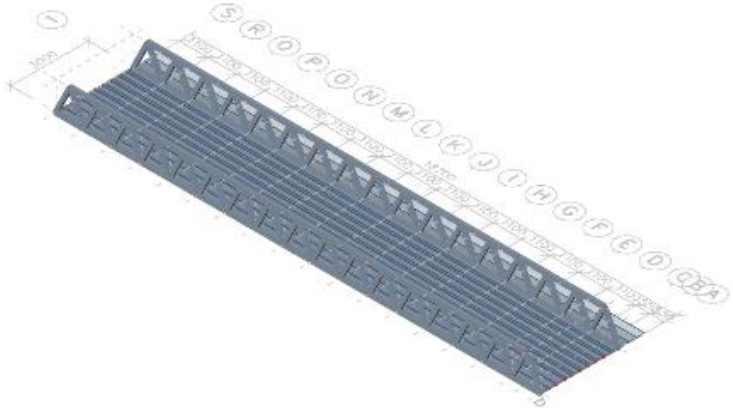

Figure 112: Steel truss used in the analysis

5.2.1 Modular aluminium girder first and second service lives (FU1 and FU2)

The services lives of the modular aluminium girder have been combined in order to demonstrate the reuse of material from the first phase; the same stages can be identified as for the steel truss however reuse and recycling of only takes place at the end of FU2 and comprises the sum of material from FU1 and FU2. The dotted line represents the start of FU2, here only the components needed to meet the new requirements are added while the original structure from FU1 remains in place.

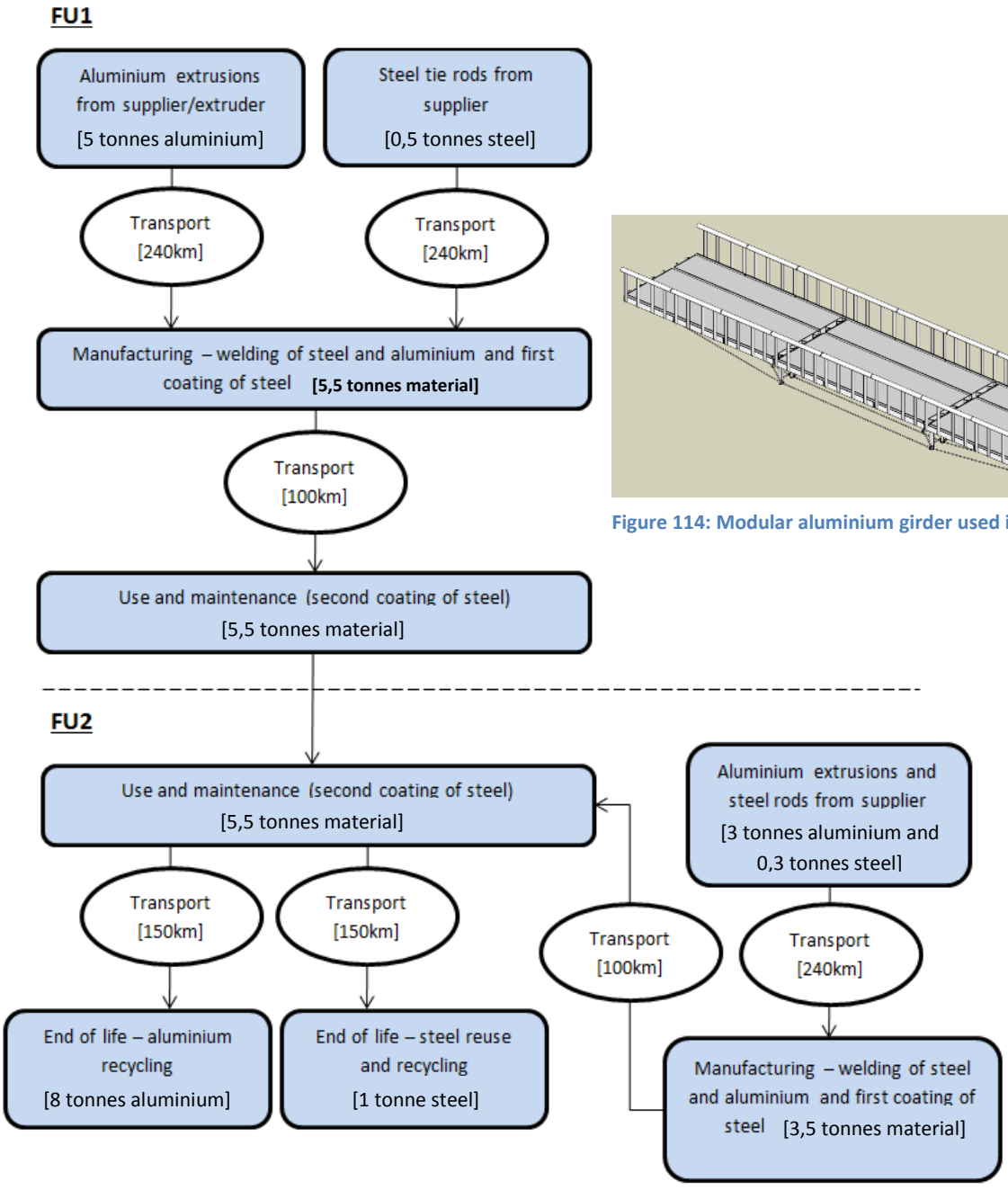

Figure 114: Modular aluminium girder used in the analysis

Figure 115: LCI diagram for the modular aluminium girder in FU1 and FU2

5.3 Life cycle impact assessment

5.3.1 Environmental Product Declaration

In accordance with European norms, an Environmental Product Declaration (EPD) is required for all construction products. The EPD is determined using a framework established in EN 15804 and consists of four stages, A through D, which collect materials and processes present in the life cycle of the structure. Stages A, B, and C all contribute to the impact of the structure while stage D falls outside of service life and allows for impact to be subtracted after the end of life depending on the applied LCA methodology. In The Netherlands the bonus, i.e. reduction in impact, attained from reuse and recycling of the material at the end of life is subtracted from the total impact of the structure. The though behind this is that in The Netherlands construction materials will be reused and recycled in accordance with the NEN8006 guidelines and the benefits can therefore be attributed to the structure being built from the offset. The European method of LCA does not account for this reduction in environmental impact from Stage D such that a more conservative result is produced which shows the impact between construction and demolition. The products and processes shown in the LCI diagrams above are placed within the framework of the four life cycle stages shown below, these can then be linked to the relevant entries in the environmental database to determine impact.

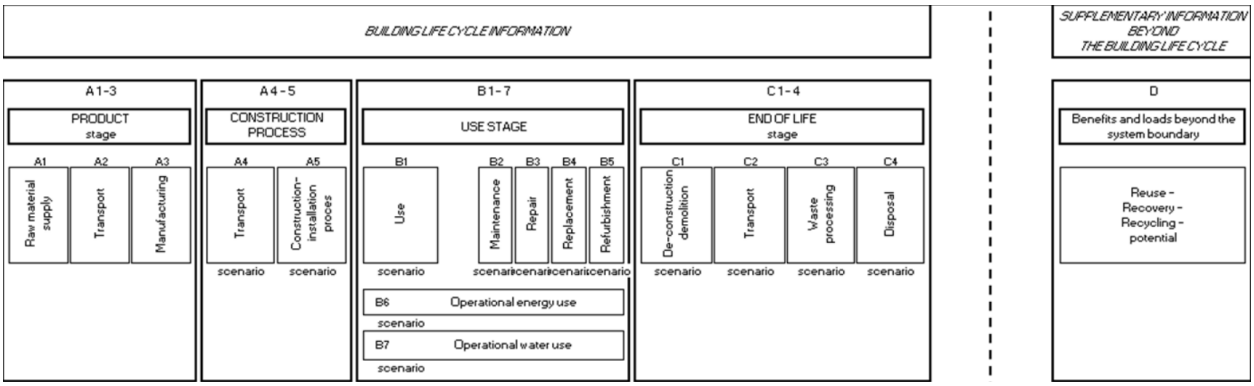

Figure 116: Stages of the life cycle used to determine impact

5.3.2 Impact categories

The impact categories are taken from the Dutch National Environmental Database; 12 impact categories are used to measure the impact of each process. Eleven of these are expressed in an equivalent value per unit while the last is the energy used in the process; these first eleven categories each have an Environmental Cost Indicator (ECI) which expresses the shadow cost of this impact, i.e. the cost of offsetting it, into euros which normalises the results and allows for valid comparison between results. The impact is therefore calculated by multiplying the ECI for the impact category by the equivalent impact per unit variable and then by the variable used by the process; for materials this is expressed in kilograms, for welding it is metres, and for transport it is tonne-kilometres. The energy use per process is calculated but not used in the comparison of the structures as it cannot be expressed in costs, the complete list of impact categories, ECIs, energy use, and impacts can be found in Appendix F.

5.4 Results and discussion

5.4.1 Comparison of the traditional and circular approach

In first instance the environmental impact of the four scenarios are presented separately as shown in Figure 117; the results are consistent with the LCIs presented in the previous section with the steel truss showing two similar charts with that of FU2 having a larger impact due to the greater quantity of material used. The modular aluminium girder also affirms the LCI from Figure 115 showing the large impact from production of steel and aluminium in dark blue in FU1 while in FU2 this is much smaller with a significant negative area shown in light blue, meaning impact has the potential to be subtracted depending on the method used, due to the recycling of the material at the end of life.

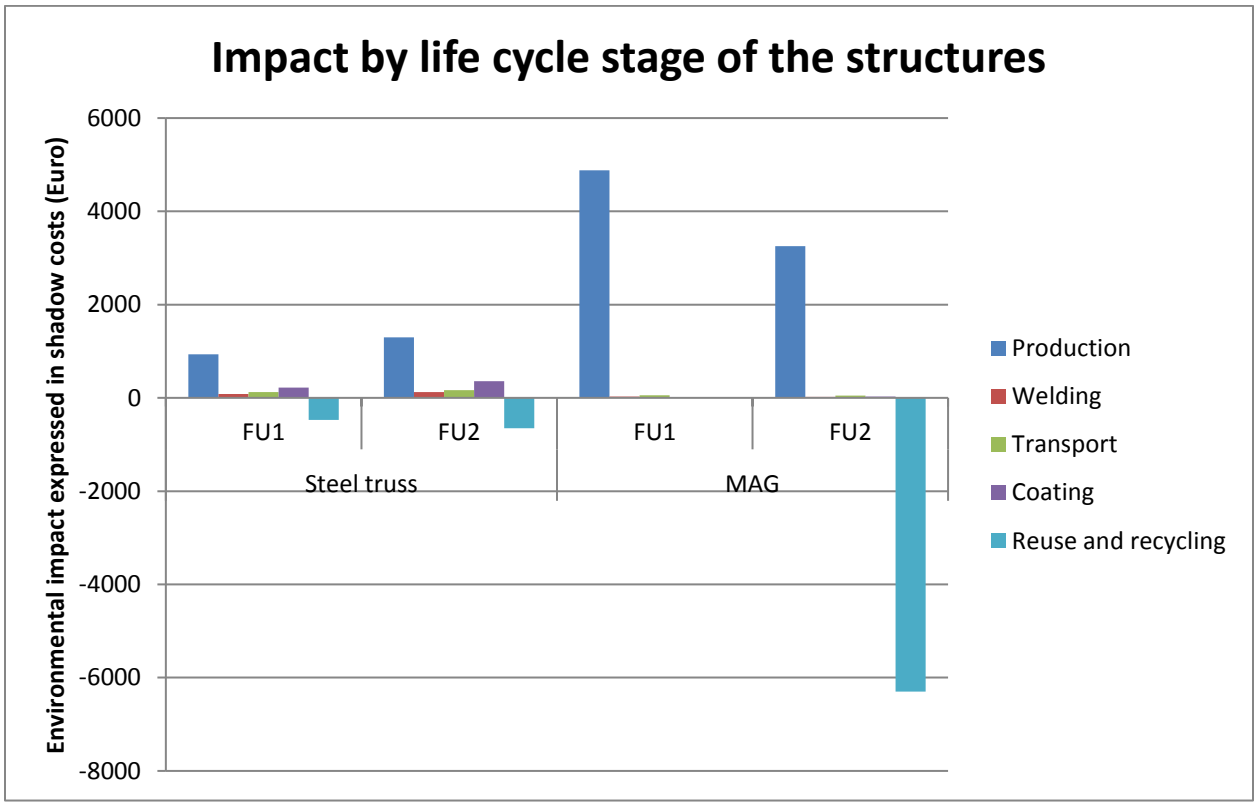

Figure 117: Environmental impact of the truss and modular girders in FU1 and FU2

In order to represent the scenario in which each structure is widened from 3m to 5m after 50 years, the results from FU1 and FU2 are summed and displayed in a single chart. The Dutch method is shown first in which the bonus from reuse and recycling is subtracted from the impact from production; Figure 117 shows the largest contribution to the impact for both structures to come from the production processes. Consistent with expectations, the impact of aluminium production exceeds that of steel by over 60% however the significant contributions of coating, transport, and welding result in a net benefit for the modular aluminium girder (MAG) which represents the circular approach.

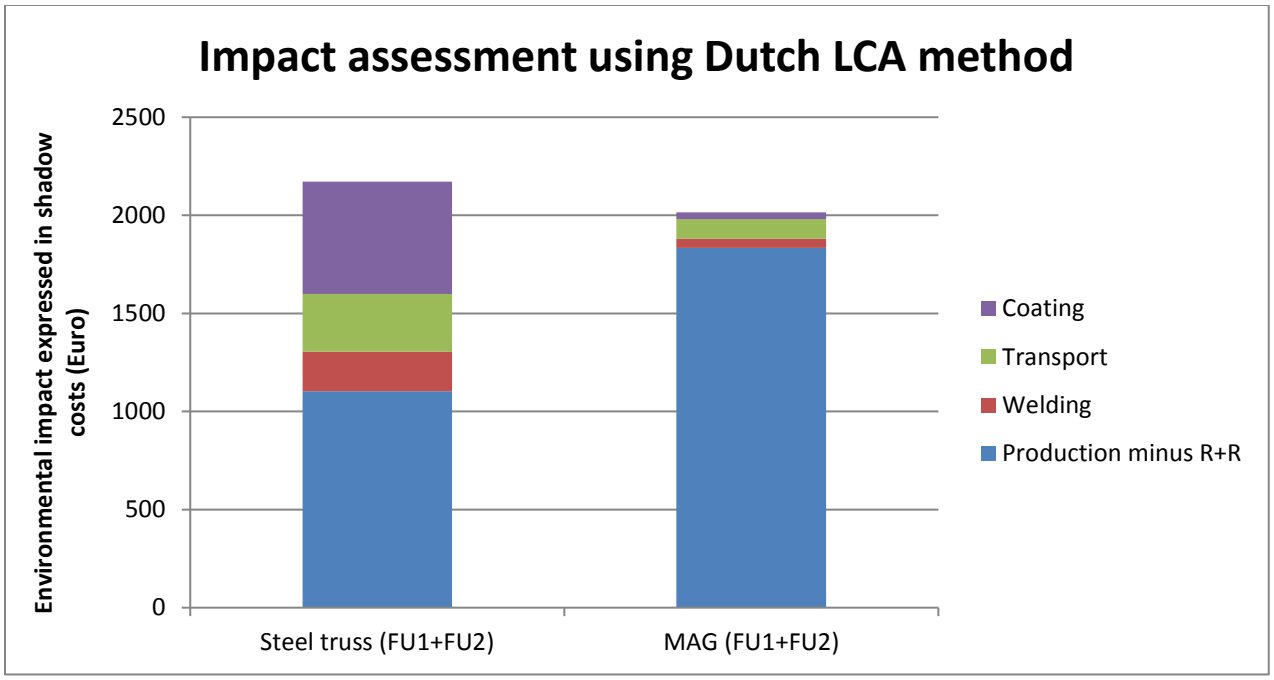

Figure 118: Impact assessment of the structures using Dutch LCA method

Comparing this result to that obtained using the European method shown in Figure 119, the critical influence of the impact subtraction from reuse and recycling can be seen.

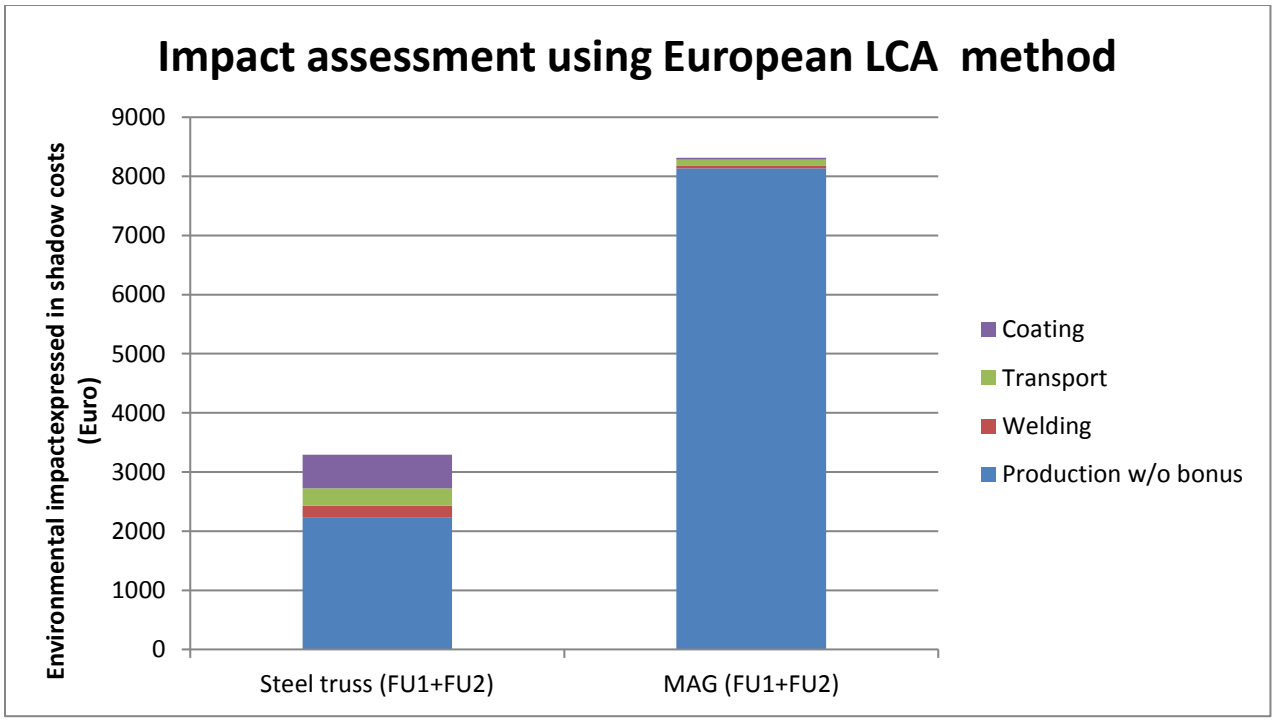

Figure 119: Impact assessment of the structures using European LCA method

The bonus from reuse and recycling represents a 75% reduction in impact for the aluminium structure while reducing the total impact of the steel structures by only one third. This demonstrates that the chosen method for LCA is critical to the outcome; implementing the Dutch method favours the use of the modular aluminium structure which in this case has an 8% lower impact. Neglecting the bonus however yields the opposite result with the steel truss having a factor 2,5 lower impact. The bonus for the reuse and recycling can be attributed to the recycling rate of 95% given in environmental database as well as the relatively low energy required to re-melt aluminium in electric arc furnaces.
Although conservative analysis, as is the case with the European method, is an important aspect in providing accurate results altogether neglecting the fact that the aluminium will be recycled at the end of life is excessively stringent. In practice due to the high value of aluminium and the ease with which it can be recycled the stated recycling rate is not excessively favourable and the subtraction of the impact is justifiable.

For this reason the Dutch method is considered to be the more accurate of the two methods assuming reuse and recycling takes place consistent with NEN8006. The total impact of the steel truss structures totals €2171 while that of modular aluminium structure is €2016. The initial assumption regarding the impact of coating during an extensive lifespan is shown to be correct, contributing to over 25% of the impact; transport also played a significant role due to the large weight compared to the aluminium structure and represented 14% of the total. Welding is not a process which is commonly included in LCA processes, particularly for small scale projects such as this, however the contribution to the impact is not negligible and is four times higher in the steel structure than that in aluminium. The impact of disassembly and demolition processed has not been considered in the analysis as the environmental database contains no information regarding these processes, given the unexpectedly large impact of welding however it would be interesting to compare the added advantage that manual disassembly offers compared to sawing of the steel trusses.
Overall it can be concluded that within the boundaries of this thesis the circular design represents an improvement on the traditional take-make-dispose approach of civil engineering, the difference in shadow costs is of approximately €100 however which represents a negligible sum compared to the additional material cost of aluminium and the associated manual assembly. Furthermore, this results depends on the application of the Dutch LCA approach; if the European approach is used the steel structures are significantly more favourable.

5.4.2 Comparison by impact category

It is also of interest to look at the results of total cost per impact category to determine in which aspects each structure is most harmful and where the most critical aspects lie. Firstly, the most significant impact categories are global warming (GW), acidification of soil and water (ASW), human toxicity (HT); both structures contribute approximately equally to each of these and show the impact of the remaining categories to be negligible by comparison. It is important to note that while aluminium has a more severe contribution than steel during production it also detracts more during recycling hence the similar impact. The similarity of the results can be attributed to the fact that both are structures are made of metal and are manufactured with processes requiring large quantities of energy, using harmful substances contributing to ASW and HT. Impact from the depletion of abiotic resources however is

remarkably low for both materials, negative for steel in fact, considering the fact that both consume non-renewable resources. The reasoning behind this ECI value is that by producing steel and aluminium a contribution is being made to the global pool of available material rather than considering the depletion of steel, coal, bauxite, and other constituents of the two metals.

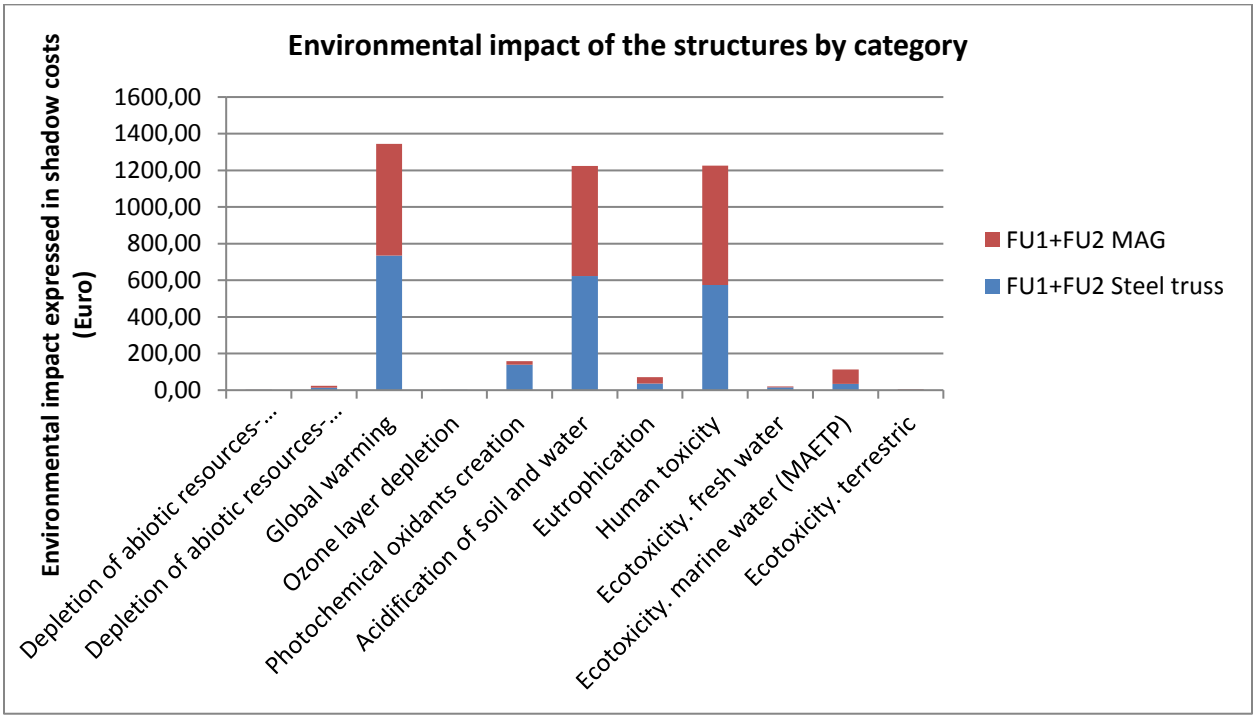

Figure 120: Shadow costs of the structures per impact category

Figure 117 from Page 109 shows that the impact of steel production is significantly lower than aluminium, this difference of more than a factor three lies mainly in the production process of aluminium. Large quantities of energy are used in heating the molten salts used to separate the aluminium from its oxides which, together with large resistance losses in anode and cathode process, results in a difference of embodied energy of 211 GJ/tonne of aluminium compared to 22,7 GJ/tonne of steel ((Brooks, 2012)). Furthermore, the corrosiveness of salts used in the Hall-Heroult process represents results in the large impact seen in the HT and ASW categories. Despite having an entirely different production process, steel, matches the impact in the three categories. The contribution to GW is from the burning of coal and the heating of the blast furnaces used, ASW and HT is instead derived from the sintering process which emits heavy metals and other toxic substances (Renzulli, Notarnicola, Tassielli, Arcese, & Di Capua, 2016).

Figure 121 and Figure 122, for the steel truss and modular aluminium girder respectively, show the contribution each stage of the life cycle has for the impact per category, it is important to note here that 100% of the value here refers to the totality of only that impact category. For the most significant impact categories, GW, ASW, and HT, the steel production process is most significant for the first two while HT is caused in large part by coating and welding. The presence of toxic substances used in thinning agents and additives for paint is particularly severe; this can be traced back to the combination

of high per kilogramme toxicity equivalence and ECI value for HT in the environmental database. For the aluminium structure production is the greatest contributor for the reasons discussed in the previous paragraph.

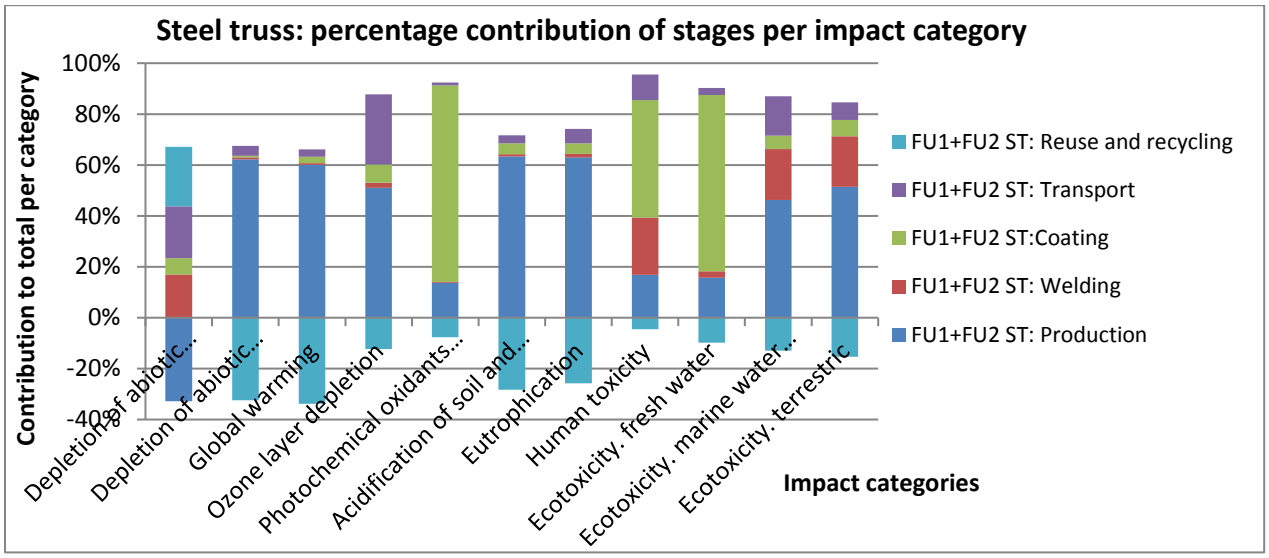

Figure 121: Percentage contribution to the impact categories of different life cycle stages for the steel truss structure

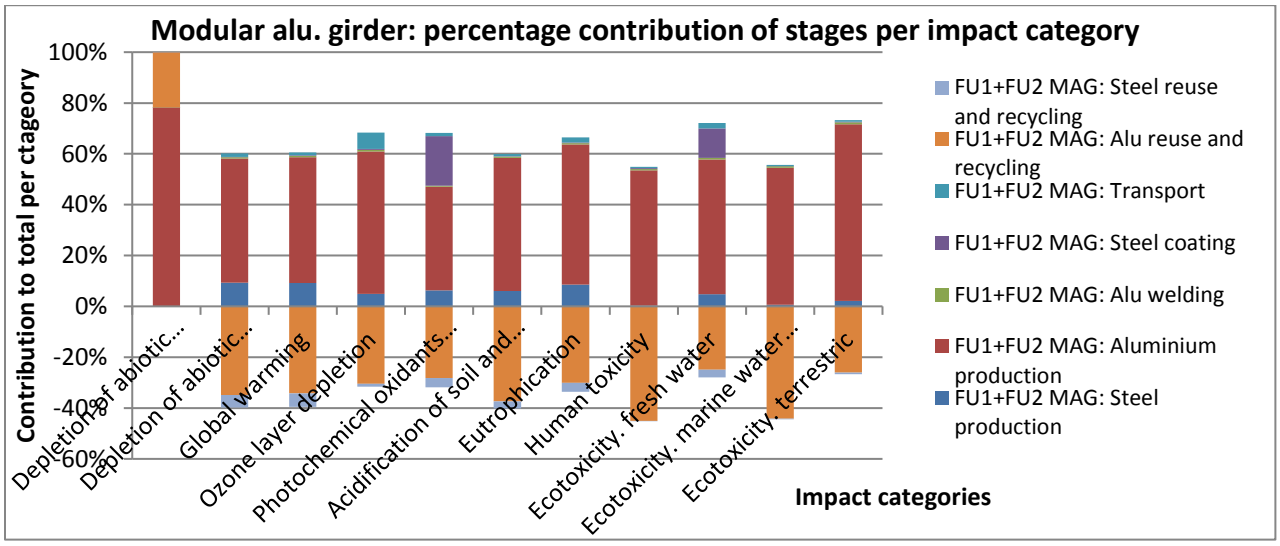

Figure 122: Percentage contribution to the impact categories of different life cycle stages for the aluminium girder structure

5.4 Conclusions for the Life Cycle Analysis

In conclusion, within the system boundaries of this analysis, the modular aluminium girder marginally more sustainable than the standard solution provided by steel trusses; the modular aluminium girder has a 7% lower impact than the steel truss in terms of shadow costs when the Dutch LCA is applied. A significant aspect in this result is the number and length of service lives chosen, as well as the number of modifications, these are relatively brief when compared to the potential product life of steel and aluminium elements and thereby favour a structure which is designed with a traditional approach. Coating was a significant contributor to the total impact of the steel truss at over 25% together with transport at 15%, welding also proved to have some environmental impact which had not been anticipated in the advantages of choosing aluminium. If the bonus from reuse and recycling is not counted, as is the case in the European method, the steel truss offers a significantly more favourable result despite requiring more coating, transport, and welding. This is due to the high impact of aluminium production which uses large quantities of energy and toxic materials.

The impact of the two structures was divided into 11 impact categories from the Dutch National Environmental Database; out of these global warming, acidification of soil and water, and human toxicity proved to be most significant. For the steel truss, the production process was most impactful for the GW and ASW categories while coating contributed to the largest portion of HT category followed by welding. In the life cycle of the modular aluminium girder the production process comprised on average 60% of the impact for every category.

The issue of whether circularity is reflected in sustainability, specifically within the context of this thesis, depends on the life span(s) of the structures and their (expected) function. If a structure is expected to fulfil precisely its function at a particular site over a brief period then material efficient design as represented by the steel truss is the most sustainable option; here the environmental impact compared to the direct costs is lowest. The added value of the aluminium girder is dependent foremost on whether modification is expected to take place, if this is not the case then this type of structure should not be considered, and secondly on how long it is expected to be in use. Within the boundaries of the life cycle analysis presented in this thesis a structure which undergoes one modification after 50 years demonstrates circular design is narrowly better in terms environmental impact. The longer the structure remains in use, and the more modifications it must undergo, the more favourable the circular design becomes. Currently however the ease of disassembly and lower impact over time of the modular aluminium structure are outweighed by the low costs of steel production and the difficulty of efficiently organising logistics surrounding reuse of structures and modules.

6. Discussion

6.1 Circularity design criteria and choice of structural system

Circular Economy as a concept is very broad and may encompass a multitude of strategies to be implemented; when designing a structure with no constraints dictated from the outset determining the optimal solution requires self-imposed constraints to be set. Incorporating every collected aspect of circularity and weighting each individually produced too nuanced of a result, with the relative score of each alternative depending strongly on subjectively assigned aspects. Choosing the solution based on material use, and reuse in different configurations, provided a quantifiable aspect around which the structural design could be focused. Other strategies for circular design such as designing for disassembly and upgradability were included but not measured.

Comparing the material use throughout different configurations the integrated deck girder allowed for 64% of all material in the structure to be reused compared to 20% for a structure using truss girders, this significant improvement increases in value the greater the number of times the structure is reused. The initial weight of this girder however was approximately three times that of the truss used in the same analysis meaning three to four reuse phases were necessary to achieve a net reduction in material use over time. When considering the final design however the post-tensioned girder was around 10% lighter than the truss while still offering the same opportunities for reuse as the previous iteration; this makes implementation of the girder much more appealing from an economic standpoint due to lower material, fabrication, and transport costs.

6.2 Preliminary structural design

The use of a prestressing system allows the bridge to meet the requirement for deflection without the need to add large amounts of material by increasing the cross-sectional dimensions, the ideal shape for the prestressed tendon would be curved to match the distributed load however a tendon with kinks offers a solution which can be realised with fewer and simpler elements; this is favourable for both disassembly and reuse in different configurations. When comparing the alternatives with either one or two kinks it was found that despite the single kink alternative supporting the span where the deflection is greatest it did not offer sufficient reduction in bending moment.

The truss core girder is able to achieve a span of 18 metres with a deck height of only 200mm, the use of an extruded profile allows for the implementation of large radius fillets to be taken into account when determining the cross-section class meaning the sensitivity to local buckling can be neglected. This creates a slender and weight-efficient structure with a 97% effective cross-section

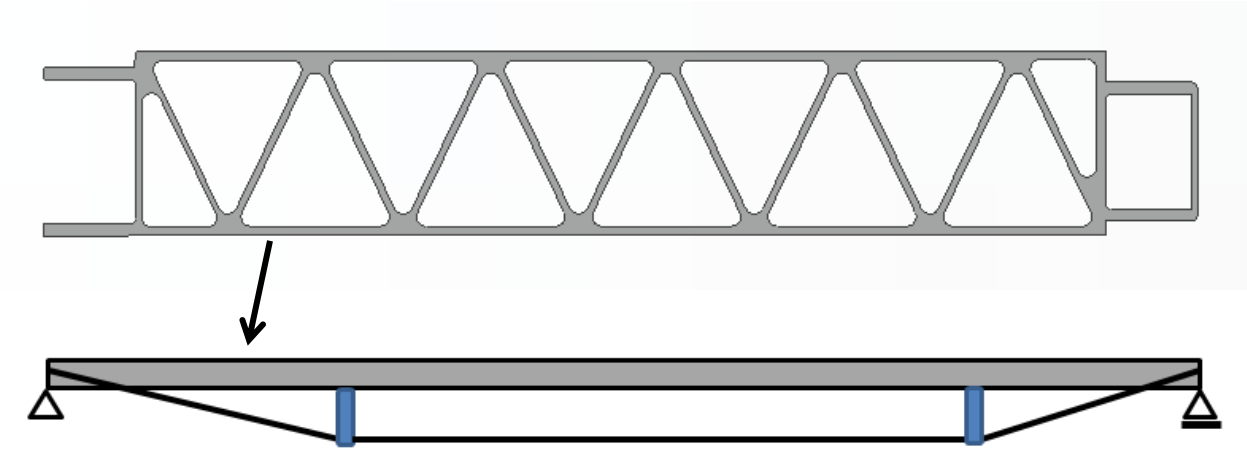

6.3 Post-tensioned support system

Successful implementation of the concept of modularity is achieved through the implementation of the post-tensioned system; while contributing to less than 10% of the weight of the structure the maximum span is doubled and the bending moment is reduced by almost 90%. Turnbuckles are used to introduce an initial prestressing force of almost 20 kN each such that the resting position of the structure is horizontal; each rod can be can be tightened individually and is accessible from the exterior of the structure. Replacing or modifying components of the support system can take place without disassembly of the main structure meaning hindrance from construction work is minimised. Furthermore, the structure can be split into 1 metre wide segments each supported by their own post-tensioned system meaning any width is achievable both when increasing the width of an existing structure or reducing it for a new application.

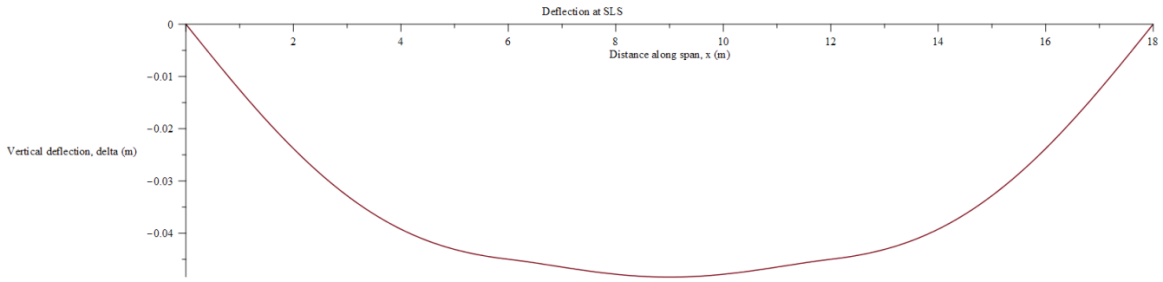

Figure 123: Deflection of the structure at SLS

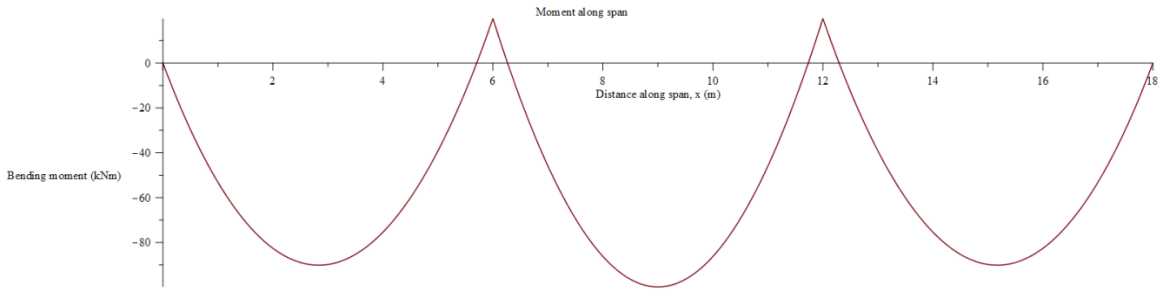

Figure 124: Bending moment along the span

For the 18m long and 3m wide configuration of the bridge six tie rods M24 are needed in total, these can be carried and assembled manually reducing the hindrance during construction. The tie rods are anchored to the structure using the transverse connections at the ends, these are demountable and accessible from the underside of the structure, in this way the number of components is reduced and reuse is facilitated.

6.4 Transverse connections

The transverse connection is designed to transfer the combined loading from the bending moment along the span, the axial prestressing, and the vertical force from the struts. The connection consists of two pre-loaded M27 Grade 10.9 bolts connecting one plate from each side; the plates are welded to a backing plate by means of fillet welds and the backing plate is then welded to the ends of the girders, the tail of the plates is welded to the underside of the girders. Welding of these plates requires the same fabrication method as the support module to the limited spacing between them.

Pre-tensioning of the bolts ensures slip does not occur at SLS, this creates an even deck and removes the influence of joint rotation on the deformation of the structure. The friction coefficient for the slip verification is given as 0,4 for a clamping package thickness of over 30mm, this is double the normal slip coefficient for aluminium and may have been increased to account for the pressure between the faces. As assembly of the structure takes place, in the step before pre-tensioning of the bolt occurs, filler elements (most likely washers) must be applied to ensure contact forces develop between plates and gaps left for tolerances are closed.

The transverse connections furthermore allow struts to be connected at each pair of plates thereby transferring the upward load from the tie rods to the girders.

6.5 Longitudinal connections

The low stiffness of the bridge in longitudinal compared to the transverse direction results in significantly lower loads to be taken by connections along the former, this allowed a greater variety of connections to be investigated with the goal of fast and simple assembly on site. Slotted connections, while sufficiently strong, required too many individual components to fit thereby hindering feasibility in a realistic scenario.

As an alternative, wedged plug-and-play connections were investigated to determine whether an end profile extruded together with the main cross-section of the girder could be used to form a continuous connection along the span. The connections showed low stresses being developed in the material for a moment of 31,4kNm/m' however the gap between the connecting parts resulted in unacceptable rigid body rotation of the connection. The gap was determined in accordance with fabrication tolerances set by HYDRO extrusions in The Netherlands and Dutch norms, the out of plane straightness resulted in a required gap of over 5mm which contributed to the majority of the 4 degree rotation in the connection. Resin injection of the connection in a finite element analysis eliminated this rotation and reduced stresses significantly by ensuring a greater part of the connection became effective, implementation however would require physical testing which falls outside the scope of this thesis.

Finally, a standard bolted connection was investigated which, although not innovative, ensures the structure remains feasible. The connection consists of two sets of plates, inner and outer, which transfer the moment by means of the two shear planes created. The bolted connection was first designed using a hand calculation according to NEN 1999-1-1, for resistance of the connection only one two bolts per meter length (along the span) were found to be necessary. FEA of the connection was used to not only verify the resistance from the norms but determine the deformation under concentrated loading. When using five bolts per meter, in accordance with the corrosion resistance requirement, the connection showed good agreement with the theory for bolted connections used in the hand calculation meaning implementation is safe and reliable.

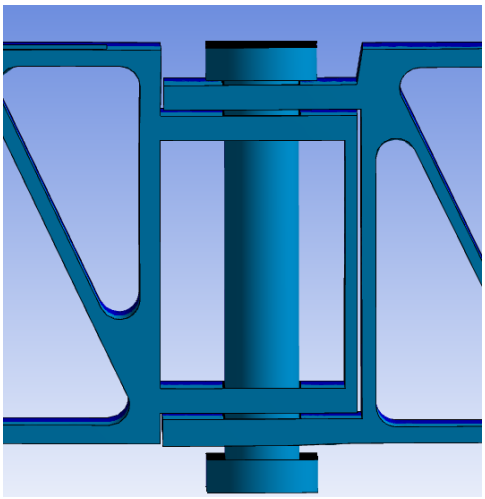

Figure 125: Deformation of the bolted connection under the service vehicle load

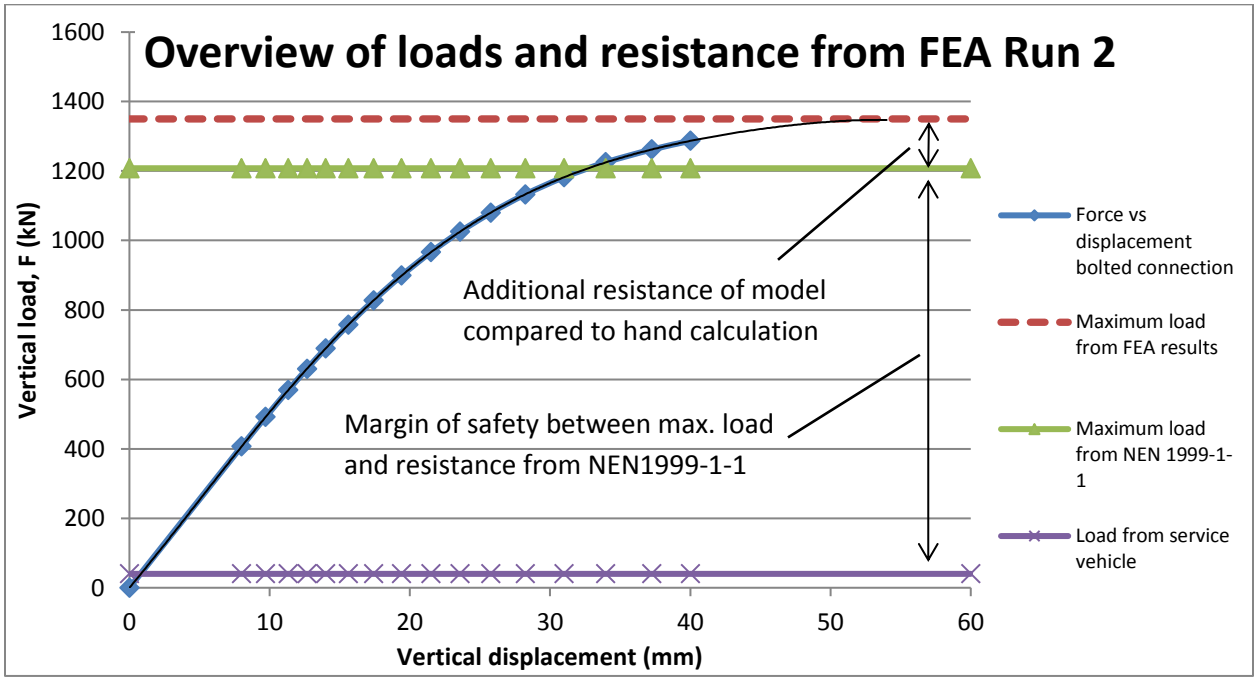

Figure 126: Load and resistances of the longitudinal bolted connection

7.5 Life cycle analysis

As mentioned in the conclusion for the LCA chapter the success of the modular aluminium structure, that is the degree to which it reduces impact with respect to a traditional steel structure, is dependent on the LCA method used; the Dutch method marginally favours the modular structure while the European method neglects the benefit of aluminium recycling and attributes a significantly lower impact to the steel truss structures. The results of the analysis were also shown to be sensitive to the service life chosen as the coating process has a large impact which was counted several times over the course of

the analysis. Choosing a longer service favours the low maintenance requirements offered by aluminium and increases the chance that the structure becomes obsolete due to changing functional requirements, thereby also favouring the modular structure. This raises the issue of modifications being made to the structure; the functional units chosen in the analysis consider only one modification which although not common is possible in practice, more likely however is the reuse of components in new applications with different functions. Forecasting a realistic series of scenarios for the modules as they are used in a variety of bridges, each with different functions, and in different locations, would be too complex and inaccurate and therefore falls outside the scope of this thesis. The ideal scenario for the modular aluminium girder bridge would be a governmental or private party with a stock of standardised modules able to deploy the structures as necessary, interchanging parts for changing functional or maintenance needs.

One barrier to realising this is the combined function of a bridge as both a structure and a monumental item, for many city or state councils creating an appealing bridge will likely be more important than the achievable saving in environmental impact. Another aspect which has neglected in this thesis is the cost of manufacturing these structures in practice which will significantly favour the steel structure, seeing as the modular aluminium structure offers only a marginal benefit to sustainability it is unlikely it would be chosen in a direct comparison. Increasing the service life considered by decision-makers is again pivotal in allowing the benefits of circular design to be seen.

Given the lower production impact of steel found in the LCA a brief analysis was performed using the same modular structure but with the extruded elements replaced a corrugated core steel sandwich panel (CCSSP) with a similar shape. It was assumed that the same cross-section as for aluminium could be replaced using steel, the weight was multiplied by three to account for the difference in density and the coating area was recalculated.

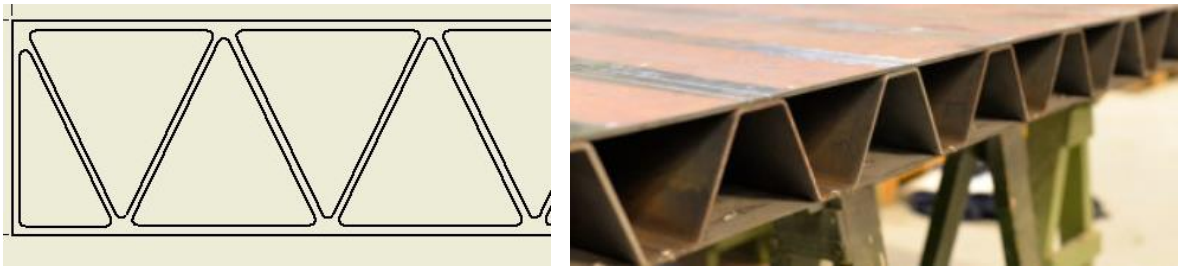

Figure 127: Extruded aluminium profile (left) and steel corrugated core sandwich panel used as a substitute for additional LCA (right) ((Nilsson, Al-Emrani, & Rasoul Atashipour, 2017).

While the added analysis makes quite a broad assumption regarding the use of steel, the stockiness of the cross-section and the added resistance, potentially up to 460 MPa which is almost double that of the chosen aluminium alloy, is expected be more than sufficient to resist the added self-weight. The results, shown in Figure 128 below, give a potential short-term solution with lower direct costs and LCA results which are less varied across methods.

The modular steel girder structure offers the solution with the lowest impact within the system boundaries defined in the original analysis and will have costs greater than the steel truss, due to the required laser arc welding process, but lower than aluminium. The improvement is achieved for both Dutch and European LCA methods and could aside from extrusion be manufactured and assembled in the same way as the aluminium structure. This assessment has been made however with significant assumptions and should not be taken as a conclusive result, rather it is used to illustrate the applicability and benefits of the circular design methods used in this thesis for other scenarios.

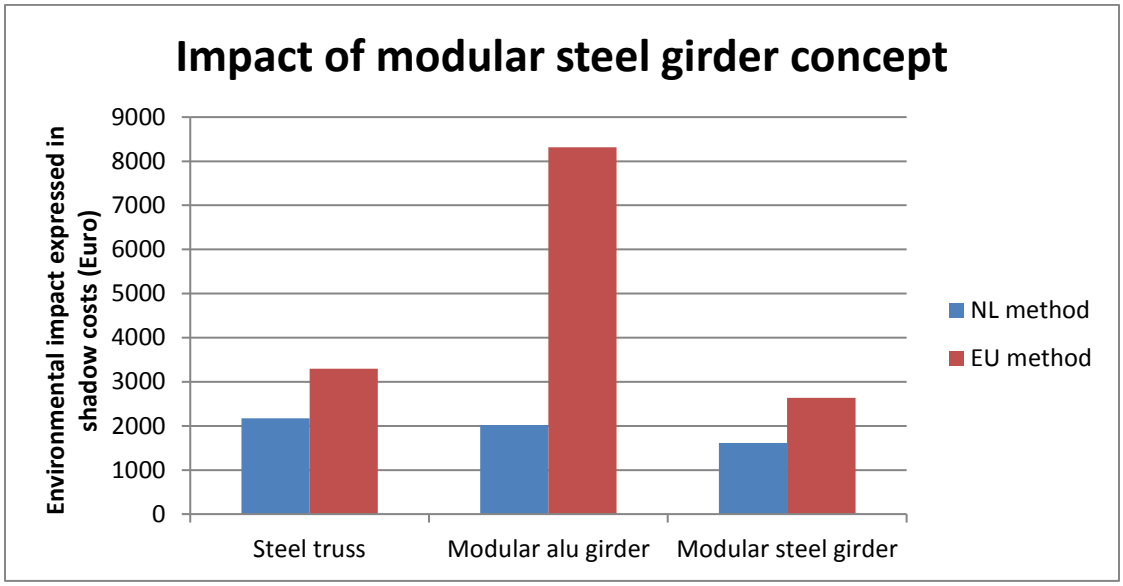

Figure 128: Environmental impact of the modular steel girder compared steel truss and modular aluminium girder

7. Conclusion & Recommendations

7.1 Conclusion

The main goal of the thesis was to perform the design and structural analysis of a bicycle and pedestrian bridge for implementation in the Circular Economy; the main aspects herein are the type of structure chosen, the connections which enable demountability and reuse, and a life-cycle assessment to verify whether circularity was achieved in the final design.

There are numerous types of structures which can potentially be applied in bridge design and each can further be modified in some respect to allow upgradability in some regard; this may be a change in span, width, configuration, or stiffness. With a large set of design criteria available as well as structures to be chosen from a multi-criteria analysis was used to find an optimal solution covering all aspects of circularity. With both rounds of qualitative analysis the different upgradable structures proved almost indistinguishable and for the latter results between the four best structures differed less than 5%. For this reason an analysis of different structure focused around material use was performed, in the analysis various configurations of the structure were considered to represent different possible functions that may be required should reuse take place. This resulted in the girder bridge being chosen as it reused over 60% of material when used in a different configurations meaning less material is used cumulatively over time.

Deflection was found to be the governing criterion for the bridge, in order to increase the stiffness while maintaining the high degree of reuse offered by the girder structure a combination with prestressing system was investigated. In a configuration with two kinks the upward force was such that the bending moment was significantly reduced, this reduced deformation and the influence of bending moments due to eccentricity. A cable system and a tie rod system with turnbuckles were investigated; the cable system offered the possibility to use only three tendons to support the entire structure resulting in a negligible contribution to the self-weight as well as speeding up assembly time. The tie rod system was chosen however as the contribution to the stiffness of the structure is significantly higher, furthermore the turnbuckles are accessible from several points and do not require disassembly of the structure to be adjusted or replaced. The higher degree of redundancy and ease of maintenance were determined to be key aspects in ensuring the service life of the structure is as long as possible.

Bolted connections were used for both the transverse and longitudinal connections in the structure; for the transverse connections this choice was based on the high resistance required to take the axial prestressing force and bending moment along the span, furthermore the possibility to preload the bolts allowed slip to be prevented at serviceability limit state thereby limiting the total deflection. Two sets M27 Grade 10.9 stainless steel bolts applied per module are able to resist the loads for a 18 meter long and 3 meter wide structure, the transverse connection are also used to connect the tie rods to the girders and serve as anchorage for the tie rods at the ends; in this way the number of different elements is reduced such that reuse is facilitated. Slip of the connections is prevented for maximum deflections larger than those occurring at the first natural frequency, the loads will therefore also be lower meaning no slip will occur due to dynamic excitation.

Slotted, wedged, and bolted connections were investigated for the longitudinal connections; key aspects for these were stiffness and ease of assembly due to their widespread use throughout the structure. The slotted connection required 24 studs to line up in order to assembly the connection making it too sensitive to execution tolerances to be feasible in practice. The wedged connection required a 5mm gap to compensate for extrusion tolerances, this resulted in poor stiffness of the joint and a doubling of the deflection due to rigid body rotation. Resin injection was shown to eliminate the issue of rotation however the lack of physical test data, as well as the challenge of disassembling this connection, meant it could not be reliably implemented. For the bolted connection, calculations performed according to European norms showed two M20 bolts per meter length were sufficient to resist the applied load for a connection consisting of two sets of 12mm plates. Due to the slenderness of the plates a finite element analysis was performed in which the connection is infinitely stiff; in this way the behaviour under local loading was to be determined. The behaviour of this connection is consistent with that predicted by the hand calculations with a resistance of 1350kN compared to the expected value of 1167kN. This is a significant margin of safety with respect to the load of 40kN; the associated deformation is also minimal, less than 2mm under the wheel load, thereby ensuring safety for users.

The life cycle assessment resulted in the traditional civil engineering approach represented by two trusses having a 7% higher impact than the modular aluminium girder when applying the reduction from recycling and reuse, instead neglecting this leads to a 2,5 times higher impact of the aluminium girder. This can be attributed almost exclusively to the production of aluminium which contributed to 70% of the impact of the structure. Neglecting the reduction due to reuse and recycling was considered excessively conservative, particularly in the context of circular economy, meaning the Dutch approach provided the more accurate results overall. The initial assumption that coating and transport have sufficient environmental impact to justify the use of aluminium was correct to a certain degree with contributions of 25% and 15% however these remain minor when compared to the impact of aluminium production without reduction. Extending the service life and number of modification would favour the adaptable and low-maintenance modular aluminium girder. In terms of impact categories global warming, acidification of soil and water, and human toxicity were most significant; for the steel trusses these was due to both production and coating while production of aluminium was responsible for 60% of the impact in all categories.

7.2 Recommendations for future research

From the analyses and results in this thesis the following topics are recommended for future research:

- Scenario analyses for bridges over multiple life spans:
  The different possible scenarios a structure may undergo over its lifespan should be investigated; these can be used to provide accurate functional requirements for structures which are used multiple times.

- Upgradability systems for bridges:
  Using the information from the scenario analysis, the types of required upgradability and the systems available to achieve these should be further investigated. This may result in more optimised structures or demonstrate the need for different system groups to be created based on the expected reuse.

- Feasibility of reuse for bridges in a region:
  By means of a case study an investigation should be made into the cost, logistics, and feasibility associated with reusing a bridge or its components. This may for example be useful for a city or town council to demonstrate benefits compared to standard engineering practice, and include practical aspects such as transport, storage, and maintenance of the bridge.

- Reliability analysis and certification for reuse:
  The reliability of the structure for long service lives should be investigated to determine whether reuse of the structure and/or its components is a safe practice; aging, corrosion, or damage due disassembly may all contribute to this. By looking at similar structures and assessing their integrity at the end of life a value can be determined for how long a structure or components should remain in use.

- Corrosion resistance of aluminium:
  The resistance of aluminium to chlorides present in de-icing salts should be investigated; this represents a significant potential risk to the longevity of the structure particularly when both steel and aluminium are present in near contact.

- Environmental impact of demolition:
  Establishing the environmental impact of demolishing a structure could be used to highlight the added benefit of designing a structure which is easily demountable, the increased quality of elements and time saved in disassembly may also prove to have a significant benefit to the post-demolition value.

Bibliography

(n.d.). Retrieved December 29, 2018, from Architectural Timber & Millwork, Inc.: http://atimber.com/the-depot

Alunoor. (n.d.). *Quality standards and recommendations.* Retrieved January 1, 2019, from http://alunoorqa.com/wp-content/uploads/2018/04/01-Quality-standards-and-recommendation.pdf

Benyus, J. (1997). *Biomimicry: Innovation Inspired by Nature.*

Bijlaard, F., Girao Coelho, A., & Magalhaes, V. (2009). Innovative joints in steel construction. *Steel Construction 2*, 243-247.

Boulding, K. E. (1966, March 8). Economics of the Coming Spaceship Earth. (H. Jarrett, Ed.) *Environmental Quality in a Growing Economy*, 3-14.

Braungart, M., & McDonough, W. (2002). *Cradle to Cradle: Remaking the Way We Make Things.* North Point Press.

CBS. (2018, September 2018). *Bromfietsen; aantal (per 1000 inwoners), soort voertuig, regio's, 1 januari*. Retrieved January 3, 2019, from Centraal Bureau voor de Statistiek: http://statline.cbs.nl/Statweb/publication/?DM=SLNL&PA=81568NED&D1=0&D2=l&D3=0-4&D4=a&HDR=T,G1,G2&STB=G3&CHARTTYPE=2&VW=G

Công Ty Cổ Phần Kỹ Thuật Namcong. (2015, November 15). *Structure strengthening with external post tensioning*. Retrieved December 29, 2018, from YouTube: https://www.youtube.com/watch?v=ytA2Rf9t7NY

ConXTech. (n.d.). *On-Site Construction services*. Retrieved December 26, 2018, from ConXTech: http://www.conxtech.com/conx-system/on-site-construction-services/)

CROW, DTV Consultants. (2018). Hoe breed moet een fietspad zijn. *Nationaal Fietscongres.* CORW.

De Telegraaf. (2017, May 22). PostNL gaat met elektrische bakfiets bezorgen in Amsterdam. *De Telegraaf*.

De Waard, C. (2018, July 18). *Tijdelijke brug over Rijnsburgersingel wegens aanleg nieuwe Valkbrug*. Retrieved January 8, 2019, from Sleutelstad: https://sleutelstad.nl/2018/07/18/tijdelijke-brug-over-rijnsburgersingel-wegens-aanleg-nieuwe-valkbrug/

Ellen MacArthur Foundation. (2013). *Towards a Circular Economy: Economic and Business Rationale for an Accelerated Transition.*

Ellen MacArthur Foundation. (2015). *Circularity Indicators: An Approach to Measuring Circularity.*

Ellen MacArthur Foundation. (2015). *Delivering the Circular Economy: A Toolkit for Policymakers.*

Ellen MacArthur Foundation. (n.d.). *Industrial ecology*. Retrieved July 24, 2018, from https://www.ellenmacarthurfoundation.org/circular-economy/schools-of-thought/industrial-ecology

Ellen MacArthur Foundation, Granta Design. (2015). *Circularity Indicators: An Approach to Measuring Circularity.*

European Comission. (2008). *Directive 2008/98/EC of the European Parliament and of the Council of 19 November 2008 on Waste and Repealing Certain Directives.* Retrieved July 24, 2018, from http://eur-lex.europa.eu/legal-content/EN/TXT/PDF/?uri=CELEX:32008L0098&from=EN

European Comission. (2015). *Closing the loop - An EU action plan for the Circular Economy.* Communication from the Commission to the European Parliament, the Council, the European Economic and Social Committee and the Committee of the Regions, Brussels.

European Commission. (2018). *Circular economy*. Retrieved July 25, 2018, from https://ec.europa.eu/growth/industry/sustainability/circular-economy_en

European Environment Agency. (2016, January 18). *Circular economy to have considerable benefits, but challenges remain*. Retrieved July 26, 2018, from https://www.eea.europa.eu/highlights/circular-economy-to-have-considerable

FDN Engineering. (n.d.). *Structural System*. Retrieved December 19, 2018, from Ultrabridge: https://www.ultrabridges.com/structure

FDN Group. (n.d.). *Effectief modulair systeem*. Retrieved 12 19, 2018, from Ultrabrug.

FDN Group. (n.d.). *Ultrabrug*. Retrieved December 19, 2018, from https://www.ultrabrug.nl/

Geissdoerfer, M., Savaget, P., Bocken, N. M., & Hultink, E. J. (2017). The Circular Economy - A new sustainability paradigm? *Journal of Cleaner Production, 143*, 757-768.

Gemeente Amsterdam. (n.d.). *Sprong over 't IJ – Snel, makkelijk, veilig naar de overkant*. Retrieved January 2, 2019, from Gemeente Amsterdam: https://www.amsterdam.nl/bestuur-organisatie/volg-beleid/sprong-ij-snel/

Groff, A. (2015, October 1). *The construction industry looks to renewable energy and sustainability*. Retrieved July 26, 2018, from https://www.energydigital.com/renewable-energy/construction-industry-looks-renewable-energy-and-sustainability

Groot, P., Errami, S., & Saitua, R. (2017). *Building blocks for movable bridges. Exploration of social costs and benefits.* EIB.

HALFEN. (n.d.). *DETAN Rod System*. Retrieved December 29, 2018, from HALFEN: https://www.halfen.com/uk/780/product-ranges/construction/tension-rod-system/detan-rod-system/introduction/

Hawken, P., Lovins, A. B., & Lovins, L. H. (1999). *Natural Capitalism.* Little, Brown & Company.

Heeres, R., Vermeulen, W., & de Walle, F. (2004). Eco-industrial park initiatives in the USA and the Netherlands: first lessons. *Journal of Cleaner Production, 12*(8-10), 985-995.

Hegger, S., & de Graaf, D. (2013). *Vergelijkende LCA studie bruggen (Comparative LCA study of bridges).* Beco.

Heistermann, C. (2014). *Resistance of connections with open slotted holes in towers for wind turbines.* Luleå University of Technology.

inStore. (2017, January 5). Nieuwe elektrische bakfietsen Albert Heijn. *inStore*.

Janson Bridging. (n.d.). Retrieved December 22, 2018, from Janson Bridging: https://www.jansonbridging.com/fileadmin/media-archive/Downloads/Films/janson_bridging.webm

Janson Bridging . (2011, September 15). *Janson Plate Girder Bridges JSB 200 series.* Retrieved December 22, 2018, from Janson Bridging: https://www.jansonbridging.nl/fileadmin/media-archive/Downloads/Bridges/Plate_Girder_Bridges/96.pdf

Janson Bridging. (2011). *Janson Plate Girder Bridges JSB 100 Series.* Retrieved from Janson Bridging : https://www.jansonbridging.nl/fileadmin/media-archive/Downloads/Bridges/Plate_Girder_Bridges/99.pdf

Johnson, D. H. (n.d.). *Principles of Simulating Contact Between Parts using ANSYS.* Erie: Penn State-Erie .

Karlsruhe Institute of Technology. (n.d.). *Safe Bridges*. Retrieved December 29, 2018, from https://www.kit-technology.de/en/technology-proposals/details/451/

Kim, S. (2011, October 31). *Europe's first bridge made from recycled plastic*. Retrieved December 19, 2018, from ZDNet: https://www.zdnet.com/article/europes-first-bridge-made-from-recycled-plastic/

Kirchherr, J., Reike, D., & Hekkert, M. (2017). Conceptualizing he circular economy: An analysis of 114 defnitions. *Resources, Conservation & Recycling, 127*, 221-232.

Lyle, J. T. (1994). *Regenerative Desiign for Sustainable Development.*

Miljanović, S., & Zlatar, M. (2015). Theoretical and experimental research of external prestressed timber beams in variable moisture conditions. *Coupled Systems Mechanics*, 191-209.

Ministry of Infrastructure and Water Management. (2016). *Nederland circulair in 2050.*

Moriche Quesada, S. (2016). *Optimization of a snap-fit connection: a steel connection for the built environment.* Student Thesis: Master.

NEN. (2003). *Eurocode 1: Actions on structures - Part 2: Traffic loads on bridges.* NEN.

NEN. (2006). *Eurocode 3: Design of steel structures - Part 1-8: Design of Joints.* Delft: NEN.

NEN. (2007). *Eurocode 9: Design of aluminium structures - Part 1-1: general structural rules.* NEN.

Pauli, G. (2010). *The Blue Economy: 10 years – 100 innovations – 100 million jobs.* Paradigm Publications.

Piniarski, S. (2014). *The analysis of a column splice with long open slotted holes.* Luleå University of Technology.

Portland Bolt. (n.d.). *Tie Rod Assemblies*. Retrieved December 29, 2018, from https://www.tierodassemblies.com/

Potting, J., Hanemaaijer, A., Delahaye, R., Ganzevles, J., Hokestra, R., & Lijzen, J. (2018). *Circular economy: what we want to know and can measure. System and baseline assessment for monitoring the progress of the circular economy in the Netherlands.* The Hague: PBL Netherlands Environmental Assessment Agency.

Potting, J., Hekkert, M., Worrell, E., & Hanemaaijer, A. (2017). *Circular Economy: Measuring Innovation in the Supply Chain.* PBL Netherlands Environmental Assessment Agency.

PRC. (2008). *Circular Economy Promotion Law of the People's Republic of China.* Retrieved July 24, 2018, from https://ppp.worldbank.org/public-private-partnership/sites/ppp.worldbank.org/files/documents/China_CircularEconomyLawEnglish.pdf

Provincie Noord-Holland. (n.d.). *maximaal toegestane scheepsafmetingen en doorvaarthoogtes van vaste bruggen over provinciale vaarwegen (maximum allowable ship dimenions and passage heights of fixed bridges over provincial waterways).* Provincie Noord-Holland.

Raoul, J., & Ortega Cornejo, M. (n.d.). *Overview of Eurocode 4 part 2.* Retrieved December 24, 2018, from JRC: https://eurocodes.jrc.ec.europa.eu/doc/WS_334_1/2010_Bridges_EN1994_JRaoul_MOrtega.pdf

Ross, K. (2002). *Non-traditional housing in the UK - A brief review.* Building Research Establishment (BRE).

RRFW. (n.d.). *Is the UK's waste infrastructure ready for a circular economy?* Retrieved July 27, 2018, from https://rrfw.org.uk/2018/01/08/is-the-uks-waste-infrastructure-ready-for-a-circular-economy/

SHARCNET. (n.d.). *2D Analyses*. Retrieved December 27, 2018, from https://www.sharcnet.ca/Software/Ansys/17.0/en-us/help/wb_sim/ds_2d_simulations.html

SHARCNET. (n.d.). *Contact Formulation Theory*. Retrieved December 27, 2018, from https://www.sharcnet.ca/Software/Ansys/17.0/en-us/help/wb_sim/ds_contact_theory.html

Short Span Steel Bridge Alliance. (2012). *Pedestrian Bridges*. Retrieved January 1, 2019, from Short Span Steel Bridge Alliance: https://www.shortspansteelbridges.org/steel-solutions/pedestrian-bridges

Short Span Steel Bridge Alliance. (n.d.). *Pedestrian Bridges*. Retrieved December 27, 2018, from Short Span Steel Bridge Alliance: https://www.shortspansteelbridges.org/steel-solutions/pedestrian-bridges

SICUT. (n.d.). *Key Benefits*. Retrieved December 19, 2018, from SICUT.

Soetens, F., Maljaars, J., van Hove, W., & Pawiroredjo, F. (n.d.). *Aluminium structural design: Lecture handbook "Aluminium Structures".* Eindhoven University of Technology.

Spencer, R. (2016, November 22). *Some quick thoughts on Infrastructure and the Circular Economy*. Retrieved July 27, 2018, from http://constructingexcellence.org.uk/quick-thoughts-infrastructure-circular-economy/

Stahel, W. R. (2006). *The Performace Economy.* Palgrave Macmillan UK.

Stanners, D., Bosch, P., Dom, A., Gabrielsen, P., Gee, D., Martin, J., et al. (2009). *Frameworks for Environmental Assessment and Indicators at the EEA.* EEA.

SteelConstruction.info. (n.d.). *Simple Connections*. Retrieved December 22, 2018, from SteelConstruction.info: https://www.steelconstruction.info/Simple_connections

StructX. (n.d.). *Beam Design Formulas*. Retrieved January 9, 2019, from StructX: https://www.structx.com/beams.html

Tirimanna, D., & Falbr, J. (2014). *FDN Sustainable Modular UHPFRC.* FDN Engineering.

US Department of Transportation. (2011). *Accelerated bridge construction; experience in design, fabrication and erecvtion of prefabricated bridge elements and systems.*

Uttam, K., Balfors, B., & Mortberg, U. (2010). *Promoting renewable energy in the construction sector using environmental impact assessment as a tool.* Royal Institute of Technology, Department of Land and Water Resources Engineering, Stockholm.

van Buren, N., Demmers, M., van der Heijden, R., & Witlox, F. (2016). Towards a Circular Economy: The Role of Dutch Logistics Industries and Governments. *Sustainability, 8*(7).

Vertech. (n.d.). *Road Bridge made from Rubbish?*

Vogels, A. (n.d.). *Bouwafval: 40% van de afvalberg*. Retrieved July 25, 2018, from http://www.overruimte.nl/2012/minder-bouwafval/

VSL. (2013). *Post-Tensioning Solutions.* VSL.

VSL. (n.d.). *STRAND POST-TENSIONING SYSTEMS.* VSL.

Waagner-Biro. (2012). *Modular Bridges for the Philippines*. Retrieved December 19, 2018, from Waagner-Biro.

Waste and Resource Action Programme. (n.d.). *WRAP and the circular economy*. Retrieved July 25, 2018, from http://www.wrap.org.uk/about-us/about/wrap-and-circular-economy

Willems Anker. (n.d.). *2017 Specificaties.* Retrieved December 29, 2018, from Willems Anker: https://www.willems.nl/fileadmin/bestanden/downloads/WIL18_115%20Leaflet%20Willems%20Ankers_LR.pdf

WRAP. (2009). *Designing out Waste: A design team guide for buildings.*

Young, W., & Budynas, R. (2002). *Roark's Formulas for Stress and Strain* (7th ed.). McGraw-Hill.

Zwolle City Council. (n.d.). *Fietspaden* . Retrieved January 4, 2019, from toegankelijkestad: https://toegankelijkestad.zwolle.nl/ontwerprichtlijnen/fietspaden

Appendices

Appendix A:

Example splice calculation for girder bridge

Height of the girder	h =	1060	mm
Width of the top flange	b top =	3500	mm
Width of the bottom flange	b bot =	420	mm
Thickness of the webs	tw =	10	mm
Thickness of the flanges	tf=	16	mm
Position of NA from top fibre	z =	252,434783	mm
Second moment of area	I_y =	1,2756E+10	mm4
Uniformly dist. Load at SLS	qSLS=	37,6245007	N/mm
Uniformly dist. Load at ULS	qULS =	55,518076	
Point load of vehicle	F =	600000	N
Span of the bridge	L =	19060	mm
Young's modulus of steel	E =	210000	N/mm2
Deflection at mid span	w_mid =	56,4466671	mm
Allowable deflection at ULS	w_allow =	57,18	mm
Maximum moment at ULS	M_mid =	6766	kNm

Appendix B: Example splice calculation for girder bridge

Project : State of the art - Beam Splice

Part : Standard bolted connection

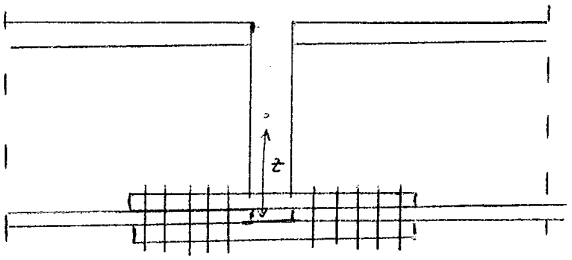

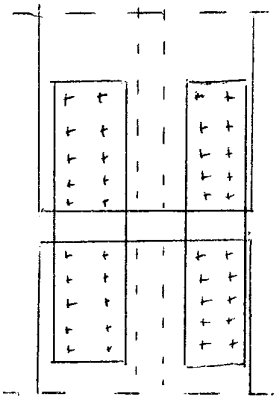

Bearing resistance

$e_1 = 120\,mm$ $e_2 = 75\,mm$ Bolts 8.8 M42 $\rightarrow d = 42\,mm$

$p_1 = 150\,mm$ $p_2 = 110\,mm$ $\rightarrow d_0 = 45\,mm$

$\rightarrow f_{ub} = 800\,N/mm^2$

Flange $\rightarrow$ S355

$\rightarrow f_u = 470\,N/mm^2$

$\rightarrow t = 2 \cdot 9\,mm = 18\,mm$

$$\alpha_b = \min\left\{\alpha_d ; \frac{f_{ub}}{f_u} ; 1{,}0\right\}$$

$$\alpha_d \begin{cases} end = e_1/3d_0 = 120/3\cdot 45 = 0{,}89 = \alpha_{b,end} \\ inner = p_1/3d_0 - 0{,}25 = \frac{150}{3\cdot 45} - 0{,}25 = 0{,}86 = \alpha_{b,inner} \end{cases}$$

$$k_{1,edge} = \min\left\{2{,}8 \cdot \frac{e_2}{d_0} - 1{,}7 ; 2{,}5\right\}$$

$$= \min\{3{,}8 ; 2{,}5\}$$

$$= 2{,}5$$

$$F_{b,Rd,end} = \frac{k_1 \cdot \alpha_{b,end} \cdot f_u \cdot d \cdot t}{\gamma_{M2}} = \frac{2{,}5 \cdot 0{,}89 \cdot 470 \cdot 42 \cdot 18}{1{,}25} \cdot 10^{-3} = 632{,}4\,kN$$

$$F_{b,Rd,inner} = \frac{k_1 \cdot \alpha_{b,inner} \cdot f_u \cdot d \cdot t}{\gamma_{M2}} = \frac{2{,}5 \cdot 0{,}86 \cdot 470 \cdot 42 \cdot 18}{1{,}25} \cdot 10^{-3} = 611\,kN$$

$$F_{b,Rd} = 5 \cdot 2 \cdot 2 \cdot 611 + 1 \cdot 2 \cdot 2 \cdot 632{,}4 = 14748\,kN$$

$$F_{Ed} = M_{Ed}/z = 6766/\tfrac{1}{2} \cdot 1{,}06 = 12766\,kN \rightarrow u.c = \frac{12766}{14748} = 0{,}87 \rightarrow OK.$$

Name:	Date:	Page:	Rev:

Project : State of the art - Beam splice

Part : Slip-resistant connection

$$F_{s,Rd} = \frac{k_s \cdot n \cdot \mu}{\gamma_{ms}} \cdot F_{p,c}$$

$$F_{p,c} = 0,7 \cdot f_{ub} \cdot A_s$$

$k_s = 0,63$

$n = 2$

$\mu = 0,2$, friction coefficient for

Bolts 8.8 M48 $\rightarrow f_{ub} = 800\ mm^2$

$\rightarrow A_s = 1473\ mm^2$

$$F_{p,c} = 0,7 \cdot 800 \cdot 1473 \cdot 10^{-3} = 824,9\ kN$$

$$F_{s,Rd} = \frac{0,63 \cdot 2 \cdot 0,2}{1,25} \cdot 824,9 = 166,3\ kN$$

Use : 4 bolts per slotted hole. 20 ~~slotted~~ slotted holes across the width

$$F_{s,Rd} = 4 \cdot 20 \cdot 166,3 = 13304$$

$$F_{Ed} = M_{Ed}/z = \frac{6766}{1/2 \cdot 1,06} = 12766$$

$$U.C = 12766/13304 = 0,96 \rightarrow OK.$$

Name: Date: Page: Rev:

Project : State of the art - Beam splice

Part : slotted connection

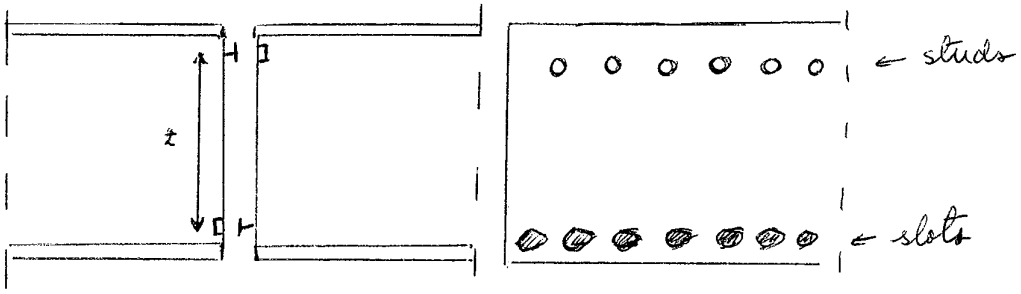

Stud tensile strength

$$F_{t,Rd} = \frac{k_2 \cdot f_{ub} \cdot A_s}{\gamma_{M2}}$$

M42 studs → $A_s = 1121\ mm^2$

$k_2 = 0,9$ for steel "bolts"

$f_{ub} = 470$ assuming S355 studs

$$F_{t,Rd} = \frac{0,9 \cdot 470 \cdot 1121}{1,25} \cdot 10^{-3} = 379\ kN$$

Assuming $z = 1m$ and 20 studs top and bottom

$M_{Rd} = F_{t,Rd} \cdot z \cdot n = 379 \cdot 20 \cdot 1 = 7580\ kNm$

$M_{Ed} = 6766\ kNm$

$M.C. = 6766/7580 = 0,89 \rightarrow OK.$

Punching shear strength

$$B_{p,Rd} = \frac{0,6 \cdot \pi \cdot d_m \cdot t_p \cdot f_u}{\gamma_{M2}}$$

$$= \frac{0,6 \cdot \pi \cdot (1,5 \cdot 42) \cdot 12 \cdot 470}{1,25} \cdot 10^{-3}$$

$= 535,8\ kN > F_{t,Rd} \rightarrow OK.$

Name:	Date:	Page:	Rev:

Project : State of the art – Beam Splice

Part : slotted connection (2)

Equivalent T-stub approximation

Failure pattern { circular / straight

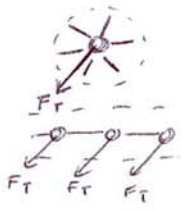

$\Sigma l_{eff,circ} = 2\pi m$

m = diameter = spacing between studs

assuming $n_{studs} = 20 \rightarrow m = \frac{b}{n_{studs}+1} = \frac{3500}{20+1} = 166,7$ mm

$\Sigma l_{eff,circ,tot} = 2\pi m n = 2 \cdot \pi \cdot 166,7 \cdot 20 \cdot 10^{-3} = 20,94$ m

$\Sigma l_{eff,straight,tot} = b = 3,5$ m $< 20,94 \quad \therefore \Sigma l_{eff} = 3,5$ m

Assume : no prying forces

Failure mode :

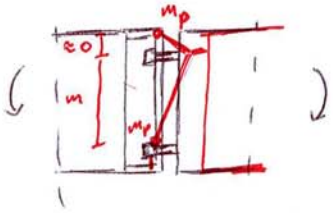

$M_{pl,1,Rd} = 0,25 \cdot \Sigma l_{eff} \cdot t_f^2 \cdot \frac{f_y}{\gamma_{M0}}$

$= 0,25 \cdot 3500 \cdot 15^2 \cdot 355/1,0 \cdot 10^{-6}$

$= 69,9$ kNm

$F_{T,1-2,Rd} = \frac{2 \cdot M_{pl,1,Rd}}{m} = \frac{2 \cdot 69,9}{1} = 139,8$ kN

$M_{Rd} = F_{T,1-2,Rd} \cdot z = 139,8 \cdot 1 = 139,8$ kNm

$M_{Ed} = 6766$

$M.C. = 6766/139,8 = 48 \rightarrow$ does not suffice!

Note : Failure mode unlikely to occur due to position of the stud line

Name: Date: Page: Rev:

Appendix C1: Multi-criteria analysis: comparison of alternatives

Aspect of circular economy		Structural variant: 1A	3A	1C / 3C	α	β	γ	ε	ζ	λ
Optimised material use										
Structure designed for the capacity without over-specification	Grade	Average	Average	Poor	Good	Excellent	Average	Poor	Good	Poor
	Comment	Large modules adjusted to bending moment but not precisely	Large modules adjusted to bending moment but not precisely	Only two main modules which give poor possibilities for optimisation	Truss members will be designed and optimised according to internal forces but somewhat over-designed to cover span extensions	The truss memebers will be completely optimised based on the internal forces	Large modules adjusted to bending moment but not precisely	Only two main modules which give poor possibilities for optimisation	Also based on large modules but sub-divided in more types giving more possibilities for optimisation	The outer profiles will have to be over-dimensioned to allow the inner profiles to fit and have sufficient capacity
Explanation: The modules in are adjusted to match the required capacity										
Use of higher strength materials*	Grade	Good	Good	Good	Good	Good	Good	Good	Good	Good
	Comment									
Explanation: The structure and elements used lend themselves to using high-strength materials										
Optimised cross-sections for performance	Grade	Average	Excellent	Average/Good	Excellent	Excellent	Excellent	Average	Excellent	Good
	Comment	Capacity is determined by different standard profiles available meaning some over-dimensioning is inevitable	The integrated deck girders can be accurately designed to match the required capacity	Outer profile can be optimised for main span, innner profiles have less freedom unless extrusions are used	Wide variety of cross-sections which can be adjusted to required capacity	Wide variety of cross-sections which can be adjusted to required capacity	Height of the cross-section can be speficially adjusted according to changing capacity requirements	Mid-span deck modules can be optimised but the telescopic span much less so	Almost all of the modules will be optimised for the required capacity	Wide variety of cross-sections available to optimise the design with some over-dimensioning
Explanation: The cross-sections used are optimised for material use or strength										
Robustness of the structure	Grade	Good	Excellent	Good	Excellent	Good	Very poor	Good	Good	Poor
	Comment	Within modules beams will be cross-connected with welded beams providing good strength	Hollow core sandwich panels, particularly CCSSPs, have high rigidity and torsional stiffness	Modules made up of individually strong components with few connections between then	Trusses provide high strength and stiffness, these support the (extending) deck elements	Truss structure is robust, this is somewhat reduced by the connections	Large number of connections in the structure contributing to risk of failure	Only two modules used with few connections between them	Mainly built up of robust modules but with more connections and telescopic parts	Large number of connections within members and to nodes
Explanation: Simplicity of the structure and number and type of moving parts										
Use of low-waste production processes	Grade	Poor	Excellent	Good	Poor	Average	Average	Average	Excellent	Very poor
	Comment	Requires extensive cutting to shape of components	Uses plate material efficiently to produce required cross-sections to specification	Central modules produced to specification while inner profiles will be somewhat over-dimensioned, this can be improved by using extrusions	Truss elements must be cut to specific shape and length producing waste, internal profiles must also be specifically produced for small applications	Truss memebers must be cut to shape but with less off-cuts as they must only be made to fit node connectors	Flanges must be specifically produced and webs must be cut to shape however these will have a high dregree of repetition	Middle span can be manufactured efficiently however folding and telescopic components less so due to customised application	Mainly comprised of hollow core panels with efficient production, use of internal profiles will be limited and have some repetition	Large number of elements which must be produced to very specific requirements
Explanation: The elements applied are produced through material efficient processes										
Adaptability and upgradability										
Range of span expandability	Grade	Average	Good	Good	Average	Excellent	Good	Good	Excellent	Excellent
	Comment	Span is limited by available cross-sections and end-end connections of modules at mid span	Cross-sections can be customised to accomodate large loads/spans as well as allowing for end-end connections to be placedalong the entire width	If cross-sections are made sufficiently large capacity will be high with no mid-span connections, minimum span will be an issue to due outer profile needing to house inner	Maximum span is large due to truss structure however range of spans is limited by available extension material and initial design span	Truss structure allows for longer spans to be achieved, as many elements as required can be added or removed to achieve a variety of spans	Cross-sections can be adjusted to accomodate large spans and modular assembly allows for a variety of spans to be composed	Middle section can be dimensioned to accomodate large spans however connection between this module and foldable module will be limiting, moderate range of spans possible	Large spans possible due to strong middle module however connections will be critical, good variety of spans possible due to extendable end modules	Completely adjustable structure which allows for large span to be created due to strength of truss structure, range of spans limited only by length of inner profiles
Explanation: The distance the span can be extended/retracted as well as the max. achievable span										
Size of dimension adjustments	Grade	Very poor	Very poor	Excellent	Excellent	Excellent	Very poor	Good	Good	Excellent
	Comment	Large modules improve efficiency meaning achievable spans will be heavily segmented	Large modules improve efficiency meaning achievable spans will be heavily segmented	Extendable modules allow for continuous adjustments to be made to the span	Extendable modules allow for continuous adjustments to be made to the span	Span is adjusted by changing truss members which can be prdouced to any length and adding deck modules which will divided into small segments	Large modules improve efficiency meaning achievable spans will be heavily segmented	Telescopic profiles make a variety of spans possible however size of middle module will limit minimum	Built up out of large modules however extendable spans provide good flexibility	All lengths adjustable giving great flexibility
Explanation: How small/accurate of an adjustment can be made to the span										
Range of width expandability	Grade	Good	Good	Average	Good	Excellent	Good	Good	Good	Good
	Comment	Modules can be connected between or at end(s) of modules	Modules can be connected between or at end(s) of modules	Hard to create modules to adjust width which can easily attach to outer and inner profile, 'filling' the core also provides less points for connections to be added	Modules can be connected between or at end(s) of modules	Modules can be connected between or at end(s) of modules and structure can easily be adjusted to increase required capacity	Modules can be connected between or at end(s) of modules	Modules can be connected between or at end(s) of modules	Modules can be connected between or at end(s) of modules	Modules can be connected between or at end(s) of modules
Explanation: The ease with which the width of the structure can be increased										
Upgradability of strength	Grade	Average	Poor	Poor	Very poor	Excellent	Excellent	Poor	Poor	Excellent
	Comment	Some possibility to add beams to increase strength	Closed profile which is difficult to modify appropriately	Closed profile which is difficult to modify appropriately	Truss structures difficult to retrofit to increase strength	Load-bearing elements can easily be replaced to increase strength	Cross-section height can easily be adjusted to meet strength requirements	Middle module is a closed section which is difficult to modify appropriately	Middle module is a closed section which is difficult to modify appropriately	Geometry of the truss can be adjusted to meet changing capacity requirements
Explanation: The ease with which the load-bearing capacity of the structure can be increased										
Standardisation/repetition of components	Grade	Good	Excellent	Good	Average	Good	Excellent	Average	Good	Poor
	Comment	Repeated use of certain types of profiles	Repeated use of sandwich panel structure with similar components	Repetition of internal profiles and only one type of outer profile	Truss will use a variety of different profiles as well as deck elements	A small variety of different cross-sections will be used for truss memebers, good degree of repetition for node connectors and deck elements	Repeated use of flange elements and repetition of web elements within the same module	Little repetition of elements however there are only few types of modules used	Repetition of internal profiles and similar structure of outer profiles	Truss will use a variety of different profiles as well as deck elements, inner profiles increase variety further
Explanation: The degree to which components are repeated in the structure										
Maintenance and repair										
Accessibility of parts within the structure	Grade	Good	Average/Good	Poor	Very Poor	Good	Very poor	Good	Average	Very poor
	Comment	Open modules with most connections accessible	Closed modules with some connections accessible depending on type of connections used	Connections within closed profiles difficult to access	Connections within small closed profiles are particularly difficult/time-conuming to access	All connections visible and accessible from the outside	Large number of connections hidden inside the structure	External connections used with good accessibility	Depends on type of connections used, connections for inner profiles reduce accessibility	Very large number of connections used, may hidden inside small profiles in the structure
Explanation: The ease with which components in the structure can be accessed or inspected										
Fault diagnostics (monitoring/expected failure points)	Grade	Good	Good	Poor	Poor	Average	Very poor	Average	Poor	Poor
	Comment	Relatively few connections which are easy to monitor	Relatively few connections which are easy to monitor	Behaviour of inner profiles difficult to monitor and critical areas more difficult to predict	Behaviour of inner profiles difficult to monitor and critical areas more difficult to predict	Large number of potentiall critical connections which are however easily monitored	Very large number of connections which are difficult to monitor with many possible failure paths	Fairly simple structure but monitoring of structural integrity may be challenging	Behaviour of inner profiles difficult to monitor with several possible critical points	Large number of connections however monitoring is feasible and critical points are clear
Explanation: Whether there are clear critical points in the structure and how easily can they be monitored										
Safety for techinicians	Grade	Average	Average	Good	Excellent	Good	Average	Good	Average	Average
	Comment	Possibility of large blocks deatching	Possibility of large blocks detaching	All profiles stored fairly tightly inside	Extension constrained by truss and deck	No large elements used and truss provides robustness	Possibility of large blocks detaching	Comprised of robust elements and connections, simple assembly process	Possibility of large blocks detaching	Truss provides robustness but large number of connections increases sensitivity to failure
Explanation: What kind of risks does the structure pose during assembly and maintenance										
Use of industry standard ("off-the-shelf") components	Grade	Excellent	Average	Average/Good	Good	Excellent	Poor	Poor	Average	Good
	Comment	Comprised of I- or H-beams as well as welded plate material	Profile is made up of standard sheet material however it must be specifically manufactured to specification	Good if standard inner profiles are used, average if extrusions/custom profiles are applied instead, outer profiles > see 3A	Truss built up from standard cross-sections, good possibilities for deck and inner profiles to use standard elements also	Truss built up from standard cross-sections, good possibilities for deck to use standard elements also	Profiles mainly uses elements made to specification	Structure mianly uses elements made to specification	Profile is made up of standard sheet material however it must be specifically manufactured to specification, may be improved if standard inner profiles are used	Use of standard profiles for the truss structure, deck may potentially also make use of these
Explanation: How common are the profiles, connections, and processes applied in the structure										
Redundancy features / alternative load paths	Grade	Poor	Poor	Good	Excellent	Excellent	Poor	Poor	Poor	Excellent
	Comment	Modules connected in 1/2 directions with few alternative load paths	Modules connected in 1/2 directions with few alternative load paths	Alternative load paths provided by other inner profiles, robust main profile	Truss provides many alternative load paths and good robustness	Truss provides many alternative load paths and good robustness	Modules connected in 1/2 directions with few alternative load paths	Robust middle module but no alternative load paths for end modules	Modules connected in 1/2 directions with few alternative load paths	Truss provides many alternative load paths and good robustness
Explanation: How sensitive is the structure to an element failing										
Refurbishment and reuse/re-assembly										
Degree of prefabrication	Grade	Good	Good	Good	Good	Good	Excellent	Good	Good	Good
	Comment	Almost all of the structure can be assembled off-site with only some on-sire adjustments necessary	Almost all of the structure can be assembled off-site with only some on-sire adjustments necessary	Most of the structure will be assembled off-site with final assembly taking place on-site	Most of the structure will be assembled off-site with final assembly taking place on-site	Main components can be assembled off-site with final connection/assembly taking place on-site	Almost all of the structure can be assembled off-site with only some on-sire adjustments necessary	Most of the structure will be assembled off-site with final assembly taking place on-site	Most of the structure will be assembled off-site with final assembly taking place on-site	Most of the structure will be assembled off-site with final assembly taking place on-site
Explanation: How much of the structure can be assembled off-site										
Ease of disassembly	Grade	Good	Good	Excellent	Average	Good	Average	Excellent	Good	Average
	Comment	Straightforward disassembly process with few connections	Straightforward disassembly process with few connections	Disassembly only requires loosening and sliding elements back into place	Partial disassembly only requires loosening and sliding elements back into place, full disassembly would be complex	Bolted connections with good accessibility requiring no specialist techniques/equipment	Partial disassembly only requires separating modules, full disassembly would be complex	Disassembly only requires folding (and removing) end modules	Partial disassembly only requires sliding profiles back in, full disassembly also only requires disassembly into modules	Partial disassembly only requires sliding elements back into place, full disassembly will be very complex
Explanation: How complicated, time-consuming, and dangerous is it to disassemble the structure										
Total number of connections	Grade	Excellent	Excellent	Good	Average	Very poor	Very poor	Excellent	Good	Very poor
	Comment	Only end-end and side-side connections between large modules	Only end-end and side-side connections between large modules	Moderate number of connections between inner and outer profiles	Moderate number of connections between inner and outer profiles however these are present in both deck and truss structure	Very large number of connection connecting nodes to truss members	Very large number of connections connecting modules and within modules connecting flanges to webs	Few connections present in the structure	Moderate number of connections between inner and outer profiles as well as some connections between modules	Very large number of connections between nodes and members of the truss as well as connections between inner and outer profiles
Explanation: The number of connections needed to assemble the structure, more is less favourable										
Tools required for disassembly	Grade	Good	Good	Average	Average	Good	Average	Excellent	Average/Good	Good
	Comment	Simple bolted connections	Simple bolted connections	May require some more specialist tools or techniques to disassemble	May require some more specialist tools or techniques to disassemble	Simple bolted connections	May require some more specialist tools or techniques to disassemble	Simple connections used	Mainly simple bolted connections, may require some more specialist tools or techniques for connection between inner and outer profile	Simple bolted connections
Explanation: The tools and processes required for disassembly, more intensive is less favourable										
Damage caused by disassembly / quality of elements after disassembly	Grade	Good	Good	Excellent	Average	Poor	Poor	Good	Excellent	Very poor
	Comment	Robust modules and simple connections which are not very sensitive to damage	Robust modules and simple connections which are not very sensitive to damage	Simple disassembly process with sturdy elements	Some damage may occur when disassembling truss elements	Connections at nodes not very robust and may incur damage during disassembly	Large number of connections increases sensitivity to damage	Fairly sturdy structural elements with simple disassembly process	Robust elements with simple disassembly process	Very large number of connections greatly increases sensitivity to damage
Explanation: The likelihood of damage occurring during disassembly										
Ease of re-assembly	Grade	Good	Good	Excellent	Good	Very poor	Very poor	Excellent	Good	Excellent
	Comment	Few and simple connections used	Few and simple connections used	Re-assembly only requires sliding required profile length out and fixing in place	Re-assembly only requires sliding required profile length out and fixing in place, slightly more complex due to both truss and deck being telescopic	Many connections using unique profiles which require precise re-assembly procedures	Re-assembly will require the profiles to be chaged and put back together before being re-used	Simple and fast deployment of end-span modules	Few and simple connections used	Structure can be adjusted and re-deployed without any changes being required for the main structure
Explanation: The labour, time, transport, and parts required to re-assemble the structure for reuse										
Reusability of modules for different conigurations ("Part interchangeability")	Grade	Good	Good	Average	Poor	Good	Excellent	Poor	Excellent	Excellent
	Comment	Modules may be used to increase width or after upgrading span be applied where required capacity is lower	Modules may be used to increase width or after upgrading span be applied where required capacity is lower	Only one module so no other configurations	Specifically designed structure with poor possibilities of fulfilling other functions	Nodes and deck can be easily reused while truss members can be applied in less critical areas after upgrading	The flanges will be reused for the new configurations while obsolete webs may be applied in less critical areas after upgrading	Specifically designed structure with poor possibilities of fulfilling other functions	Modules have increased flexibility due to telescopic profiles	Structure is extremely flexible and almost all elements can be reused for new configurations
Explanation: Which fraction of the elements can be reused when the structure is changed or upgraded										
Sensitivity to tolerances and execution errors	Grade	Good	Good	Poor	Very poor	Very poor	Very poor	Good	Poor	Very poor
	Comment	Standard bolted connections	Standard bolted connections	Inner profiles must fit and be able to be joined which requires good degree of precision	Inner profiles must fit and be able to be joined which requires good degree of precision, this is required for both deck and truss elements	Large number of bolted connections which require precise production and assembly processes	Large number of bolted connections which require precise production and assembly processes	Simple structure requiring only basic assembly	Inner profiles must fit and be able to be joined which requires good degree of precision	Large number of bolted connections which require precise production and assembly processes
Explanation: How sensitive is the structure to the manufacturing tolerances of profiles and connections										
Ease of identification of components	Grade	Excellent	Excellent	Excellent	Good	Average	Good	Excellent	Good	Very poor
	Comment	Few and easily recognisable modules	Few and easily recognisable modules	Few and easily recognisable modules	Modules have clear functions in the structure	Deck and node modules are clearly recognisable however truss members may lead to incorrect assemblies	Clearly defined modules and elements within modules	Few and easily recognisable modules	Clearly defined modules with relatively few components	Large number of specifically designed modules
Explanation: How clear the function of an element is within a structure such that reuse is simplified										
Recycling of materials and sustainability										
Minimising volume of waste	Grade	Average	Average	Average	Poor	Poor	Poor	Average	Average	Very poor
	Comment	Disassembly does not favour or hinder recovery of material in any particular way	Disassembly does not favour or hinder recovery of material in any particular way	Disassembly does not favour or hinder recovery of material in any particular way	Disassembly and upgrading may lead to some loss of material	Disassembly and upgrading may lead to some loss of material	Disassembly and upgrading may lead to some loss of material	Disassembly does not favour or hinder recovery of material in any particular way	Disassembly does not favour or hinder recovery of material in any particular way	Large number of components increases chances of loss during disassembly
Explanation: The amount of material that is lost when the structure is disassembled										
Reducing spectrum of materials and profiles	Grade	Excellent	Excellent	Excellent/Good	Average	Poor	Good	Average	Good	Poor
	Comment	Modules will be composed of a single material and similar elements	Modules will be composed of a single material and similar elements	Modules will be composed of a single material and similar elements, depends on whether inner and outer profiles will use the same material	Deck and truss will use different materials but same ones within modules	Several different types of modules used with different materials and profiles	Profiles will be composed of similar materials and good use of repeated elements	Different modules use different profiles however the same material will liekly be used	Modules will be composed of a single material and similar elements, depends on whether inner and outer profiles will use the same material	Large variety of cross-sections used within truss, number of different materials will be limited
Explanation: The different types of profiles and connectors used, and the materials from which they are made										
Ecological footprint of materials	Grade	Poor	Poor	Poor	Poor	Poor	Poor	Poor	Poor	Poor
	Comment									
Explanation: The ecological footprint of the materials (likely to be) present in the structure										
Opportunities for green procurement	Grade	Average	Poor	Poor	Average	Average	Poor	Poor	Poor	Average
	Comment	Standard profiles with wide variety of possible suppliers; may offer opportunities for green procurement	Green procurement may be possible for plate material however this will depend mainly on the manufacturer	Green procurement may be possible for plate material however this will depend mainly on the manufacturer	Standard profiles with wide variety of possible suppliers; may offer opportunities for green procurement	Standard profiles with wide variety of possible suppliers; may offer opportunities for green procurement	Elements made to specification with fewer opportunities for green procurement	Elements made to specification with fewer opportunities for green procurement	Green procurement may be possible for plate material however this will depend mainly on the manufacturer	Standard profiles with wide variety of possible suppliers; may offer opportunities for green procurement
Explanation: Do the elements and materials used lend themselves to be procured from green sources										
Overall grade	Grade	Good	Good	Average/Good	Average	Good	Poor	Good	Good	Average/Good
	Comment									

Appendix C2: Multi-Criteria Analysis: Second round qualitative analysis

Aspect of circular economy	Weighting		Structural variant 1A	3A	1C / 3C	α	β	γ	ϵ	Ω	λ
Optimised material use											
Structure designed for the capacity without over-specification	8	Score	3	3	2	4	5	3	2	4	2
Use of higher strength materials*	8	Score	4	4	4	4	4	4	4	4	4
Optimised cross-sections for performance	10	Score	3	5	3,50	5	5	5	3	5	4
Robustness of the structure	5,0	Score	4	5	4	5	4	1	4	4	2
Use of low-waste production processes	2	Score	2	5	4	2	3	3	3	5	1
Adaptability and upgradability											
Range of span expandability	10	Score	3	3	4	3	5	4	4	5	5
Size of dimension adjustments	3	Score	1	1	5	5	5	1	4	4	5
Range of width expandability	8	Score	4	4	3	4	5	4	4	4	4
Upgradability of strength	8	Score	3	2	2	1	5	5	2	2	5
Standardisation/repetition of components	6	Score	4	4	4	3	4	5	3	4	2
Maintenance and repair											
Accessibility of parts within the structure	7	Score	4	3,5	2	1	4	1	4	3	1
Fault diagnostics (monitoring/expected failure points)	2	Score	4	4	2	2	3	1	3	2	2
Safety for techinicians	5	Score	3	3	4	5	4	3	4	3	3
Use of industry standard ("off-the-shelf") components	6,0	Score	5	3	3,5	4	5	2	2	3	4
Redundancy features / alternative load paths	2	Score	2	2	4	5	5	2	2	2	5
Refurbishment and reuse/re-assembly											
Degree of prefabrication	6	Score	4	4	4	4	4	5	4	4	4
Ease of disassembly	8	Score	4	4	5	3	4	3	5	4	3
Total number of connections	6	Score	5	5	4	3	1	1	5	4	1
Tools required for disassembly	3	Score	4	4	3	3	4	3	5	3,5	4
Damage caused by disassembly / quality of elements after disassembly	6	Score	4	4	5	3	2	2	4	5	1
Ease of re-assembly	6,0	Score	4	4	5	4	1	1	5	4	5
Reusability of modules for different conigurations ("Part interchangeability")	7	Score	4	4	3	2	4	5	2	5	5
Sensitivity to tolerances and execution errors	5	Score	4	4	2	1	1	1	4	2	1
Ease of identification of components	1	Score	5	5	5	4	3	4	5	4	1
Recycling of materials and sustainability											
Minimising volume of waste	6	Score	3	3	3	2	2	2	3	3	1
Reducing spectrum of materials and profiles	5	Score	5	5	4,5	3	2	4	3	4	2
Ecological footprint of materials	6	Score	2	2	2	2	2	2	2	2	2
Opportunities for green procurement	3	Score	3	2	2	3	3	2	2	2	3
Overall Score		Score	571	575,5	548,5	504	582	483	545	589,5	489

Appendix D: Comparison of material use and reuse in different scenarios

			Truss	Integrated deck girder	Tied Arch
Scenario A					
Original situation:	15m span, 5m width	Weight:	3191	10465	15700
Modification:	25m span	Weight:	9362	17633	27936
	Weight of new material required:		7072	8403	15943
	Percetage of material reused:		24%	52%	43%
Scenario B					
Original situation:	25m span, 5m width	Weight:	9362	17633	27936
Modification:	7m width	Weight:	10591	25721	36870
	Weight of new material required:		10008	9141	26367
	Percetage of material reused:		6%	64%	28%
Scenario C					
Original situation:	25m span, 5m width	Weight:	9362	17633	27936
Modification:	33m span	Weight:	14657	24480	35655
	Weight of new material required:		10450	5935	15778
	Percetage of material reused:		29%	76%	56%
Scenario D					
Original situation:	33m span, 5m width	Weight:	14657	24480	35655
Modification:	7m width	Weight:	15993	34272	46139
	Weight of new material required:		12885	12778	19048
	Percetage of material reused:		19%	63%	59%

```
> Appendix E1; Complete calculation of the structure at SLS
```

Appendix E1

Complete calculation of the structure at SLS **(1)**

```
> restart;
> ODE1 := EI·diff(w1(x), x$4) = q; ODE2 := EI·diff(w2(x), x$4) = q; ODE3 := EI
      ·diff(w3(x), x$4) = q;
```

$$ODE1 := EI\left(\frac{d^4}{dx^4}\, w1(x)\right) = q$$

$$ODE2 := EI\left(\frac{d^4}{dx^4}\, w2(x)\right) = q$$

$$ODE3 := EI\left(\frac{d^4}{dx^4}\, w3(x)\right) = q \quad \textbf{(2)}$$

```
> sol := dsolve({ODE1, ODE2, ODE3}, {w1(x), w2(x), w3(x)}) : assign(sol) :
> w1 := w1(x); w2 := w2(x); w3 := w3(x);
```

$$w1 := \frac{q\,x^4}{24\,EI} + \frac{\_C9\,x^3}{6} + \frac{\_C10\,x^2}{2} + \_C11\,x + \_C12$$

$$w2 := \frac{q\,x^4}{24\,EI} + \frac{\_C5\,x^3}{6} + \frac{\_C6\,x^2}{2} + \_C7\,x + \_C8$$

$$w3 := \frac{q\,x^4}{24\,EI} + \frac{\_C1\,x^3}{6} + \frac{\_C2\,x^2}{2} + \_C3\,x + \_C4 \quad \textbf{(3)}$$

```
> phi1 := -diff(w1, x) : kappa1 := diff(phi1, x) : M1 := EI·kappa1-H·w1 : V1 := diff(M1, x) :
> phi2 := -diff(w2, x) : kappa2 := diff(phi2, x) : M2 := EI·kappa2-H·w2 : V2 := diff(M2, x) :
> phi3 := -diff(w3, x) : kappa3 := diff(phi3, x) : M3 := EI·kappa3-H·w3 : V3 := diff(M3, x) :
> x := 0 : eq1 := w1 = 0 : eq2 := M1 = 0 :
> x := a : eq3 := w1 = w2 : eq4 := phi1 = phi2 : eq5 := M1 = M2 : eq6 := V1 - V2 + F = 0 :
> x := a + b : eq7 := w2 = w3 : eq8 := phi2 = phi3 : eq9 := M2 = M3 : eq10 := V2 - V3 + F = 0 :
> x := a + b + a : eq11 := w3 = 0 : eq12 := M3 = 0 :
> sol := solve({eq1, eq2, eq3, eq4, eq5, eq6, eq7, eq8, eq9, eq10, eq11, eq12}, {_C1, _C2, _C3,
      _C4, _C5, _C6, _C7, _C8, _C9, _C10, _C11, _C12}) : assign(sol);
> #Input parameters:
> a := 6 : b := 6 : B := 3 : q := B·(5 + (89·9.81)/1000) + 8/(a + b + a)^2 ·H·(0.0135) : EI := B
      ·70·10^6·0.000175 : f := 1.0 : n := 6 : T := 20 : A_tierod := 0.25·3.14·0.024^2 : E_tierod :=
      210·10^6 :
> #Deflection at a:
> delta_a := 0.03447 :
> #Force in tie rod due to elongation:
> l_inc1 := sqrt(a^2 + f^2) : l_inc2 := sqrt(a^2 + (f + delta_a)^2) : delta_l := l_inc2 - l_inc1 :
      eps_l := delta_l/l_inc1 : N := A_tierod·E_tierod·eps_l :
```

```
> #Force components of the tie rod:
> alpha := arctan((f + delta_a)/a); N_total := n·N; F := n·sin(alpha)·(T + N) − 1.4; H := n
  ·cos(alpha)·(T + N); Force_per_tie_rod := N + T;
```

$$\alpha := 0.1707331465$$

$$N\_total := 539.6570960$$

$$F := 110.6789608$$

$$H := 650.0659895$$

$$Force\_per\_tie\_rod := 109.9428493 \qquad \textbf{(4)}$$

```
> x := 'x': AA := plot(-w1, x = 0..a, title = "displacement in metres") : BB := plot(-w2, x = a..a
  + b) : CC := plot(-w3, x = a + b..a + b + a) :
> plots:-display([AA, BB, CC]); maximum_deflection := -1·minimize(-w2, x = a..a + b);
  allowable_deflection := evalf((a + b + a)·3/1000); x := a : deflection_at_a := w1;
```

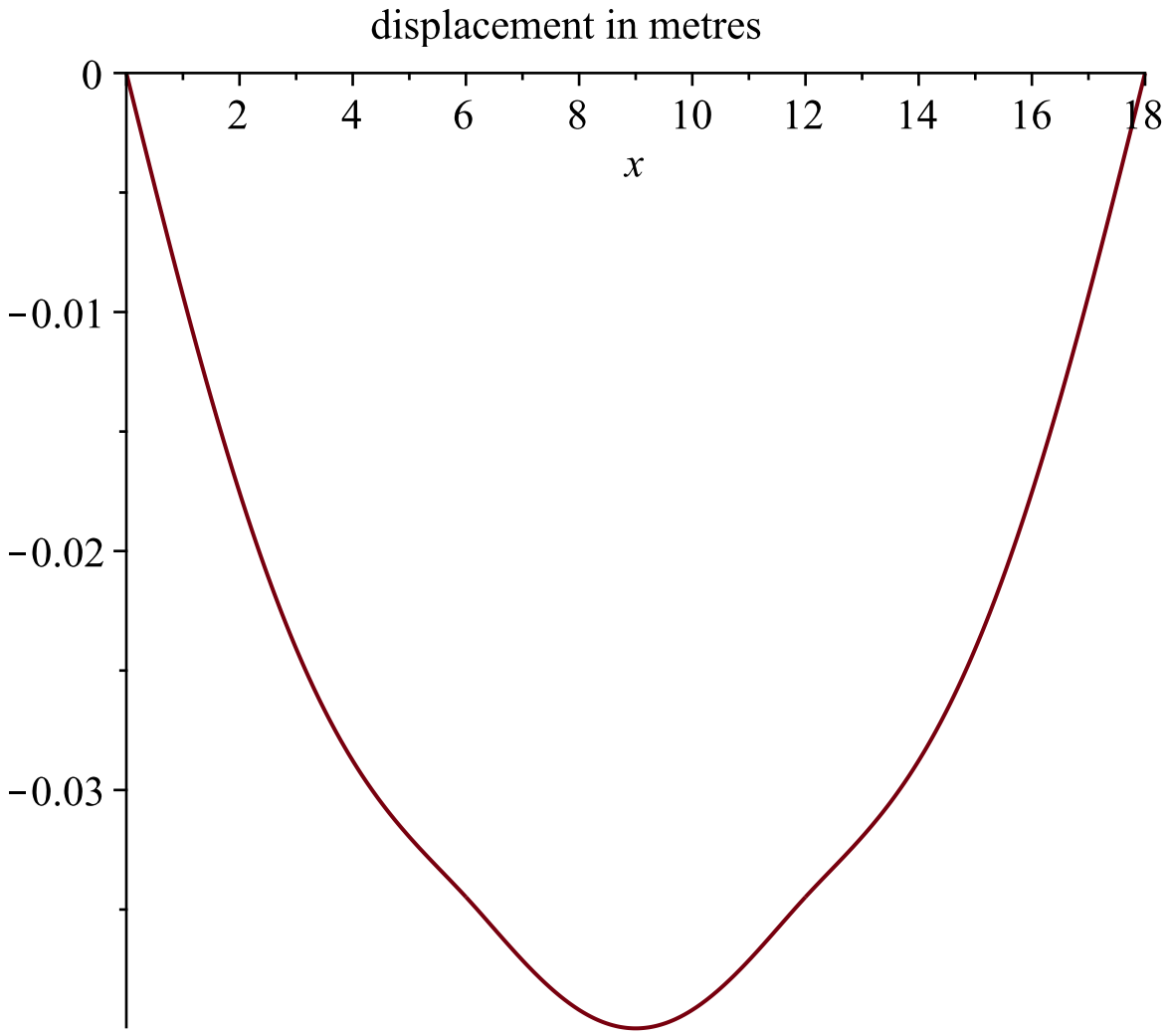

$$maximum\_deflection := 0.03997227500$$

$$allowable\_deflection := 0.05400000000$$

$$deflection\_at\_a := 0.03447363106 \qquad \textbf{(5)}$$

```
> x :='x': AA := plot( -M1, x = 0 ..a, title = "bending moment") : BB := plot( -M2, x = a ..a + b) :
      CC := plot( -M3, x = a + b ..a + b + a) :
> plots:-display( [AA, BB, CC]); x := a : M1;
```

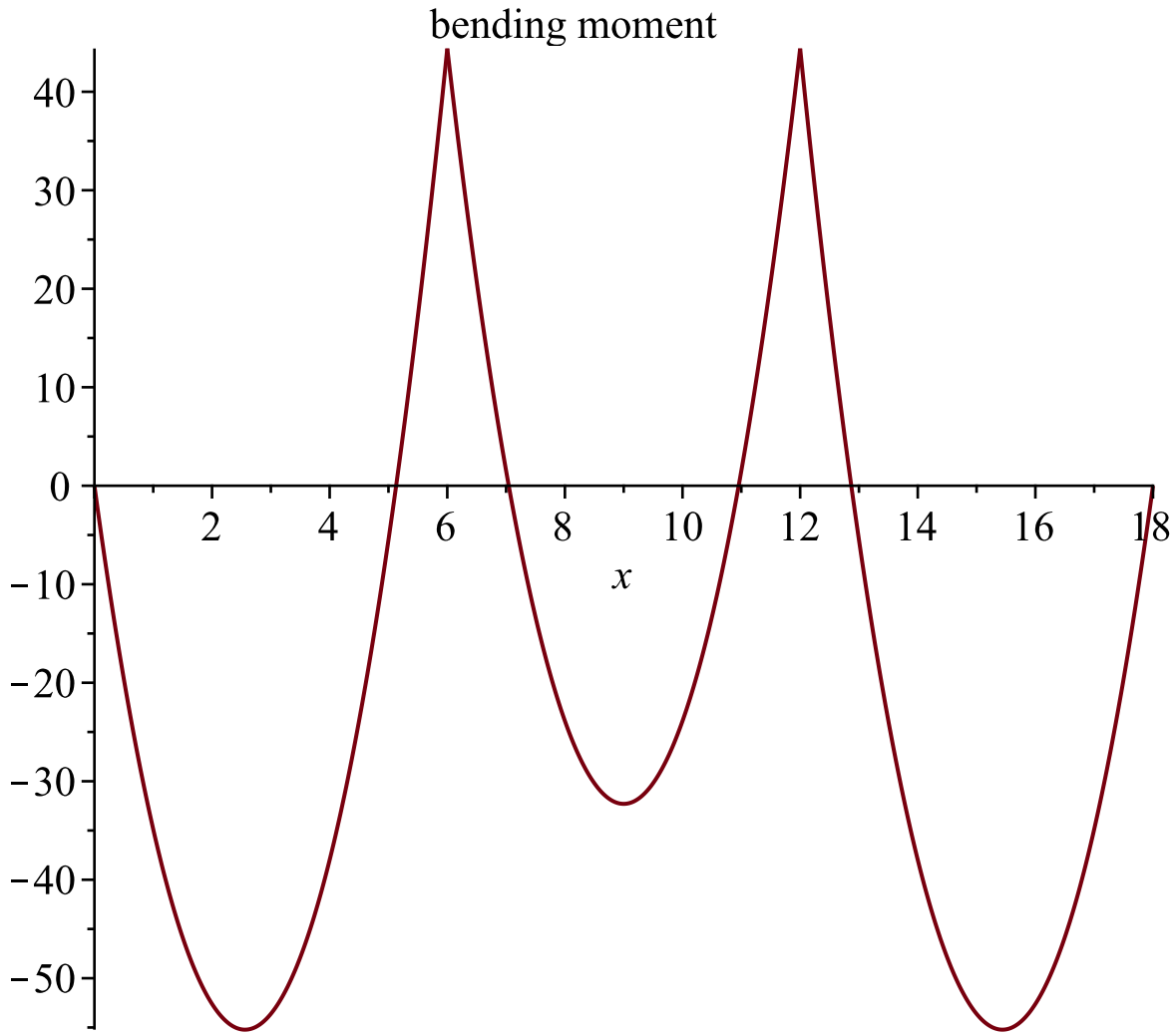

$$-44.38938789 \qquad (6)$$

```
>
> x :='x': AA := plot( V1, x = 0 ..a, title = "shear force") : BB := plot( V2, x = a ..a + b) : CC :=
      plot( V3, x = a + b ..a + b + a) :
> plots:-display( [AA, BB, CC]);
```

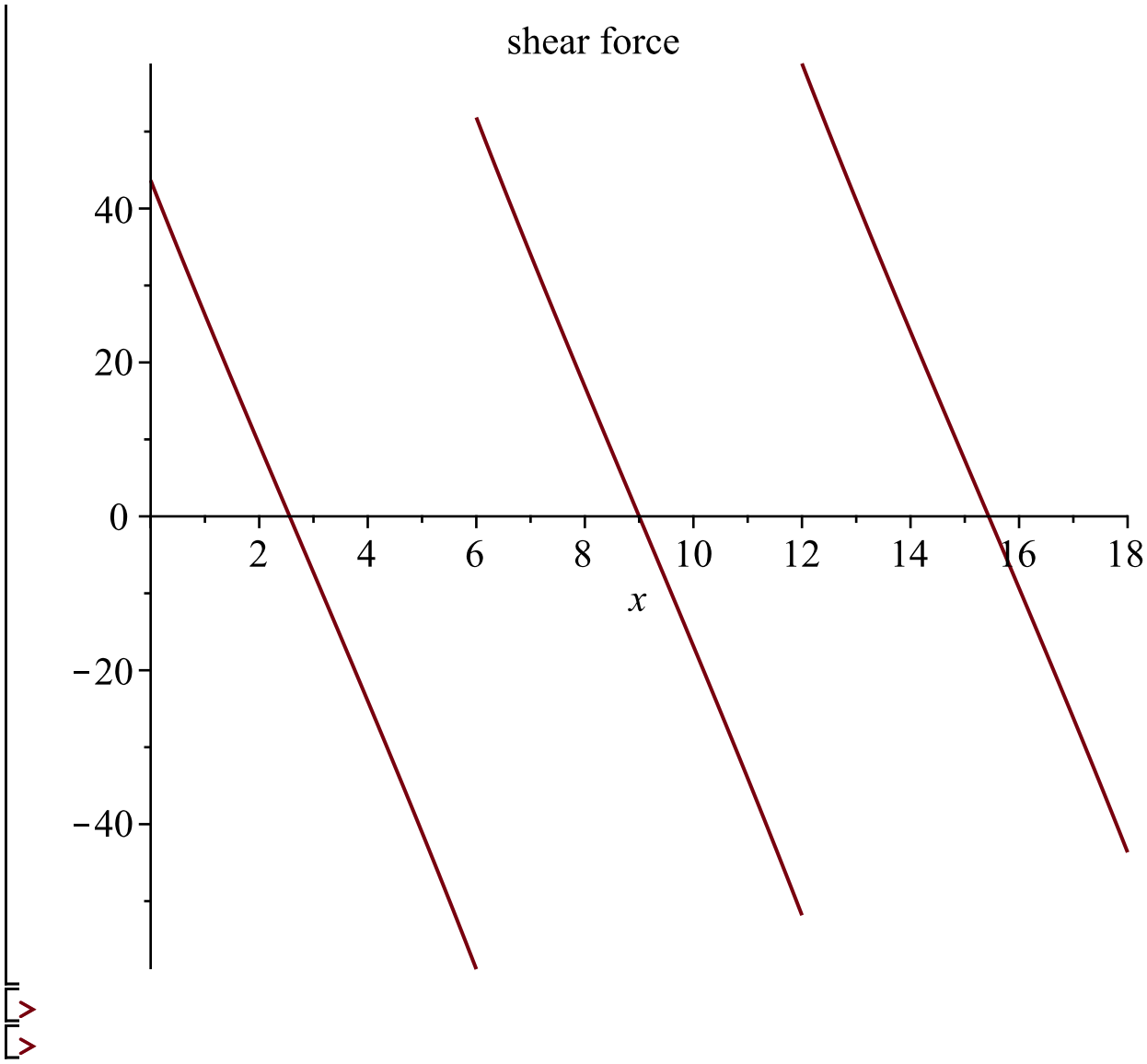
shear force
40
20
0
−20
−40
2
4
6
8
10
12
14
16
18
x

> *Appendix E2; Complete calculation of the structure at ULS*

Appendix E2

Complete calculation of the structure at ULS **(1)**

> *restart;*

> $ODE1 := EI \cdot diff(w1(x), x\$4) = q;\ ODE2 := EI \cdot diff(w2(x), x\$4) = q;\ ODE3 := EI \cdot diff(w3(x), x\$4) = q$;

$$ODE1 := EI\left(\frac{d^4}{dx^4}\, w1(x)\right) = q$$

$$ODE2 := EI\left(\frac{d^4}{dx^4}\, w2(x)\right) = q$$

$$ODE3 := EI\left(\frac{d^4}{dx^4}\, w3(x)\right) = q \quad \textbf{(2)}$$

> $sol := dsolve(\{ODE1, ODE2, ODE3\}, \{w1(x), w2(x), w3(x)\}) : assign(sol) :$

> $w1 := w1(x);\ w2 := w2(x);\ w3 := w3(x);$

$$w1 := \frac{q\,x^4}{24\,EI} + \frac{\_C9\,x^3}{6} + \frac{\_C10\,x^2}{2} + \_C11\,x + \_C12$$

$$w2 := \frac{q\,x^4}{24\,EI} + \frac{\_C5\,x^3}{6} + \frac{\_C6\,x^2}{2} + \_C7\,x + \_C8$$

$$w3 := \frac{q\,x^4}{24\,EI} + \frac{\_C1\,x^3}{6} + \frac{\_C2\,x^2}{2} + \_C3\,x + \_C4 \quad \textbf{(3)}$$

> $phi1 := -diff(w1, x) : kappa1 := diff(phi1, x) : M1 := EI \cdot kappa1 - H \cdot w1 : V1 := diff(M1, x) :$

> $phi2 := -diff(w2, x) : kappa2 := diff(phi2, x) : M2 := EI \cdot kappa2 - H \cdot w2 : V2 := diff(M2, x) :$

> $phi3 := -diff(w3, x) : kappa3 := diff(phi3, x) : M3 := EI \cdot kappa3 - H \cdot w3 : V3 := diff(M3, x) :$

> $x := 0 : eq1 := w1 = 0 : eq2 := M1 = 0 :$

> $x := a : eq3 := w1 = w2 : eq4 := phi1 = phi2 : eq5 := M1 = M2 : eq6 := V1 - V2 + F = 0 :$

> $x := a + b : eq7 := w2 = w3 : eq8 := phi2 = phi3 : eq9 := M2 = M3 : eq10 := V2 - V3 + F = 0 :$

> $x := a + b + a : eq11 := w3 = 0 : eq12 := M3 = 0 :$

> $sol := solve(\{eq1, eq2, eq3, eq4, eq5, eq6, eq7, eq8, eq9, eq10, eq11, eq12\}, \{\_C1, \_C2, \_C3, \_C4, \_C5, \_C6, \_C7, \_C8, \_C9, \_C10, \_C11, \_C12\}) : assign(sol);$

> *#Input parameters:*

> $a := 6 : b := 6 : B := 3 : q := B \cdot \left(1.5 \cdot 5 + 1.35 \cdot \frac{(89 \cdot 9.81)}{1000}\right) + \frac{8}{(a+b+a)^2} \cdot H \cdot (0.0135) :$

$EI := B \cdot 70 \cdot 10^6 \cdot 0.000175 : f := 1.0 : n := 6 : T := 20 : A\_tierod := 0.25 \cdot 3.14 \cdot 0.024^2 :$

$E\_tierod := 210 \cdot 10^6 :$

> *#Deflection at a:*

> $delta\_a := 0.03883 :$

> *#Force in tie rod due to elongation:*

> $l\_inc1 := \sqrt{a^2 + f^2} : l\_inc2 := \sqrt{a^2 + (f + delta\_a)^2} : delta\_l := l\_inc2 - l\_inc1 :$

$$eps\_l := \frac{delta\_l}{l\_inc1} : N := A\_tierod \cdot E\_tierod \cdot eps\_l :$$

> #Force components of the tie rod:

> $alpha := \arctan\left(\frac{f + delta\_a}{a}\right)$; $N\_total := 1.35 \cdot n \cdot N$; $F := 1.35 \cdot (n \cdot \sin(alpha) \cdot (T + N) - 1.4)$; $H := 1.35 \cdot n \cdot \cos(alpha) \cdot (T + N)$; $Force\_per\_tie\_rod := 1.35(N + T)$;

$$\alpha := 0.1714387499$$

$$N\_total := 822.3961444$$

$$F := 166.0481629$$

$$H := 969.9652275$$

$$Force\_per\_tie\_rod := 164.0660241 \quad \textbf{(4)}$$

> $x := 'x'$: $AA := plot(-w1, x = 0..a, title = \text{"displacement in metres"})$: $BB := plot(-w2, x = a..a + b)$: $CC := plot(-w3, x = a + b..a + b + a)$:

> $plots{:}\text{-}display([AA, BB, CC])$; $maximum\_deflection := -1 \cdot minimize(-w2, x = a..a + b)$; $allowable\_deflection := evalf\left(\frac{(a + b + a) \cdot 3}{1000}\right)$; $x := a$: $deflection\_at\_a := w1$;

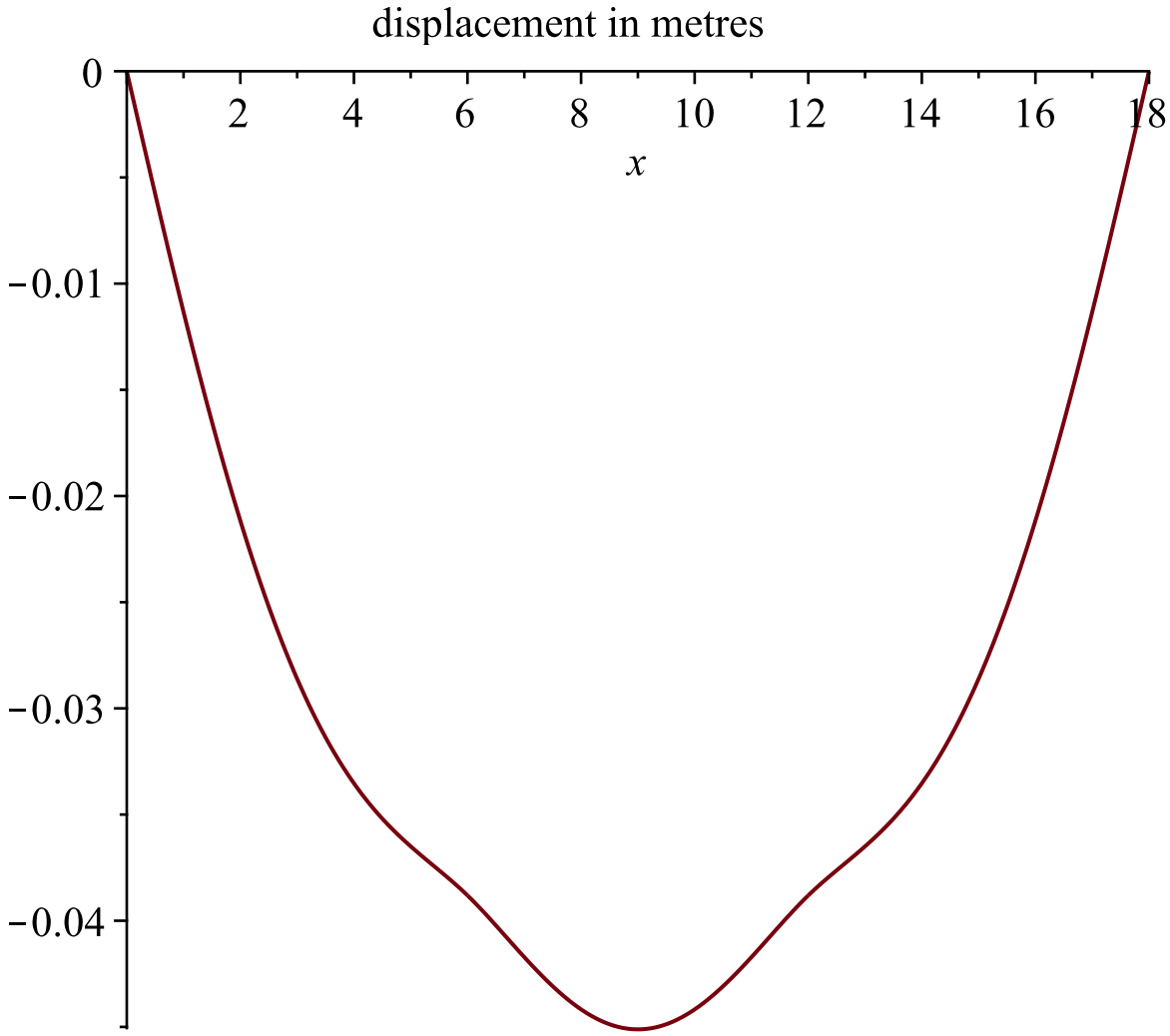

$$maximum\_deflection := 0.04511423057$$

$$allowable\_deflection := 0.05400000000$$

$$deflection\_at\_a := 0.03880876546 \quad \textbf{(5)}$$

```
> x :='x': AA := plot( -M1, x = 0 ..a, title = "bending moment") : BB := plot( -M2, x = a ..a + b) :
      CC := plot( -M3, x = a + b ..a + b + a) :
> plots:-display( [AA, BB, CC]); x := a : M1;
```

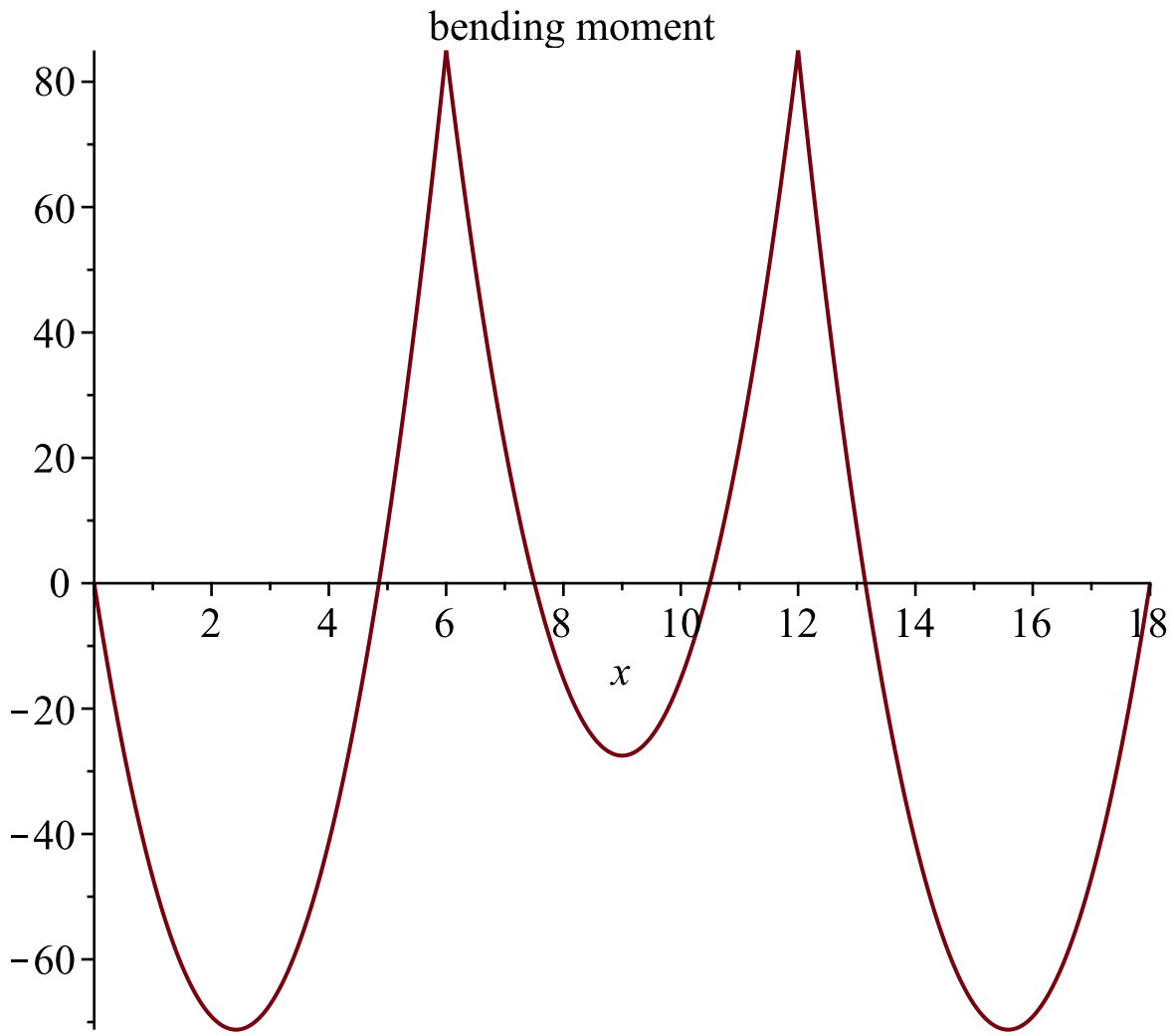

$$-84.99602598 \quad \textbf{(6)}$$

```
>
> x :='x': AA := plot( V1, x = 0 ..a, title = "shear force") : BB := plot( V2, x = a ..a + b) : CC :=
      plot( V3, x = a + b ..a + b + a) :
> plots:-display( [AA, BB, CC]);
```

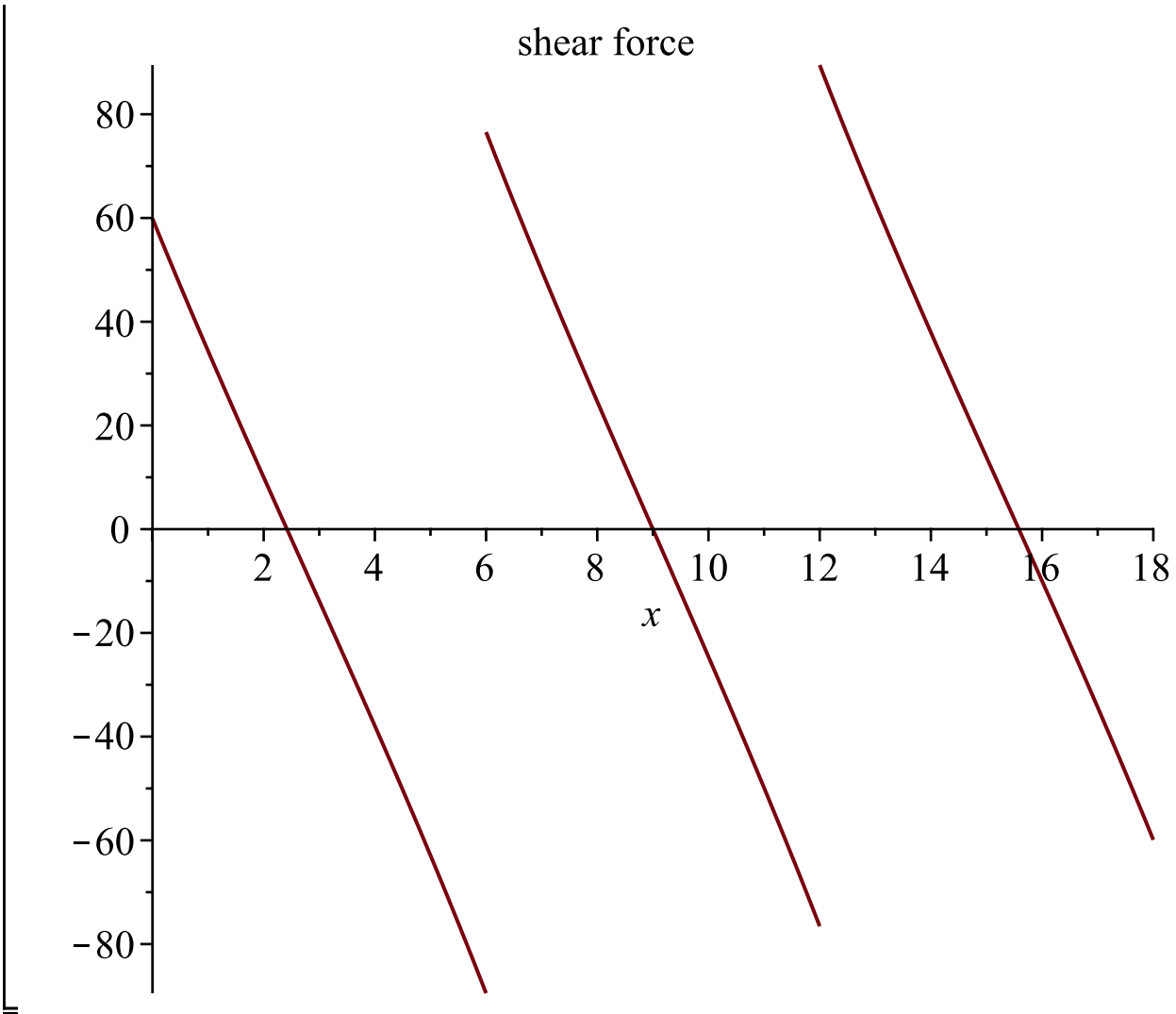

> $x := a : -V1 + V2$

166.0481629 **(7)**

>

Appendix E3: Buckling verification of the structure at ULS

N_Ed =	904	kN	Reduced axial force and bending moment due to moment
M_Ed =	71	kNm	eccentricity assumption used in this calculation

E =	70000000	kN/m2
I =	0,000525	m4
L =	6	m
M1 =	60	kNm
θ1 =	0,007935	rad
M2 =	85	kNm
θ2 =	2,59E-03	rad

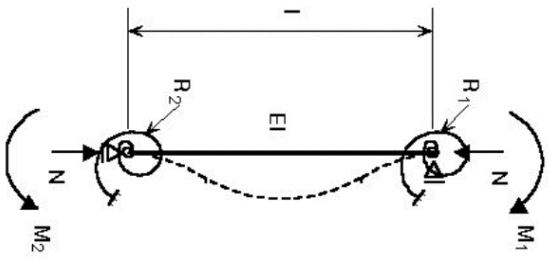

f1 =	0,03	-	(= 0 when excluding eccentricity of anchorage)
f2 =	0,14	-	
n =	0,228025	-	
k =	2,094153	-	
L_k =	12,56492	m	
N_cr =	2297,406	kN	
λ =	3,343626	-	
ϕ =	6,41428	-	
χ_y =	0,084117	-	
κ =	0,997254	-	
ω_x =	0,63		
N_Rd =	23286	kN	
M_Rd =	1184	kNm	
U.C. =	0,874807	-	

$$f_i = \frac{1}{6{,}5\,EI}\frac{M_i}{\Theta_i}$$

$$n = \frac{1{,}2(f_1+f_2)+7{,}2\,f_1 f_2}{1+1{,}4\,(f_1+f_2)+1{,}8\,f_1 f_2} \qquad K = 1/\sqrt{n}$$

$$\bar{\lambda} = \sqrt{\frac{A_{eff}\,f_o}{N_{cr}}} \qquad \phi = 0{,}5(1+\alpha(\bar{\lambda}-\bar{\lambda}_0)+\bar{\lambda}^2)$$

$$\chi = \frac{1}{\phi+\sqrt{\phi^2 - \bar{\lambda}^2}}$$

Table 6.6 - Values of α and $\bar{\lambda}_0$ for flexural buckling

Material buckling class according to Table 3.2	α	$\bar{\lambda}_0$
Class A	0,20	0,10
Class B	0,32	0,00

Appendix F: Life Cycle Analysis comparing circular and traditional bridge design methodology

NMD data			Unit:	EPD Data		Steel truss bridge FU1	Steel truss bridge FU2	Modular aluminium girder bridge FU1	Modular aluminium girder bridge FU2	Modular steel girder	Steel truss bridge FU1 (EPD DATA USED)	Steel truss bridge FU2 (EPD DATA USED)
Steel	SBK Steel, Heavy Construction Products PRODUCTIE, BmS, 2013, c2		kg	kg								
	1 ton heavy construction products consist of 900 kg sections (10% BF and 90% EAF) and 100 kg plate (BF). No coilcoating or hot dip galvanising is included. MRPI-CODE 9.2.00011.004				ECI value in Euro per unit:	11276	15706	381	254	24662		
1	Depletion of abiotic resources-elements	Kg Sb		-1,34E-07	4,92E-07	0,16	-2,42E-04	-3,37E-04	-8,17E-06	-5,45E-06	-5,29E-04	8,88E-04	1,24E-03
2	Depletion of abiotic resources-fossil fuels	Kg Sb		5,21E-03		0,16	9,40E+00	1,31E+01	3,18E-01	2,12E-01	2,06E+01	9,40E+00	1,31E+01
3	Global warming	Kg CO2 Equiv.		9,08E-01	1,13E+00	0,05	5,12E+02	7,13E+02	1,73E+01	1,15E+01	1,12E+03	6,37E+02	8,87E+02
4	Ozone layer depletion	Kg CFC-11 Equiv.		1,55E-08	1,96E-10	30	5,24E-03	7,30E-03	1,77E-04	1,18E-04	1,15E-02	6,63E-05	9,24E-05
5	Photochemical oxidants creation	Kg Ethene Equiv.		3,30E-04	4,02E-04	2	7,44E+00	1,04E+01	2,51E-01	1,68E-01	1,63E+01	9,07E+00	1,26E+01
6	Acidification of soil and water	Kg SO2 Equiv.		3,38E-03	2,16E-03	9	3,43E+02	4,78E+02	1,16E+01	7,73E+00	7,50E+02	2,19E+02	3,05E+02
7	Eutrophication	Kg PO43- Equiv.		3,74E-04	2,19E-04	4	1,69E+01	2,35E+01	5,70E-01	3,80E-01	3,69E+01	9,88E+00	1,38E+01
8	Human toxicity	kg 1.4 DB		3,33E-02		0,09	3,38E+01	4,71E+01	1,14E+00	7,61E-01	7,39E+01	3,38E+01	4,71E+01
9	Ecotoxicity. fresh water	kg 1.4 DB		3,02E-03		0,03	1,02E+00	1,42E+00	3,45E-02	2,30E-02	2,23E+00	1,02E+00	1,42E+00
10	Ecotoxicity. marine water (MAETP)	kg 1.4 DB		6,34E+00		0,0001	7,15E+00	9,96E+00	2,42E-01	1,61E-01	1,56E+01	7,15E+00	9,96E+00
11	Ecotoxicity. terrestric	kg 1.4 DB		4,68E-04		0,06	3,17E-01	4,41E-01	1,07E-02	7,13E-03	6,93E-01	3,17E-01	4,41E-01
14	renewable primary energy total	MJ		5,28E-01									
18	use of secondary material	Kg		5,00E-01									
							9,31E+02	1,30E+03	3,15E+01	2,10E+01	2,04E+03	9,27E+02	1,29E+03
Steel	steel heavy construction products - BmS (MRPI) - D	Recycling and re-use	kg										
	The recycling and re-use process for steel are included in the MRPI of steel from demolition until the point the steel can be re-used in a product system.												
							11276	15706	0	635	24662		
1	Depletion of abiotic resources-elements	Kg Sb		9,55E-08	-8,92E-07		1,72E-04	2,40E-04	0,00E+00	9,70E-06	3,77E-04	-1,61E-03	-2,24E-03
2	Depletion of abiotic resources-fossil fuels	Kg Sb		-2,72E-03			-4,91E+00	-6,84E+00	0,00E+00	-2,76E-01	-1,07E+01	-4,91E+00	-6,84E+00
3	Global warming	Kg CO2 Equiv.		-5,12E-01	-4,13E-01		-2,89E+02	-4,02E+02	0,00E+00	-1,63E+01	-6,31E+02	-2,33E+02	-3,24E+02
4	Ozone layer depletion	Kg CFC-11 Equiv.		-3,72E-09	1,62E-09		-1,26E-03	-1,75E-03	0,00E+00	-7,09E-05	-2,75E-03	5,48E-04	7,63E-04
5	Photochemical oxidants creation	Kg Ethene Equiv.		-1,84E-04	-1,78E-04		-4,15E+00	-5,78E+00	0,00E+00	-2,34E-01	-9,08E+00	-4,01E+00	-5,59E+00
6	Acidification of soil and water	Kg SO2 Equiv.		-1,51E-03	-8,07E-04		-1,53E+02	-2,13E+02	0,00E+00	-8,63E+00	-3,35E+02	-8,19E+01	-1,14E+02
7	Eutrophication	Kg PO43- Equiv.		-1,53E-04	-6,66E-05		-6,90E+00	-9,61E+00	0,00E+00	-3,89E-01	-1,51E+01	-3,00E+00	-4,18E+00
8	Human toxicity	kg 1.4 DB		-8,85E-03			-8,98E+00	-1,25E+01	0,00E+00	-5,06E-01	-1,96E+01	-8,98E+00	-1,25E+01
9	Ecotoxicity. fresh water	kg 1.4 DB		-1,87E-03			-6,33E-01	-8,81E-01	0,00E+00	-3,56E-02	-1,38E+00	-6,33E-01	-8,81E-01
10	Ecotoxicity. marine water (MAETP)	kg 1.4 DB		-1,78E+00			-2,01E+00	-2,80E+00	0,00E+00	-1,13E-01	-4,39E+00	-2,01E+00	-2,80E+00
11	Ecotoxicity. terrestric	kg 1.4 DB		-1,40E-04			-9,47E-02	-1,32E-01	0,00E+00	-5,33E-03	-2,07E-01	-9,47E-02	-1,32E-01
14	renewable primary energy total	MJ		-2,48E-01									
25	Components for re-use	Kg		4,90E-01									
26	Materials for recycling	Kg		5,10E-01									
							-4,70E+02	-6,54E+02	0,00E+00	-2,64E+01	-1,03E+03	-3,38E+02	-4,71E+02
Steel coati	wetpainting steel, per kg coating [BmS]						211	345	7,8	26	465,8		
	SBK Natlakken van staal, per kg lak, cradle to gate, BmS, 2013, c2		kg										
1	Depletion of abiotic resources-elements	Kg Sb		1,62E-06			5,47E-05	8,94E-05	2,02E-06	6,74E-06	6,48E-05		
2	Depletion of abiotic resources-fossil fuels	Kg Sb		3,00E-03			1,01E-01	1,66E-01	3,74E-03	1,25E-02	1,20E-01		
3	Global warming	Kg CO2 Equiv.		2,43E+00			2,56E+01	4,19E+01	9,48E-01	3,16E+00	3,04E+01		
4	Ozone layer depletion	Kg CFC-11 Equiv.		1,37E-07			8,67E-04	1,42E-03	3,21E-05	1,07E-04	1,03E-03		
5	Photochemical oxidants creation	Kg Ethene Equiv.		1,16E-01			4,90E+01	8,00E+01	1,81E+00	6,03E+00	5,80E+01		
6	Acidification of soil and water	Kg SO2 Equiv.		1,42E-02			2,70E+01	4,41E+01	9,97E-01	3,32E+00	3,20E+01		
7	Eutrophication	Kg PO43- Equiv.		1,55E-03			1,31E+00	2,14E+00	4,84E-02	1,61E-01	1,55E+00		
8	Human toxicity	kg 1.4 DB		5,68E+00			1,08E+02	1,76E+02	3,99E+00	1,33E+01	1,28E+02		
9	Ecotoxicity. fresh water	kg 1.4 DB		8,29E-01			5,25E+00	8,58E+00	1,94E-01	6,47E-01	6,22E+00		
10	Ecotoxicity. marine water (MAETP)	kg 1.4 DB		4,45E+01			9,39E-01	1,54E+00	3,47E-02	1,16E-01	1,11E+00		
11	Ecotoxicity. terrestric	kg 1.4 DB		3,64E-03			4,61E-02	7,53E-02	1,70E-03	5,68E-03	5,46E-02		
14	renewable primary energy total	MJ		8,52E-01									
							2,17E+02	3,55E+02	8,02E+00	2,67E+01	2,57E+02		
Steel coati	Pouder coating steel, per kg coating [BmS]						0	0	0	0			
	SBK Poedercoaten van staal, per kg poedercoat, cradle to gate, BmS, 2013, c2		kg										
1	Depletion of abiotic resources-elements	Kg Sb		1,39E-05									
2	Depletion of abiotic resources-fossil fuels	Kg Sb		1,32E-01									
3	Global warming	Kg CO2 Equiv.		1,58E+01									
4	Ozone layer depletion	Kg CFC-11 Equiv.		1,80E-06									
5	Photochemical oxidants creation	Kg Ethene Equiv.		5,59E-03									
6	Acidification of soil and water	Kg SO2 Equiv.		4,56E-02									
7	Eutrophication	Kg PO43- Equiv.		5,92E-03									
8	Human toxicity	kg 1.4 DB		4,59E+00									
9	Ecotoxicity. fresh water	kg 1.4 DB		7,81E-02									
10	Ecotoxicity. marine water (MAETP)	kg 1.4 DB		6,77E+02									

11	Ecotoxicity. terrestric	kg 1.4 DB		3,82E-03								
14	renewable primary energy total	MJ		5,02E+00								
						800	1200	0	0		2289,6	
Steel weldi	Welding, arc, steel {RER}| processing | Alloc Rec, U		m									
1	Depletion of abiotic resources-elements	Kg Sb		1,33E-06		1,70E-04	2,55E-04				1,72E-04	
2	Depletion of abiotic resources-fossil fuels	Kg Sb		1,26E-03		1,61E-01	2,42E-01				1,63E-01	
3	Global warming	Kg CO2 Equiv.		1,89E-01		7,56E+00	1,13E+01				7,65E+00	
4	Ozone layer depletion	Kg CFC-11 Equiv.		1,13E-08		2,71E-04	4,07E-04				2,75E-04	
5	Photochemical oxidants creation	Kg Ethene Equiv.		1,51E-04		2,42E-01	3,62E-01				2,45E-01	
6	Acidification of soil and water	Kg SO2 Equiv.		9,23E-04		6,65E+00	9,97E+00				6,73E+00	
7	Eutrophication	Kg PO43- Equiv.		1,53E-04		4,90E-01	7,34E-01				4,96E-01	
8	Human toxicity	kg 1.4 DB		8,51E-01		6,13E+01	9,19E+01				6,20E+01	
9	Ecotoxicity. fresh water	kg 1.4 DB		9,19E-03		2,21E-01	3,31E-01				2,23E-01	
10	Ecotoxicity. marine water (MAETP)	kg 1.4 DB		5,29E+01		4,23E+00	6,35E+00				4,28E+00	
11	Ecotoxicity. terrestric	kg 1.4 DB		3,48E-03		1,67E-01	2,51E-01				1,69E-01	
14	renewable primary energy total	MJ		2,43E-01								
						8,10E+01	1,21E+02				8,20E+01	
						0	0	0	0			
Steel weldi	Welding, gas, steel {RER}| processing | Alloc Rec, U		m									
1	Depletion of abiotic resources-elements	Kg Sb		1,25E-06								
2	Depletion of abiotic resources-fossil fuels	Kg Sb		1,19E-03								
3	Global warming	Kg CO2 Equiv.		2,10E-01								
4	Ozone layer depletion	Kg CFC-11 Equiv.		1,00E-08								
5	Photochemical oxidants creation	Kg Ethene Equiv.		1,68E-04								
6	Acidification of soil and water	Kg SO2 Equiv.		8,83E-04								
7	Eutrophication	Kg PO43- Equiv.		1,47E-04								
8	Human toxicity	kg 1.4 DB		8,47E-01								
9	Ecotoxicity. fresh water	kg 1.4 DB		9,16E-03								
10	Ecotoxicity. marine water (MAETP)	kg 1.4 DB		5,28E+01								
11	Ecotoxicity. terrestric	kg 1.4 DB		3,45E-03								
14	renewable primary energy total	MJ		2,06E-01								
						0	0	4806	3203			
Aluminium	Aluminium, cast alloy {GLO} | market for | Alloc Rec, U		kg									
	Allocation based on economic values. Aluminium consists of 20% primary and 80% secondary material (26,7% post-cosumer).											
1	Depletion of abiotic resources-elements	Kg Sb		2,87E-04	4,94E-06			2,21E-01	1,47E-01		3,80E-03	2,53E-03
2	Depletion of abiotic resources-fossil fuels	Kg Sb		2,48E-02				1,91E+01	1,27E+01		1,91E+01	1,27E+01
3	Global warming	Kg CO2 Equiv.		4,43E+00	7,51E+00			1,06E+03	7,09E+02		1,80E+03	1,20E+03
4	Ozone layer depletion	Kg CFC-11 Equiv.		1,63E-07	8,27E-10			2,35E-02	1,57E-02		1,19E-04	7,95E-05
5	Photochemical oxidants creation	Kg Ethene Equiv.		1,93E-03	2,71E-03			1,86E+01	1,24E+01		2,60E+01	1,74E+01
6	Acidification of soil and water	Kg SO2 Equiv.		2,67E-02	4,92E-02			1,15E+03	7,70E+02		2,13E+03	1,42E+03
7	Eutrophication	Kg PO43- Equiv.		2,20E-03	2,74E-03			4,23E+01	2,82E+01		5,27E+01	3,51E+01
8	Human toxicity	kg 1.4 DB		5,32E+00				2,30E+03	1,53E+03		2,30E+03	1,53E+03
9	Ecotoxicity. fresh water	kg 1.4 DB		3,02E-02				4,35E+00	2,90E+00		4,35E+00	2,90E+00
10	Ecotoxicity. marine water (MAETP)	kg 1.4 DB		5,01E+02				2,41E+02	1,60E+02		2,41E+02	1,60E+02
11	Ecotoxicity. terrestric	kg 1.4 DB		1,36E-02				3,92E+00	2,61E+00		3,92E+00	2,61E+00
14	renewable primary energy total	MJ		5,37E+00								
18	use of secondary material	Kg		8,02E-01								
								4,85E+03	3,23E+03		6,58E+03	4,39E+03
								0	8009			
Aluminium	Aluminium for civil construction - D		kg									
	Allocation based on economic values. The output side is assumed to be 95% recycling.											
1	Depletion of abiotic resources-elements	Kg Sb		7,98E-05	-2,63E-06				1,02E-01		-3,37E-03	
2	Depletion of abiotic resources-fossil fuels	Kg Sb		-1,77E-02					-2,27E+01		-2,27E+01	
3	Global warming	Kg CO2 Equiv.		-3,07E+00	-4,91E+00				-1,23E+03		-1,97E+03	
4	Ozone layer depletion	Kg CFC-11 Equiv.		-8,85E-08	-2,08E-10				-2,13E-02		-5,00E-05	
5	Photochemical oxidants creation	Kg Ethene Equiv.		-1,34E-03	-1,76E-03				-2,15E+01		-2,82E+01	
6	Acidification of soil and water	Kg SO2 Equiv.		-1,91E-02	-3,51E-02				-1,38E+03		-2,53E+03	
7	Eutrophication	Kg PO43- Equiv.		-1,20E-03	-1,45E-03				-3,84E+01		-4,65E+01	
8	Human toxicity	kg 1.4 DB		-4,51E+00					-3,25E+03		-3,25E+03	
9	Ecotoxicity. fresh water	kg 1.4 DB		-1,42E-02					-3,41E+00		-3,41E+00	
10	Ecotoxicity. marine water (MAETP)	kg 1.4 DB		-4,11E+02					-3,29E+02		-3,29E+02	
11	Ecotoxicity. terrestric	kg 1.4 DB		-5,10E-03					-2,45E+00		-2,45E+00	
14	renewable primary energy total	MJ		-3,78E+00								
25	Components for re-use	Kg		0,00E+00								
26	Materials for recycling	Kg		9,50E-01								
								0	-6,27E+03		0	-8,18E+03
								320	214			
Alu weldin	Welding, arc, aluminium {RER}| processing | Alloc Rec, U		m									
1	Depletion of abiotic resources-elements	Kg Sb		2,94E-07				1,51E-05	1,01E-05			

2	Depletion of abiotic resources-fossil fuels	Kg Sb	2,25E-03				1,15E-01	7,70E-02		
3	Global warming	Kg CO2 Equiv.	3,92E-01				6,27E+00	4,19E+00		
4	Ozone layer depletion	Kg CFC-11 Equiv.	1,50E-08				1,44E-04	9,63E-05		
5	Photochemical oxidants creation	Kg Ethene Equiv.	1,61E-04				1,03E-01	6,89E-02		
6	Acidification of soil and water	Kg SO2 Equiv.	2,30E-03				6,62E+00	4,43E+00		
7	Eutrophication	Kg PO43- Equiv.	1,70E-04				2,18E-01	1,46E-01		
8	Human toxicity	kg 1.4 DB	4,82E-01				1,39E+01	9,28E+00		
9	Ecotoxicity. fresh water	kg 1.4 DB	2,84E-03				2,73E-02	1,82E-02		
10	Ecotoxicity. marine water (MAETP)	kg 1.4 DB	4,69E+01				1,50E+00	1,00E+00		
11	Ecotoxicity. terrestric	kg 1.4 DB	1,33E-03				2,55E-02	1,71E-02		
14	renewable primary energy total	MJ	5,45E-01							
							2,88E+01	1,92E+01		

Transport, freight, sea, transoceanic ship {GLO}| market for | Alloc Rec, U — tkm

1	Depletion of abiotic resources-elements	Kg Sb	2,49E-09							
2	Depletion of abiotic resources-fossil fuels	Kg Sb	7,82E-05							
3	Global warming	Kg CO2 Equiv.	1,14E-02							
4	Ozone layer depletion	Kg CFC-11 Equiv.	1,80E-09							
5	Photochemical oxidants creation	Kg Ethene Equiv.	1,23E-05							
6	Acidification of soil and water	Kg SO2 Equiv.	2,38E-04							
7	Eutrophication	Kg PO43- Equiv.	2,12E-05							
8	Human toxicity	kg 1.4 DB	5,10E-03							
9	Ecotoxicity. fresh water	kg 1.4 DB	9,00E-05							
10	Ecotoxicity. marine water (MAETP)	kg 1.4 DB	4,36E-01							
11	Ecotoxicity. terrestric	kg 1.4 DB	1,64E-05							
12	renewable primary energy ex. raw materials	MJ	0,00E+00							
13	renewable primary energy used as raw materials	MJ	0,00E+00							
14	renewable primary energy total	MJ	3,76E-03							

Transport, freight, lorry >32 metric ton, EURO4 {GLO}| market for | Alloc Rec, U

1	Depletion of abiotic resources-elements	Kg Sb	1,70E-07							
2	Depletion of abiotic resources-fossil fuels	Kg Sb	6,77E-04							
3	Global warming	Kg CO2 Equiv.	8,97E-02							
4	Ozone layer depletion	Kg CFC-11 Equiv.	1,71E-08							
5	Photochemical oxidants creation	Kg Ethene Equiv.	5,58E-05							
6	Acidification of soil and water	Kg SO2 Equiv.	3,53E-04							
7	Eutrophication	Kg PO43- Equiv.	6,85E-05							
8	Human toxicity	kg 1.4 DB	4,07E-02							
9	Ecotoxicity. fresh water	kg 1.4 DB	1,10E-03							
10	Ecotoxicity. marine water (MAETP)	kg 1.4 DB	4,36E+00							
11	Ecotoxicity. terrestric	kg 1.4 DB	1,29E-04							
12	renewable primary energy ex. raw materials	MJ	0,00E+00							
13	renewable primary energy used as raw materials	MJ	0,00E+00							
14	renewable primary energy total	MJ	2,05E-02							
				5880	7840	1700	2220		12250	

Transport, freight, lorry 16-32 metric ton, EURO4 {GLO}| market for | Alloc Rec, U

1	Depletion of abiotic resources-elements	Kg Sb	4,97E-07	4,68E-04	6,23E-04	1,95E-04	1,77E-04		9,74E-04	
2	Depletion of abiotic resources-fossil fuels	Kg Sb	1,21E-03	1,14E+00	1,52E+00	4,74E-01	4,30E-01		2,37E+00	
3	Global warming	Kg CO2 Equiv.	1,66E-01	4,88E+01	6,51E+01	2,03E+01	1,84E+01		1,02E+02	
4	Ozone layer depletion	Kg CFC-11 Equiv.	3,03E-08	5,34E-03	7,13E-03	2,23E-03	2,02E-03		1,11E-02	
5	Photochemical oxidants creation	Kg Ethene Equiv.	8,32E-05	9,78E-01	1,30E+00	4,08E-01	3,69E-01		2,04E+00	
6	Acidification of soil and water	Kg SO2 Equiv.	6,51E-04	3,45E+01	4,59E+01	1,44E+01	1,30E+01		7,18E+01	
7	Eutrophication	Kg PO43- Equiv.	1,27E-04	2,99E+00	3,98E+00	1,24E+00	1,13E+00		6,22E+00	
8	Human toxicity	kg 1.4 DB	6,21E-02	3,29E+01	4,38E+01	1,37E+01	1,24E+01		6,85E+01	
9	Ecotoxicity. fresh water	kg 1.4 DB	1,71E-03	3,02E-01	4,02E-01	1,26E-01	1,14E-01		6,28E-01	
10	Ecotoxicity. marine water (MAETP)	kg 1.4 DB	6,61E+00	3,89E+00	5,18E+00	1,62E+00	1,47E+00		8,10E+00	
11	Ecotoxicity. terrestric	kg 1.4 DB	2,21E-04	7,80E-02	1,04E-01	3,25E-02	2,94E-02		1,62E-01	
12	renewable primary energy ex. raw materials	MJ	0,00E+00						0,00E+00	
13	renewable primary energy used as raw materials	MJ	0,00E+00						0,00E+00	
14	renewable primary energy total	MJ	3,20E-02						0,00E+00	
				1,25E+02	1,67E+02	5,23E+01	4,74E+01		2,61E+02	

TOTAL	8,85E+02	1,29E+03	4,97E+03	-2,95E+03		
	2171,24		2015,79		1,61E+03	
		3,29E+03		8,32E+03		2,64E+03

	NL method	EU method	NL method w/ manual EPD
Steel truss	2171	3295	2,48E+03
Modular alu girde	2016	8317	3,00E+03
Modular steel gir	1610	2637	

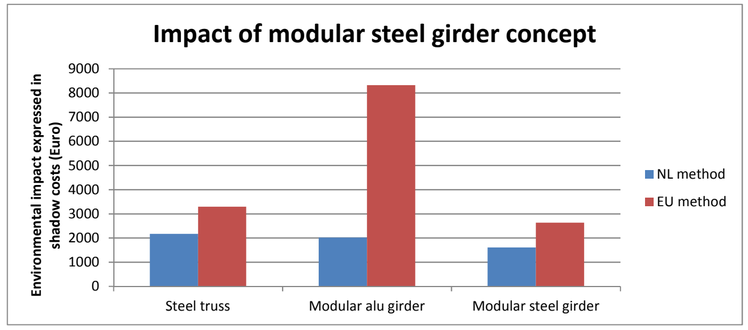
Impact of modular steel girder concept
Environmental impact expressed in shadow costs (Euro)
9000
8000
7000
6000
5000
4000
3000
2000
1000
0
Steel truss
Modular alu girder
Modular steel girder
NL method
EU method

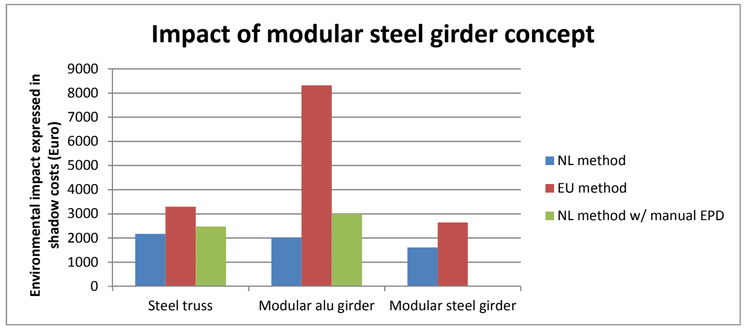
Impact of modular steel girder concept
Environmental impact expressed in shadow costs (Euro)
9000
8000
7000
6000
5000
4000
3000
2000
1000
0
Steel truss
Modular alu girder
Modular steel girder
NL method
EU method
NL method w/ manual EPD